THE CONFORMATION OF LYSOZYME IN SOLUTION

A thesis submitted in partial fulfilment
of the requirements for the degree of
Doctor of Philosophy

C.M. Dobson

Merton College

1975

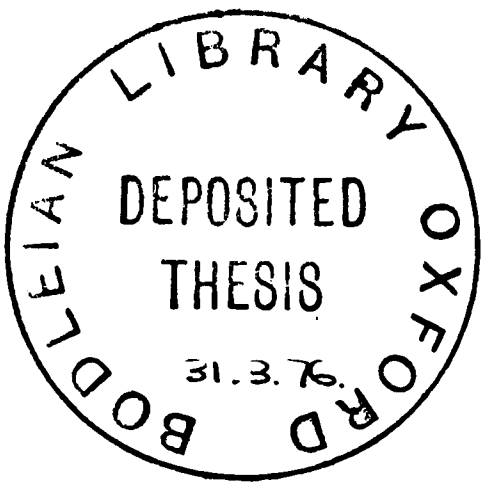

ACKNOWLEDGEMENTS

I should like first to thank Professor R.J.P. Williams for his constant supervision and encouragement of the work described in this thesis.

I am indebted to those people who have contributed directly to the experimental work reported here. In particular, Dr. I.D. Campbell devised the means of performing many of the experimental techniques without which much of the data in this thesis would not have been obtained. Dr. A.V. Xavier was responsible for introducing me to nuclear magnetic resonance spectroscopy, particularly to techniques involving lanthanide ions. Dr. Janet Thornton instructed me in the use of the MSEARCH computer programme, and performed various calculations for me. I am also indebted to those people who have contributed through discussion to many of the ideas expressed in this thesis. In particular, this refers to Drs Campbell and Xavier, but I should also like to thank Drs L.O. Ford, G. Jeminet, B.A. Levine, D.R. Martin, D.A. Sweigart and P.E. Wright, and Messrs. G.R. Moore and R.G. Ratcliffe.

I am grateful to Professor D.C. Phillips and his department for providing crystallographic data for lysozyme, and for information and discussions about the X-ray diffraction method. I thank Mrs H.M. Holloway for typing this thesis.

This work was carried out during the course of a Senior Scholarship and Junior Research Fellowship, for which I am grateful to the Warden and Fellows of Merton College.

ABSTRACT

This thesis describes an investigation of the conformation of a small protein, lysozyme from hen egg-white, in aqueous solution which was carried out by means of nuclear magnetic resonance (nmr) spectroscopy. The conformation in the crystalline state had previously been investigated by X-ray diffraction, and a model of this conformation (the X-ray structure) was available. The solution and crystalline states could therefore be compared.

Before conformational studies could be undertaken, several problems associated with the nmr spectroscopy of a protein had to be overcome. The spectrum of lysozyme (in this work ^{1}H resonances were studied) consists of a large number of broad overlapping lines. The individual resonances needed to be resolved and then assigned to specific protons in the molecule. Two different methods were devised to increase the resolution of the spectrum. First, the linewidths of resonances were reduced by a factor of about two by a mathematical manipulation of the spectrum (convolution difference). Secondly, the number of resonances observed in any given spectrum was reduced. This was achieved either by difference spectroscopy (the subtraction of two slightly different spectra) or by use of specific sequences of rf pulses in the Fourier transform nmr experiment. Using these methods, about sixty resonances were completely and separately resolved.

Techniques for assignment of the spectrum were next considered. A general scheme for assignment was devised and applied to lysozyme. The first stage consisted in assigning an observed resonance to a type of proton, and for the resolved resonances these types were mainly either aromatic protons or

methyl groups. The second stage of assignment was to assign to a type of amino acid residue, and this was achieved by observation of spin-spin coupling and by using double resonance techniques. Unlike these first two stages, the final stage of assignment, to a specific residue in the sequence, required that conformational information was used. The approach taken was to perturb selectively the spectrum in ways which depended on the molecular conformation, and then to interpret the observed perturbations by making use of the X-ray structure. This procedure will only be possible if the solution conformation closely resembles the X-ray structure, and the consistency of the results showed that, at least to a first approximation, this was the case for lysozyme. The spectral perturbations were brought about by the specific binding of paramagnetic species (Gd^{3+} and $Cr(CN)_6^{3-}$) and of protons, or were intrinsic perturbations arising from the presence of aromatic residues in the protein. These procedures permitted the total assignment of about thirty methyl group and aromatic proton resonances, and of about 10 other resonances, mostly of protons coupled to a methyl group. The totally assigned resonances were from 16 different residues, including many of those in the active site of lysozyme, but also residues from all parts of the protein. Partial assignment of other resonances was achieved.

The detailed conformational analysis was divided into three stages. First, use was made of the spectral perturbations induced by paramagnetic lanthanide cations. In certain circumstances the degree of relaxation of a nuclear resonance induced by Gd^{3+} is proportional to $1/r^6$, and the shift induced by each of the other lanthanides is proportional to $(3\cos^2\theta-1)/r^3$, where θ is the angle between the vector of

length r joining the nucleus and the metal ion, and the direction of the principal axis of magnetic susceptibility. The shifts induced by binding of different lanthanides was first used to characterise the binding site of lysozyme. It was shown that only one tight binding site exists, and that this is analagous to the binding site found in the X-ray structure. The shift and relaxation effects were then measured for different assigned resonances, and used to show that within the limits of experimental error the solution structure is well described by the X-ray structure provided allowance is made for the mobility of certain groups in the protein. This led to the second stage of the conformational analysis, that concerned with the dynamic structure of the protein. Information was collected from various nmr experiments which can detect processes occurring at widely different rates. These experiments were concerned either with the measurement of relaxation phenomena (T_1,T_2, nuclear Overhauser effects) or with the observation of exchange phenomena (e.g. linebroadening, equivalence of resonances in different environments). The conclusions from these studies were that motions of groups in the protein were described by correlation times ranging from shorter than 10^{-10} sec to longer than 10^{-2} sec. All the groups in the protein appear to experience motion with a correlation time in the region of 10^{-9} sec, which is independent of the molecular tumbling which has a correlation time in the same region. Faster than this are rotations about C-CH_3 bonds, and motions of groups on the molecular surface. Somewhat slower motions are experienced by bulky groups in the interior of the protein, but it was shown that even tyrosine groups are undergoing rotation about the C_β-C_γ bond at rates faster than

10^4 sec^{-1}. Of particular interest was the detection of slow conformational fluctuations of groups in the active site of the protein, of a type not seen elsewhere in the molecule. This type of mobility was observed to be altered on binding species into the active site, and this led to the third stage of conformational analysis, that is the detection of conformational changes which can occur in response to an applied perturbation. These changes were studied by observing changes in chemical shift values and in relaxation times of assigned resonances. There are small changes in conformation accompanying the binding of protons, metal ions and inhibitors to lysozyme. These changes are most pronounced when binding takes place in the active site region rather than elsewhere. It was first shown that changes of conformation occur as a consequence of the binding of these species in the active site. It was then shown that changes in conformational mobility occur also, the active site being less mobile in the bound form. The rates of the conformational changes were also studied, and these changes were always faster than 10^3 sec^{-1}, with the exception of the change induced by binding of the inhibitor $(GlcNAc)_3$ which was quite slow (ca. 10 sec^{-1} at 25^oC). This result allowed the conclusion to be drawn that the slow step in the binding of this inhibitor was the rearrangement of the protein conformation. Additionally certain aspects of the dynamic behaviour of the protein in solution could be correlated with the diffuse electron density observed in certain regions of the X-ray structure.

Finally, a comparison was made of the conformation and conformational behaviour of human lysozyme with that of hen lysozyme. Human lysozyme differs from hen lysozyme in 40%

of its sequence, but close similarities were found between the two enzymes.

The overall conclusions of this conformational work were drawn as follows. The X-ray structure is a good description of the solution conformation of lysozyme, provided that the average position of the groups over a long period of time is required. Many groups in the protein, however, possess considerable independent mobility. This is particularly clear for groups in the active site, and binding of species (even protons) in the active site can result both in conformational changes, which may be quite slow and therefore possible rate determining steps in catalysis, and also in changes in the mobility of protein groups, and this must be important when considering the mechanism and energetics of enzymic action.

CONTENTS

NOTE

In Appendix F, several diagrams are reproduced to illustrate aspects of the crystal structure of lysozyme. These are helpful in the interpretation of the nmr observations.

CHAPTER I

INTRODUCTION

This thesis is concerned with an investigation of the conformation in solution of a small protein, lysozyme*, by means of proton nuclear magnetic resonance (nmr). The conformation of the protein in the crystalline state has already been investigated by X-ray diffraction methods (see Imoto *et al.*, 1972). These studies enabled a three dimensional model of the protein to be constructed, which will be referred to as the X-ray structure.

I.1 Lysozyme

Lysozyme consists of a single polypeptide chain of 129 amino acid residues, and has a molecular weight of *ca.* 14,400. Recent reviews (Imoto *et al.*, 1972; Osserman *et al.*, 1974) summarise the properties of the protein. The amino-acid composition and sequence have been determined, and are given in Appendix A. Lysozyme is readily available in high purity, it is soluble in water to high concentration (more than 10mM), and is stable in solution in its native form between pH 1 and pH 11 at 25°C and over a wide temperature range (up to 70°C at pH 5.0). Its thermal denaturation is fully reversible at pH values less than 7, and aggregation does not occur in solution except at pH values above 7. In addition, the protein is known to bind lanthanide cations both in the crystal (Blake and Rabstein, 1970) and in solution (Morallee *et al.*, 1970).

---

* unless otherwise stated, 'lysozyme' refers to the protein from hen egg-white.

These cations are valuable nmr probes. Prior to the present work, a number of nmr experiments had been carried out on lysozyme (McDonald and Phillips, 1970) and these showed that the ^{1}H nmr spectrum was relatively well resolved.

Lysozyme promotes the dissolution of bacterial cell walls, as it is able to catalyse the hydrolysis of β-1,4-glycosidic linkages between residues in the polysaccharide components of the cell walls. The cell wall is a copolymer of N-acetylglucosamine (GlcNAc) and N-acetylmuraminyl (GlcNAm). Lysozyme also catalyses the hydrolysis of $(GlcNAc)_n$ polymers where $n>4$, whilst when $n<3$ the molecules inhibit the enzymic activity. On the basis of the X-ray studies (see below) and chemical information, the binding of these inhibitors and substrates is well understood and a mechanism of action for the enzyme has been proposed (Blake et al., 1967). This work has been fully described by Imoto et al. (1972).

I.2 The X-ray structure

The X-ray structure of lysozyme is a model, representing the positions of the atoms in the molecule, deduced from the electron density distribution calculated from the observed scattering of X-rays by tetragonal crystals of lysozyme. The model shows the molecule as being roughly ellipsoidal in shape, with dimensions about 45 x 30 x 30 Å. The molecule has a deep cleft on one side, divided into six sites A-F, in which the polysaccharide inhibitors and substrates bind. Two catalytically important ionisable groups are the carboxylic acid groups of glu 35 and asp 52 situated between sites D and E.

The outline conformation of the molecule in solution is presumed to be similar to the X-ray structure, because of the correlation between known chemical properties of the molecule

and those expected from the X-ray structure. On a quantitative basis the degree of similarity remains unknown. It is useful here to consider the way in which the X-ray structure of a protein is derived. First, measurements of the intensities of scattered X-radiations are recorded over a relatively long period of time. Next, these time-averaged intensities are converted into a three dimensional electron density distribution. The known sequence of the protein is then fitted as a single molecular conformation to this electron density distribution. This fitting procedure cannot be carried out without the sequence information. If any of the parts of the molecule can exist in a number of different conformations, a fitting procedure of this type will result in an incorrect interpretation of the electron density map. A similarly incorrect interpretation will be reached if parts of the molecule have sufficient freedom to move between different conformations in the time taken for acquisition of the scattering intensities. It is therefore possible that correlation between the experimental electron density map and the expected electron density for a given group may be rather less satisfactory for some residues than for others. In the electron density map of lysozyme, certain groups cannot be well defined from the electron density map. For example, the indole ring of trp 62 cannot be clearly placed in the native enzyme, although in the presence of a bound inhibitor this group is well defined (Imoto et al., 1972). Parts of the side-chains of other residues such as met 12 and many surface groups (see Appendix A) are not well defined, and their conformations in the X-ray structure are not certain (Imoto et al. 1972). This situation arises in all protein X-ray structures. It seems likely therefore that the

reasons for the diffuse nature of the electron density map in some regions of a protein is due either to the existence of various conformations in the crystal or to the motion of groups in the time taken for data collection.

The exact meaning of a protein conformation becomes more difficult to define once the situation in solution is considered. The constraints which could result in the existence of a single immobile conformation are less than those operating in the crystal state. The questions which need to be answered may be summarised as follows. First, how closely does the X-ray structure resemble the time-averaged solution structure? Secondly, how different are the conformers which contribute to the observed time-averaged conformation, or in other words how much freedom of movement do the groups in a protein in solution possess? Thirdly, how fast do the groups in a protein move independently of the overall molecular motion? Fourthly, what are the changes in the protein conformation which arise from the binding of species or from change in conditions, and how fast do they occur?. All these questions are concerned with the nature of the structure of a protein molecule in solution. At the end of the analysis, one may ask whether or not it is valid to discuss the mechanism of enzymic action simply by considering a static model of the solution conformation based on the X-ray structure.

Diffraction methods cannot be applied to the determination of protein conformation in solution. Nmr spectroscopy is the only technique at present which can provide detailed information of the type required. However, the application of nmr to the study of proteins is not well developed. Thus, much of this thesis must be concerned with the development of techniques which will permit detailed conformational studies to be performed.

I.3 The Purpose of the Present Work

The aims of the work described in this thesis fall into three sections. First, methods for the improvement of the resolution of protein spectra are to be developed. Secondly, assignments are to be made in the spectrum of lysozyme. Thirdly, the conformation and conformational behaviour of lysozyme in solution are to be investigated. In each section, the application of paramagnetic lanthanide ion probes is of particular interest.

The existence of the X-ray structure of lysozyme means that comparison between this and the nmr observations in solution may be made. This is likely to be the most straightforward procedure for investigation of the solution conformation. The conformation of lysozyme itself is of greatest interest in the region of the active site cleft, and particularly close to glu 35 and asp 52. It would be hoped that observations concerning the conformation and conformational changes in this region could be related to the X-ray studies of inhibitor binding and to the known enzymatic activity.

Aside from the specific conclusions concerning lysozyme, it is hoped that general conclusions may be reached. First, nmr procedures may be laid down for investigation of other proteins. Secondly, the question of the nature of a protein solution structure may be substantially answered by a study in depth of a single system.

References for Chapter I

Blake, C.C.F., Johnson, L.N., Mair, G.A., North, A.C.T., Phillips, D.C. and Sarma, V.R. (1967), Proc. Roy. Soc. B167, 378.

Blake, C.C.F and Rabstein, M.A. (1970), personal communication, cited in Morallee et al., 1970.

Imoto, T., Johnson, L.N., North, A.C.T., Phillips, D.C. and Rupley, J.A. (1972), in The Enzymes, Vol. VII, (3rd ed.) (Boyer, P.D. ed.). Academic Press (N.Y.), 666.

McDonald, C.C. and Phillips, W.D. (1970), in Fine Structure of Proteins and Nucleic Acids, Vol. IV, (Fasman, G.D. and Timasheff, S.N. eds), Dekker (N.Y.), 1.

Morallee, K.G., Nieboer, E., Rossotti, F.J.C., Williams, R.J.P., Xavier, A.V. and Dwek, R.A. (1970), J.C.S. Chem. Comm. 1132.

Osserman, E.F., Canfield, R.E., Beychok, S. (eds) (1974), Lysozyme, Academic Press (N.Y.).

CHAPTER II

MATERIALS AND METHODS

II.1 Materials

II.1.1 The Proteins

Lysozyme from hen egg-white was obtained from the Sigma Chemical Company. It was Grade I, three times crystallised, dialysed and lyophilised. The activity was quoted as 20,000-25,000 units per mg. No differences in the pmr spectra were observed in samples from different batches. Each sample, however, contained an impurity which was identified from the singlet pmr resonance at ca. 2.1 ppm to be acetate. Attempts to remove this by dialysis at pH 6.0 were not completely successful. Attempts to dialyse from 8M urea, followed by dialysis against H_2O to remove the urea were also not entirely satisfactory. Then, arguing that the acetate must interact with the charged groups on the protein in order to be so difficult to remove, the pH was lowered below the pK value of acetate (ca. 4.8) and dialysis against water carried out. This resulted in rapid total removal of acetate. Routinely, 1g of lysozyme was dissolved in 20ml of H_2O and the pH was adjusted to 3.0 using dilute HCl. This was dialysed at 20°C against three changes of 500ml of H_2O at pH 3.0 for a total time of 24 hours. The solution was then lyophilised and the powder stored at -5°C. No change in the pmr spectrum other than the removal of the acetate peak resulted from this procedure. Concentrations were usually obtained from the weight of dry solid. Where necessary the UV absorption was measured (ε = 37,600 ± 400 M^{-1} cm^{-1}, Imoto et al., 1972, at pH 5.0 and changes by only 1-2% from this between pH 2 and 7).

Lysozyme extracted from the urine of patients with chronic monocytic leukaemia was donated by Dr. C.C.F. Blake (Molecular Biophysics, Oxford) from material originally prepared by Dr. E.F. Osserman (Columbia University, New York). This material was purified as described above for hen lysozyme, with an additional centrifugation step before lyophilisation to remove a small amount of insoluble material. Concentrations were estimated from the weight of dry solid.

II.1.2 Other Materials

N-acetyl glucosamine (GlcNAc) was obtained from BDH Limited. The pmr spectra showed that this material was mainly the α- isomer, but that after some hours mutarotation results in almost equal concentrations of the α- and β- isomers. This has been discussed by Dalquist and Raftery (1968). The dimer $(GlcNAc)_2$ being GlcNAc-β-(1→4)-GlcNAc, and the trimer $(GlcNAc)_3$ being GlcNAc-β-(1→4)-GlcNAc-β-(1→4)-GlcNAc were donated by Dr. L.N. Johnson (Molecular Biophysics, Oxford). The proportions of α- and β- isomers were not investigated, but this has been shown to be unimportant in interactions of the molecules with lysozyme (Dalquist and Raftery, 1969). Concentrations were estimated from the weight of dry, lyophilised solid. Bacitracin was obtained from the Sigma Chemical Company and lyophilised from H_2O before use.

D_2O (99.8%) was obtained from Norsk Hydro-Elektrisk. NaOD (40% in D_2O, isotopic purity greater than 99%) and DCl (35% in D_2O, isotopic purity 99.6%) were obtained from Ciba Limited. DSS, 2:2-dimethyl-2-sila-pentane-5-sulphonate (sodium salt), was obtained from Merck.

Hexacyano chromate (potassium salt), $K_3Cr(CN)_6$, was obtained from Alfa Inorganics. The material was recrystallised from water

and solutions were stored in the dark at 5°C.

Lanthanide oxides (99.9% or better) were obtained from Koch-Light Laboratories. Lanthanide nitrates (hexahydrates, 99.9%) were obtained from Rare Earth Products Limited. The lanthanide chlorides were prepared as 0.50M stock solutions in D_2O. This was achieved by roasting the oxides (Ln_2O_3) at 900°C for at least three hours, then cooling in a desiccator and weighing the solids into volumetric flasks. To these an excess of concentrated DCl was added (1.5ml of 35% DCl for 10ml of 0.5M solution), and an equal volume of D_2O. The flasks were sealed and warmed in an oven at 70°C for several hours (Cl_2 was released from the flasks containing Pr^{3+}, as the oxide, Pr_6O_{11}, contains Pr^{4+} which oxidises DCl). The volume was then made up and the pH adjusted to ca. 5. The solutions were then of known concentration and ionic strength. The nitrates were simply dissolved in D_2O and the pH adjusted.

All other reagents were of Analar grade. Glassware was thoroughly cleaned before use. Singly distilled H_2O was used for all solutions. Standard buffer solutions (pH 4 and 9.2) for calibration of the pH meter were obtained from BDH Limited.

II.2 Preparation of Solutions for nmr

Solutions of the proteins were prepared by dissolution of the weighed lyophilised solids in the required volume of 99.8% D_2O or of 90% H_2O and 10% D_2O. Pipetting was carried out using Oxford Laboratories disposable pipettes. If required, exchangeable hydrogens were replaced by deuterons by heating solutions in D_2O, at pH values below 5 and in the absence of added salt, to 80°C for several minutes. This process relies on the unfolding of the protein which is reversible under these

conditions, though not at high pH or high ionic strength. Lanthanide, or other, solutions were added after this exchange process as concentrated solutions, to give solutions of the required concentrations.

pH values were measured using a Radiometer pH 24 meter with a GK2321C combination glass electrode. Values in D_2O are pH meter readings and are not corrected in any way. The pH meter was standardised using buffers at pH 4.0 and 9.2 (at 20°C or at quoted values for other temperatures). pH measurements were generally made at 20°C, except for detailed pH titrations where measurements were made at the temperature at which the spectra were run using a constant temperature dry block. Littl difference was found between the two methods. In titrations, pH values were measured of solutions in small glass sample tube before and after running spectra and a mean pH value was taken. However if the difference was more than 0.1 pH units, the spectrum was rerun and the pH value checked again.

The pH of the lysozyme solution was adjusted using about 1M DCl or NaOD in D_2O. With NaOD, some precipitate occurred on addition, but this redissolved on shaking. However, for pH values above ca, 9.5, it was necessary to adjust the pH value to ca. 11.0 in dilute solution, and then to centrifuge and lyophilise the solution. This solid was dissolved to give a solution at high pH, and decrease in pH could then be readily carried out using DCl. Above ca. pH 12.0 irreversible denaturation occurred. At pH values above about 7 lysozyme is markedly less soluble and irreversible precipitation occurred in solutions taken to higher temperatures.

Lanthanide solutions precipitate on formation of the hydroxide complexes at pH values above ca. 6.5, the pH at which precipitation occurs decreasing across the series from La^{3+} to

Lu^{3+}. However, the use of NaOD to adjust pH even at pH values below this results in local precipitation which may be slow to redissolve. Thus, lanthanide solutions where possible were left for several hours and the pH values remeasured. Lowering the pH was again straightforward. The lanthanide solutions of lysozyme were quite soluble, in fact more soluble than equivalent protein solutions containing KCl to the same ionic strength. The maximum KCl concentration for 5mM protein solution is ca. 0.05M, whilst 0.2M lanthanide chloride solutions are quite soluble below pH 6.

Buffers were not used in the nmr solutions because of the possibility of binding to the lanthanides, and to avoid any additional resonance appearing in the spectrum.

A list of all experiments (other than preliminary ones or those totally defined in the text) which are discussed in this thesis is given in Appendix C.

II.3 Accumulation of nmr spectra

II.3.1 Spectrometers

All the nmr spectra reported in this thesis are Fourier transform (FT) proton spectra (see Appendix B). Some spectra were recorded at 90 MHz using the Bruker HFX 90 spectrometer of the Oxford Enzyme Group. However most spectra were recorded at 270 MHz using the Oxford Enzyme Group Bruker spectrometer fitted with an Oxford Instrument Company magnet. This spectrometer employs a Nicolet 1085 computer, a Nicolet 294 disc storage system and a Nicolet 293 pulse controller, although the latter two devices only became available towards the end of this work. Both spectrometers had temperature controllers, and both required 5mm (O.D.) sample tubes contain-

ing a minimum of 0.4ml of sample. Both employed a deuterium field-frequency lock. Peak positions could be measured directl from the spectrometer computer using a cursor address system.

The operation of the spectrometer depended on the type of experiment performed, as discussed in Chapter III. However, some comments can be made here. The majority of the normal spectra were accumulated (2048 scans) in about 17 minutes using an interpoint time (dwell time) of 125 μsec and a pulse repetition time of 0.513 sec. The 90° pulse length was generally ca. 20 μsec and a ca. 45° pulse was employed. The interpoint time of 125 μsec corresponds to a sweep width of 4000 Hz. Generally, 4096 data acquisition points were employed but spectra were Fourier transformed over 8192 points using the zero-addition technique (see Farrar and Becker, 1971). For difference spectra, to avoid saturation effects, the repetition time was generally 1.2 sec, and the pulse length reduced. Befo: accumulation, it was ensured that saturation was not occurring. In T_1 and T_2 pulse sequences, 5 T_1 (ca. 5 secs) was left between pulse repetition. For spectra of samples in 90% H_2O solvent, the long pulse method was normally employed to saturat the solvent resonance (see Section III.2.2.2) and a repetition rate of 0.913 sec was generally used.

II.3.2 Measurement of Chemical Shift Values

All chemical shift values in this thesis are, unless otherwise stated, quoted for a pH value of 5.3 and temperature of 54°C in ppm (parts per million) downfield from DSS. However DSS was not used as an internal standard for the protein spectr because of its possible interaction with the protein and becaus the resonance at 0 ppm obscures peaks of interest. Acetone and dioxan (at concentrations of about 10mM) were used as

internal standards, giving singlet peaks at 2.214 ppm and 3.741 ppm respectively. Peak positions were generally obtained directly from the computer using the cursor address system.

II.4 Computation of Lanthanide Probe Data

The programme MSEARCH (Barry et al., 1973a, b) was employed on the University ICL 1906A computer for performing calculations concerned with the interpretation of lanthanide shift and broadening data. The X-ray co-ordinates of lysozyme were the RS5D set described by Diamond (1973), which differ slightly from those given by Imoto et al. 1972. These co-ordinates did not include the hydrogen atoms required in this work. These were calculated by making use of standard bond lengths and angles (see Ford, 1975) with the help of Dr. Janet M. Thornton (Molecular Biophysics, Oxford). The details of the calculations using MSEARCH will be described in Chapter VII. The operation of the programme has been described fully by Ford (1975).

References for Chapter II

Barry, C.D., Dobson, C.M., Ford, L.O., Sweigart, D.A. and Williams, R.J.P. (1973a), in Nuclear Magnetic Resonance Shift Reagents (Sievers, R.E. ed.), Academic Press, (N.Y.), 173.

Barry, C.D., Hill, H.A.O., Sadler, P.J. and Williams, R.J.P. (1973b), Ann. N.Y. Acad. Sci. 206, 247.

Dalquist, F.W. and Raftery, M.A. (1968), Biochemistry, 7, 3269.

Dalquist, F.W. and Raftery, M.A. (1969), Biochemistry, 8, 713.

Diamond, R. (1973), J. Molec. Biol. 82, 371.

Farrar, T.C. and Becker, E.D. (1971), Pulse and Fourier Transform NMR, Academic Press (N.Y.).

Ford, L.O. (1975), D.Phil. Thesis, Oxford.

Imoto, T., Johnson, L.N., North, A.C.T., Phillips, D.C. and Rupley, J.A. (1972), in The Enzymes Vol. VII, 3rd ed. (Boyer, P.D. ed.), Academic Press, (N.Y.), 666.

CHAPTER III

ACCUMULATION OF THE SPECTRUM - DEVELOPMENT OF Nmr TECHNIQUES

In this Chapter, a variety of nmr techniques are described. These techniques were designed to overcome the major difficulties encountered in protein nmr spectroscopy, which are (i) the resolution of individual resonances (spectral simplification) and (ii) the observation of multiplet structure and of the effects of double resonance experiments.

Two essentially different methods of spectral simplification have been developed in this work. The first method, that of difference spectroscopy, is well known in many branches of spectroscopy but has not yet been greatly exploited in nmr spectroscopy. This lack of exploitation is mainly a consequence of technical difficulties which have been much reduced with the advent of spectrometers operating in the pulsed mode. The second method, the use of specific sequences of pulses, has not previously been exploited for spectral simplification.

The observation of multiplet structure has been aided by two techniques. First, convolution difference methods have allowed the apparent linewidth of a resonance to be reduced. Secondly, specific sequences of pulses distinguish resonances by their J values and multiplet structure. Double resonance effects have been observed by means of both difference spectroscopy and pulse methods, and the different effects which arise (decoupling and/or nuclear Overhauser effects) have been distinguished using pulse techniques.

III.1 Difference Spectroscopy

In protein nmr, the major requirement is to reduce

the number of observed resonances. Each resonance in the spectrum is characterised by the parameters of chemical shift, linewidth, multiplet structure, intensity and spin-lattice relaxation time. The key to a good difference spectrum is to change one or more of these parameters for a small class of resonances in one of two spectra. The two spectra are then scaled, aligned and phase adjusted before subtraction. Only the perturbed resonances are then observed. Various types of difference spectra will be considered in turn. Each will be illustrated with reference to lysozyme.

III.1.1 The Convolution Difference Method

The convolution difference method is concerned with the observation of the difference between a broadened spectrum and a normal spectrum. The broadening is non-selectiv (cf. III.1.2) and is brought about by multiplication of a free induction decay by an exponentially decaying function (convolution).

It is a straightforward mathematical manipulation which sacrifices signal to noise to achieve increased resolution and in this respect is very similar to deconvolution or the multiplication of a free induction decay by an exponentially increasing function (Ernst, 1966; Ernst et al., 1967). The method does not suffer, however, from truncation and overflow problems which are especially difficult in protein spectra with a large HDO peak, and it has the additional feature of removing broad peaks from a spectrum (cf. method described by Seiter et (1972) which can lead to problems with phase correction and baseline distortion).

Assume that a free induction decay from a proton resonance is of the form $e^{-t/T_2^*} \cos(\omega^1-\omega_o)t$, where T_2^* is a decay

constant which includes the natural T_2 and magnetic inhomogeneities, ω^1 is the resonant frequency and ω_o is the frequency of the applied rf pulse. The Fourier transform of this decay is a Lorentzian line shape:

$$L(T_2^*) \alpha \quad T_2^*/(1 + \Delta\omega^2 T_2^{*2}) \qquad (1)$$

where $\Delta\omega = \omega - \omega^1$.

If the free induction decay is multiplied by e^{-t/τ_1} the resulting lineshape $L(T_A)$ is also Lorentzian with T_2^* replaced by T_A where $1/T_A = 1/T_2^* + 1/\tau_1$. Similarly convolution with e^{-t/τ_2} leads to a Lorentzian $L(T_B)$ with T_2^* replaced by T_B where $1/T_B = 1/T_2^* + 1/\tau_2$.

If $L(T_B)$ is multiplied by a constant K and subtracted from $L(T_A)$ a new lineshape is generated:

$$L(CD) \quad \alpha \quad \frac{T_A - KT_B + \Delta\omega^2(T_A T_B^2 - KT_B T_A^2)}{1 + \Delta\omega^2(T_A^2 + T_B^2) + \Delta\omega^4 T_A^2 T_B^2} \qquad (2)$$

K is usually adjusted empirically to give a convenient lineshape but two cases are worth noting.

a) $K = T_B/T_A$. The term in $\Delta\omega^2$ in the numerator now disappears and the lineshape functions L(CD) and $L(T_2^*)$ may be readily compared. Note that (i) an additional term $\Delta\omega^4 T_A^2 T_B^2$ appears in the denominator of L(CD) resulting in a rapid reduction of the resonance to zero with increasing $\Delta\omega$. (ii) The relative intensity at resonance (I_o) is reduced from T_2^* to $(T_A - T_B^2/T_A)$ resulting in a loss in signal to noise ratio. This ratio is however a more complicated function than this equation implies. (iii) The linewidth at half height is reduced from $1/\pi T_2^*$ to les than $1/\pi(T_A^2 + T_B^2)^{\frac{1}{2}}$. (iv) If $T_A = T_B$, L(CD) = 0. This occurs if the normal decay is unaffected by the convolution i.e. $\tau_1, \tau_2 >> T_2^*$. Thus the method eliminates broader lines from a spectrum.

b) K = 1. The integrated intensity of the spectrum is now zero and the term $\Delta\omega^2 (T_A T_B^2 - T_B T_A^2)$ in L(CD) causes the wings of a resonance to be negative. The intensity at resonance $I_o = T_A - T_B$. The improvement in resolution is hard to quantify but if the linewidth at half height is used as a criterion the maximum improvement is roughly a factor of 2. (see Fig. III.1). Fig. III.2 shows simulated spectra of L(CD) for $K = T_B/T_A$ and K = 1. These are compared with the original spectrum, the sum of two shifted Lorentzian lines.

The following procedure is carried out to obtain a convolution difference spectrum:

(i) A free induction decay (FID) is collected and duplicated either in another block of memory or in a storage system.

(ii) One FID is multiplied by e^{-t/τ_1} where $\tau_1 >$ the T_2^* of interest. This step is useful in protein spectra to reduce the HDO peak and phase anomalies resulting from echoes (Freeman and Hill, 1971a) but may be omitted when the FID is dominated only by the resonances of interest.

(iii) The convoluted FID is transformed and phase corrected.

(iv) The duplicate FID is convoluted with e^{-t/τ_2} where τ_2 is in the range $3T_2^*$ to $7T_2^*$ (see Fig. III.1).

(v) This FID is transformed and phase corrected.

(vi) The real part of the second transform is multiplied by a constant (-K) and added to the real part of the second transform. The multiplicative constant may be varied to optimise the convolution difference spectrum.

This procedure has been found to be easy in practice and has the advantage that both a normal spectrum and a CD spectrum are obtained. To obtain a CD spectrum only, the collected FID

FIGURE III.1

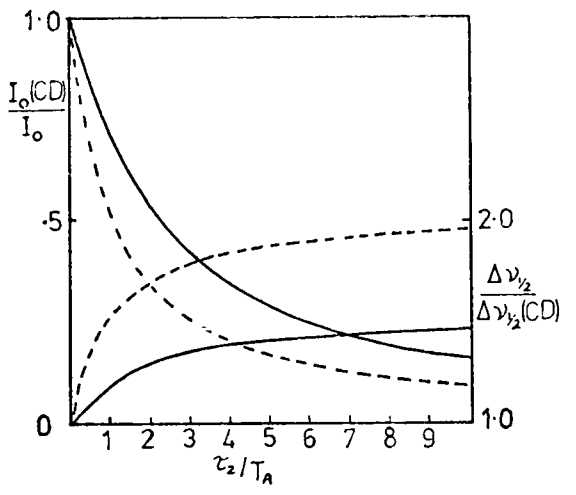

Curves showing the loss of intensity and increase in resolution resulting from a CD operation on a single line for K = 1 (---) and K = T_B/T_A (——).

FIGURE III.2

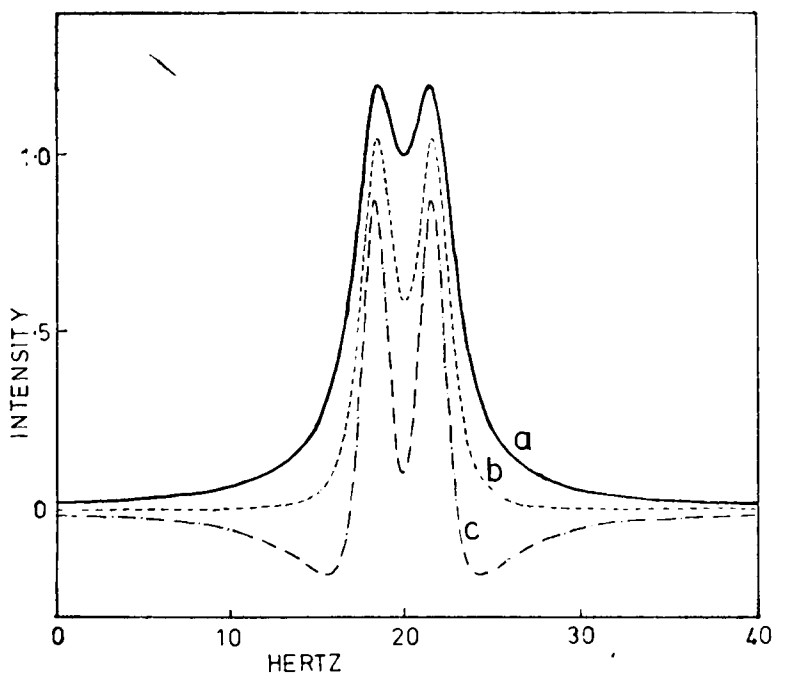

Simulated spectra of (a) the sum of two Lorentzian lines (T_2^* = 0.1 sec), (b) CD spectrum with τ_1 = 10 sec, τ_2 = 0.5 sec, K = 0.84, (c) as (b), but K = 1.

FIGURE III.3

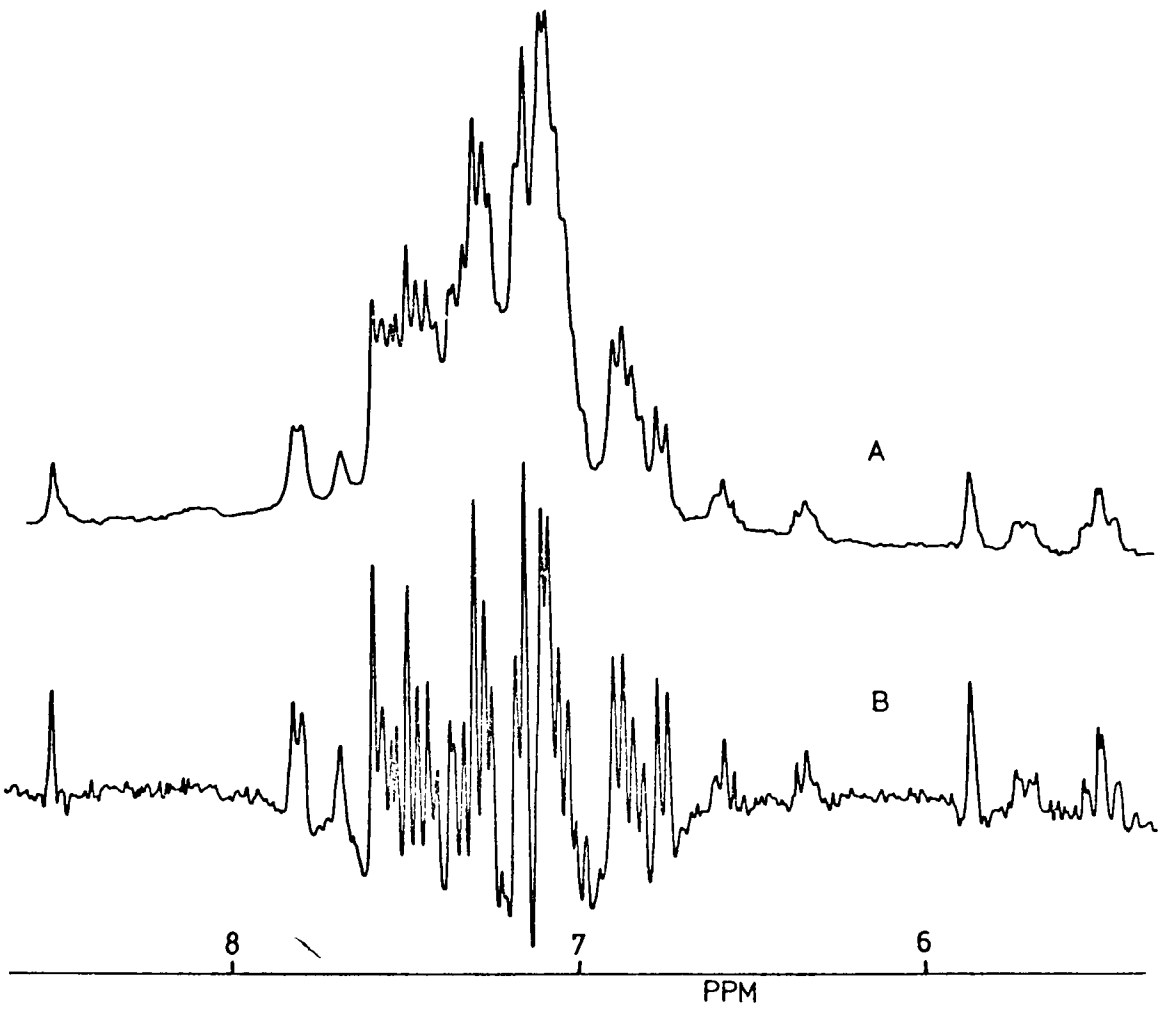

Low field region of the lysozyme spectrum. A, normal spectrum; B, convolution difference spectrum with τ_1 = 0.25 sec, τ_2 = 0.08 sec, K = 1.0. 5mM lysozyme, pH 4.8, 66^{o}C.

FIGURE III.4

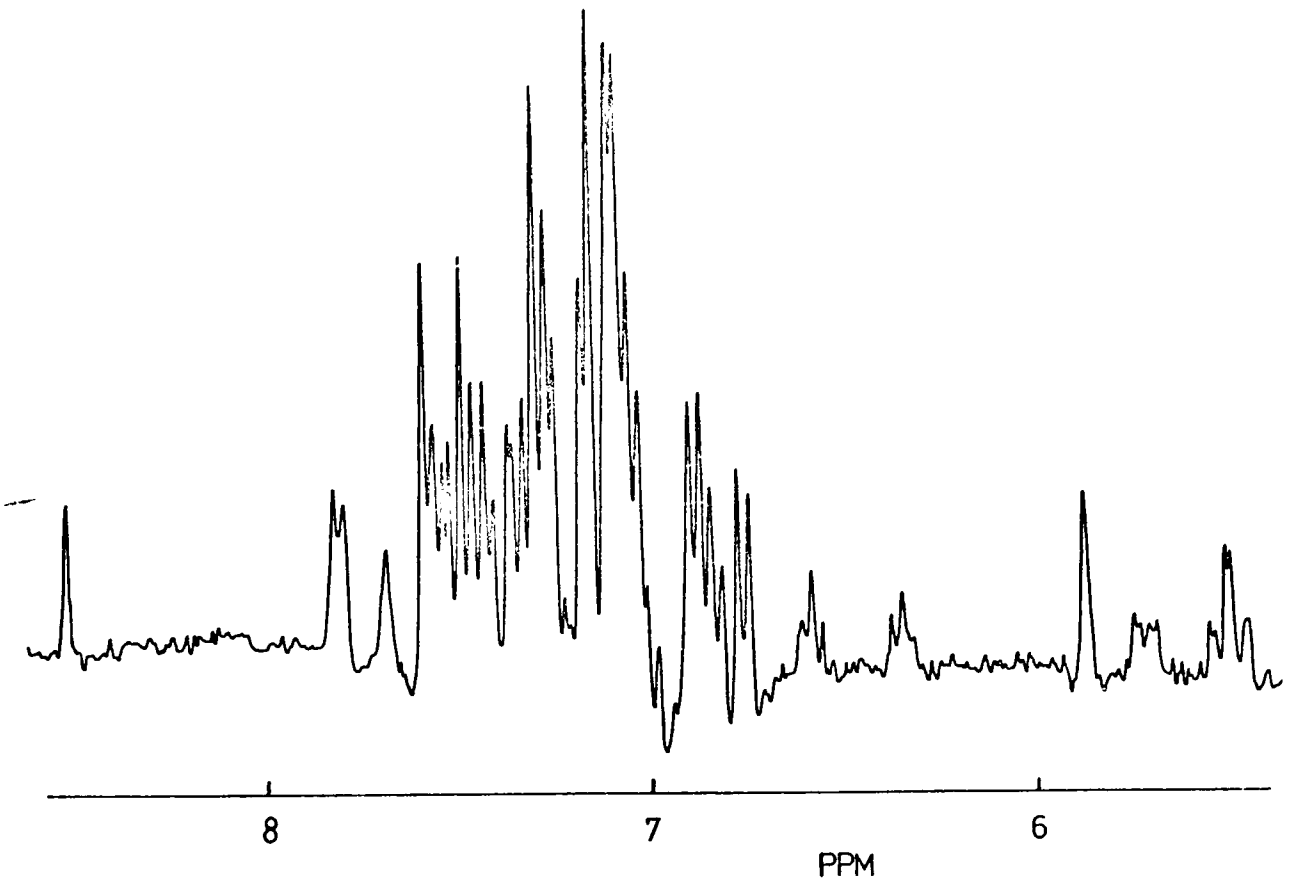

Convolution difference spectrum as Fig. III.3, but K = 0.93. Note the nearly complete elimination of the regions of the spectrum with negative intensity and the higher signal to noise ratio.

may be multiplied by $(e^{-t/\tau_1} - Ke^{-t/\tau_2})$ thus eliminating a number of steps.

Some illustrations of the application of CD spectra are shown in Figs III.3 and III.4. Note that multiplet structure is readily seen.

III.1.2 The Paramagnetic Difference Method

This method depends on the selective broadening of resonance lines, brought about by the specific binding of a paramagnetic species with a long electron relaxation time. This species may be a cation for example Gd^{3+}, Eu^{2+} or Mn^{2+}, an anion for example $Cr(CN)_6^{3-}$ or a neutral molecule such as a spin label.

The simulated spectra in Fig. III.5 illustrates the principle of this method. In spectrum b one peak has been broadened because of the proximity of specifically bound paramagnetic ions. In spectrum c, which is the difference between a and b, the only peak revealed is that one peak affected by the paramagnetic ion.

The influence of a paramagnetic ion on nuclei in its environment is, in general, complicated. If the paramagnetic ion exchanges between free solution and a bound complex there may be changes in the chemical shift and/or the linewidth of the observed resonances depending on the relative values of the parameters T_{2M}, $\Delta\omega_M$, τ_M and f. T_{2M} is the paramagnetic contribution to the spin-spin relaxation time of the ion/molecule complex, $\Delta\omega_M$ and τ_M are the induced shift and lifetime of this complex respectively and f is the fraction of the observed molecule complexed with a paramagnetic metal ion. The theory giving the observed paramagnetic contribution to the linewidth $(1/\pi T_{2p})$ in the presence of exchange has been presented by many

FIGURE III.5

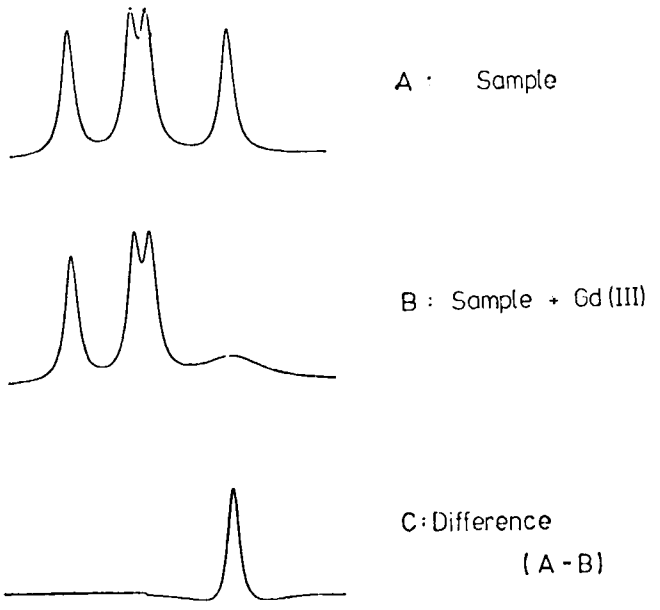

Simulated paramagnetic broadening difference spectrum. It is assumed that one of the four resonances shown is broadened substantially more than the others. This one resonance is revealed in the difference spectrum.

FIGURE III.6

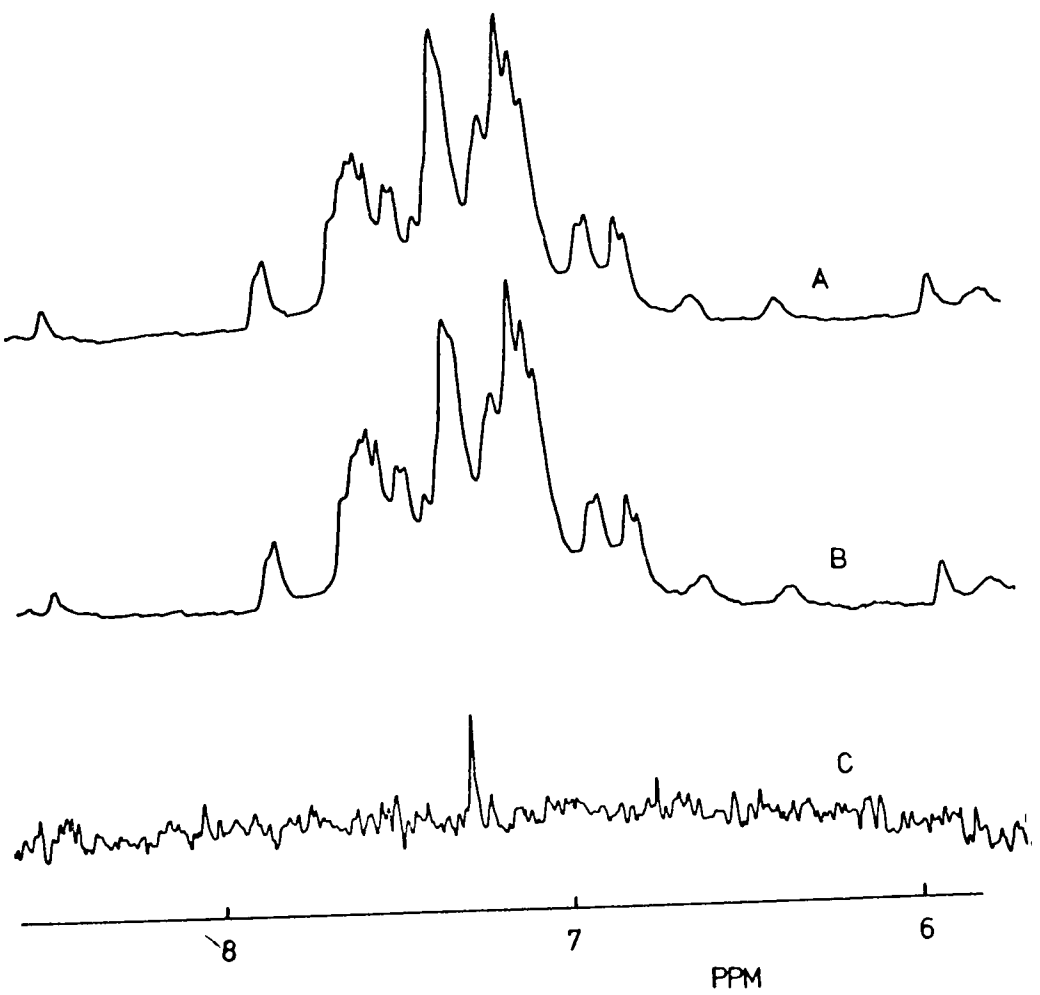

A Gd^{3+} difference spectrum of lysozyme. A, low field region of the spectrum of 5mM lysozyme containing 23.8 mM La^{3+}, pH 5.3, 54°C. B, same sample but with 1.12×10^{-5} M Gd^{3+}. C, difference A minus B with four times the vertical scale. One resonance is observed (see Chapter V).

authors (Solomon, 1955; Bloembergen, 1957; Swift and Connick, 1962).

If the electron relaxation time of the metal ion is long, e.g. Gd^{3+}, Mn^{2+}, the relaxation due to the ion is very efficient and the condition $^{1}/_{T_{2M}} >> \Delta\omega_M$ usually applies. If, in addition fast exchange occurs, i.e. $\tau_M << T_{2M}$ then, at constant temperature

$$^{1}/_{T_{2p}} = \text{const.} \times \frac{f}{r^6} \qquad (3)$$

Assume that equation (3) is applicable and return to the lineshape for a convolution difference spectrum given in equation (2). T_{2p} is now equivalent to τ_2 and K = 1. If $\tau_1 >> T_2^*$ the intensity of a singlet resonance (I_o) is proportional to $T_2^* - T_B$ in the difference spectrum, i.e.

$$I_o(PD) = \text{const.} \times T_2^{*2}/(T_{2p} + T_2^*) \qquad (4)$$

If $T_{2p} << T_2^*$, $I_o(PD) = \text{const.} \times T_2^*$, i.e. it is the intensity of a normal spectrum. If $T_{2p} >> T_2^*$, $I_o(PD) = 0$. T_{2p} is readily adjusted between these extremes by varying the concentration of the paramagnetic ion provided the distance between the ion binding site and the observed nucleus is not too large.

In the case of hen and human lysozyme Gd^{3+} binds between glu 35 and asp 52 (See Chapter V). From available crystal structure data the methyl groups of val 109 and ala 110 are nearest to this site. The PD spectra of both proteins when $[Gd^{3+}] = 5 \times 10^{-5}M$ do reveal groups which may be attributed to these residues. This is illustrated in Fig. V.7 At higher Gd^{3+} concentrations more resonances appear in the PD spectra as the T_{2p} of the observed resonance becomes of the same order as its T_2^*. These experiments will be discussed in detail in later chapters.

It is important in quantitative conformational studies to be able to measure T_{1M} and T_{2M}. The pulse sequences discussed below may enable this to be done. However, the difference method allows T_{2M} to be estimated in regions of the spectrum which are highly complex, using a simple graphical method.

Consider the case where f is proportioned to the concentration of paramagnetic ion, [P], (this is the case in the lysozyme experiments). Then from equations (3) and (4) we have

$$\frac{1}{I_o(PD)} \quad \alpha \quad \frac{1}{[P]} \quad x \quad \frac{T_{2M}}{T_2^{*2}} + \frac{1}{T_2^*} \qquad (5)$$

Thus a plot of $\frac{1}{I_o(PD)}$ vs $\frac{1}{[P]}$ has a slope proportional to T_{2M}/T_2^{*2} and the intercept (when $1/[P] = 0$) is related to the inverse of the intensity of the peak in the normal spectrum. Thus if T_2^* is the same for a series of resonances (a good approximation for many groups in lysozyme) the slopes of $1/I_o$ vs $1/[P]$ for different resonances produces ratios of $1/T_{2M}$ and so of $1/r^6$. This analysis applies strictly only to singlet lines. For example it may be observed in Fig. III.2 that for a doublet the intensity depends on the separation between the lines (J) and the value of T_{2p}, since although each singlet is normalised to unit intensity, the doublet does not normalise. These corrections may be allowed for by spectral simulation. A plot of $\frac{1}{I_o(PD)}$ vs $1/[Gd^{3+}]$ for different resonances in hen lysozyme is shown in Fig. VI.16. It can be readily seen that good linear graphs are obtained.

III.1.3 Shift Difference

This method is quite straightforward. If the chemical shift values of a small number of resonances are perturbed, subtraction of the perturbed spectrum from the original spectrum permits the affected resonances to be observed. Each resonance gives rise to a positive and a negative peak, the areas and chemical shift values of these peaks being those of the individual spectra provided that the difference in chemical shifts is significantly greater than the linewidths.

This method was originally used by Bradbury and King (1971) to follow the titrations with pH of the histidine resonances of ribonuclease. In the work described in this thesis shift difference spectra have been used to observe not only pH effects, but also the binding of metal ions and of inhibitor molecules. Fig. III.7 illustrates this technique.

III.1.4 Intensity Difference

If the intensity of a number of resonances is altered, this is easily revealed by difference spectroscopy. One method of changing peak intensities is by observation of nuclear Overhauser effects (see Appendix B). However, in this work difference spectroscopy has also been developed as a method of following the exchange of NH protons with solvent. This is illustrated in Fig. III.8. Fig. III.8a shows the 270 MHz proton magnetic resonance spectrum of a sample of hen lysozyme dissolved in D_2O at 25°C and pH 2.6. Fig. III.8b shows the spectrum of the same sample after it was subjected to a temperature of 80°C for two minutes. Lysozyme reversibly denatures at temperatures above 75°C, resulting in rapid equilibrium between solvent (D_2O) and all exchangeable hydrogens. Fig. III.8c shows the result of

FIGURE III.7

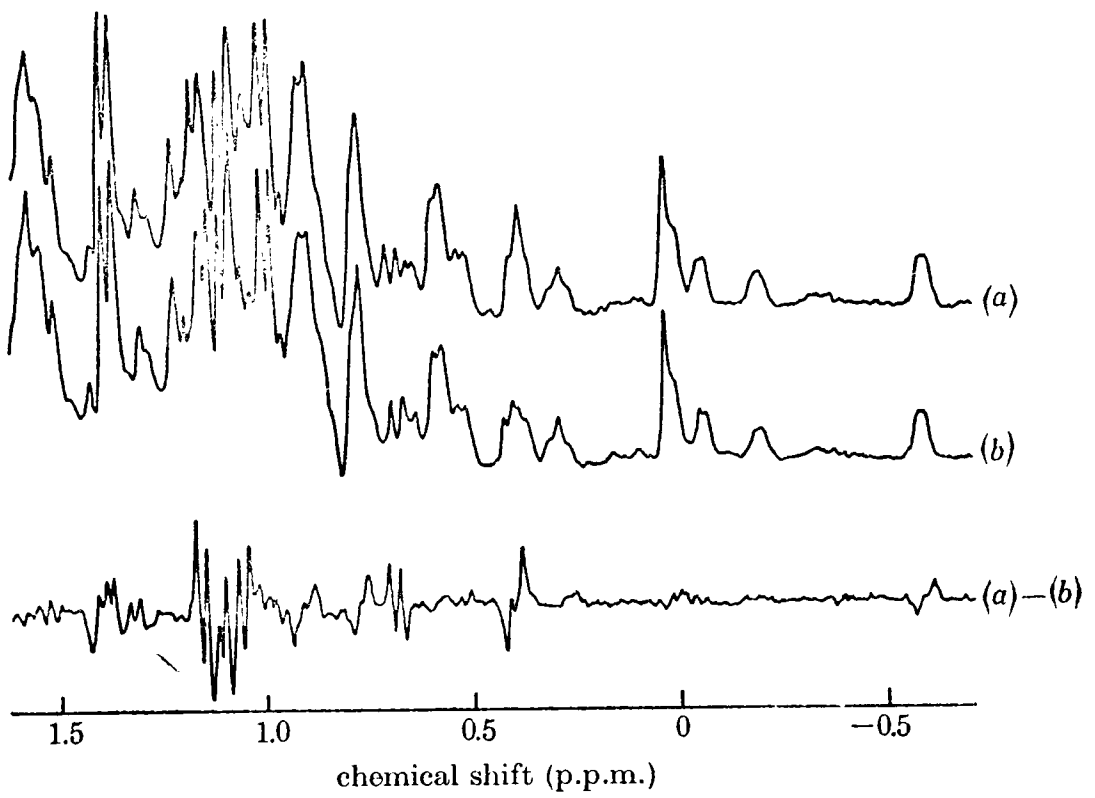

A shift difference spectrum. (a) is part of the high field CD spectrum of 5mM lysozyme containing 23.8 mM La^{3+} at pH 5.3. In (b), O.6mM of La^{3+} has been replaced by the shift probe Pr^{3+}. The difference, (a)-(b), reveals only those resonances which have been shifted significantly.

FIGURE III.8

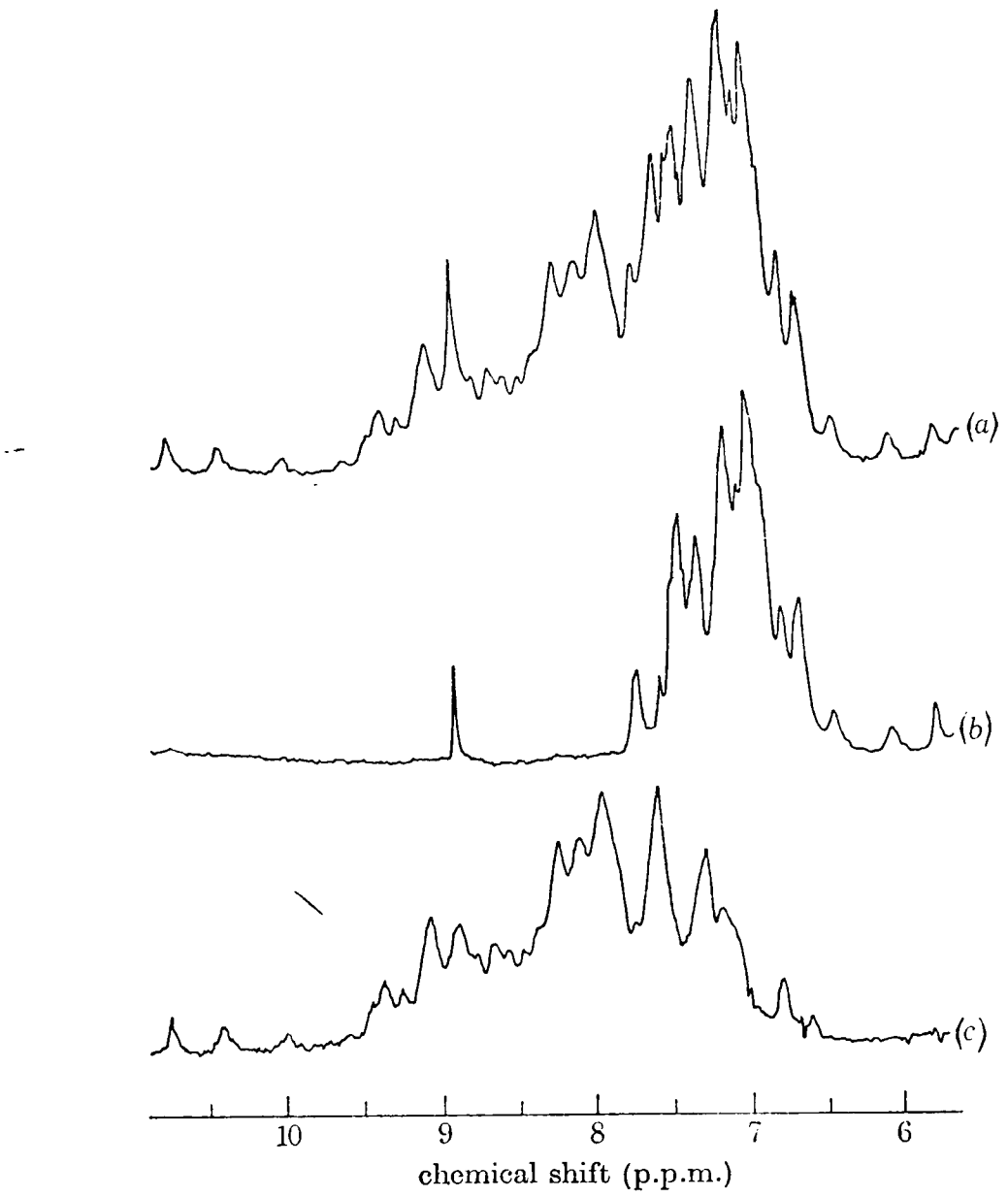

Intensity difference spectrum. (a) low field part of the spectrum of 5mM lysozyme at pH 2.6, 21°C. The accumulation of the spectrum started 10 min after dissolution of the protein in D_2O, and took 9 min. (b) spectrum of the same sample after heating to 80°C for several minutes. (c) difference between (a) and (b).

subtracting these two spectra. The resonances observed in this difference spectrum correspond to exchangeable hydrogens which are not replaced by deuterium after ca. 10 mins in D_2O at 25°C and pH 2.6. This is a use of difference spectroscopy for simplifying a spectrum by observing separately a small number of proton resonances of interest. The difference spectrum clearly illustrates that proton magnetic resonance can be used to perform quantitative isotope exchange studies.

III.1.5 Double Resonance Difference

Three effects can accompany the application of a selective rf pulse in the double resonance method. One, is the change in intensity of a resonance through the nuclear Overhauser effect (see Noggle and Schirmer, 1971; Campbell and Freeman, 1973). The second is the change in multiplet structure of a resonance spin-spin coupled to a resonance at the frequency of the applied rf pulse. This is spin-decoupling. The third effect is that perturbation to chemical shift values near to the frequency of the applied rf pulse can occur (Bloch-Siegert shifts, see for example Hoffmann and Forsén, 1966). The use of difference spectroscopy to measure intensity changes has been mentioned. In Section III.2.2.1 it will be shown that the nuclear Overhauser effect and spin decoupling can be separated by the use of pulse sequences. In this section the use of difference spectroscopy to observe changes in spin-coupling will be described. In principle this is straightforward. Spectra with and without decoupling irradiation are subtracted. If any resonance is decoupled, a peak is observed in the difference spectrum. The shape of this peak depends on the multiplet structure and coupling constant in the two spectra (note that as with most forms of difference spectra except for that des-

cribed in Section III.1.4, the overall integrated intensity in the difference spectrum is zero).

In practice, the procedure is not easy unless the irradiatio frequency and the decoupled resonance are well separated. In order to achieve good results, the following procedure is proposed. One spectrum is accumulated with the irradiation applied at x ppm, and another with irradiation at x + Δx ppm. Δx (ca. 0.1 ppm) is chosen such that no resonance occurs at x + Δx ppm. Any peaks which occur in the difference between these two spectra correspond to resonances coupled to resonances at x ppm. The reason for recording the second spectrum with irradiation applied is to minimise the effect of non-specific perturbations caused by the irradiation. It is also advantageous to use the lowest effective rf decoupling power to minimise Bloch-Siegert shifts and loss of signal-to-noise ratio and to minimise intensity changes in the region of the applied rf frequency.

The use of the difference method to observe decoupling of tyrosine resonances in lysozyme is shown in Fig. III.9. The intensity and shape of the peaks in the difference spectrum indicates quite unambiguously that a two proton intensity doublet is coupled to a second two proton intensity doublet.

As a warning note, the intensity of any peak in the spin-decoupling difference spectrum is reduced as the linewidths increase. It is also smaller for the change triplet to doublet than for doublet to singlet. Care must therefore be taken to ensure that negative results, that is the observation of no significant peaks in the difference spectrum, are correctly interpreted. An alternative method of detecting coupling is described in Section III.2.3.3.

FIGURE III.9

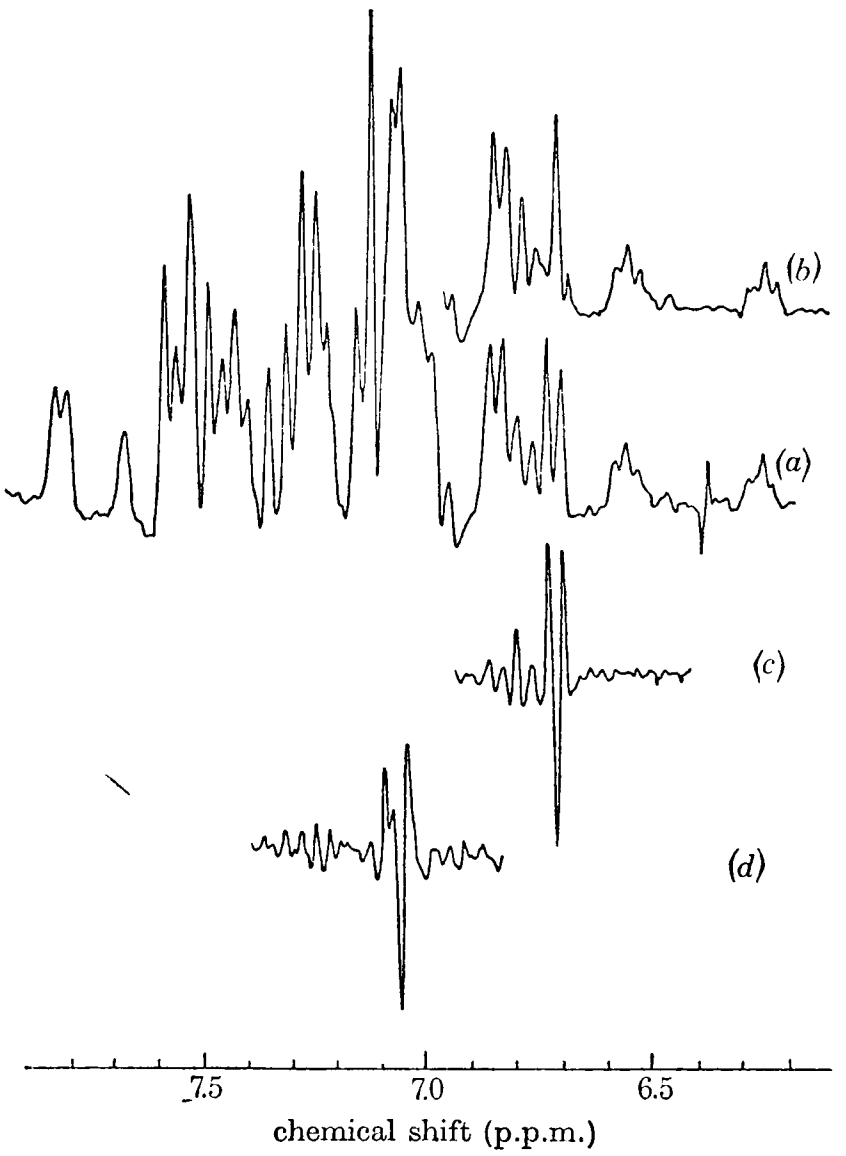

Spin-decoupling difference spectra. (a) Low field part of the spectrum of 10mM lysozyme, pH 4.0 at 68^{o}C. Irradiation at 6.4 ppm causes no change in the spectrum. (b) irradiation at 7.05 ppm causes decoupling at 6.71 ppm. (c) spectrum (a) minus spectrum (b). (d) difference between spectrum (a) and a spectrum obtained whilst irradiating at 6.71 ppm.

III.1.6 Chemical Difference

If the spectrum of a molecule which has been chemically modified is subtracted from the spectrum of the unmodified molecule, the spectral changes due to the modification are observed. A particularly simple case is chemical replacement of hydrogen atoms by deuterium atoms as already mentioned. It is possible to make more substantial modifications, for example to specific side-chains of proteins. Also, proteins of slightly different sequence may be available. The interpretation of the observed changes however becomes more difficult as the complexity of the modification increases. No modifications other than deuteriation are discussed in this work.

III.1.7 Pulse Methods and Difference Spectroscopy

At present the spectra to be subtracted have always been assumed to be direct spectra. It is however possible to add or subtract spectra accumulated using a pulse sequence. It will be shown below that, by these means, considerable spectral simplification can be achieved without the need for an induced spectral perturbation. Differences between the intrinsic relaxation times and multiplet structure of individual resonances are made use of in these methods.

III.1.8 Combinations of Methods

In some cases it is desirable to use several types of difference spectroscopy at the same time. In particular, convolution difference may be combined with any of the other forms of difference spectroscopy (see for example Fig. III.9) or with pulse sequences.

III.2 Pulse Methods

III.2.1 Types of Pulse

In the category of pulse methods are included all techniques which require the application of more than one pulse of rf power. Some details of pulsed nmr are given in Appendix B. A pulse of rf power may be characterised by (i) frequency (ii) power and (iii) length of time applied (pulse length).

The pulse may be defined in terms of its effect on the net magnetisation of a nuclear resonance. Thus, for example, a 90^{o} pulse usually tips the net magnetisation from the magnetic field direction (z) through 90^{o} into the xy plane. The angle through which the magnetisation is tipped depends on the applied power (H_1) and on the pulse length (τ), for a 90^{o} pulse $\frac{\pi}{2}=\gamma H_1 \tau$ (Farrar and Becker, 1971). Now, consider a 90^{o} pulse. This can be achieved either by high power and a short pulse length or by low power and a long pulse length. The rf pulse is applied for a finite time, and so the frequency is not defined exactly, and may be considered as a band of frequencies around the value chosen. The effective range of this band is proportional to $1/\tau$ for a 90^{o} pulse. Thus, a short pulse is non-selective, whilst a long pulse is selective and can be used to selectively tip the magnetisation of resonances occurring in a narrow frequency range. A 100 msec pulse has a spread of about 10Hz. In the normal pulsed nmr spectrometer, the non-selective pulse applied in the conventional FT experiment is ca. 10μ sec. To summarise, the types of pulses are:

(i) High power, short pulse length. These pulses are non-selective and are used for the normal FT experiment. By adjusting the pulse length, for a given power, non-selective 90^{o} and 180^{o} pulses are generated for T_1 and T_2 sequences.

(ii) Low power, long pulse length. This pulse is used for a selective tip of the magnetisation of selected nuclear spins. Selective 90^{o} and 180^{o} pulses may be generated. Pulses of this type are used for spin-decoupling, and other forms of double resonance.

III.2.2 Multiple Resonance

The key to the experiments described in this section is that the selective irradiation pulse required for spin-decoupling or to obtain a nuclear Overhauser effect may be applied in two ways. These are the time shared and the gated pulse methods illustrated in Fig. III.10.

The time shared method (Jesson et al. 1973) involves the application of a pulse of the required frequency for short time periods in between data acquisition points. This is approximately equivalent to a continuous (and selective) application of rf power provided that the individual flip angles are small (Pines and Ellet, 1973). This method therefore gives rise to Bloch-Siegert shifts, but is the usual means of causing spin-decoupling in FT experiments.

The gated pulse method has previously been used in ^{13}C spectroscopy (Freeman and Hill, 1971b; Freeman et al., 1972). Here, a selective pulse (of length say 0.5 sec) is applied (Schaefer, 1972), just before the usual non-selective pulse (of length say 10μ sec), as shown in Fig. III.10. This gated pulse can result in no Bloch-Siegert shifts or decoupling, but can cause nuclear Overhauser effects or cross-saturation. The fall-off of the latter effects depends on the T_1 relaxation processes which are generally long (>0.1 sec) compared to the delay between the selective and non-selective pulses (ca. 100 μsec). Some applications of these pulse methods developed in

FIGURE III.10

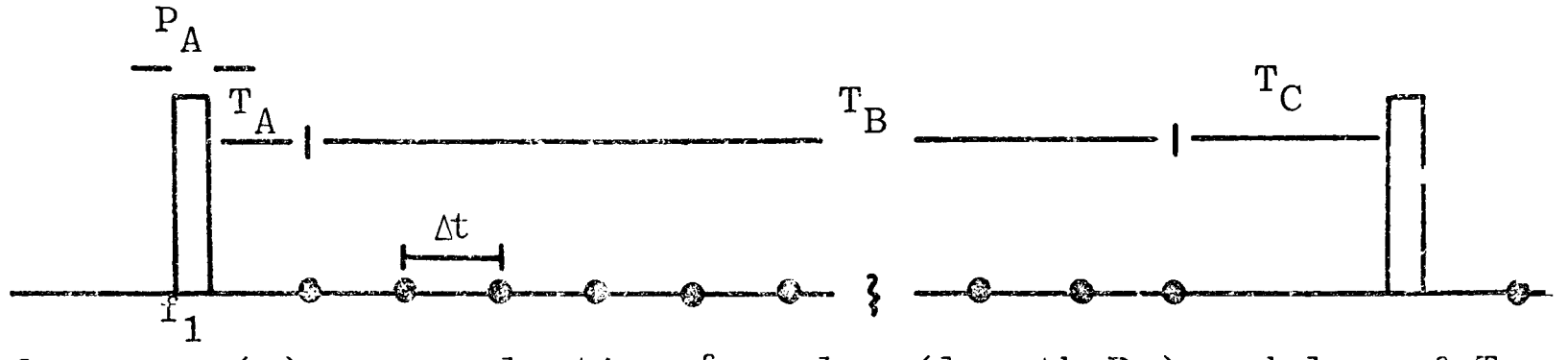

Sequence (a): non-selective f_1 pulse (length P_A); delay of T_A; accumulation for a time T_B, sampling magnetisation at intervals Δt; delay of T_C; repeat.

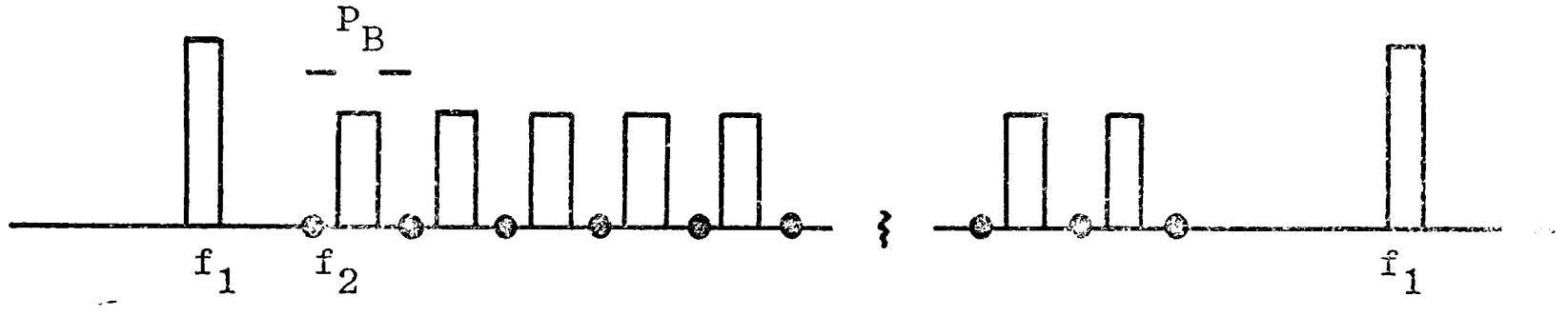

Sequence (b): as (a) but selective f_2 pulses (length less than Δt) applied in between sampling times.

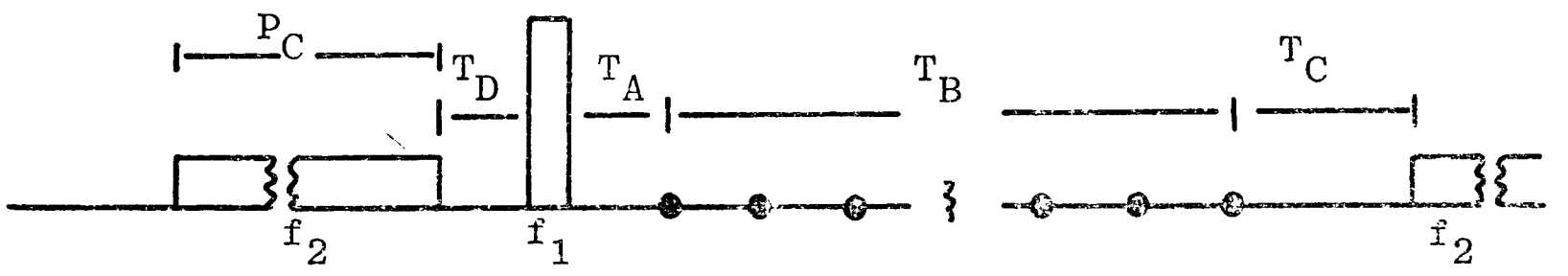

Sequence (c): as (a) but selective f_2 pulse (length P_C) and delay T_D applied before f_1.

Illustration of (a) normal FT, (b) time-shared irradiation, (c) gated irradiation. For observing (i) decoupling and NOE, sequence (b) with $T_C = 0$; (ii) decoupling but no NOE, sequence (b) with $T_C > 5T_1$; (iii) NOE but no decoupling, sequence (c) with $T_D << T_1$.

the present work will now be considered.

III.2.2.1 Separation of nuclear Overhauser and spin-decoupling effects

The pulse sequences used to separate spectral changes due to the nuclear Overhauser effect (which arises from selective saturation of transitions in a spin system coupled through a through-space dipolar relaxation mechanism) from decoupling effects (which arise from selective saturation of transitions in a spin system coupled through a scalar interaction of nuclear magnetic moments via the electrons in the adjoining bands) make use of the different timescales of the effects. After the application of rf power, the magnitude of the observed nuclear Overhauser effect decays at a rate dependent on the T_1 of the coupled transitions. The decoupling effect decays effectively instantaneously. Thus, the pulse sequences illustrated in Fig. III.10 may be used to separate the two effects, as is illustrated in Fig. III.11.

Fig. a shows a small part of the spectrum of lysozyme. The resonance at 6.28 ppm is a triplet and has an area corresponding to one proton. It is shifted by ring current effects outside the main envelope of aromatic proton resonances and is thus easy to observe. The 6.28 ppm triplet can be shown to be spin-spin coupled to a doublet at 6.76 ppm and a triplet at 6.82 ppm (Section V.2.2). The triplet at 6.82 ppm is also coupled to a doublet at 7.76 ppm. These decoupling experiments confirm that these resonances are from the benzenoid ring of a tryptophan residue. Since the two resonances coupled to the observed peak at 6.28 ppm are close together, time-shared irradiation at 6.8 ppm can be used to saturate these two resonances and to totally decouple the triplet resonance (Fig. b). The area of

FIGURE III.11

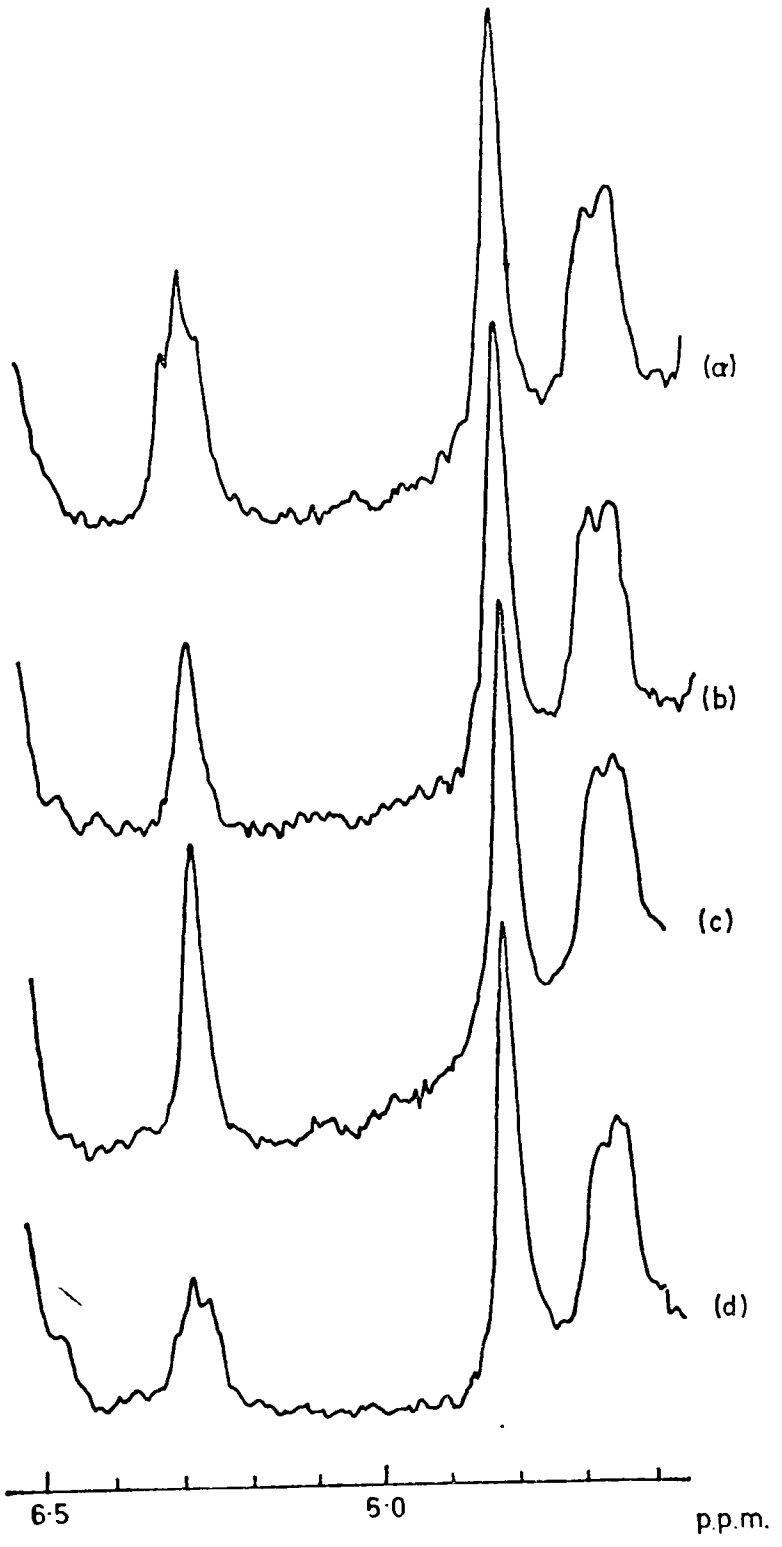

(a) Part of the spectrum of 10mM lysozyme, pH 4.0, 68^{o}C.

(b) The effect of continuous time-shared irradiation at 6.8 ppm.

(c) The effect of time-shared irradiation with a delay of 5 sec between pulses. Only the decoupling effect is observed.

(d) The effect of gated decoupling. Only the nuclear Overhauser effect is observed.

the triplet resonance is reduced by 45 $\pm$ 10% in this experiment, whilst other nearby resonances are unaffected. Irradiation at positions other than 6.8 ppm causes no decoupling or area change at 6.28 ppm. Fig. c shows the spectrum decoupled but without an Overhauser effect. The area of the 6.28 ppm resonance is the same in figures a and c within experimental error ($\pm$ 10%). A spectrum showing the Overhauser effect, without decoupling is shown in Fig. d. The area of the 6.28 resonance in this figure is 55 $\pm$ 10% less than that in figure a. In Chapter VIII the interpretation of this result is discussed.

The observation of the large negative enhancement parameters may be particularly valuable when macromolecules larger than lysozyme are studied. In such systems the spin-coupling is unlikely to be observable and the Overhauser effects would then have to be used for assignment purposes.

III.2.2.2 Solvent Suppression

The concentration of protons in 90% H_2O is 100M whilst the concentration of the protein is 5×10^{-3}M in the experiments to be described. Detection of the protein resonances in the presence of 90% H_2O thus requires a dynamic range of 20,000:1. This is beyond the range of virtually all known detectors. It is thus necessary to avoid selectively the excitation of the water resonance. This has previously been achieved by using conventional continuous wave techniques (Dadok and Sprecher, 1974), stochastic resonance (Tomlinson and Hill, 1973) and null methods which depend either on differential relaxation (Patt and Sykes, 1972) or on a certain amplitude of radio-frequency pulse (Redfield and Gupta, 1971). However, all the spectra using H_2O solvent reported in this thesis were obtained by suppressing the H_2O resonance using Fourier transform double

resonance methods. The selective irradiation at the H_2O frequency was applied using either the time shared method or preferably using the gated method.

Fig. III.12 shows a spectrum of hen lysozyme in H_2O, accumulated using the long pulse method. The residual H_2O resonance is smaller than that observed when the protein is dissolved in 99.8% D_2O and the spectrum accumulated in the normal way. Distortion in the spectrum is negligible, and resonances close to the H_2O resonance may be observed readily. This is in itself a considerable improvement over continuous wave spectroscopy. The signal-to-noise ratio is as good as that for a spectrum of an equivalent sample in 99.8% D_2O, as is the resolution. All forms of difference spectroscopy may be used in conjunction with this technique. Difficulties however will arise if the T_1 of the H_2O resonance is very much reduced, for example by high concentrations of a paramagnetic ion. The power required for saturation would then be excessive.

One advantage of the long pulse method is that resonances coupled to other resonances in the region of the H_2O peak will not be decoupled, although any Overhauser and cross-saturation effects will be observed. This is not generally a serious problem but the intensity of some exchangeable NH protons (exchanging with the H_2O) may be decreased by cross saturation (Glickson et al., 1974).

III.2.2.3 Triple Resonance

One disadvantage of running spectra in H_2O solution was that spin-decoupling experiments could not easily be performed. This is of particular annoyance because assignment of the NH protons is therefore very difficult. The problem of irradiating α-CH resonances in peptides to decouple the peptide

FIGURE III.12

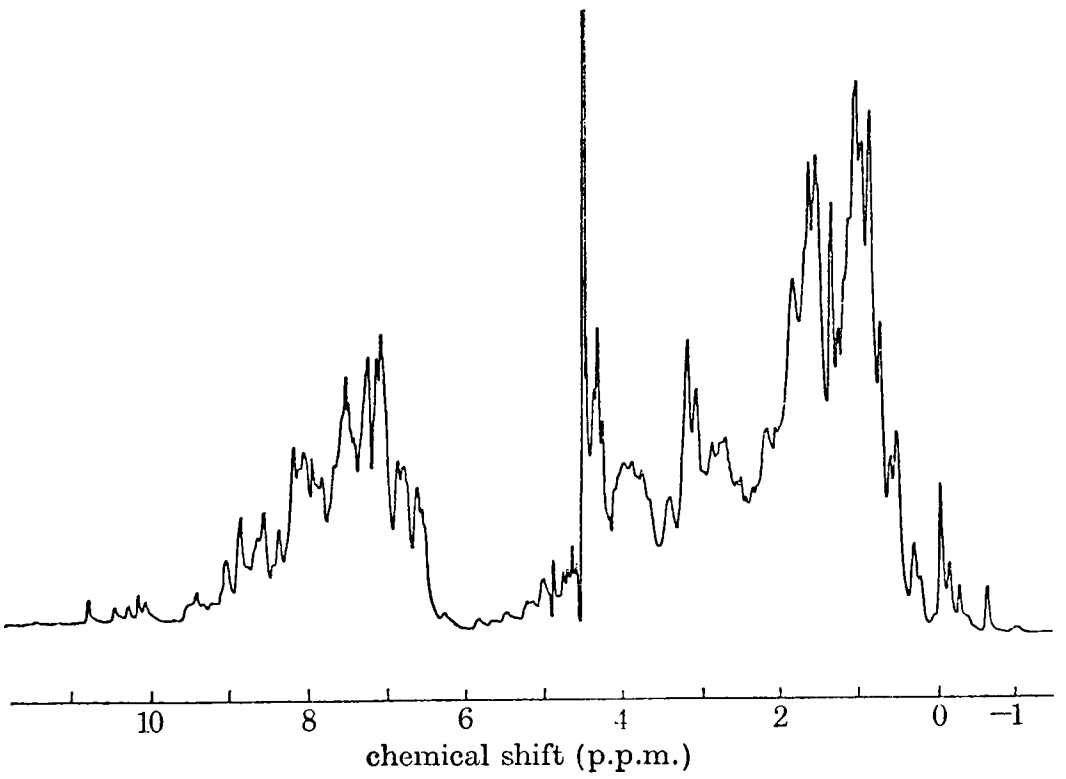

Spectrum of 5mM lysozyme in 90% H_2O, 10% D_2O at pH 3.2, 54°C. The H_2O resonance was saturated by a selective gated pulse of length 0.4 sec, finishing 80 μsec before the non-selective pulse. The overall repetition time was 1.1 sec, and 2048 scans were accumulated.

FIGURE III.13

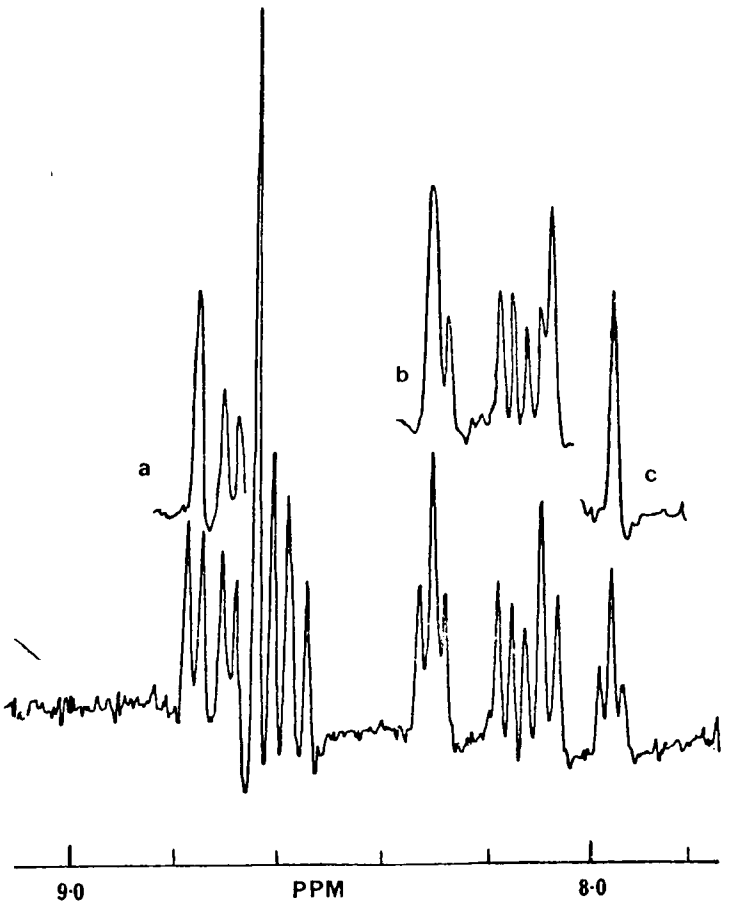

Pulsed triple resonance. Decoupling of the peptide NH proton resonances of the polypeptide bacitracin. The lower trace shows part of the CD spectrum of 20mM bacitracin in 90% H_2O, 10% D_2O, pH 3.2, 20°C. (a) The decoupling of a doublet at 8.73 ppm caused by irradiation at 4.71 ppm. (b) Effect of irradiation at 4.20 ppm. (c) Effect of irradiation at 3.23 ppm. The H_2O resonance was suppressed as described for Fig. III.12.

NH resonances has been discussed for continuous wave spectroscopy by Dadok et al. (1972). It was shown that careful detuning of the amplification network in their spectrometer allowed irradiation to be used. This method is difficult, does not permit FT experiments, and does not allow simultaneous observation of the whole spectral region.

However, once the solvent has been suppressed, as described here, normal hormonuclear decoupling methods can be applied by applying another pulse. This third frequency (f_3 where f_1 is the non-selective pulse frequency and f_2 the solvent saturation frequency) has been applied using a time-shared pulse. The frequency f_3 was derived from a Schomandl frequency synthesiser. In order to prove the success of this technique, the decoupling of peptide NH resonances of a polypeptide, bacitracin, are shown in Fig. III.13.

III.2.3 Non-selective Pulse Sequences

Non-selective pulse sequences, involving short pulses of high power, have been used to measure relaxation times. In this work these measurements have been made on lysozyme, but the pulse sequences have also been developed for spectral simplification. This spectral simplification has been achieved by making use of intrinsic differences in relaxation times or in spin-spin coupling. Each case will be treated separately.

III.2.3.1 Relaxation Times

T_1 values were readily measured by using a 180°-τ-90° pulse sequence (Farrar and Becker, 1971). The recovery of equilibrium magnetisation in the z direction following the complete inversion caused by the 180° pulse is measured by recording spectra at different values of the time τ. Then, for each peak a

plot of log (h_o-h) against τ is linear, h being the observed peak height at time τ, and h_o being the peak height following a 90° pulse only. T_1 is obtained from $t_{1/2}$ ($t_{1/2}$ is the time taken for (h_o-h) to fall to half its value). For any first order process, $t_{1/2} = \ln 2/k_1$, and as T_1 is defined as the reciprocal of the rate constant (k_1), $T_1 = t_{1/2} / \ln 2$. Values for lysozyme are given in Chapter VIII. Only small differences between T_1 values of resonances of a given class of proton (e.g. of methyl groups) exist. T_1 pulse sequences are thus not very valuable for spectral simplification on the basis of differential T_1 values.

T_2 values were measured using the Carr-Purcell sequence with the Meiboom-Gill modification (Farrar and Becker, 1971). This sequence is denoted by $90^\circ_{x'}$, τ, $(180^\circ_{y'}, 2\tau)_n$ $180^\circ_{y'}$, τ [measure]. The x' and y' subscripts refer to the application of a 90° phase shift between the 90° and 180° pulses in the Meiboom-Gill manner. Provided τ is small (less than 10 m sec, generally 1 m sec) spectra recorded at different values of T (defined as $(n+1)2\tau$, i.e. the total time between the 90° pulse and the measurement of magnetisation) can be used to measure T_2. Here, a plot of log (h) against T is used to measure $t_{1/2}$, the time taken for the observed peak height at time T (h) to fall to half its value. Then, $T_2 = t_{1/2} \cdot \ln 2$. Values of T_2 for lysozyme are given in Chapter VIII. One application of this pulse sequence is to remove broad resonances from the spectrum. This is illustrated in Fig. III.14. After T = 0.1 sec, the resonances of NH protons, which have short T_2 values because of the quadrupolar relaxation effect of ^{14}N are essentially eliminated from the spectrum, whilst the resonances of CH protons with longer T_2 values are still clearly observed. This will be

FIGURE III.14

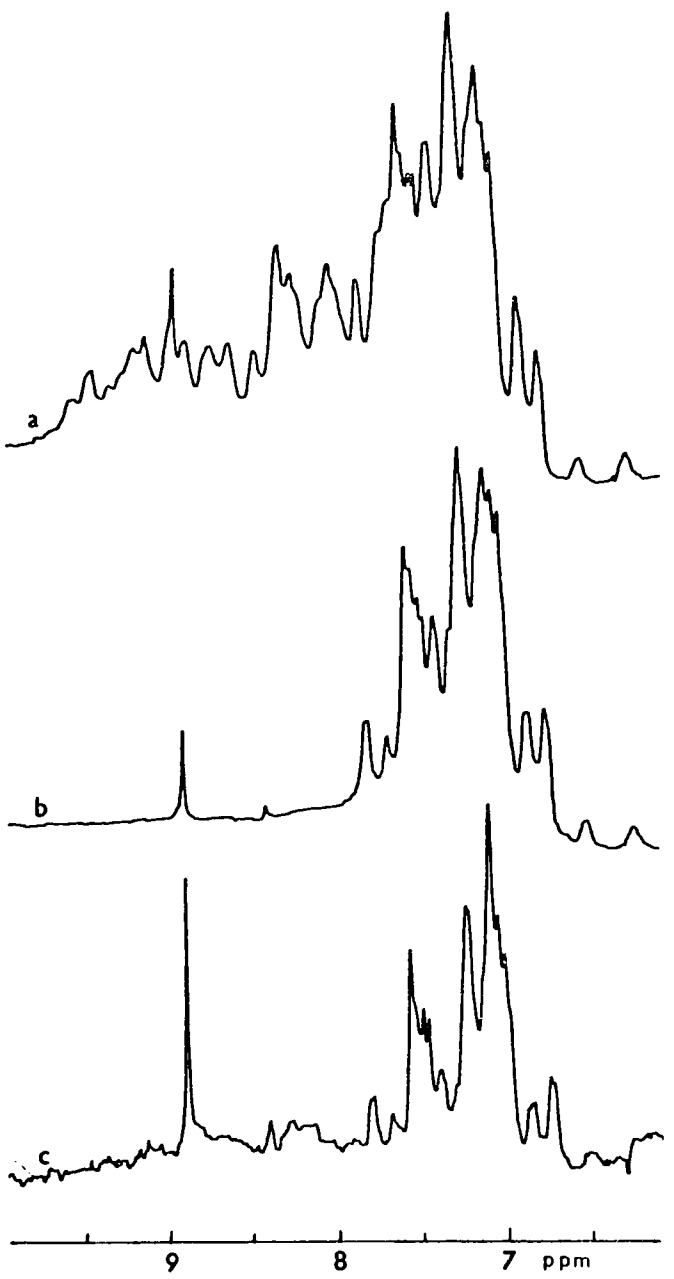

Low field region of the lysozyme spectrum. (a) normal spectrum of lysozyme freshly dissolved in D_2O; (b) as (a) but after exchanging the NH proton resonances by heating to $80^{o}C$; (c) spectrum obtained of sample corresponding to (a) using CPMG sequence with T = 90 msec, τ = 1 msec. 5mM lysozyme, pH 4, $54^{o}C$.

of particular value for large proteins where the NH resonances cannot be removed by exchange methods. It seems likely also that this pulse sequence will permit the observation of the sharp resonances of surface histidine and other groups of large proteins. However, in lysozyme little useful spectral simplification other than that of the NH resonances has been achieved. One potential application is however to observe separately the sharp resonances of a small molecule such as an inhibitor in the presence of a large one, such as a protein.

III.2.3.2 Multiplet Selection Techniques

If, instead of using a train of n 180^{o} pulses in the Carr-Purcell-Meiboom-Gill (CPMG) method a single 180^{o} pulse is used, a very different result is obtained. This pulse sequence is then $90^{o}_{x'}$, τ, $180^{o}_{y'}$, τ [Measure], which is here called the Carr-Purcell method A (CPA), and the behaviour of resonances as τ is varied depends on their multiplet structure and coupling constants (Freeman and Hill, 1975). For a singlet resonance, the intensity decays as a function of τ as in the CPMG sequence. For a doublet resonance, the phase of the two components varies with τ. When $T = 1/J$ ($T = 2\tau$) the components are 180^{o} out of phase with the singlet, and at $T = 2/J$ they are in phase and so on. For triplet resonances, the centre component behaves as a singlet, but the outer components are 180^{o} out of phase at $1/2J$ and in phase at $1/J$, and so on. This behaviour follows directly from a consideration of the precession of the components of each multiplet. Thus, the coupling of resonances may be investigated using this sequence. However, a particular application is to observe selectively resonances of given multiplet structure. Consider the aromatic region of a protein. To a first approximation, the resonances at first order are

either singlets, or doublets or triplets with J = 8.5 $\pm$ 0.5 Hz. Secondary couplings are less than 2Hz, and are neglected here. Thus, by setting T = 1/8.5 = 0.12 secs doublets are totally inverted (see Fig. III.15), whilst triplets and singlets are normally in phase. If, for the same value of T_1 the CPMG pulse sequence is used, all peaks are in phase. Thus, by addition and subtraction of these spectra it is possible to observe separately doublet or singlet and triplet resonances (Fig. III.15). Thus this sequence gives considerable spectral simplification. Of course, the areas of resonances in the spectra will depend on their T_2 values. Similarly the methyl group resonances are singlets or doublets and triplets, with J values of 6.5 $\pm$ 1.0 Hz. Thus T = 0.155 sec should be used here. A variety of other methods for performing these experiments has been briefly investigated. For example, addition and subtraction of spectra using the CPA method but different values of T (e.g. T = 1/2J and 3/2J) is effective. Also, use of the CPMG method at values of n which give τ in the region of 10-20 msec is interesting, and doublet resonances may be effectively removed from the spectrum by this method. All these possibilities for multiplet selection deserve further study.

III.2.3.3 Spin Echo Double Resonance

The dependence of the phase of different multiplets is the key to this method of detecting coupling. If selective irradiation is applied in the CPA sequence during the period between the 90° pulse and the start of data acquisition, the multiplicity and thus the phase of the coupled resonances can be changed. The observed multiplicity, however, is that of the original spectrum since the irradiation is not applied during data acquisition. Only the phase is observed to be changed.

FIGURE III.15

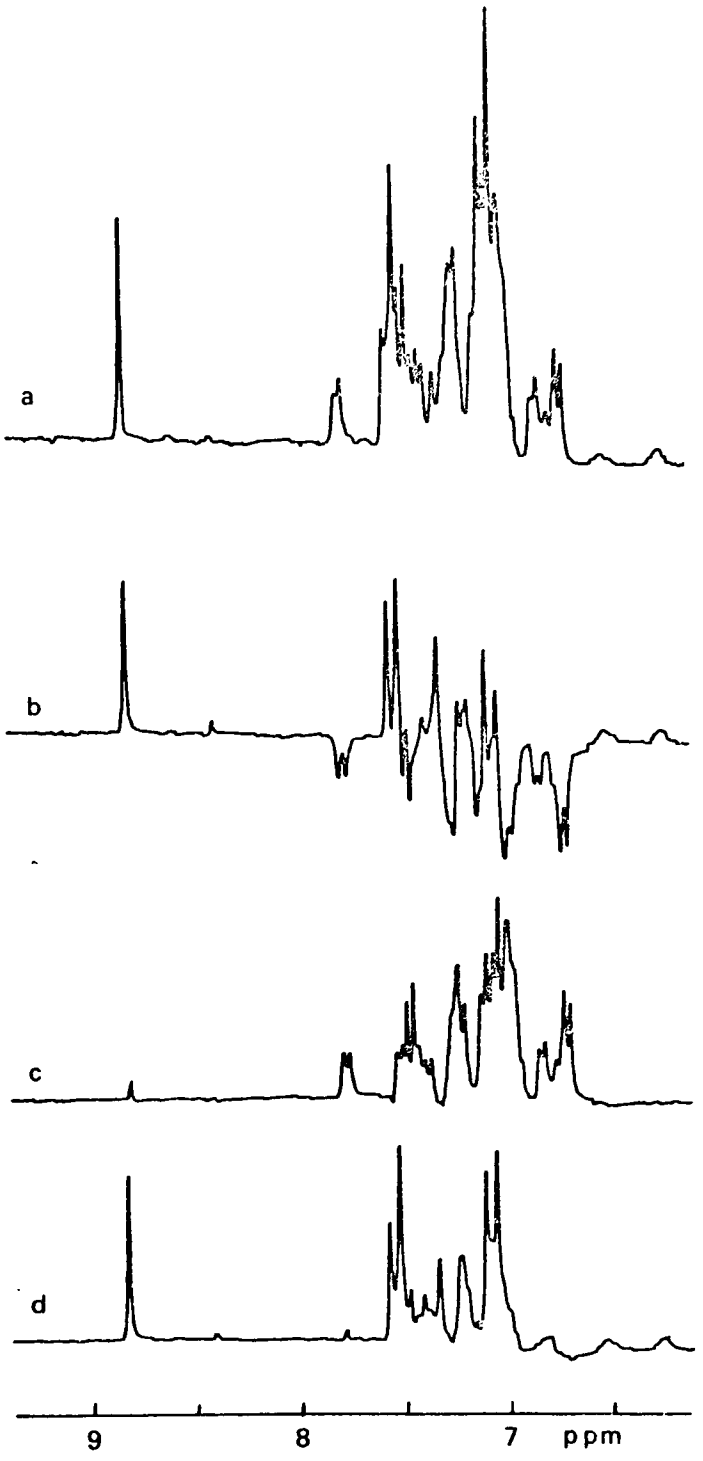

Illustration of multiplet selection. (a) low field region of lysozyme spectrum obtained with CPMG sequence, T = 120 msec, τ = 1 msec. (b) spectrum of same sample using CPA sequence, T = 120 msec, τ = 60 msec. The doublet resonances are inverted. (c) spectrum (a) minus (b) showing doublet resonances only. (d) spectrum (a) plus (b) showing singlet and triplet resonances. 5mM lysozyme, pH 4, 54^{o}C.

FIGURE III.16

Low field region of spectrum of 20mM tryptophan plus 1mM Pr^{3+} in D_2O, pH 5. (a) normal spectrum; (b) spectrum obtained using CPA sequence, T = 118 msec, τ = 59 msec; (c) as (b) but with selective irradiation applied at the frequency of the low field doublet during the 118msec pre-acquisition period; (d) the difference (b) minus (c); (e) the difference between spectrum (a) and a spectrum accumulated whilst irradiating the low field doublet in the usual time-shared mode (cf. Section III.1.5).

This is indicated in Fig. III.16 for tryptophan. Spectrum (a) shows the normal spectrum and (b) the spectrum obtained using the CPA sequence with T = 118 msec (as J ≃ 8.5 Hz for all coupled resonances). Irradiation of the low field doublet in the pre-acquisition period causes inversion of the phase of the high field triplet (spectrum (c)), since during the irradiation time this resonance behaves as a doublet. The difference spectrum (d) contains a positive peak with an area twice that of the original triplet. If a doublet is collapsed to a singlet during the pre-acquisition period, the difference spectrum contains a negative peak. This type of double resonance method has considerable potential in protein spectra, and has advantages over the continuous decoupling method illustrated in spectrum (e).

References for Chapter III

Balaram, P., Bothner-By, A.A. and Dadok, J. (1972). J.Amer. Chem. Soc. 94, 4015.

Bloembergen, N.J. (1957), J. Chem. Phys. 27, 572.

Bradbury, J.H. and King, N.L.R. (1971), Nature, 229, 404.

Campbell, I.D., Dobson, C.M., Jeminet, G.J. and Williams, R.J.P. (1974), FEBS Lett. 49, 115.

Campbell, I.D. and Freeman, R. (1973), J. Magnetic Resonance 11, 143.

Coates, H.B., McLauchlan, K.A., Campbell, I.D. and McColl, C.E. (1973), Biochim. Biophys. Acta 310, 1.

Dadok, J. and Sprecher, R.F. (1974), J. Magnetic Resonance 13, 243.

Dadok, J., Von Dreele, P.H. and Scheraga, H.A. (1972), J.C.S. Chem. Comm., 1055.

Ernst, R.R. (1966), in Advances in Magnetic Resonance (Waugh, J.S. ed.), Academic Press (N.Y.), 1.

Ernst, R.R., Freeman, R., Gestblom, B.O. and Lusebrink, T.R. (1967), Molec. Phys. 13, 283.

Farrar, T.C. and Becker, E.D. (1971), Pulse and Fourier Transform NMR, Academic Press (N.Y.)

Freeman, R. and Hill, H.D.W. (1971a), J. Magnetic Resonance 4, 366

Freeman, R. and Hill, H.D.W. (1971b), J. Magnetic Resonance 5, 278

Freeman, R. and Hill, H.D.W. (1975), in Dynamic Nuclear Magnetic Resonance Spectroscopy (Jackman, L. and Cotton, F.A. eds.), Academic Press (N.Y.), 131.

Glickson, J.D., Dadok, J. and Marshall, G.R. (1974), Biochemistry 13, 11.

Hoffmann, R.A. and Forsén, S. (1966) in Progress in NMR Spectroscopy (Emsley, J.W., Feeney, J. and Sutcliffe, L.H. eds.), Pergamon Press, 15.

Imoto, T., Johnson, L.N., North, A.C.T., Phillips, D.C. and Rupley, J.A. (1972), in The Enzymes (3rd Ed.) (Boyer, P.D. ed.), Academic Press (N.Y.), 666.

Jesson, J.P., Meakin, P. and Kneissel, G. (1973), J. Amer. Chem. Soc. 95, 618.

Noggle, J.H. and Schirmer, R.E. (1971), The Nuclear Overhauser Effect, Academic Press (N.Y.).

Patt, S.L. and Sykes, B.D. (1972), J. Chem. Phys. 56, 3182.

Pines, A. and Ellet, J.D. Jr. (1973), J. Amer. Chem. Soc. 95, 4437

Redfield, A.G. and Gupta, R.K. (1971), J. Chem. Phys. 54, 1418.

Schaefer, J. (1972), J. Magnetic Resonance 6, 670.

Seiter, C.H.A., Feigenson, G.W., Chan, S.I. and Ming-chu Hsu (1972), J. Amer. Chem. Soc. 94, 2535.

Solomon, I. (1955), Phys. Rev. 99, 559.

Swift, T.J. and Connick, R.E. (1962), J.Chem. Phys. 37, 307.

Tomlinson, B.L. and Hill, H.D.W. (1973), J.Chem.Phys. 59, 1775.

CHAPTER IV

ASSIGNMENT OF THE SPECTRUM - DEVELOPMENT OF A SCHEME

IV.1 Introduction

In this Chapter, a strategy for the assignment of protein nmr spectra is developed. This strategy is general, but will be illustrated by specific examples to the proton spectrum of lysozyme. The actual assignment of the lysozyme spectrum is however dealt with in Chapter V.

For a small molecule, the principles of assignment are well known (Pople et al., 1959), although not always easy to apply. Generally, measurement of chemical shift values, peak areas, multiplet structure, and the application of decoupling methods are sufficient for total assignment. The assignment process does require, or itself leads to, a knowledge of the molecular structural formula. Occasionally, supplementary information is required to distinguish between a small number of different possible assignment schemes. For example, comparison of the spectra of similar chemical species may be carried out, or use made of a paramagnetic probe.

Unfortunately, methods used previous to this work for assignments of protein spectra are not at all rigorous. This situation arose for two reasons. First, very few resonances could be resolved, and the multiplet structure was not observable. This meant that no decoupling experiments were performed. Secondly, distinction between a large number of chemically identical groups has to be made (for example, there are 12 alanine residues in lysozyme). This means in practice that distinction between these resonances must be made by reference to the molecu-

lar conformation. In other words, for protein spectra the assignment process is intimately linked with knowledge not only of the molecular formula but also of the molecular conformation. The scheme put forward in this chapter aims to distinguish between the information concerning assignments which is independent of the conformation, and that which is dependent on the conformation. For this reason, the methods previously used for attempting assignment do not enter this scheme until a very late stage. These methods include ring-current shift calculations (Sternlicht and Wilson, 1967), pH titrations (Roberts and Jardetzky, 1970), chemical modification (Glickson et al., 1971), comparison of proteins from different species (Stellwagen and Shulman, 1973), and the use of paramagnetic probes (McDonald and Phillips, 1969).

The scheme put forward here is divided into four stages. These are (i) the resolution of resonances of individual nuclei; (ii) the assignment of an observed resonance to a type of proton (e.g. CH_3, NH); (iii) the assignment to a type of amino-acid residue, and (iv) the assignment to a specific residue in the sequence.

IV.2 The Resolution of Individual Resonances

The resolution problem is the result of too many resonances of finite linewidth occurring in too small a frequency range (see for example, Fig. IV.1). Solutions to the problem therefore lie in methods which increase the chemical shift range, decrease the linewidth or reduce the number of resonances observed at a given time.

IV.2.1 Shift range

One approach to protein nmr is to concentrate on

FIGURE IV.1

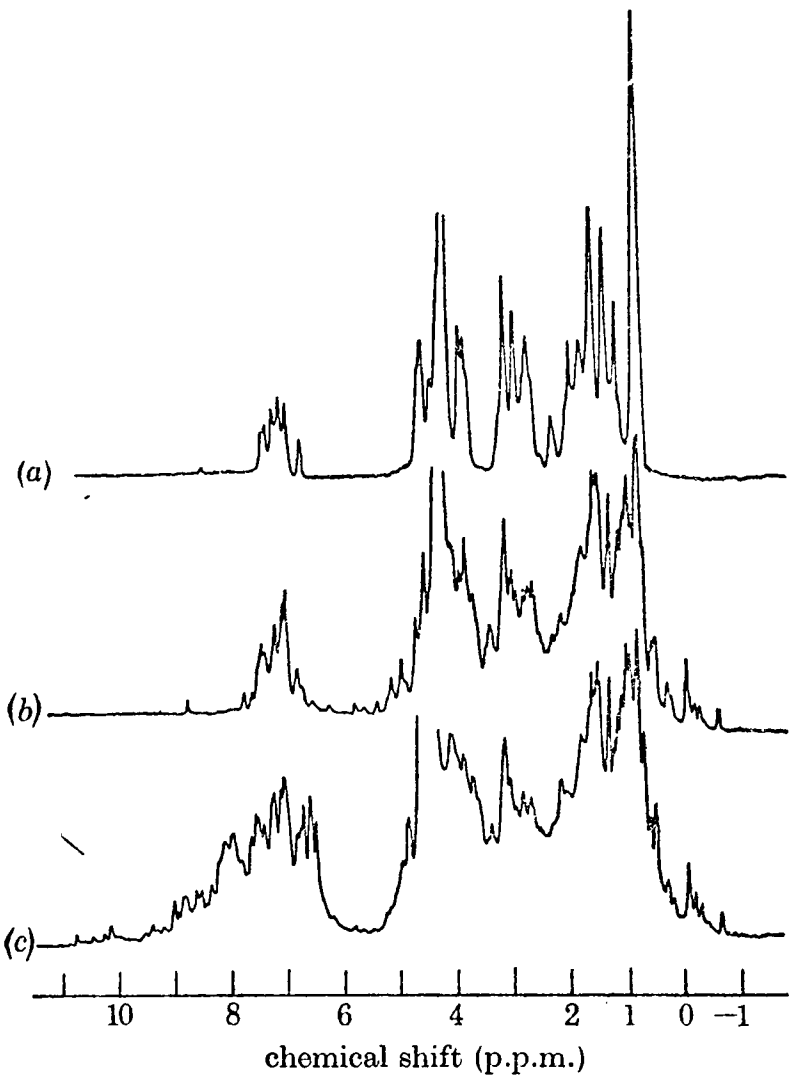

Spectra of 5mM lysozyme (a) in D_2O at 80°C; (b) in D_2O at 58°C and (c) in 90% H_2O, 10% D_2O at 58°C. In (c) the H_2O resonance has been saturated by the gated irradiation technique.

resonances which occur outside the main spectral envelope of resonances. Sometimes these resonances occur fortuitously; for example, the C(2) proton of histidine resonates at about 8.5 ppm at low pH and some methyl resonances are shifted to high field (above 0 ppm) by secondary shifts (see Fig. IV.1). In H_2O solvent the tryptophan indole resonances are also easily observed at about 10 ppm in Fig. IV.1. Resonances may also be shifted by a paramagnetic species and McDonald and Phillips (1969) showed that the addition of Co^{2+} to lysozyme shifted some resonances outside the main spectral envelope. This is a general method and lanthanide probes such as Eu^{3+} are even more effective. These shift methods are particularly important for separating overlapping resonances prior to spin-decoupling.

IV.2.2 Linewidths

The linewidths of the lysozyme resonances are of the order of 8 Hz in Fig. IV.1. These linewidths are mainly dominated by dipole-dipole interactions between proton neighbours, in the absence of a paramagnetic centre. Line narrowing is therefore brought about either by increasing the molecular motion by, for example, raising the temperature or by reducing the number of proton neighbours by, for example, extensively deuterating the protein (see Crespi *et al.*, 1973). In certain cases lines are also broadened by some sort of exchange process; line narrowing can then be brought about by speeding up the rate of exchange, e.g. by adding buffer to carbonic anhydrase (Campbell *et al.*, 1974) or by preventing the exchange, e.g. by adding an inhibitor to lysozyme (Chapter VIII).

Having achieved the most favourable condition, the observed linewidth of an isolated resonance can be further reduced by up to about a factor of two by using the method of convolution

difference (Section III.1.1). In a spectrum of overlapping peaks this method also discriminates against broad peaks and changes the observed lineshape, thus making it much easier to observe sharp peaks and to measure precise chemical shift values.

IV.2.3 Reduction of the Number of Resonances

An effective resolution enhancement method is to alter the chemical composition of the protein to allow certain resonances to be observed more easily. The number of ^{1}H atoms may be reduced by selective deuteriation (for example, Crespi *et al.*, 1973); the ^{13}C signal from one particular type of amino acid may be increased by selective enrichment (for example, Hunkapillar *et al.*, 1973) or a new nucleus may be introduced into the protein (for example, Sykes *et al.*, 1973). These chemical modification methods also reduce the assignment problems and their use and importance will no doubt increase, although the synthetic chemistry can become difficult and one may be limited to macromolecules from bacteria.

The methods of which most use have been made in this work are, however, all based on difference spectroscopy or on pulse sequences. These have been fully described in Chapter III. Once an observed resonance has been resolved as well as possible, the assignment itself can be considered.

IV.3 Assignment to a Type of Proton

The first classification is to assign a resonance to an hydrogen attached to a carbon atom or a nitrogen atom. Even in H_2O solvent -OH and -SH protons are not generally observed because their solvent exchange rate is too rapid. Those resonances which are not observed after exchange in D_2O has been carried out are of -CH protons. Those observed only in H_2O solvent, or in

D_2O before exchange are of -NH protons (see Section III.1.4).

In small molecule systems, further assignment to a type of proton can generally be done directly from chemical shift values (see tables in for example Pople *et al.*, 1959). The secondary (ring current) shifts which accompany the folding of a globular protein such as lysozyme (Fig. IV.1) make this process more difficult. However, provided large induced shifts from a group such as haem are not involved, the following guidelines may be laid down as the secondary shifts are generally less than 1 ppm.

IV.3.1 Exchangeable Hydrogens

(a) A resonance of an exchangeable proton can be assumed to arise from an NH group. These resonances are generally observed below 6 ppm.

(b) A resonance to very low field (below 12 ppm) may be assigned to an imidazole NH proton, and therefore arises from histidine. This assignment is made firm where a titration with pH can be observed (Patel *et al.*, 1971; Robillard and Shulman, 1972).

(c) A resonance between 9.5 and 11 ppm may be assigned to the N(1)H proton of indole, and therefore arises from tryptophan. This assignment may be made firm by associating the resonance with the corresponding singlet C(2)H resonance.

(d) Resonances close to 7.0 ppm which arise from rapidly exchanging protons may be assigned to guanidino (arginine) or amide NH protons.

(d) Resonances between 7.0 and 9.5 ppm may be assigned to peptide NH protons. This assignment becomes rigorous if the coupling to non-exchangeable resonances of α-CH protons can be proved by spin-decoupling.

IV.3.2 Non-exchangeable Hydrogens

Resonances which persist in the pmr spectrum even after rigorous exchange processes may be assigned to CH protons. If rigorous exchange procedures cannot be applied, some distinction can be made on the basis of T_2 values using the Carr-Purcell sequences (Section III.2.3). NH resonances are considerably broader (have a shorter T_2) than CH resonances. Using the known chemical shift values and multiplet structure of different types of proton resonance, it is possible to proceed as follows:

(a) A single resonance of three proton intensity with a chemical shift value between 3.0 and -1 ppm may be assigned to a methyl group. The resonance will be a singlet or a doublet or triplet with $J = 6.5 \pm 1$ Hz.

(b) A resonance between 6 and 9 ppm probably arises from an aromatic proton. This is confirmed by the observation of singlet or doublet or triplet multiplet structure with $J = 8.5 \pm 1$ Hz, (if first order), the coupled resonance also falling into this same category.

(c) Any resonance coupled to an exchangeable peptide NH resonance may be assigned to an α-CH resonance. The chemical shift value is usually 4 to 6 ppm.

(d) Any resonance which does not fall into any of the above categories arises from an aliphatic CH or CH_2 proton.

IV.4 Assignment to a Type of Amino Acid

The observation of coupling between α-CH resonances and peptide N-H resonances (see Fig. III.8) means that assignment to all types of amino acids may be possible from studies of these resonances. However, at the present time a limitation to aromatic amino acids and the amino acids containing methyl groups is

generally made in this thesis. This limits the resonances to those of the NH protons of tryptophan and histidine; the aromatic CH protons of histidine, tryptophan, tyrosine and phenylalanine; the CH_3 groups of methionine, leucine, isoleucine, valine, alanine and threonine, and the CH resonances coupled to these CH_3 resonances.

The parameters of the resonances of the five amino acids containing aromatic side chains and the six containing methyl groups are summarised in Tables IV.1 and IV.2. All of these resonances can be shifted from the primary positions shown by ring current or other secondary effects in a folded protein. These secondary shifts allow two amino acids of the same kind to be distinguished but do not allow us to use the primary shift positions alone to make assignments, except in a few cases where the primary shifts are rather unusual.

There are a few selective methods available for identifying a particular amino acid. The best of these is the identification of the C(2)H and C(4)H proton resonances of histidine by the upfield shift which occurs on ionisation of the histidine side chain (see Table IV.2 and, for example, Roberts and Jardetzky, 1970). Another group which may ionize in an accessible pH range is tyrosine (see Table IV.2). Other selective binding reagents exist in addition to the proton; for example, $PtCl_4^{2-}$ has been used to identify a methionine resonance (Sadler et al., 1974).

However, the most important assignment aid is undoubtedly the observation of multiplet structure and the interrelationship of various multiplets as determined by double resonance. As shown in Tables IV.1 and IV.2 the observed coupling constants in the proton resonances of amino acids are in the 5-9 Hz range. To observe either these multiplets or effects due to double resonance the inherent linewidth of the resonances must be less

TABLE IV.1

Characteristics of Methyl Group Resonances

Type of Amino Acid	No. of Methyl Groups	Multiplet Structure[c]	Chemical Shift (ppm)[a] Methyl Group	Coupled Resonance	Difference	J^b (Hz)
Ala	1	d	1.4	4.0	2.6	7.3
Thr	1	d	1.3	4.1	2.8	6.6
Met	1	s	2.1	None		
Ile	2	d	0.92	1.6	0.68	7.0
		t	1.0	1.4	0.4	7.3
Leu	2	d	0.92	1.6	0.68	6.5
		d	0.93	1.6	0.67	6.5
Val	2	d	0.96	2.3	1.34	7.0
		d	1.02	2.3	1.28	7.0

[a] Mainly from McDonald and Phillips (1969); Values are for a random coil protein.

[b] Variations may be $\pm$ 0.15 depending on conditions (see Roberts and Jardetzky 1970).

[c] Singlet (s), doublet (d), triplet (t).

TABLE IV.2

Characteristics of Aromatic Proton Resonances[a]

Type of Amino Acid	No. of Carbon Bound Protons	Expected[b] Multiplet Structure		Area of Multiplet	Chemical Shift (ppm)
His	2	s	C(4)	1	7.7[c]
		s	C(2)	1	8.8[d]
Phe	5	t	p	1	7.3
		t	m	2	7.3
		d	o	2	7.3
Tyr	4	d	o	2	6.9[e]
		d	m	2	7.2[f]
Trp	5	s	C(2)	1	7.2
		d	C(4)	1	7.5
		d	C(7)	1	7.5
		t	C(5)	1	7.1
		t	C(6)	1	7.1

[a] non-exchangeable protons only. Chemical shift data mainly from McDonald and Phillips, 1969.

[b] this multiplicity assumes (a) first order spectra, (b) rotation of tyr and phe (see text), (c) that only the larger coupling constants (ca. 8 Hz) are resolved. The proton from which the resonance arises is indicated (ortho (o), meta (m), or para (p) or by number).

[c] this value is for the protonated (low pH) form. At high pH the resonance shifts ca. 0.5 ppm upfield.

[d] as (c) but moves ca. 1.0 ppm upfield

[e] as (c) but moves ca. 0.3 ppm upfield

[f] as (c) but moves ca. 0.15 ppm upfield.

than twice the coupling constant (J). If the linewidth is greater than about J/2, the observed splitting is significantly less than J and a correction must be made by, for example, spectral simulation. As discussed above the observed linewidths in lysozyme are small enough for multiplet structure to be observed. This structure, however, has been hitherto almost completely unseen and unused in protein spectra. The difference between observations in this and in previous work must arise partly because of improved instrumentation and techniques like convolution difference, but it may also be due to the fact that T_1 is longer at higher fields (see Chapter VIII). For example, at 90 MHz where most of the multiplet structure in lysozyme is hard to observe, the measured T_1 value of the protons coupled to the methyl groups is about 0.2 secs. In other words T_1 is of the order of 1/J, when the observed multiplet structure can be reduced or removed completely (Navon and Polak, 1974). At 270 MHz the T_1 values are about 3 times longer and this reduction of the multiplet structure is less likely. (In this frequency dependent region the linewidth is also predicted to be somewhat less at higher field).

Since multiplet structure and double resonance have not previously been used in assignment procedures for proteins the approach is described in some detail.

IV.4.1 NH Resonances

The assignment of histidine NH resonances and tryptophan indole NH resonances may be made on the basis of their primary chemical shift positions in many cases. Assignment of other resonances to specific types of amino acid residue is not easy. The procedures for peptide NH resonances must involve spin-decoupling, and will generally require assignment to have

been made of the corresponding α-CH resonance. These experiments will not however be considered in this thesis.

IV.4.2 Methyl Group Resonances

As shown in Table IV.1, the methyl group resonances from a particular amino acid are characterized uniquely by the observed multiplet structure, the measured separation between the coupled resonances, the coupling constant and the number of coupled resonances. For example, one of the isoleucine methyl group resonances and the methionine methyl group resonances are immediately identified by their observed triplet and singlet character respectively. To distinguish the various doublets double resonance experiments are necessary.

The double resonance experiments were performed using time shared homonuclear decoupling. The object of these experiments is to search for the position at which a resonance is collapsed and to determine the number of resonances which collapse simultaneously. Since there is often severe overlap of resonances, difference spectroscopy was used to reveal decoupled resonances. There is usually overlap at the irradiation position too and care must be taken to apply as selective an irradiation as possible and to repeat the experiment after shifting the resonances by a change in pH or the addition of a paramagnetic shift probe.

Using these double resonance experiments the alanine and threonine methyl doublets can be distinguished from other doublets since the number of collapsed doublets is one, and since the separation between the irradiation position and the observed methyl doublet is about 2.5 ppm (see Table IV.1). Even with large secondary shifts in a system it was found that the separation between coupled resonances does not usually deviate by more than about 0.5 ppm from the primary shift separation .

Only one doublet is collapsed also for one of the isoleucine methyl resonances. In this case, however, the irradiation position is only about 0.7 ppm to low field of the collapsed resonance (see Table IV.1). Leucine and valine are identified by the collapse of 2 pairs of doublets simultaneously, and by an irradiation position at about 1 ppm to low field of the observed resonances.

The double resonance experiments reduce the problem to the separation of alanine and threonine methyl resonances and of leucine and valine methyl resonances. In certain cases this separation can be made by measuring the coupling constants. If the splitting is >6.8 Hz, the methyl resonance must be from alanine or valine. If the splitting is <6.6 Hz the methyl resonance is probably from a threonine or a leucine, but in this case, there is some uncertainty because of T_1 effects on the multiplets (Navon and Polak, 1974) which reduce the measured coupling constant. Thus a measured coupling constant could be less than the true J value.

These procedures therefore make it possible to assign to types of amino acid all the methyl group resonances and their coupled resonances. At worst assignment is to one of two possibilities. If the resonances can be resolved, further decoupling permits assignment of all protons in the residue. In the next chapter the results of extensive studies on lysozyme are presented.

IV.4.3 The Aromatic Proton Resonances

The aromatic region of the spectrum is made up of the resonances listed in Table IV.2. The multiplet structure, as listed, contains several simplifications which have been made as a result of the observations described in this thesis. For

example, tyrosine is listed as consisting of two doublets, each of area corresponding to two protons. This assumes that the ortho and meta protons of tyrosine are always equivalent, which would not initially be expected of a tyrosine which was rigidly held in a protein. To explain observations in several proteins, it is proposed that the tyrosine side chain is able to flip rapidly about its axis of symmetry thus causing the two ortho and the two meta proton resonances to be equivalent (see Chapter VIII). Similarly, for phenylalanine with sufficient motion, the pairs of ortho and of meta protons become equivalent. This simplification has also been incorporated in the table. In practice, the equivalence of the pairs of ortho and of meta protons of tyrosine and phenylalanine is not assumed to be necessarily the case. This is investigated in the course of spin-decoupling experiments. If the motion was less rapid or if the inherent inequivalence was very large, an intermediate exchange situation could arise and lead to severe broadening of the ortho and meta proton resonances of tyrosine or phenylalanine (not the para phenylalanine proton resonance). The table also shows that the tryptophan resonances are not simplified by motion because, of course, this side chain has little symmetry. In addition to the above simplifications the coupling is assumed to be approximately first order and that smaller couplings (<3 Hz) are not resolved. In practice, it is desirable, and often necessary, to ensure that the first order approximation is valid. This is best done by causing differential shifts of the resonances, for example by using added lanthanide shift probes. To detect coupling and multiplet structure it is possible to use the pulse sequences described in Section III.2.3.2. These lead to considerable simplification of the procedures.

One interesting feature of double resonance experiments

in the aromatic region is that nuclear Overhauser effects are observed. These effects, which arise from a dipolar relaxation mechanism, can be distinguished from spin coupling using certain types of pulsed double resonance (Section III.2.2.1). Most of the Overhauser effects observed in this work arise from intra amino acid effects, e.g. the tyrosine ortho protons are mainly relaxed by the tyrosine meta protons although inter amino acid effects could also occur. Since the homonuclear Overhauser effects in proteins can be large (a 100% reduction in intensity is possible) and since this effect occurs whether or not spin multiplets are observed, this phenomenon could be a useful assignment aid on systems where the multiplets are obscured by large linewidths.

IV.4.4 Other Proton Resonances

To this stage, assignment only of resonances of aromatic (including NH) protons, and of methyl groups, with their coupled protons, have been described. This is because resonances of these protons are relatively easy to observe, resolve and decouple. There are also relatively few resonances (ca. 60 in lysozyme) of each class. The resonances of aliphatic -CH and $-CH_2$ groups are more difficult to deal with. First, there are a large number of these resonances (ca. 500 in lysozyme) in a relatively small frequency range, normally between 2 and 5 ppm. Secondly, the multiplet structure of these resonances is complicated compared to that of the aromatic proton and methyl group resonances (which are all singlets, doublets or triplets). These resonances therefore are only considered in this thesis when they are fortuitously resolved. Assignment procedures are not discussed here, and generally require detailed spin-decoupling experiments to be performed. No simple rules can be laid down as was possible in Sections IV.4.2 and IV.4.3.

IV.5 Assignment to a Particular Residue

Assignment to the level above has required no knowledge of the molecular conformation. The next stage of assignment is closely dependent upon this knowledge about the protein structure. The object is to perturb the protein spectrum in such a way that resonances can be identified with a particular amino acid in space and thus perhaps indirectly with a particular amino acid in the sequence. The rest of this chapter describes ways in which a resonance can be perturbed deliberately and how intrinsic perturbations such as ring current shifts can be used in the assignment/structure procedures.

IV.5.1 Perturbation by the binding of diamagnetic ligands

Since proteins exhibit very specific binding properties, one of the most obvious ways of locating resonances from groups in, for example, the active site of an enzyme is to monitor the effect of a substrate or inhibitor on the resonances. This procedure has been applied for example to ribonuclease (Roberts and Jardetzky, 1970) and carbonic anhydrase (Campbell et al., 1974) to assign histidine resonances. The perturbed resonances are likely to be, but are not necessarily, near to the binding site. This uncertainty arises because the precise mechanism of the perturbation is usually not known. The changes in the resonances could, for example, arise because of a conformational change at some other part of the protein. This uncertainty is much less likely to arise with paramagnetic ligands (see below). In the case of lysozyme, N-acetyl glucosamine (GlcNAc) is an inhibitor and the binding of this molecule causes very many changes in the lysozyme spectrum (see Chapter VIII). Because GlcNAc causes such large pertubations of an unknown nature it is not a good

method for assignment in this case. However, the information obtained from this type of experiment once assignments have been made gives very valuable information about the binding process.

IV.5.2 Perturbation by the binding of Paramagnetic Species

The use of paramagnetic species particularly lanthanide ions for conformational studies on small molecules is well known. (See Chapter VII). In these experiments, attempts are made to correlate the observed perturbations of assigned resonances with a unique conformation of the molecule. If the conformation were known, it should be possible to perform the reverse procedure and obtain the spectral assignments. The first attempt to carry out a procedure of this type for a protein was by McDonald and Phillips (1969) who studied the shifts induced by Co^{2+} binding to lysozyme. However, two major objections to this study may be made. First, the nature of the shifts induced by Co^{2+} is not fully understood, and secondly their geometrical dependence is unknown. However in principle this method is extremely important. In the work reported in this thesis the complexity of induced shift data was considered to be too great to permit their immediate use for assignment. However, isotropic dipolar relaxation data are well understood, a simple $1/r^6$ dependence being followed where r is the distance between the paramagnetic species and a nucleus. Gd^{3+} or Mn^{2+} are suitable probes for assignment as they give rise to isotropic dipolar relaxation. The next Chapter considers in detail the use of Gd^{3+} for assignment of lysozyme resonances. Provided that the binding sites for Gd^{3+} are well defined, the types of amino acid residue at different relative distances from the Gd^{3+} may be deduced. These are then compared to predictions for different residues in the sequence based on the X-ray structure If sufficient agreement between the two sets of relative distances

is obtained, it may be concluded that the conformation in solution resembles the X-ray structure. Assignment of the resonances of types of amino acid to specific residues in the sequence may then be made. A major difficulty arises in the observation and quantitative measurement of the induced relaxation. This may be overcome by the use of paramagnetic difference spectra described in Section III.1.2.

The use of paramagnetic species other than cations is possible. In particular the anion $Cr(CN)_6^{3-}$ has proved useful in this work. Other possible probes include neutral spin-label molecules which may either be introduced by chemical modification experiments, or by non-covalent binding of the molecules.

IV.5.3 Perturbation by the Binding of Protons

The specific binding of protons is of course well understood for it is concerned with the ionisation of acidic or basic groups. The effects of ionisation on the chemical shifts of histidine and tyrosine have already been discussed. If the pK value of specific residues is known independently, then assignment in the nmr spectra of groups which titrate according to the defined pK values may be straightforward. However, in the present work it has been observed that local conformational changes often accompany the ionisation of side-chains, and these cause small shifts of the resonances of nearby groups. It is sometimes possible by this method to assign resonances to residues close together in space and then, by using the X-ray structure, to specific residues in the sequence.

IV.5.4 Ring Current Shifts

In addition to the binding of extrinsic perturbing probes, intrinsic probe centres exist. These are the aromatic

rings which give rise to ring current shifts (see Sternlicht and Wilson, 1967). A common assignment method is to assume that in the absence of ring current shifts, the protein spectrum will be exactly that of the sum of the component amino acids. Then, the magnitude of the ring current shift experienced by different resonances is calculated using standard formulae and the X-ray co-ordinates. These calculated shifts are then used to predict the native spectrum, and assignments made from this comparison (see McDonald and Phillips, 1970). Unfortunately, the accuracy of the formulae for the ring current shifts is not very good. In the next chapter the quantitative value of this approach is discussed.

IV.5.5 Intrinsic Paramagnetic Centres

Intrinsic paramagnetic centres occur, for example, in haem proteins and may occur naturally or be substituted into many metalloproteins. These centres do not occur in lysozyme and their use will not be discussed here.

IV.5.6 Other ways of classifying resonances

Chemical modification has been used as an assignment aid and many proteins contain residues which can be changed very specifically. This method is very valuable for identifying resonances from a modified residue and residues close to it but it is very often not possible to identify unambiguously the resonances of the modified residue. The best known example of this is probably the case of ribonuclease A where histidine 12 or histidine 119 can be modified by iodoacetate. In either case the resonances from both residues are perturbed when one histidine is modified (see Roberts and Jardetzky, 1970). Chemical modification of tryptophan 108 in lysozyme (Glickson *et al.*, 1971)

also leads to ambiguous results (see below).

In many cases proteins from different species or a mutant species contain small known changes in amino acid composition. Comparison of the spectra of these proteins can sometimes lead to the identification of resonances (see, for example Stellwagen and Shulman, 1973) although the problem of ambiguity described above still applies. In this thesis the spectra of human and hen lysozymes are compared and although these proteins are only 60% homologous the similarity between certain resonances in the active site is striking and lends considerable weight to some of the assignments.

When NH resonances are studied there is an additional parameter which can be measured, this is the rate of exchange of NH to ND when the solvent is changed to D_2O. This parameter can then be related to the degree of 'exposure' to solvent of a particular NH proton in the structural model. This method has been used by Glickson et al. (1971) in assignments of the tryptophan indole resonances of hen lysozyme.

IV.6 Summary

In the next chapter the application to lysozyme of the methods discussed here is described. None of the methods for the final stage of assignment, to specific residues in the sequence, is rigorous. They are only feasible if the assignment of resonances to types of amino acid has been made, for this reduces considerably the number of possibilities to be considered for assignment of a given resonance. Confidence in assignments can only arise from the accumulation of information from as many different experiments as possible.

At present, these methods require the knowledge of the X-ray structure. It is thus essential to show whether or not the

X-ray structure is a good description of the solution conformation. It is not difficult however to see how the methods may be extended to provide conformational information independently of any X-ray structure.

References for Chapter IV

Campbell, I.D., Lindskog, S. and White, A.I. (1974), J. Molec Biol. 90, 1.

Crespi, H.L., Norris, J.R., Bays, J.P. and Katz, J.L. (1973), Ann. N.Y. Acad. Sci. 222, 800.

Glickson, J.D., Phillips, W.D. and Rupley, J.A. (1971), J.Amer.Chem.Soc. 93, 4031.

Hunkapillar, M.W., Smallcombe, S.H., Whitaker, D.R. and Richards, J.H. (1973), Biochemistry, 12, 4732.

McDonald, C.C. and Phillips, W.D. (1969), Biochem. Biophys. Res. Comm. 35, 43.

McDonald, C.C. and Phillips, W.D. (1970), in Fine Structure of Proteins and Nuclei Acids (Fasman, G.D. and Timasheff, S.N. eds), Vol. IV, Dekker (N.Y.), 1.

Navon, G. and Polak, M. (1974), Chem. Phys. Lett. 25, 239.

Patel, D.J., Woodward, C.K. and Bovey, F.A. (1971), Proc.Natn.Acad.Sci. U.S.A. 69, 599.

Pople, J.A., Schneider, W.G. and Bernstein, H.J. (1959), High Resolution Nuclear Magnetic Resonance, McGraw-Hill (N.Y.).

Roberts, G.C.K. and Jardetzky, O. (1970), Adv. Protein Chem. 24, 448.

Robillard, G. and Shulman, R.G. (1972), J.Molec.Biol. 71, 507.

Sadler, P.J., Benz, F.W. and Roberts, G.C.K. (1974), Biochim. Biophys. Acta 359, 13.

Stellwagen, E. and Shulman, R.G. (1973), J.Molec.Biol. 75, 683.

Sternlicht, H. and Wilson, D. (1967), Biochemistry, 6, 2881.

Sykes, B.D., Weingarten, H.I. and Schlesinger, M.J. (1974), Proc.Natn.Acad.Sci. U.S.A., 71, 469.

CHAPTER V

ASSIGNMENT OF THE SPECTRUM - DETAILED ANALYSIS

In this Chapter the results of experiments designed to make assignments in the lysozyme spectrum are presented. The format of this Chapter preserves as far as possible that of the previous Chapter in which the general strategy was developed. For convenience, however, the spectral resolution methods are not discussed again here, but are introduced where necessary.

V.1 Assignment to a Type of Proton

V.1.1 Random Coil and Native Spectra

The spectrum of lysozyme at temperatures above 80°C is that of a random coil protein (McDonald and Phillips, 1969; McDonald *et al.*, 1971). The spectrum is very closely that of a sum of the spectra of the component amino acids except that line-widths are somewhat greater because of the increased molecular weight (McDonald and Phillips, 1969). Complete assignment to types of proton, and even to types of amino acid is thus direct. At low temperature, the native protein exists and the spectrum is perturbed (see for example Fig. IV.1). At 70°-80°C both forms of the protein are present in solution, but exchange between them is slow, and two superimposed spectra are observed. If the assigned resonances in the random coil spectrum could be related to those in the native spectrum, the assignment of the native spectrum would be much easier. One way of relating resonances of two species which are in slow nmr exchange is by the use of cross-saturation techniques. These have been used to relate resonances in oxidised and reduced cytochrome *c* (Redfield and Gupta, 1971). Here, selective irradiation of resonances of one

species results in the decrease in area of the corresponding resonances of the other species, provided that the lifetime in each state is less than or comparable to the T_1 values. In this work, application of both time-shared and gated decoupling (see Section III.2) to a variety of resonances in spectra of a mixture of random coil and native lysozyme (pH 4.0, 75°C) failed to result in observable effects. This implies that the rate of exchange of the two species is slower than ca. 1 sec^{-1} under these conditions. Further studies of the random coil spectrum are therefore under these conditions of no direct value for assignment.

V.1.2 Exchangeable Hydrogens

Fig. V.1 shows how difference spectroscopy permits the separation of the resonances of the non-exchangeable hydrogens from those of the exchangeable hydrogens to be made. From these spectra a value for the number of hydrogens observed under different conditions was obtained (Table V.1). Following the rules laid down in Chapter IV we can summarise the resonances of exchangeable hydrogens as follows. (a) At least 175 resonances are observable; (b) imidazole NH are not observable; (c) five indole N(1)H resonances are observed between 9.5 and 11 ppm; (d) for H_2O samples only, about 40 resonances from amide and guanido protons are observed between 6.5 and 7.0 ppm, and (e) probably all (126) of the peptide NH resonances are observed between 6.5 and 9.0 ppm, about half of which are not exchanged after three hours in D_2O at pH 3.2 at 54°C. It is also clear however that only the indole N(1)H resonances are very well resolved. Using convolution difference methods it is possible to resolve coupling on the peptide NH resonances but this has not yet been pursued. Both high pH and high temperatures

FIGURE V.1

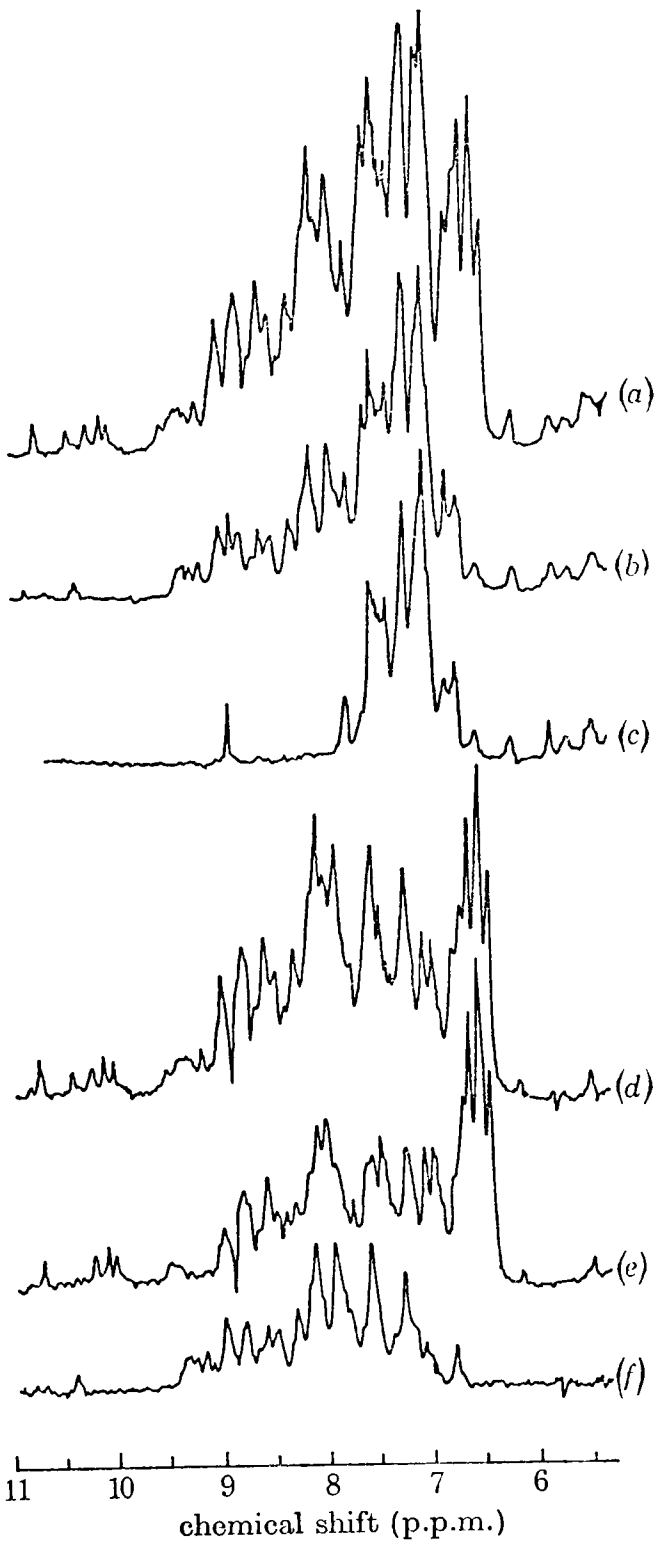

Spectra of 5mM lysozyme at pH 3.2, 54°C. (a) spectrum in 90% H_2O, 10% D_2O. (b) spectrum in D_2O after 3 hours. (c) spectrum in D_2O after heating to 80°C for several minutes. (d) difference between (a) and (c). (e) difference between (a) and (b). (f) difference between (b) and (c). The H_2O resonance was saturated by means of the time shared method.

TABLE V.1

Numbers of Exchangeable Hydrogens

Experimentally Observed[a]	in H_2O	175 ± 10
	in D_2O[b]	56 ± 5
	spectral difference	125 ± 8
Calculated from Sequence	total NH	249
	peptide NH	126

[a] at 57°C, pH 4.3

[b] after 3 hours under these conditions

reduce the number of observable resonances as exchange rates increase.

V.1.3 Non-Exchangeable Hydrogens

Fig. V.2 shows spectra of the non-exchangeable hydrogens, including convolution difference spectra. To high field of 0.7 ppm 14 resonances each of area three protons are observed. These may each be resolved separately under some conditions of pH or temperature, or in the presence of a shift probe. One resonance is a singlet, 11 are doublets and 2 are triplets. J for the doublets and triplets is 6.5 $\pm$ 1 Hz (see later) and these resonances are all therefore assigned to methyl groups. The other 47 methyl group resonances are assumed to be between 2.5 and 0.7 ppm, although less than ca. 10 resonances (1 singlet and the rest doublets) have been separately resolved, even using difference methods. Many other peaks in this region are however clearly due to overlapping doublets and triplets with J values in the 6.5 Hz region. No peaks below 2.5 ppm can be assigned to methyl groups.

All the resonances below 6.5 ppm can be assigned at once to aromatic protons, as it is most unlikely that any other resonances could be shifted into this region. The resonances at 6.28 and 6.49 ppm have been shown to be also of aromatic protons by spin-decoupling. Only about 15 peaks are resolvable separately in this region, but ca. 10 other resonances have been identified using difference spectroscopy (particularly involving double resonance) or pulse sequences. Each of the aromatic proton resonances identified is observed as a singlet, or a doublet or triplet with J = 8.5 $\pm$ 1 Hz.

Only one resonance has been definitely identified as of an α-CH proton from its clearly observed coupling to an exchangeable

FIGURE V.2

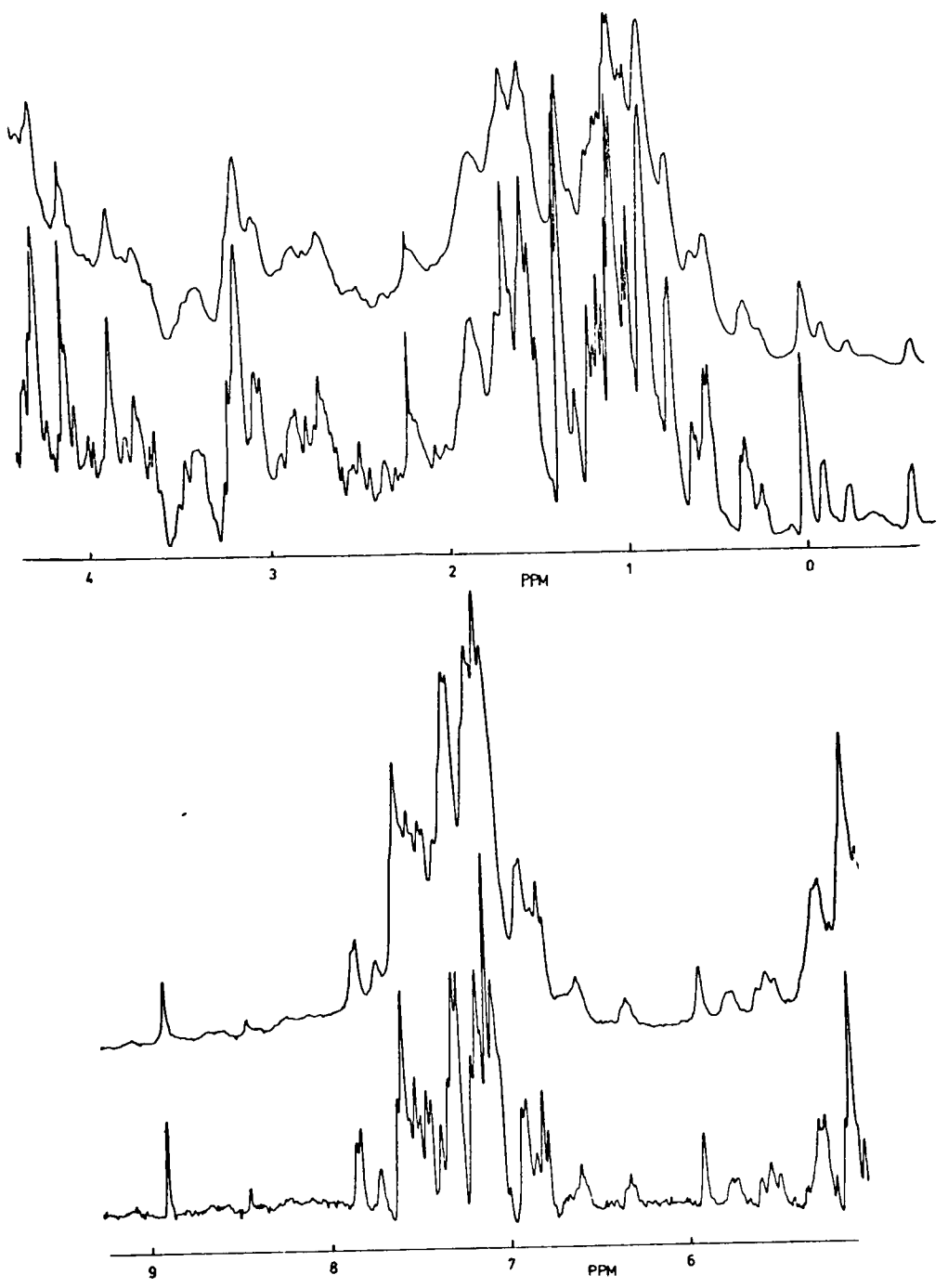

Normal and convolution difference spectra of the non-exchangeable proton resonances of lysozyme. The HOD peak is at ca. 4.5 ppm and is not shown here. 5mM lysozyme, pH 4, 54^{o}C.

proton. This is the resonance at 5.81 ppm, which is approximately a singlet (J<3 Hz in D_2O, but a doublet (J = 5 Hz) in H_2O). All the resonances other than those of aromatic protons, observed below the HOD peak are however likely to be α-CH resonances.

Clear direct observation of other CH or CH_2 protons is difficult. Four resonances appear above 0.5 ppm and are resolved separately. One of these has been shown to be coupled to a methyl group resonance. Their multiplet structure is not directly observable. Other resonances between 0.5 and 5.5 ppm have been identified only by the double irradiation experiments described below. Other regions of the spectrum may be approximately assigned by comparison with the random coil spectrum, but no independent evidence can be presented. In the subsequent parts of this thesis, only the resonances of aromatic protons, of methyl groups and their coupled protons, and the few separately observable resonances will normally be considered. Nearly half of the protein residues are accessible from the aromatic and methyl group resonances.

V.2 Assignment to a Type of Amino Acid

In order to assign a resonance to a proton of a particular type of amino acid residue it is essential to be able to resolve the resonance separately, in order to determine unambiguously the multiplet structure, area and coupling constant (if required). This is also valuable for observing clear spin-decoupling effects. Thus, the first task is to tabulate resonances for which such clear observation is possible. This was carried out here by observation of the effects of various perturbations which cause selective shifts in the spectrum. For each of the tabulated resonances, some conditions have been determined by which the resonance may be viewed in the absence (or virtual absence) of

any overlapping peaks. In order to define the conditions in as straightforward a manner as possible, the following scheme has been drawn up. (a) For each resonance, the first consideration is whether separate observation is possible, using convolution difference, at any given pH value at a standard temperature, chosen as 54°C. The origin of the small shifts which occur with pH changes will be described subsequently. (b) In the event of no separate observation being possible under these conditions, the possibility of a variation of temperature at a standard pH value (pH 5.3, measured at 20°C) resulting in separation is considered. (c) For each resonance, conditions under which separate observation may be achieved by the use of lanthanide probes is next considered. To simplify again, conditions were standardised where possible. Thus, a temperature of 54°C, a pH value of 5.3 (measured at 20°C) and a <u>total</u> lanthanide concentration of 24 mM were selected. (This arises from addition of 50µl of 0.50M lanthanide to 1ml of lysozyme solution, resulting in 23.8 mM lanthanide). If separate observation is possible with La^{3+} only, this is indicated as La. If induced shifts are required, then conditions are given. For example 'Eu, 10mM 'means $[Eu^{3+}]$ = 10mM, $[La^{3+}]$ = 14mM, i.e. the total lanthanide concentration is still 24mM. Because of the lack of line broadening induced, Eu^{3+} and Pr^{3+} are best for this separate observation, but Yb^{3+} and other lanthanides are sometimes needed. Where Gd^{3+} difference spectra are required, the concentration is indicated, and again a total Ln^{3+} concentration of 24mM was used. In practice, this means that small quantities of Gd^{3+} were added to a solution containing 24mM La^{3+}. The effects of the Ln^{3+} will be described in more detail below. Here, it suffices to say that fast exchange conditions are operative in each case. (d) In certain cases, separate observation was not possible under any of these

conditions. In these cases the conditions required are quoted. These include spin-decoupling difference spectra. Clearly there are many conditions under which some resonances can be observed. The purpose of this classification is not to define all of these conditions. The resonances of different types of proton will be considered separately.

V.2.1 Methyl Group Resonances

Twenty-two methyl group resonances have been totally resolved (Table V.2). These are indicated in Fig. V.3.

Spin-decoupling experiments were performed using the time shared method. The procedure used was as follows. A 10mM solution of lysozyme in D_2O at pH 4.0 was made up, and spectra were obtained at 67°C. Irradiation was carried out at 30 Hz (ca. 0.1 ppm) intervals from 5.5 ppm to 0.7 ppm (and above 0.7 ppm on observed peaks), recording spectra at each position. The power and pulse width were adjusted to be such that the band of the irradiation frequency was ca. 50 Hz wide, so that decoupling of all those resonances which are coupled to a resonance in the frequency range swept (i.e. 5.5 ppm and above) would be achieved. This resulted in decoupling of all the doublet resonances observable separately in the spectrum. Many changes in other, overlapping, resonances due to decoupling effects were observed but not pursued. Then, in the regions of irradiation frequency where decoupling was observed, finer changes in the irradiation frequency were made and the position at which the most complete decoupling of a given resonance occurred was recorded. Difference spectroscopy was used in certain cases to observe the decoupling effects. In cases where there existed possible ambiguities in the results (e.g. several resonances decoupling at the same frequency) decoupling experiments under different conditions were

TABLE V.2

Conditions for Resolution of Methyl Group Resonances[a]

Resonance Number	Chemical Shift (ppm)	Multiplet Structure[b]	pH Value	Temp[c] (°C)	Ln^{3+}[d]
M1	-0.63	d	All		La
M2	-0.26	d	<6		La
M3	-0.10	d	<6		La
M4	-0.01	t		>65°	
M5	-0.01	d	<3		
M6	0.00	s			Yb 12-14mM
M7	0.27	t	<4.5		La
M8	0.28	d	<3.5		Pr 1.5-3mM
M9	0.32	d	<3.5		Pr 1.5-3mM
M10	0.48	d	>5		La
M11	0.53	d		(>65°)	
M12	0.57	d		(>65°)	
M13	0.60	d	>5.5		La
M14	0.64	d	<3.5		La
M15	0.75	d			Eu 12-24mM
M16	1.03	d			Gd (diff)
M17	1.14	d			Gd (diff)
M18	1.35	d			Eu 5-8mM
M19	1.35	d			Pr 6-16mM
M20	1.38	d			Pr 6-8mM
M21	1.49	d			Eu 5-8mM
M22	1.66	s			(La)

[a] in convolution difference spectra, at 54°C normally.

[b] singlet (s), doublet (d), triplet (t).

[c] at pH 5.3.

[d] total $[Ln^{3+}] + [La^{3+}] = 23.8mM$. Gd (diff) indicates difference spectroscopy. Ln^{3+} indicates a paramagnetic lanthanide ion.

FIGURE V.3

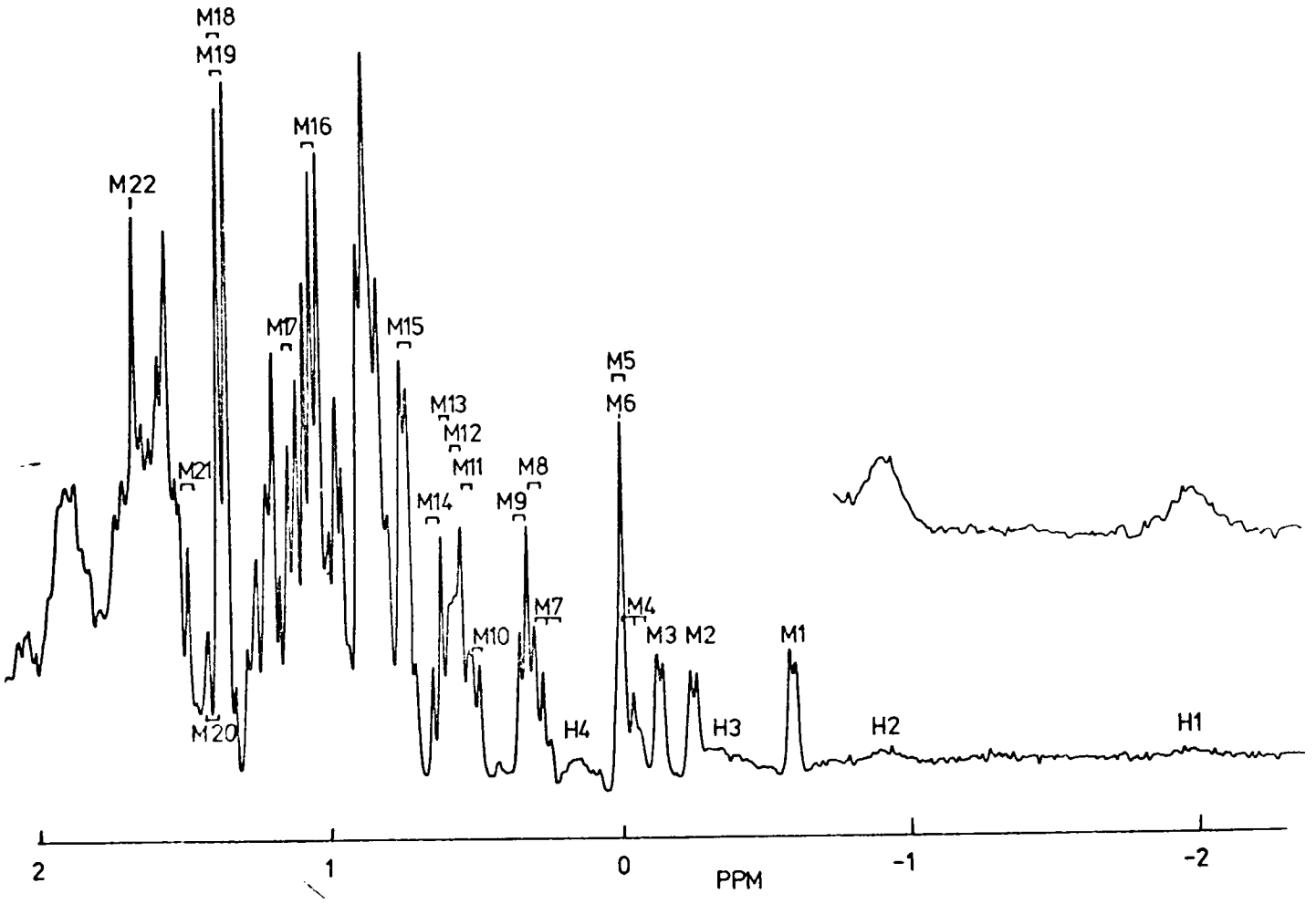

Resonance numbering scheme for the high field region of lysozyme. This spectrum (convolution difference) is at 66^{o}C. 5mM lysozyme, pH 4.8.

carried out. The results are all summarised in Table V.3, and illustrated in Figs V.4 and V.5.

Having achieved decoupling of the required resonances, in conjunction with the known multiplet structure, assignments can be made on the basis of the arguments laid down in Section IV.4.2. This then leaves only distinction between leucine and valine, and between alanine and threonine to be made. In order to achieve this, values of coupling constants were measured. This involved the measurement of the separation between the components of the multiplets in well resolved spectra. By recording spectra under different conditions, the values shown in Table V.4 were achieved. Because the components of the resonances are not totally resolved, and because of theoretical problems (see Section IV.4.2), the true J values may be larger than these measured values. Thus the large values (greater than 7.0 Hz) were used to assign doublet resonances with confidence to alanine and valine. The small values (<6.3 Hz) were used to assign to threonine and leucine, but the alternative assignments to alanine and valine were not dismissed. In future, measurements of T_1 and T_2 values may enable more definite values to be obtained for the true J values. The conclusions are summarised in Table V.4.

Having achieved these assignments the total numbers of methyl groups of different residues that there are in the sequence are summarised. These are given in Table V.5, along with the numbers of assigned resonances. It is noted from Table V.4 that the parameter Δ_{sd}. which was used in the assignment procedure, was observed, with only one exception (M2), to be as predicted in Section IV.4.2 i.e. either 1.0 ± 0.5 or 3.0 ± 0.5 ppm. This gives considerable confidence in the assignments. M2, which suffers a large secondary shift has the value of 1.8 ppm which is just out-

TABLE V.3

Spin-decoupling of Methyl Group Resonances[a]

Resonance Number	Multiplet Structure	Chemical Shift (ppm) Decoupling	Chemical Shift (ppm) Irradiation	Other Resonances Decoupled	Confirmation[b] Required By:
M1	d	-0.55	0.68	M3	
M2	d	-0.22	1.56	-	
M3	d	-0.15	0.68	M1	
M4	t	-0.02	-2.10	-	A
M5	d	0.01	1.47	M12	A
M6	s				
M7	t				
M8	d	0.32	1.22	M11	
M9	d	0.35	3.76	-	
M10	d	0.53	1.92	M13	
M11	d	0.54	1.22	M8	B
M12	d	0.56	1.47	M5	
M13	d	0.61	1.92	M10	B
M14	d	0.59	3.87	-	C
M15	d				
M16	d	1.04	2.19	M17	D
M17	d	1.15	2.19	M16	D
M18	d	1.35 }	4.2-[c]		
M19	d	1.35 }	4.4		
M20	d	1.38	4.31		C
M21	d	1.49	4.23		
M22	s				

[a] [Lys] = 10mM, pH = 4.0, T = 68°C.

[b] Conditions for confirmation. A = pH 2.5; B = 24mM La^{3+}; C = 10mM Nd^{3+} + 14mM La^{3+}; D = 50mM La^{3+}, $[Gd^{3+}] = 5 \times 10^{-5}$M in difference spectrum.

[c] Separate decoupling not observed.

FIGURE V.4

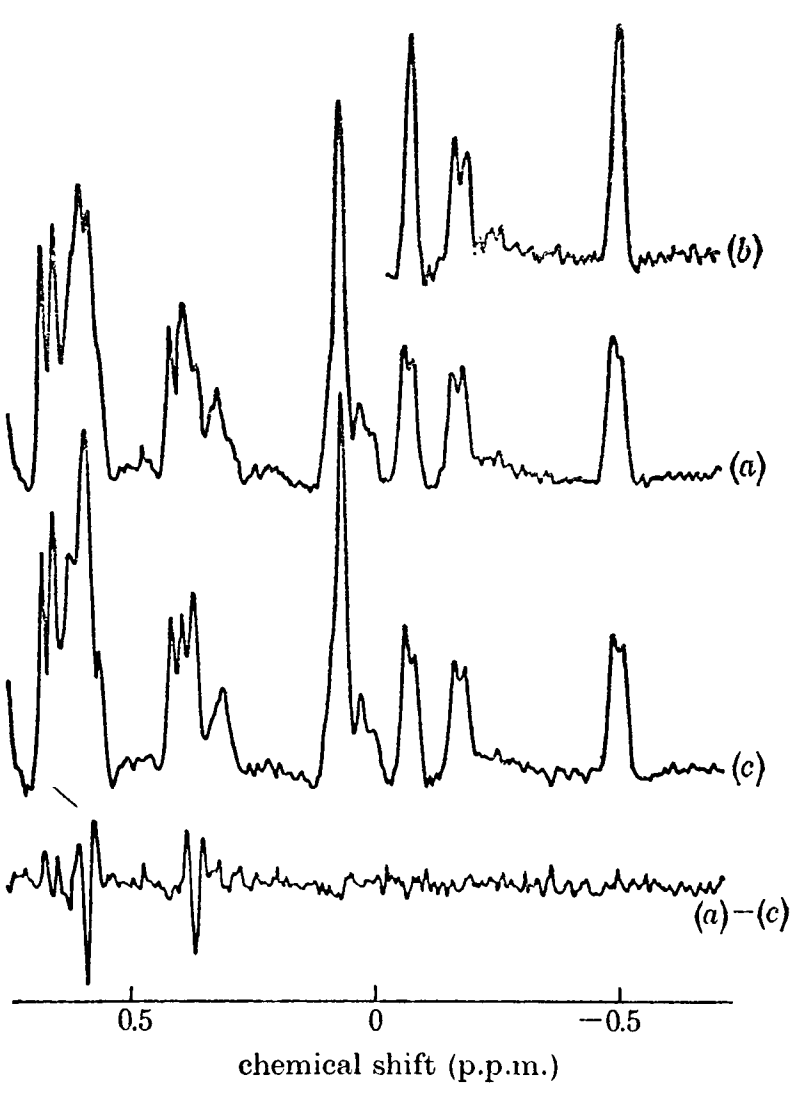

(a) High field part of the CD spectrum of 10 mM lysozyme, pH 4.0, 68°C. (b) with time-shared irradiation at 1.59 ppm showing decoupling of M1 and M3. (c) with irradiation at 1.25 ppm. The collapse of the two doublets M8 and M11 in (c) is revealed in the difference spectrum (a)-(c).

FIGURE V.5

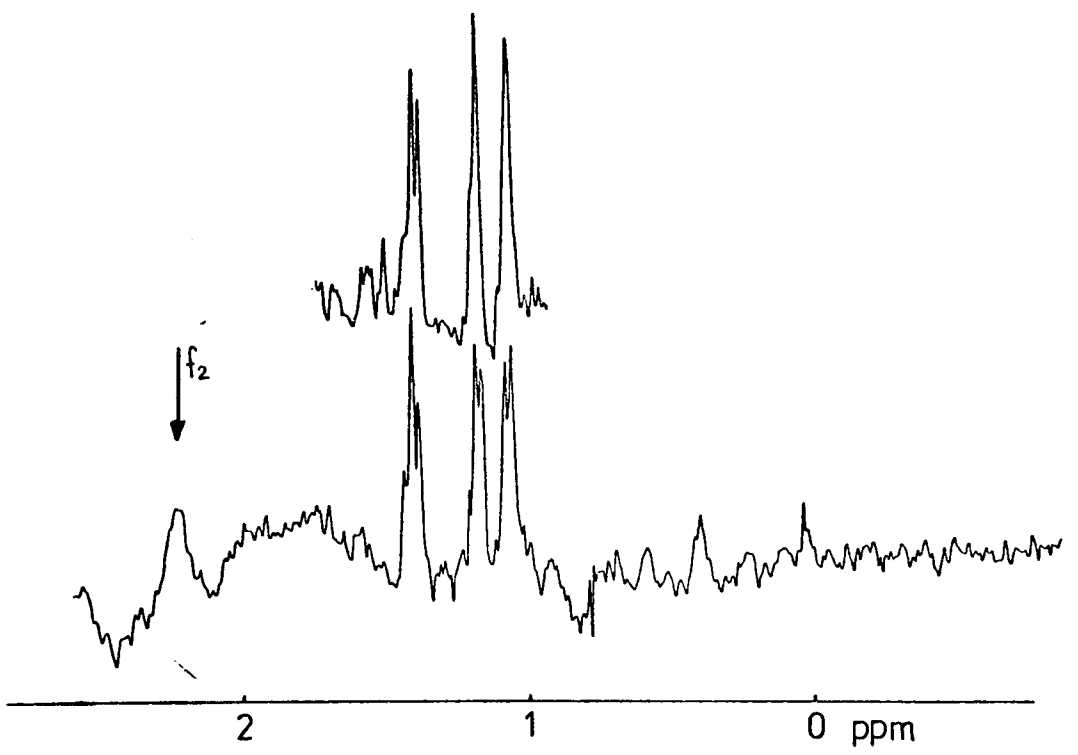

Observation of spin-decoupling in a Gd^{3+} difference spectrum. The lower trace is the difference between spectra of 5mM lysozyme with 50mM La^{3+} in the absence and in the presence of 5×10^{-5}M Gd^{3+}. The upper trace is the difference obtained in the same way except that irradiation at 2.2 ppm was applied for the two spectra. Decoupling of the two upfield resonances, M16 and M17, is observed.

TABLE V.4

Assignments of Methyl Group Resonances to Type of Amino Acid[a]

Resonance Number	Multiplet Structure	Δ_{sd}[b] (ppm)	Number Decoupled		J[c] (Hz)		Assignment[d]
M1	d	1.23	2	L/V	5.9		LEU (val)
M2	d	1.78	1	ILE γ	6.5		ILE γ
M3	d	0.83	2	L/V	5.8		LEU (val)
M4	t ILE δ				7.5		ILE δ
M5	d	1.46	2	L/V	6.0		LEU (val)
M6	s MET				0		MET
M7	t ILE δ				7.3		ILE
M8	d	0.90	2	L/V	5.9		LEU
M9	d	3.41	1	A/T	6.3		THR
M10	d	1.39	2	L/V	6.5		LEU/VAL
M11	d	0.68	2	L/V			LEU (val)
M12	d	0.89	2	L/V			LEU (val)
M13	d	1.31	2	L/V	6.5		LEU/VAL
M14	d	3.31	1	A/T	7.4	ALA	ALA
M15	d						
M16	d	1.15	2	L/V	7.1	VAL	VAL
M17	d	1.04	2	L/V	6.6		VAL
M18	d	2.95		A/T	(7.5)	(ALA)	ALA (thr)
M19	d	2.95		A/T	(7.5)	(ALA)	ALA (thr)
M20	d	2.93		A/T	7.8	ALA	ALA
M21	d	2.74		A/T	7.5	ALA	ALA
M22	s MET				0		MET

[a] the conclusions from each piece of information are recorded at each stage.

[b] Δ_{sd} = difference between irradiation and decoupling frequencies. L = leu, V = val.

[c] J values ca ±0.3 Hz.

[d] bracketed assignments have not been excluded.

TABLE V.5

Numbers of Methyl Groups in Sequence and Number of Resonances Assigned

Type of Amino Acid	Number in Sequence		Number Assigned	
	Residues	Groups	Residues	Groups
Ala	12	12	5	5
Ile	6	12	2/3	3
Leu	8	16	3/4	6/8
Met	2	2	2	2
Thr	7	7	1	1
Val	6	12	1/2	2/4
Total	41	61	15/16	21

side the expected range.

V.2.2 Aromatic Proton Resonances

V.2.2.1 Non-Exchangeable Hydrogens

The separate observation of 23 non-exchangeable aromatic proton resonances (Fig. V.6) was achieved. The relevant conditions are given in Table V.6.

The spin-decoupling experiments were more difficult to perform than those for the methyl group resonances, because many of the resonances coupled together are close to each other. The spin-decoupling experiments could not be performed satisfactorily when the separation of coupled resonances was less than ca. 0.2 ppm. However, decoupling was clearly observed in nearly every case. A similar procedure to that described for methyl group resonances was carried out. Spectra of a sample of 10mM lysozyme, pH 4.0 at 67^{o}C were recorded whilst irradiating in the time shared mode initially at 30 Hz intervals from 7.8 to 6.3 ppm. Then, the irradiation frequency was adjusted more finely, and coupled resonances identified in the manner shown in Table V.7. Confirmation in several cases was carried out in the presence of shift probes as Table V.7 indicates. Several experiments were repeated using the sequence described in Section III.2.2.1 to eliminate Overhauser effects.

Resonances A14 and A23 are considerably shifted by pH, the shifts showing the same pK value (5.3 at 54^{o}C), and the total shifts being 0.65 ppm for A14 (chemical shift values of 6.89 ppm at high pH, 7.54 ppm low pH) and 1.12 ppm for A23 (7.79 ppm at high pH, 8.91 at low pH). This at once allowed assignment to the C(4)H and C(2)H of a histidine (cf. Roberts and Jardetzky, 1970) of which lysozyme has only one. Other assignments are

TABLE V.6

Conditions for Resolution of Aromatic Proton Resonances[a]

Resonance Number	Chemical Shift (ppm)	Multiplet[b] Structure	pH Value	Ln^{3+}[c]	Other[d]
A1	6.28	t	All	La	
A2	6.49	t	All	La	
A3	6.71	d(2)	4.8-5.3		
A4	6.76	d	4.8-5.3		0.2M GlcNAc
A5	6.82	t			0.1-0.2M GlcNAc
A6	6.83	d(2)		Eu(24mM)	
A7	6.92	d			0.05M GlcNAc
A8	6.98	d(2)			sd diff
A9	7.03	s		Yb(16-24mM)	
A10	7.05	d(2)			sd diff
A11	7.08	s		Pr(20-24mM)	Gd(diff) pH diff
A12	7.09	d(2)		Pr(21mM)[e]	
A13[f]	7.18	s			CPMG
A14	7.23	s	>6.5		pH diff
A15	7.24	d(2)	(<6)		sd diff
A16	7.30	s		Dy(2-10mM)	
A17	ca. 7.41	d		(Yb(30mM,pH 5.5))	
A18	ca. 7.48	d		Yb(24mM)	
A19	7.55	s		Dy(2-6mM)	
A20	7.63	s	<6		
A21	7.74	d		Pr(9-10mM)	
A22	7.76	d		Pr(9-10mM)	
A23	8.34	s	All		

[a] in convolution difference at 54°C. Non-exchanged protons only.

[b] numbers in parentheses are numbers of equivalent protons if not one.

[c] total $[Ln^{3+}] + [La^{3+}] = 23.8mM$ (except for A17). Gd (diff) indicates use of difference spectroscopy.

[d] GlcNAc indicates in presence of GlcNAc; sd diff is spin-decoupling difference spectrum; pH diff is pH difference spectrum; CPMG is the Carr-Purcell-Meiboom-Gill pulse sequence.

[e] observed to low field of aromatic envelope.

[f] not clearly observed.

FIGURE V.6

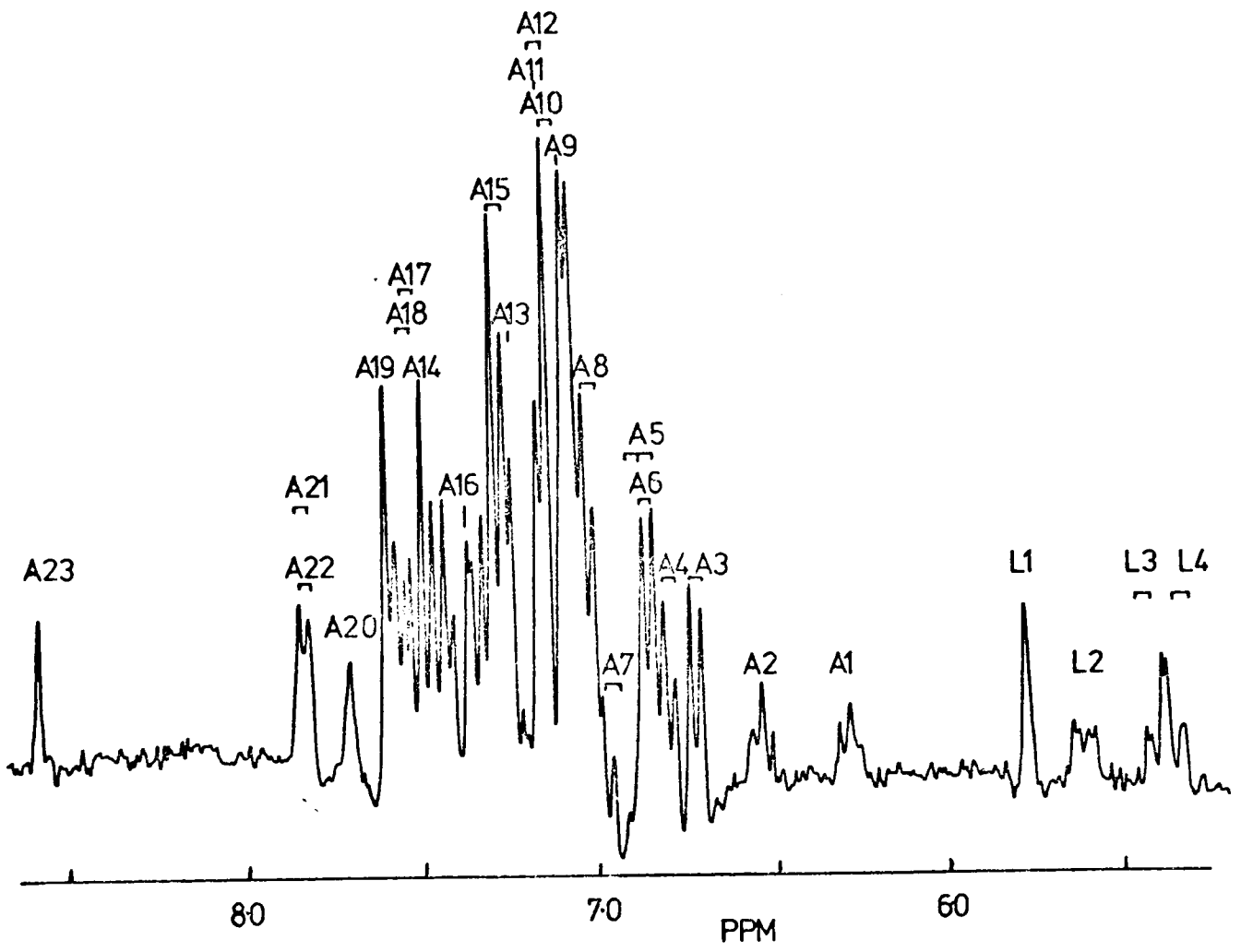

Resonance numbering scheme for the low field region of lysozyme. 5mM lysozyme, pH 4.8, 66°C.

TABLE V.7

Spin-decoupling of Aromatic Proton Resonances[a]

Resonance Number	Multiplet Structure	Coupled Resonances[b] Number	Multiplet Structure	Confirmation[c] Required By	Comment
A1	t	A4	d		
		A5	t		
A2	t	7.15ppm			
		7.38ppm			
A3	d(2)	A10	d(2)		Titrates pK = 10
A4	d	A1	t		
A5	t	A1	t		
		A22	d		
A6	d(2)	A12	d(2)	A	
A7	d				
A8	d(2)	A15	d(2)		
A9	s	-			
A10	d(2)	A3	d(2)		
A11	s	-			Titrates pK = 6.2
A12	d(2)	A6	d(2)		
A13	s	-			
A14	s	-			Titrates pK = 5.3
A15	d(2)	A8	d(2)		
A16	s	-			
A17	d				
A18	d				
A19	s	-			
A20	s	-			
A21	d	7.08ppm		B	
A22	d	A5	t	B	
A23	s				Titrates pK = 5.3

[a] [Lys] = 10mM, pH = 4.0, T = 68°C

[b] values in parentheses are chemical shift values of coupled resonance

[c] conditions for confirmation. A = 24mM Eu^{3+}, B = 24mM Pr^{3+}.

TABLE V.8

Assignments of Aromatic Proton Resonances to Types of Amino Acid

Resonance Number	Multiplet Structure	Singlet Assignments	Other Assignments[a]	Coupling Pattern
A1	t		trp 5/6[b]	
A2	t		(trp 5/6)	
A3	d(2)		tyr (o-)	
A4	d		trp 4/7	
A5	t		trp 5/6	
A6	d(2)		tyr (o-)	
A7	d		(trp 4/7)	
A8	d(2)		tyr (o-)	
A9	s	trp C(2)H		
A10	d(2)		tyr (m-)	
A11	s	trp C(2)H		
A12	d(2)		tyr (m-)	
A13	s	trp C(2)H		
A14	s	his C(4)H		
A15	d(2)		tyr (m-)	
A16	s	trp C(2)H		
A17	d		(trp 4/7)	
A18	d		(trp 4/7)	
A19	s	trp C(2)H		
A20	s	trp C(2)H		
A21	d		(trp 4/7)	
A22	d		trp 4/7	
A23	s	his C(2)H		

[a] assignments in parentheses refer to those which assume equivalence of all pairs of ortho and meta phenylalanine resonances.

[b] 4,5,6,7 refer to the protons on the tryptophan indole ring. Spin-decoupling does not allow distinction between 4 and 7 (doublets) or 5 and 6 (triplets) to be made.

given in Table V.8. These are all based on the data of Table V.7. Several points require comment. First, the tyrosine resonances are assigned from the observation of a two proton intensity doublet coupled to another two proton intensity doublet. The high field resonance in each case was assigned by comparison with tyrosine itself to the protons ortho to the -OH group, because the chemical shift values strongly indicate that no large secondary shifts are experienced. This is seen in Table V.9. In one case, A3, this could be confirmed by the observation of a 0.3 ppm upfield shift corresponding to a pK value of 10.0 ± 0.5. This shift must arise from the ionisation of the -OH group and is of the expected magnitude (see Karplus et al., 1973). Resonances A1, A4, A5 and A22 must arise from tryptophan because of the coupling pattern (d-t-t-d). All one proton doublet resonances are assigned to the C(4)H or C(7)H protons of tryptophan rather than to phenylalanine ortho protons. This assumes rapid 180^{o} flips of all phenylalanine residues, which would result in a single two proton intensity doublet for the ortho proton resonances, and is thus not necessarily rigorous in all cases. Note that all the tyrosine resonances are previously accounted for. Equally, the one proton area triplet resonance A2 is assigned to tryptophan not to a phenylalanine proton. A slow flipping rate would allow assignment to a phenylalanine meta or para proton to be conceivable. However, in the study of all these resonances over a wide range of conditions, no evidence has been observed that any of the flip rates in lysozyme are slow. The flipping process is further discussed in Chapter VIII.

The use of the multiplet selection technique allows separate observation of six clear singlet resonances, and of one possible singlet resonance (A13) (see Fig. IV.15). A20 is a singlet but

TABLE V.9

Chemical Shift Values of Tyrosine Resonances[a]

Resonances	ortho (3,5)	meta (2,6)	difference (meta-ortho)
tyrosine	6.9	7.2	0.3
lysozyme (a)	6.71	7.05	0.34
(b)	6.83	7.09	0.26
(c)	6.98	7.24	0.26

[a] at pH values below the pK of the hydroxyl group.

TABLE V.10

Numbers of Aromatic Protons[a] in sequence and Number of Resonances Assigned

Type of Amino Acid	Number in Sequence		Number Assigned	
	Residues	Protons	Residues	Protons
His	1	2	1	2
Phe	3	15	0	0
Trp	6	30	6[b]	15
Tyr	3	12	3	12
Total	13	59	10	29

[a] non-exchangeable protons only.

[b] this is 5 if A13 is not a singlet.

is rather broad (see later) and is not observed in Fig. IV.15. If A13 turns out not to be a singlet resonance, then another singlet must be broad also, for there are 8 expected from the sequence (1 His C(2)H, 1 His C(4)H, 6 Trp C(2)H). The sequence information is given in Table V.10. It is to be noted that no phenylalanine protons have been definitely assigned.

V.2.2.2 Exchangeable Hydrogens

The resonances of the indole N(1)H proton of 5 of the 6 tryptophan residues have been observed (Glickson *et al.*, 1971), as shown in Table V.11. The sixth resonance is either very broad or shifted underneath other resonances above 9.5 ppm. It is most desirable that each N(1)H resonance should be related to the C(2)H resonance corresponding to the same residue. One way of doing this would be to attempt to observe coupling between the resonances, although spectra of tryptophan itself indicate that this is only *ca.* 2 Hz. Direct irradiations of NH resonances (of solutions in D_2O, before NH exchange had taken place) failed to produce any observable effect in the aromatic CH region. The best chance however will be to use the spin echo double resonance method of Section III.2.3.3.

V.2.3 Other Resonances

V.2.3.1 High Field CH Resonances

Only four resonances to high field of the HOD resonance (*ca.* 5 ppm) have been separately observed (with the exception of those of methyl groups). These are listed in Table V.12. All are of one proton area. Spin-decoupling has revealed that H1 is coupled to the ile 98δ resonance (M4).

TABLE V.11

Indole N(1)H Proton Resonances [a]

Resonance Number	Chemical Shift (ppm)	Maximum pH at which observable [b]	Comment
N1	10.73	8	
N2	10.39	7	
N3	10.26	5.5	Broader than others
N4	10.06	5.5	
N5	10.04	5.5	
N6	-	Not observed	

[a] 54°C, H_2O resonance saturated by long pulse method.

[b] all are separately observed at low pH values.

TABLE V.12

High-Field CH Proton Resonances

Resonance Number	Chemical Shift (ppm)	Comment
H1	-2.10	Coupled to M4
H2	-0.91	
H3	-0.38	
H4	0.09	

TABLE V.13

Low-Field CH Proton Resonances

Resonance Number	Chemical Shift (ppm)	Comment
L1	5.81	Singlet in D_2O, doublet in H_2O
L2	5.64	
L3	5.50	
L4	5.42	pH shift, pK ~ 8.5

V.2.3.2 Low Field CH Resonances

A number of peaks of area equal to one proton are observed to low field of the HOD resonance. Four have been examined in some detail, and these are listed in Table V.13. Resonance L1 is coupled to a slowly exchanging NH resonance as shown by its change in coupling following solvent exchange cycles (see Fig.III.8). Resonance L4 shifts upfield with pH, and appears to titrate with a pK of 8.5 $\pm$ 0.5. This pK value, according to previous studies (Imoto *et al.*, 1972) must be of the N-terminal amino group. The large shift with pH (more than 0.3 ppm) suggests the assignment of this resonance to the α-CH of the N-terminal residue, Lys 1. In the presence of shift probes, particularly Pr^{3+}, a number of other resonances can be observed to be shifted out of the main spectral envelope but have not been characterised. A number of these have small J values, and therefore appear as sharp singlets (*cf.* L1).

V.3 Assignment to a Particular Residue

Assignment to a particular residue in the protein sequence requires conformational information. Thus, the effects of the specific binding of conformational probes, and the effects of the intrinsic probes were examined. By making use of the assignment information already obtained, any resonance perturbed by the probes could be assigned to a type (or to one of two types) of amino acid residue. Thus, the types of residue in the vicinity of the probes were discovered. At this stage, the X-ray structure of lysozyme was used. By examining the region of the structure around the known probe position, the types of amino acid residue whose resonances would be predicted to be perturbed could be discovered. These predictions were then compared to the

experimental findings. This comparison can at this stage be qualitative. Consistent assignments can be made by this approach only if the X-ray structure is a good overall description of the solution structure. Therefore the assignment process involves a 'low-resolution' definition of the solution structure in terms of similarity to the X-ray structure. An absence of correspondence between the structural data obtained by the two methods would imply that the solution and crystal structures are different.

Quantitative comparison of the X-ray and nmr results is only possible if due allowance is made for the intrinsic differences between the two methods. This quantitative comparison will be made in Chapter VII.

V.3.1 The Use of Gd^{3+}

Lysozyme has been shown to bind Gd^{3+} in the crystalline state (Blake and Rabstein, 1970) and in solution (Morallee et al., 1970). The binding is discussed in detail in Chapter VI, where it is shown that a single strong binding site exists. In the crystal, this site is between the carboxylate groups of asp 52 and glu 35. In solution, it has been independently shown that glu 35 is a binding group, which suggests strongly that the binding is similar to that in the crystal. Although other weak binding sites exist, the broadening induced by Gd^{3+} in the resonances considered in this section arises overwhelmingly from binding at the strong binding site. The conditions for fast exchange are also satisfied.

The broadening of resonances by Gd^{3+} was generally measured using difference spectroscopy. These experiments are described in Chapter VI. Several spectra are shown in Fig. V.7. From these, three resonances (M16, M17 and M20) clearly are most broadened. These are of a valine (2 resonances) and an alanine (1 resonance).

FIGURE V.7

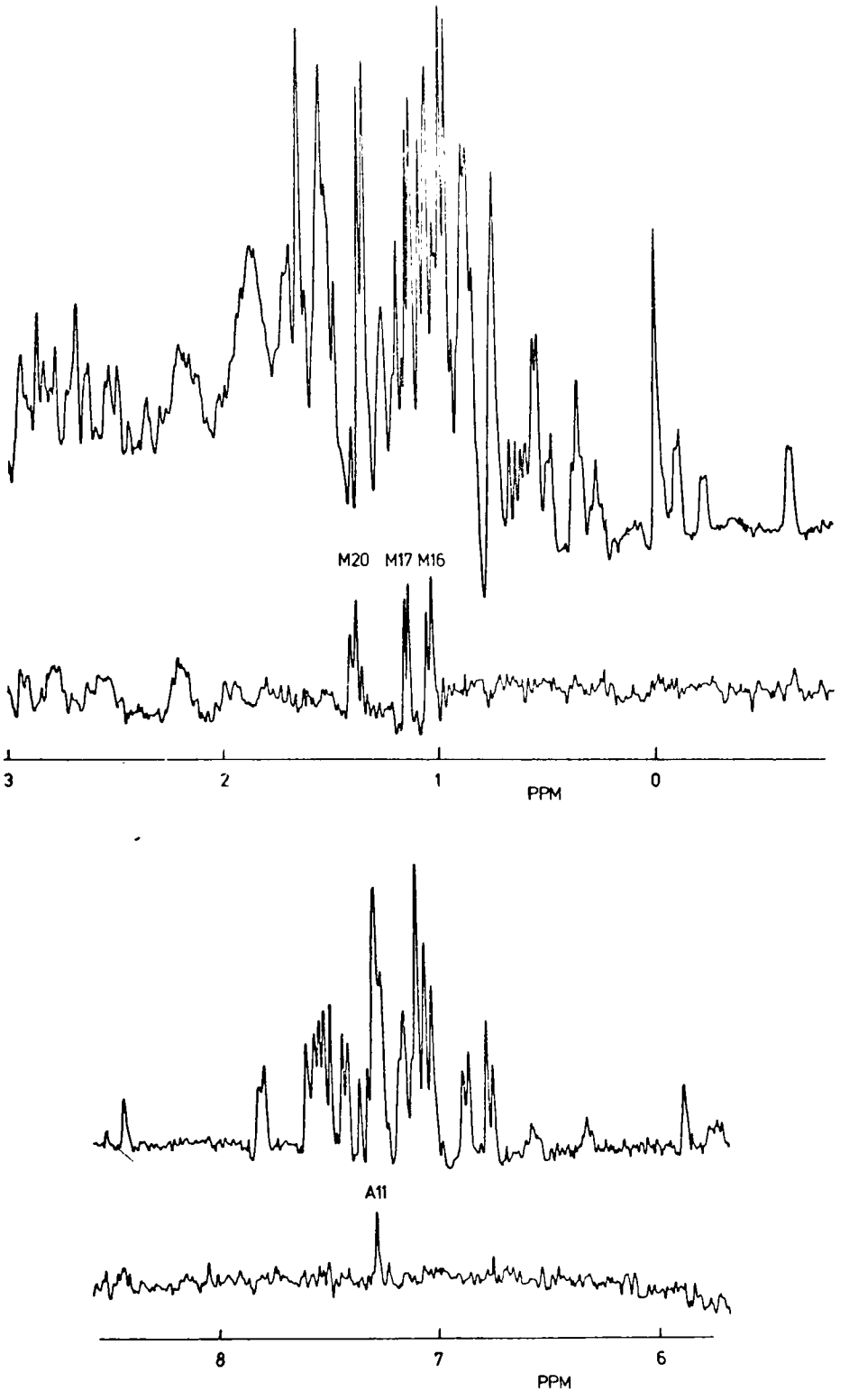

Gd^{3+} difference spectra of lysozyme (5mM lysozyme, 23.8mM La^{3+}, pH 5.3, 54°C, difference between spectra with and without 1.12×10^{-5}M Gd^{3+}) showing that M16, M17, M18 and A11 are observed to be the most broadened non-exchangeable proton resonances. Above the difference spectra are shown convolution difference spectra of the sample in the absence of Gd^{3+}.

FIGURE V.8

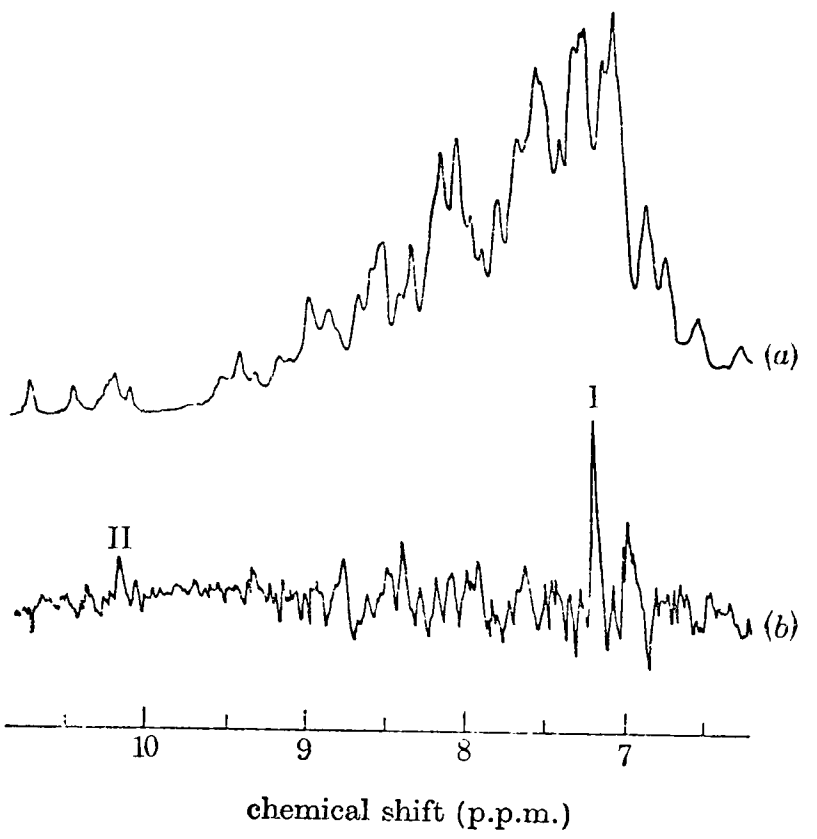

Gd^{3+} difference spectrum for 5mM lysozyme in 90% H_2O, 10% D_2O. (a) Spectrum of lysozyme containing 23.8mM La^{3+}, 54°C, pH 5.3. (b) Difference between this and a spectrum of the same solution containing 1.23×10^{-5}M Gd^{3+}. The vertical scale in (b) is four times that of (a). The H_2O resonance was saturated using the time shared method. Resonance I is A11 and II is N5. Below, the broadening of N5 is shown more clearly. (a) The spectrum of 5mM lysozyme in 90% H_2O, 10% D_2O at pH 5.3, 54°C. (b) The spectrum of the same solution containing 2.8×10^{-4}M Gd^{3+}.

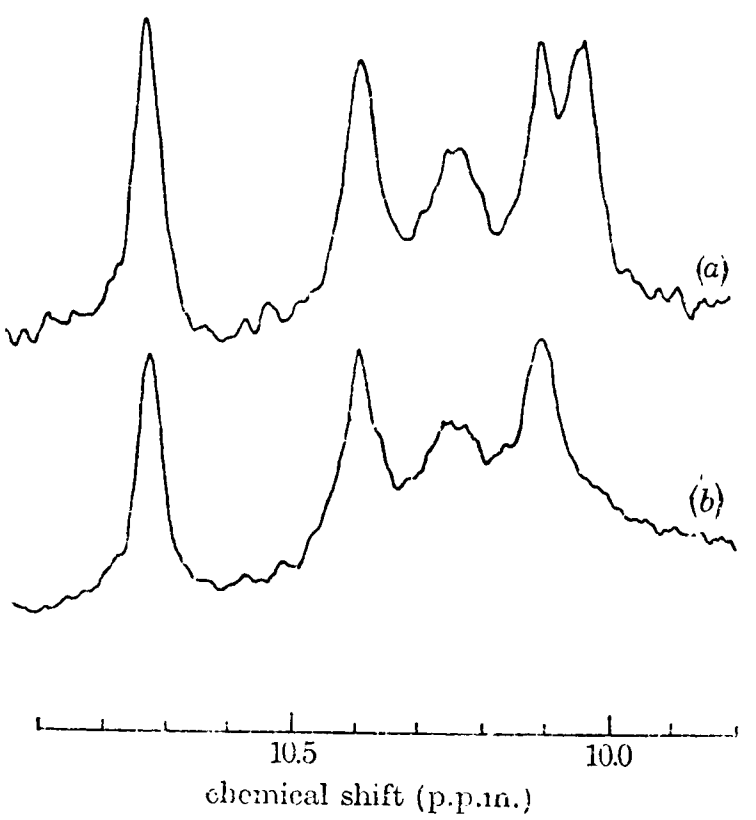

In the aromatic region, one resonance (A11) can be seen in the difference spectrum. This is from a tryptophan C(2)H proton. By performing the same experiments in H_2O solvent, one of the tryptophan N(1) proton resonance (N5) is seen to broaden rapidly (Fig. V.8). Because the broadening is proportional to $1/r^6$, these experiments reveal the binding site of Gd^{3+} in terms of the nearest residue types in solution.

Using atomic co-ordinates derived from the X-ray structure and generating co-ordinates for hydrogen atoms (see Section II.4), the relative values of r and $1/r^6$ for the hydrogens of CH_3 groups and aromatic protons were calculated from the bound Gd^{3+} (the co-ordinates are given in Section VII.2.1) in Ångstroms. This was done using the computer programme MSEARCH (Barry et al., 1973), and allowed for free rotation of CH_3 groups, and for rapid flipping of the aromatic residues tyrosine and phenylalanine through 180^{o}. Motion of both these types of group was required by the nmr observations, and will be described in Chapters VI and VII. These calculations are given in detail later, but at this stage are best illustrated by the diagram in Fig. V.9. The calculations showed that the broadening of methyl group resonances should be greatest for val 109 and ala 110, and of aromatic proton resonances for the C(2)H, and then N(1)H, of trp 108. The exact agreement of proton and residue type (1 ala, 1 val and 1 trp) demonstrates the similarity of the solution and X-ray structure in the Gd^{3+} binding site, and allows direct assignment of these resonances.

As the distance from the Gd^{3+} increases, the broadening becomes less selective, and the possibility of error as a result of a secondary binding site increases. A small number of resonances may however be assigned with confidence. Resonances of one threonine (M9) and of one leucine/valine (M8, M11) are

FIGURE V.9

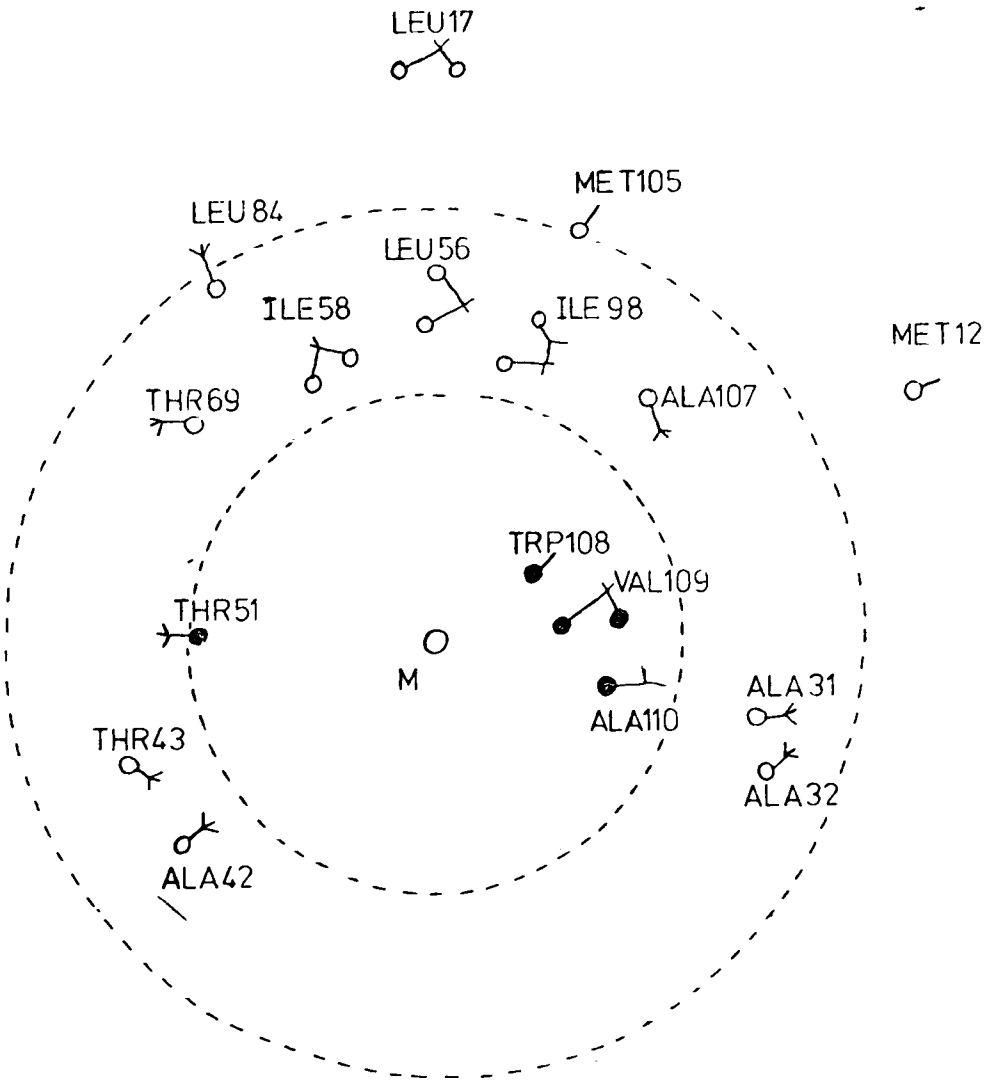

A two-dimensional illustration of some groups near to the bound metal ion. The data are based on the X-ray structure. The circles are drawn at about 10 Å and 15 Å from the metal position.

TABLE V.14

Approximate Distances of Residues[a] from Gd^{3+} in X-ray Structure

Type of Amino Acid	0-9 Å	9-12 Å	12-15 Å	More than 15 Å
Ala	110[b]	42, 107	31, 32, 95	9,10,11,82,90,122
Ile	-	58, 98	55	78, 88, 124
Leu	-	56,83,84	-	8,17, 25, 75, 129
Met	-	-	105	12
Thr	51	43, 47, 69	40	89, 118
Val	109	-	-	2, 29, 92, 99, 120
His	-	-	-	15
Phe	-	-	34	3, 38
Trp	108	62, 63	111	28, 123
Tyr	-	53	-	20, 23

[a] distance to nearest proton

[b] numbers refer to residue number

TABLE V.15

Assignments from Gd^{3+} Broadening

Resonance Number	Amino Acid Type	Relative Broadening[a]	Assignment
M9	THR (ala)	3	thr 51
M8	LEU (val)	3	leu 56[b]
M11	LEU (val)	3	leu 56[b]
M16	VAL	1	val 109
M17	VAL	1	val 109
M20	ALA	1	ala 110
A6	TYR (o-)	3	tyr 53 (o-)
A12	TYR (m-)	(3)	tyr 53 (m-)
A11	TRP C(2)H	1	trp 108 C(2)H
N5	TRP N(1)H	2	trp 108 N(1)H

[a] 1>2>3 is the order of broadening.

[b] a possible assignment to leu 83 or leu 84 is unlikely on consideration of ring current shift data.

substantially broadened. These are assigned (Note Table V.14) to thr 51 and leu 56. These assignments are confirmed subsequently. The resonance of ala 42 is predicted to be broadened, and peaks in the alanine region (i.e. 1.3-1.4 ppm) are observed in the difference spectra. No specific separately observed resonance is assigned to this residue because of the problem of overlapping resonances. Finally, resonances of only one of the three tyrosine residues are substantially broadened (A6 and A12). These are assigned to tyr 53, which in the X-ray structure is much closer (ca. 10 Å) to Gd^{3+} than are tyr 20 or tyr 23 (ca. 20 Å). These assignments are all given in Table V.15. No further assignments are made at this stage. Care has been taken to ensure that these assignments are unaffected by slight differences in the lysozyme solution and X-ray structure, and by movement of even a few Å in the metal position.

An important observation is that resonances of all the methyl groups predicted to be within about 12 Å of Gd^{3+} can be accounted for in the spectrum. No resonances are known to be broadened considerably more than is consistent with the X-ray structure. For example the methyl group singlet resonances of the two methionine residues have been resolved and, as expected from the predicted distances of these groups from the metal ion (greater than 12 Å), they are not greatly broadened. No discrepancies have been observed for aromatic proton resonances, although the analysis of this spectral region is somewhat more complicated.

V.3.2 The Use of $Cr(CN)_6^{3-}$

The addition of $Cr(CN)_6^{3-}$ to lysozyme results in broadening of specific resonances. This broadening has been revealed by difference spectroscopy (Fig. V.10). Resonance A23 is most broadened, and this is known to be of the C(2)H of his 15.

FIGURE V.10

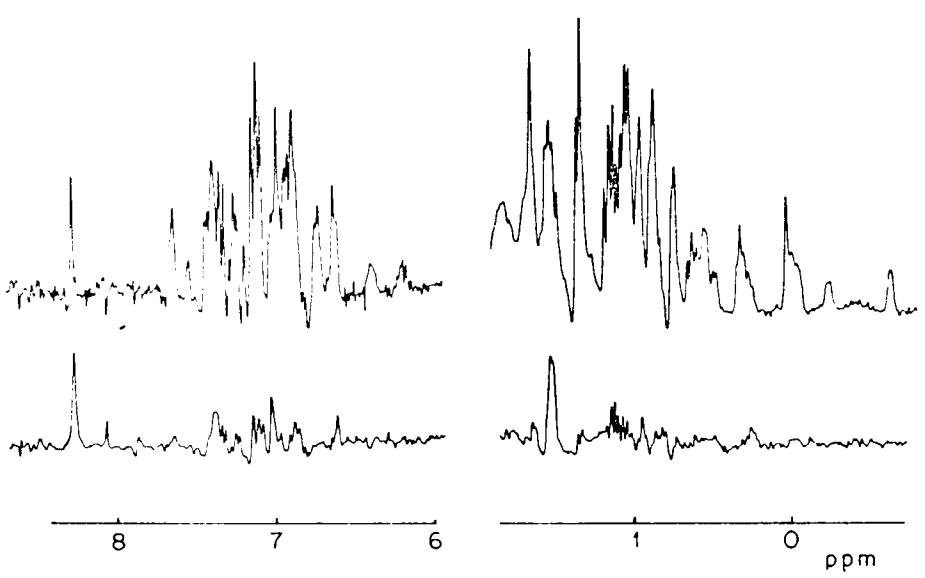

Effect of $Cr(CN)_6^{3-}$ on the lysozyme spectrum. Upper trace is the CD spectrum of 5mM lysozyme at pH 5.3, 37°C. The lower trace is the difference between this spectrum and one of the same solution containing 5×10^{-5}M $Cr(CN)_6^{3-}$.

Also strongly broadened is a resonance at 1.4 ppm. This has not been assigned but may be of CH_2 protons of lysine. Resonance A14, the C(4)H of his 15 is also broadened. In the highfield region, an isoleucine resonance (M7) is broadened. This suggests, and this is subsequently confirmed, that M7 should be assigned to ile 88. However, in order to use broadening probes it is essential to have the binding sites fully characterised. This has not been done for $Cr(CN)_6^{3-}$. An attempt to use $Fe(CN)_6^{3-}$ as a shift probe to characterise the binding sites failed because of the insolubility of the complex formed with lysozyme. Similarly, little success was achieved with anionic lanthanide complexes (e.g. $Ln(edta)^-$). However, these deserve further study. In the X-ray structure, anions such as $PtCl_6^{2-}$ bind close to his 15 (Imoto et al., 1972).

V.3.3 The Use of pH Titrations

The ionisation of side-chain groups may cause local conformational changes to occur. In Chapter IX , details of these conformational changes will be given. In this section, the perturbations of the chemical shift values of specific resonances (arising from local conformational changes) which are observed in pH titrations are used for assignment purposes. In Appendix A, the pK values proposed for the different ionisable groups in lysozyme are tabulated. Two ionisations are quite distinctive, those of his 15 and glu 35. In 0.4M KCl their pK values have been determined to be 5.7 ± 0.1 and 6.2 ± 0.2. No other pK values are between 5 and 7. These pK values are readily measured from the spectrum, that of his 15 from the characteristic shifts of the C(2)H and C(4)H resonances (A23 and A14), and that of glu 35 from its effect on the trp 108 resonances (A11 and N5). The origin of the pH shifts of the trp 108 resonances is postulated (Chapter

IX) to be due to an interaction between glu 35 and trp 108 when glu 35 is protonated. Several small changes in the spectrum with pH have been noticed. There is no evidence for any substantial conformational change in the range pH 2-11.

In 0.4M KCl, the triplet resonance M7 titrates with a pK value of 5.7 $\pm$ 0.2 (Fig. V.11). The doublet resonance M2 and triplet M4 titrate with pK values 6.0 $\pm$ 0.3. In the presence of 0.05M La^{3+}, the measured pK values (Fig. V.11) are 5.7 $\pm$ 0.2 for M7 and 4.2 $\pm$ 0.2 for M2 and M4. From the his 15 and trp 108 resonances these are the pK values of his 15 and glu 35 under these conditions. The apparent lowering of the glu 35 pK arises because of the binding of La^{3+} (see Chapter VI). Thus M7 must arise from a group close to his 15, and is of isoleucine. The only possible residue is ile 88. This assignment correlates with the conclusions from $Cr(CN)_6^{3-}$ broadening. The other resonances, M2 and M4, are also from isoleucine. Both of these are assigned to ile 98, from its proximity to trp 108 and glu 35. This is confirmed in the next section.

Other assignments from pH titrations are of M10 and M13 to val 92. Both the resonances titrate with the pK of his 15. Val 92 is the only valine or leucine residue in this region of the protein. The alanine resonance, M14, is assigned to ala 31 or ala 107. The resonance is affected by the pK value of glu 35, and is also broadened by Gd^{3+}. No definite distinction at this stage has been attempted. The resonance L4 is assigned to the α-CH of lys 1 because of its large titration with a pK value of 8.5, which must correspond to the terminal NH_2 group. Finally, the resonance A3 titrates upfield by 0.3 ppm with a pK value of 10.0 $\pm$ 0.5. This confirms the assignment to tyrosine, but cannot distinguish between tyr 20 and tyr 23. It does however show that this resonance is not from tyr 53, which is known to have a pK of 12.0

FIGURE V.11

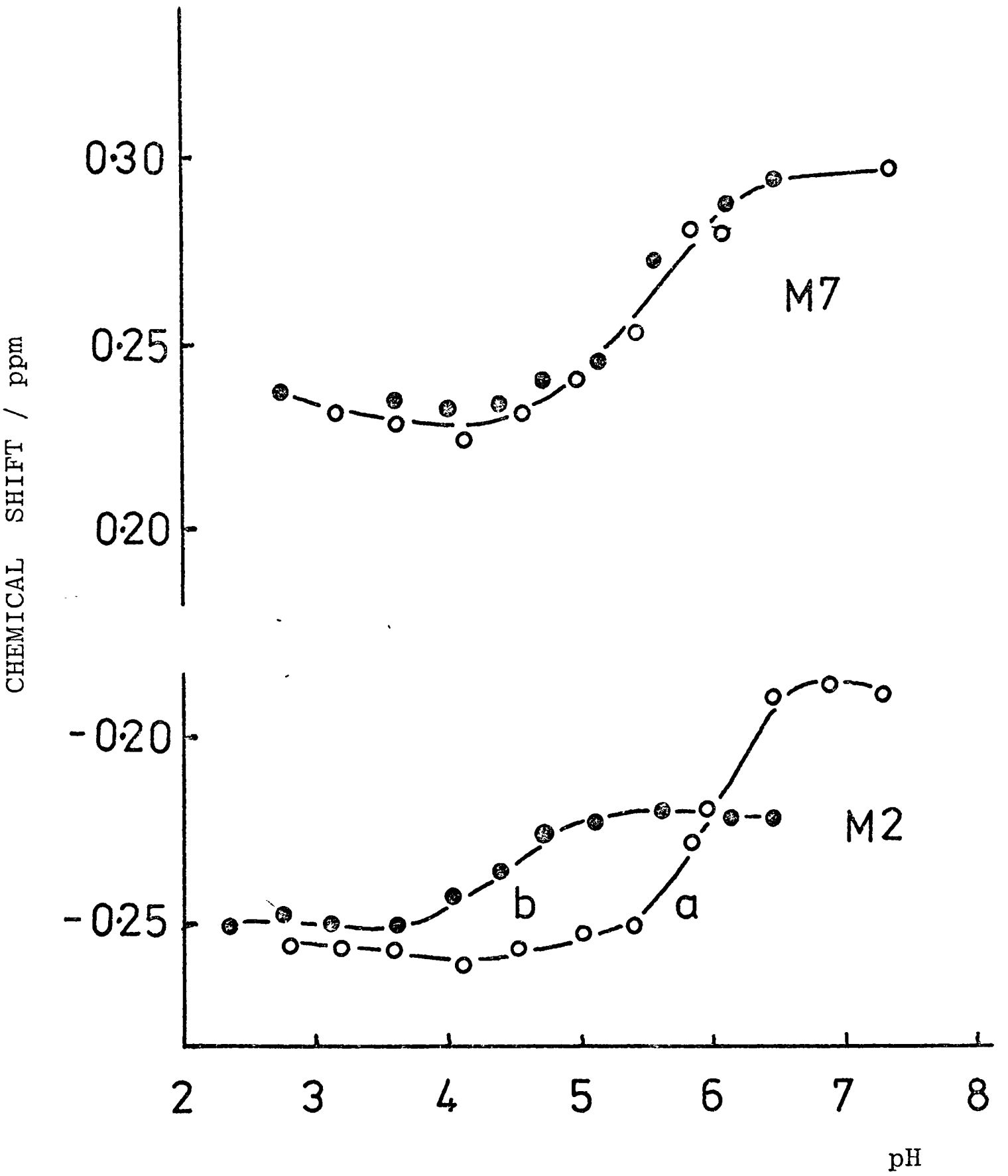

pH dependence of the chemical shift values of resonances M2 and M7 from isoleucine residues. (a) open circles, 0.4M KCl; (b) closed circles, 0.05M $LaCl_3$. 5mM lysozyme, 54°C.

TABLE V.16

Assignments from pH Titrations

Resonance Number	Amino Acid Type	pK reflected	Assignment
M7	ILE δ	his 15	ile 88 δ
M10	LEU/VAL	his 15	val 92
M13	LEU/VAL	his 15	val 92
M2	ILE γ	glu 35	ile 98 γ[a]
M4	ILE δ	glu 35	ile 98 δ[a]
M14	ALA	glu 35	ala 107 (31)[b]
L4	-	terminal NH_2	lys 1
A14	HIS C(4)	his 15	his 15 C(4)
A23	HIS C(2)	his 15	his 15 C(2)

[a] confirmed by ring current shift data.

[b] also broadened by Gd^{3+} (relative broadening 3); could be ala 31 instead of ala 107.

or higher. The assignments from pH titrations are given in Table V.16.

V.3.4 Ring current shift calculations

Previous to this work, no detailed correlation of predicted ring current shift values with observed differences between native and random coil chemical shift values had been achieved. With the assignment already made, this can now be carried out.

Tables of ring current shift predictions for methyl groups of lysozyme have been published (Cowburn et al., 1970; Sternlicht and Wilson, 1967). These are summarised in Table V.17. In Fig. V.12 these predictions have been plotted against some experimental values for the assigned resonances (see Tables V.14-V.16). The correlation is qualitatively, though certainly not quantitatively, reasonable. This results in the conclusion that the use of quantitative values of ring current shifts to make assignments is invalid. However, where qualitative information only is required, where effects are very large, or where additional evidence is available, assignment may be made. The ring current shift values confirm some assignments. For example, thr 51 is the only threonine residue where resonance is predicted to be strongly shifted. Only one threonine resonance is found to high field of 0.7 ppm. This has already been assigned to thr 51 from the Gd^{3+} experiments.

Only two methionine residues are present in lysozyme, and the two singlet methyl group resonances (M6 and M22) are shifted upfield by 2.0 and 0.5 ppm respectively. The most shifted resonance (M6) must be assigned to met 105 (predicted shift 1.4 ppm) whilst the other (M22) must be assigned to met 12 (predicted ring current shift -0.11 ppm). Similarly, leu 8 (M5

TABLE V.17

Predicted[a] Ring Current Shifts of Methyl Group Resonances

Type of Amino Acid[b]	Magnitude of Shift 1-2 ppm	0.5-1.0 ppm	0.2-0.5 ppm	0.2- -0.2 ppm	-0.20- -1.0 ppm
Ile	-	98	88	55(δ),58	55(γ)
Leu	17	8,17	8	56, 75, 83 84, 129	-
Met	105	-	-	12	-
Thr	-	51	-	40, 43, 69 89, 118	-
Val	-	-	-	2, 29, 99, 109, 120	99

[a] mean of Cowburn et al. 1970; Sternlicht and Wilson, 1967.

[b] for residues with two methyl groups, a single number shows both resonances in the same column.

FIGURE V.12

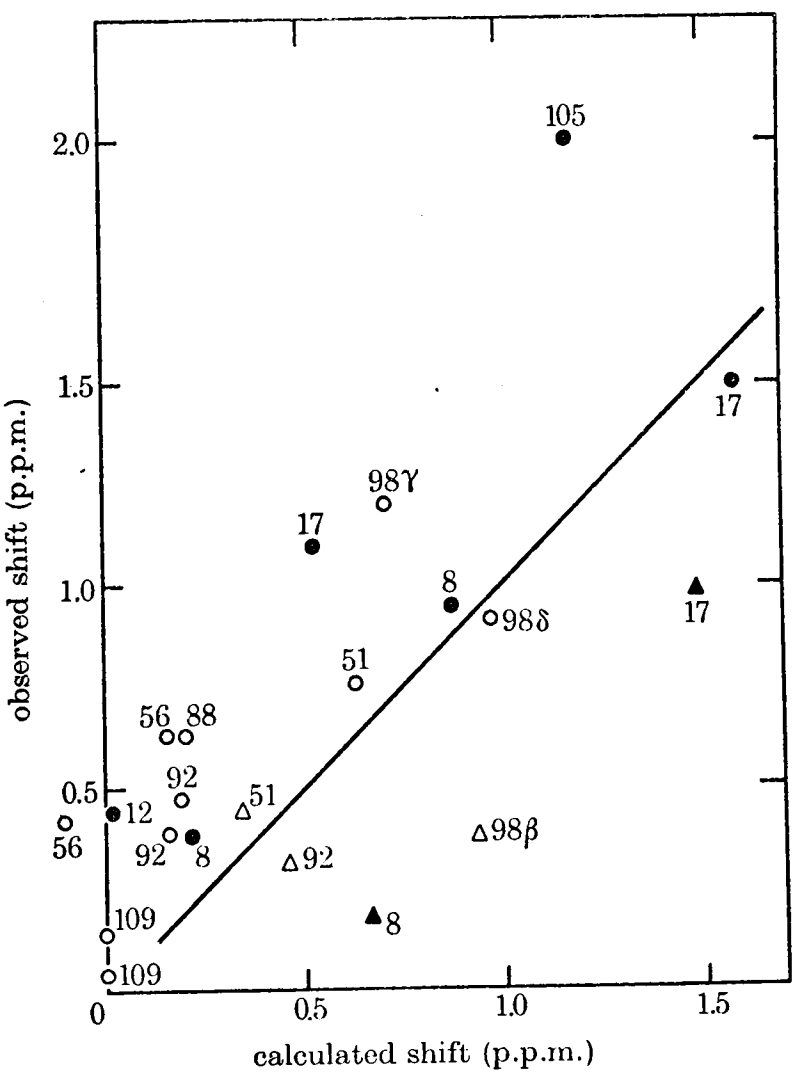

Ring current shift data for a number of resonances of lysozyme. The observed shift is the difference between the chemical shift of a given resonance and the chemical shift of the resonance of the equivalent proton in a free amino acid. The calculated shift is a mean value taken from Cowburn et al. (1970) and Sternlicht and Wilson (1967). Open points refer to resonances assigned by other methods as text. Closed points refer to resonances assigned from this ring current data. Circles refer to methyl group resonances and triangles to the coupled CH resonance. The numbers refer to residues in the sequence.

TABLE V.18

Assignments of Methyl Group Resonances from Ring Current Shift Data

Resonance No.	Amino Acid Type	Assignment	Ring Current Shift (ppm) Observed	Ring Current Shift (ppm) Predicted[a]	Ring Current Shift of Coupled Peak (ppm) Observed	Ring Current Shift of Coupled Peak (ppm) Predicted[a]
M5	LEU (val)	leu 8	0.94	0.86	0.18	0.66
M12	LEU (val)	leu 8	0.39	0.21		
M22	MET	met 12	-0.11	0.44		
M1	LEU (val)	leu 17	1.50	1.58	0.97	1.48
M3	LEU (val)	leu 17	1.10	0.51		
M6	MET	met 105	2.10	1.17		

[a] from mean of Cowburn et al. (1970) and Sternlicht and Wilson (1967) except for met 12 and met 105 which are from Cowburn et al. (1970) only.

and M12) and leu 17 (M1 and M3) may be assigned. No calculations are yet available for alanine residues, or for aromatic residues.

The overall qualitative agreement between nmr observations and the X-ray structure is again found. There are no resonances with large predicted ring current shifts which cannot be observed, nor are there resonances with large observed ring current shifts which are not predicted to be shifted. Assignments from ring current shift calculations are given in Table V.18.

V.3.5 Other Assignments

Most of the methyl group resonances have been assigned by the methods described above. Many of the aromatic proton resonances have not yet been discussed, as unambiguous interpretation of the spectral perturbations, if any, has not been made. In this section rather more tentative assignments will be made for a number of resonances.

The chemical shift values of one set of coupled tryptophan resonances are strongly perturbed (A1, A4, A5 and A22) by secondary (ring current) shifts. No substantial broadening by Gd^{3+} is experienced by these resonances. Resonance A1 and A4 are perturbed by pH with pK values of ca. 4 and of ca. 6. The pK of 6 is that of glu 35. Large shifts are experienced on binding inhibitors and will be described later. This evidence, and an examination of the X-ray structure to estimate possible ring current shifts, suggests that these resonances arise from Trp 63 or Trp 62. The ring current shifts favour Trp 63. Resonance A20, of a tryptophan C(2)H proton experiences a large ring current shift, which is perturbed by pK values of 4 and 6, and by inhibitor binding. This then associates this resonance with Trp 62 and Trp 63, the most likely assignment being to Trp 63.

Inhibitor perturbation and chemical modification studies of

tryptophan N(1)H resonances were used previously (Glickson et al., 1971) to assign the resonances N1 to N5. However, in this work these assignments have been invalidated by the assignment of N5 to trp 108 (not to trp 62 as Glickson et al. (1971) proposed). No assignments for the resonances N1 to N4 are therefore proposed here. The resonances of tyr 20 and tyr 23 have been observed (A3, A10; A8, A15) but not distinguished. A3 and A10 are both about 0.15 ppm to high field of A8 and A15. A3 is observed to titrate with a pK value of 10.0 ± 0.5, whilst A8 is unaffected by pH up to pH 11. $Cr(CN)_6^{3-}$ broadens A3 more than A8. However, none of these pieces of evidence gives an unambiguous assignment.

V.4. Summary of the Assignments

Specific assignments of ca. 40 resonances of ca. 20 residues have been made in this work. They are entirely self-consistent where evidence from various sources was available. The evidence used, and the assignments, are listed in Table V.19. Each resonance was first resolved separately, then assigned to a type of proton, then to a type or to one of two types of amino acid residue, and finally to a specific residue in the sequence.

TABLE V.19

Summary of Totally Assigned Resonances

Resonance Number	Assignment	Information From[a] Gd^{3+}	$Cr(CN)_6^{3-}$	pH	Ring Current
M1/M3	leu 17				*
M2	ile 98 γ	*		*	*
M4	ile 98 δ	*		*	*
M5/M12	leu 8			(*)	*
M6	met 105				*
M7	Ile 88 δ		*	*	(*)
M8/M11	leu 56	*			(*)
M9	thr 51	*		(*)	(*)
M10/M13	val 92			*	(*)
M14	ala 107/31	*		*	(*)
M16/M17	val 109	*			
M20	ala 110	*		(*)	
M22	met 12				*
A1/A5	trp 63 5/6[c]			(*)	*
A4/A22	trp 63 4/7[c]			(*)	*
A6	tyr 53 o-	*			
A12	tyr 53 m-	*			
A11	trp 108 C(2)	*		*	
A14	his 15 C(4)		(*)	*	
A20	trp 63 C(2)[c]			(*)	*
A23	his 15 C(2)		(*)	*	
N5	trp 108 N(1)	*		*	
H1	Ile 98 γ-CH_2	[b]			*

[a] an * indicates that positive information from the techniques here (see text) has been obtained. The brackets indicated that this information was not used in the assignment argument.

[b] coupled to M4, which has been assigned to ile 98.

[c] tentative assignment.

References for Chapter V

Barry, C.D., Dobson, C.M., Ford, L.O., Sweigart, D.A. and Williams, R.J.P. (1973), in Nuclear Magnetic Resonance Shift Reagents (Sievers, R.E. ed.), Academic Press (N.Y.), 173.

Blake, C.C.F. and Rabstein, M.A. (1970), unpublished data.

Cohen, J.S. and Jardetzky, O. (1968), Proc. Natn. Acad. Sci. U.S.A. 60, 92.

Cowburn, D.A., Bradbury, E.M., Crane-Robinson, C. and Gratzer, W.B. (1970), Eur. J. Biochem. 14, 83.

Glickson, J.D., Phillips, W.D. and Rupley, J.A. (1971), J.Amer . Chem. Soc. 93, 4031.

Imoto, T., Johnson, L.N., North, A.C.T., Phillips, D.C. and Rupley, J.A. (1972), in The Enzymes Vol. VII, 3rd Ed. (Boyer, P.D., ed.), Academic Press (N.Y.), 665.

Johnson, L.N. (1973), personal communication.

Karplus, S., Snyder, G.H. and Sykes, B.D. (1973), Biochemistry 12, 1323.

McDonald, C.C. and Phillips, W.D. (1969), J. Amer. Chem. Soc. 91, 1513.

McDonald, C.C., Phillips, W.D. and Glickson, J.D. (1971), J.Amer. Chem. Soc. 93, 235.

Morallee, K.G., Nieboer, E., Rossotti, F.J.C., Williams, R.J.P., Xavier, A.V. and Dwek, R.A. (1970), J.C.S. Chem. Comm., 1132.

Redfield, A. and Gupta, R.K. (1971), Cold Spring Harb. Symp. Quant. Biol. 36, 405.

Roberts, G.C.K. and Jardetzky, O. (1970), Adv. Protein Chem. 24, 448.

Sternlicht, H. and Wilson, D. (1967), Biochemistry 6, 2881.

CHAPTER VI

MEASUREMENT OF LANTHANIDE ION INDUCED SPECTRAL PERTURBATIONS

VI.1 Introduction

In order to make a detailed comparison of the crystal and solution structures of lysozyme, it is necessary to employ a method by which observable nmr effects may be quantitatively compared to the X-ray structure of the molecule. The most promising procedures are those based on the spectral perturbations induced by the specific binding of paramagnetic lanthanide ions (Barry et al., 1971, 1974; Dobson and Levine, 1975). As summarised in Chapter VII under certain conditions the shift induced in the resonance frequency of a nucleus by a paramagnetic lanthanide ion other than Gd^{3+} is proportional to $(3\cos^2\theta-1)/r^3$ where r is the distance from the metal ion to the nucleus, and θ is the angle between the vector joining the metal ion with the nucleus and the principal axis of symmetry of the metal ion (See Chapter VII). The broadening (relaxation) of a resonance is proportional to $1/r^6$. Thus both distance and angular information are available.

In order to use the lanthanide ions as conformational probes, a procedure has been developed from the results of a number of studies of small molecules (see Dobson and Levine, 1975). This procedure will be followed here, and its purpose is to determine the ratios of the shift and of the broadening effects experienced by different resonances as a consequence of lanthanide binding at single defined sites. These ratios are required for the conformational analysis. First, the binding of lanthanide ions must be investigated in order to define the number, characteristics

and positions of the binding sites. These investigations may be carried out using nmr methods. Secondly, from the observed shift and relaxation measurements, the ratios of these effects caused by binding at each site separately must be calculated.

VI.2 Investigation of Lanthanide Ion Binding

The binding of lanthanide cations to lysozyme in solution has been investigated by proton relaxation enhancement (pre) methods (Dwek et al., 1971; Jones et al., 1974) and by uv methods (Secenski and Lienhard, 1974). Both these studies concluded that a single relatively strong binding site exists, but neither study would have been able to detect sites of weaker binding in the presence of this site. In the solid state, binding of lanthanide ions to the tetragonal crystal form was studied at low (6Å) resolution and binding at a single site (between the carboxylate groups of glu 35 and asp 52) was observed (Blake and Rabstein, 1970). More detailed studies of binding to the tetragonal crystals (Perkins, 1975) and to the triclinic crystals (Jensen, 1974) appear to show that there are several distinct binding sites in the region of glu 35 and asp 52. There is thus some uncertainty in the binding to crystalline lysozyme. One possible reason for this can be proposed from the solution studies of binding described below. The X-ray studies were performed by soaking crystals in Gd^{3+} solutions at pH 4.7. At this pH value, asp 52 is ionised but glu 35 is not, as the pK of glu 35 is over 6.0. There may therefore be binding to asp 52 only at this pH. As binding of Gd^{3+} in solution is much stronger to the ionised form of glu 35 than to the non-ionised form this is likely to remain true in the crystal. Thus, the Gd^{3+} could also displace the proton of glu 35 on binding to lysozyme. Now in solution this results in an induced conformational change. It

is possible that in the crystalline state the conformational change is restricted. Evidence for this comes from the fact that the crystals of lysozyme crack when occupancy of more than ca. 30% of the binding sites occurs (Perkins, 1975). Taking these facts together, this could mean that the different binding sites observed in the crystals correspond to binding to different ionisation states and to different conformations of the protein. Such a situation would not arise in solution where rapid conformational changes can occur. Until more detailed studies have been made, it may be stated only that binding in the region of glu 35 and asp 52 occurs in the crystals.

The investigation of the binding in solution by nmr was carried out by performing two different types of experiment. Both of these involved measurements of lanthanide induced shifts. (The broadening induced by lanthanides is difficult to measure quantitatively over a wide range of conditions). First, at a fixed pH value and a fixed concentration of lysozyme, the concentration of lanthanide ions in solution was varied. Secondly, at a fixed concentration of lysozyme and of lanthanide ions, the pH was varied. A summary of all the experiments performed is given in Appendix C.

VI.2.1 Binding Studies by Nmr

All the shifts to be discussed below show that conditions of fast exchange apply. This means that the observed shift of a nucleus i (δ_i) induced on binding a lanthanide (M^{3+}) to a ligand (L^-) depends on the fraction (f) of ligand bound to the lanthanide. Consider the simple binding scheme

$$M^{3+} + L^- \rightleftharpoons ML^{2+}$$

where $K = [ML^{2+}]/[M^{3+}][L^-]$ and $f = [ML^{2+}]/([ML^{2+}]+[L^-])$. The

observed shift $\delta_i = f\ \Delta_i$ where Δ_i is the induced shift for the fully formed complex ML^{2+}. Thus measurement of δ_i, and therefore of f, as a function of variables such as the relative concentration of M^{3+} and L^- allows the extraction of binding parameters in the manner familiar for any spectroscopic technique (Rossotti & Rossotti, 1961). Binding schemes more complex than that illustrated above may of course be treated. Binding of other species (e.g. of H^+) may be investigated by nmr whenever binding of the species results in a change in chemical shift values.

VI.2.2 Binding Curves at Fixed pH

The effects on the nmr spectrum of lysozyme of varying concentrations of lanthanide ions were examined for each lanthanide. Detailed binding curves were calculated for Pr^{3+}, Eu^{3+} and Yb^{3+} at lysozyme concentrations of 5mM and 1mM. The effects of ionic strength changes on the spectra were investigated by using KCl to maintain a given ionic strength. The effects of the diamagnetic lanthanides, La^{3+} and Lu^{3+}, were investigated in order to calculate the paramagnetic contribution to the shifts induced by the other lanthanides.

VI.2.2.1 Titrations with Diamagnetic Ions

The effects of La^{3+} and Lu^{3+} on the spectrum of lysozyme are not large. Several of the spectral changes were also observed on addition of KCl, showing that the effects of changes in ionic strength (μ) as well as metal ion binding must be considered. For example, shifts of the his 15 resonances result from a change in the pK values of this residue from 5.2 at $\mu = 0$ to 5.6 at $\mu = 0.4$ at $54^{o}C$. Several shifts of resonance positions do result from the binding of the diamagnetic ions.

In particular resonances of trp 108 (C(2)H and N(1)H, resonances A11 and N5), and of methyl groups of thr 51 (M9), leu 56 (M8) and ala 110 (M20) are affected. The observed shifts at pH 5.3 are discussed again in Chapter IX. There are small differences between the effects of La^{3+} and Lu^{3+}. All these affected residues are close to the region of the expected binding groups, asp 52 and glu 35.

VI.2.2.2 Titrations with Paramagnetic Ions

The shifts measured for La^{3+} and Lu^{3+} were subtracted, at the relevant concentrations, from the observed shifts induced by the paramagnetic ions. The paramagnetic induced shifts were then plotted against the concentration of lanthanide ion in the solution. The behaviour of the different resonances suggested that conditions of fast exchange were satisfied, and that the shifts arose from several sources. The type of behaviour of each different observed resonance is summarised in Appendix D, and these types will now be described. Essentially similar conclusions are reached with the different paramagnetic ions.

(a) Certain resonances suffer shifts which are essentially linear in the concentration of lanthanide over a wide concentration range (0-0.2M). These shifts are independent of pH (3.5-6.0) and of the concentration of lysozyme (1-5mM), as Fig. VI.1 shows. This indicates that the shifts are not connected with the binding of lanthanide ions to ionisable groups on the protein. In addition, this type of shift is a nearly equal contribution to the shifts of all resonances in the spectrum. The similarity of these shifts for the different resonances makes it unlikely that non-specific binding to the protein is a sufficient explanation, as this would affect surface residues more than

FIGURE VI.1

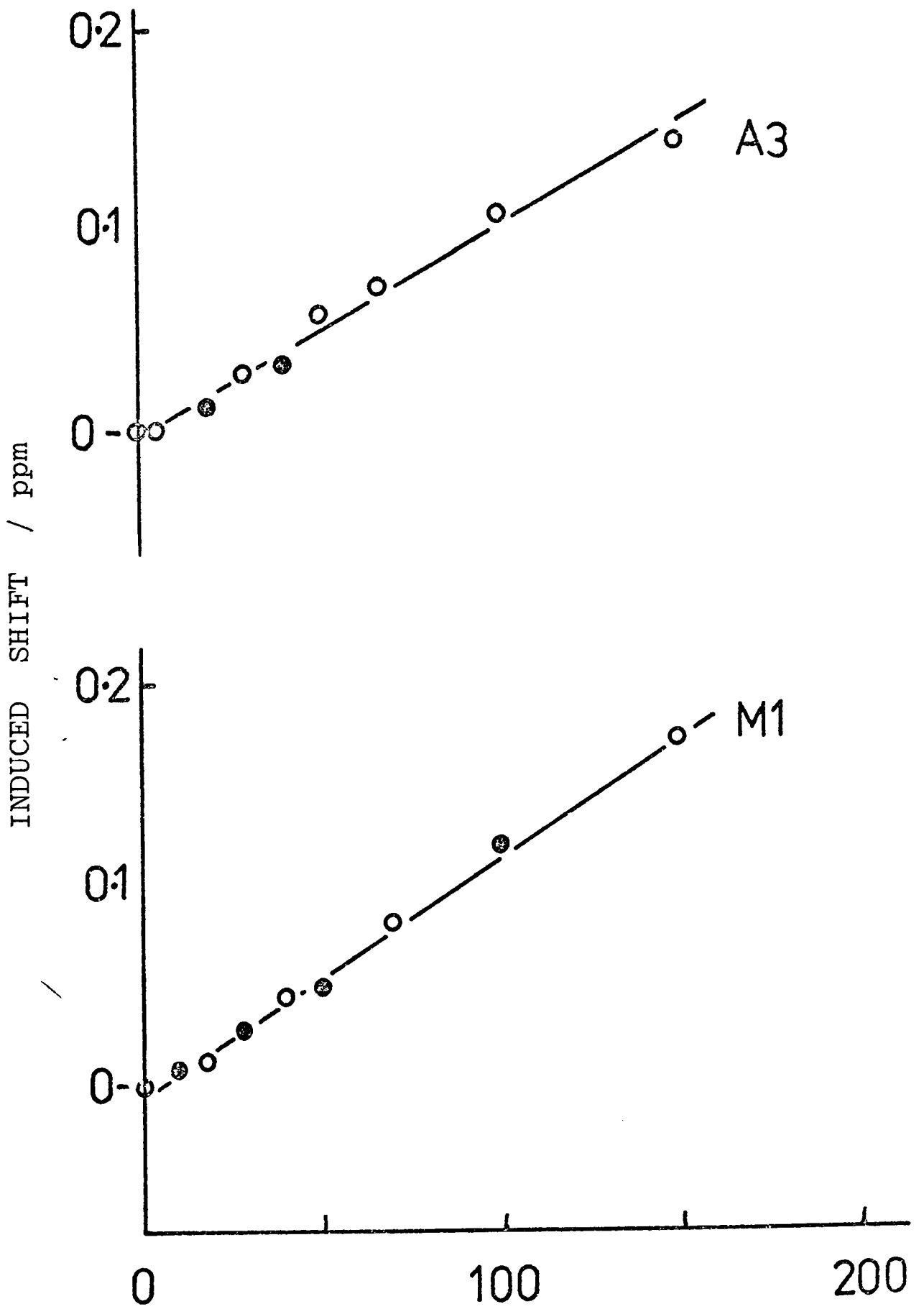

Shifts induced in the chemical shift values of resonances A3 and M1 as a function of the concentration of Yb^{3+}. Open circles, pH 5.3; closed circles, pH 4.3. 5mM lysozyme, $54^{o}C$.

internal ones. A more likely explanation of the effect is that the internal standards (acetone and dioxan) which are both in free solution are shifted by weak interactions with the lanthanides, possibly by collisional processes, whilst most of the protein groups, not being exposed to the solvent, are not shifted. The direction of the shifts with different lanthanides shows that they are due to pseudocontact and not to bulk susceptibility effects. Some support for this mechanism comes from preliminary observations that the resonance of $N(CH_3)_4^+$ is shifted relative to acetone and dioxan. This species would be repelled by the lanthanide cation and therefore behave to some extent like the internal groups of the protein. In any case, these linear shifts are readily subtracted from the observed shifts due to binding which are described below.

(b) Many resonances experience shifts which give rise to binding curves typical of those arising from binding at a specific site, provided the linear correction described above is made. Some curves are shown in Fig. VI.2. Binding constants may be obtained from these curves (see below), and these binding constants are pH dependent, implicating a group of pK value of at least 6.0. These resonances (Table VI.1) are all of groups relatively close to asp 52 and glu 35, as the Gd^{3+} broadening described in the previous chapter reveals.

(c) A number of resonances show titration curves which have different characteristics from those of category (b). These curves demonstrate binding to weaker sites, and implicate groups of pK value closer to 4 than to 6. In some cases, as in Fig. VI.3, the effect of binding at more than one site is observed. All these results are summarised in Table VI.1.

Titrations of the type above are difficult to interpret

FIGURE VI.2

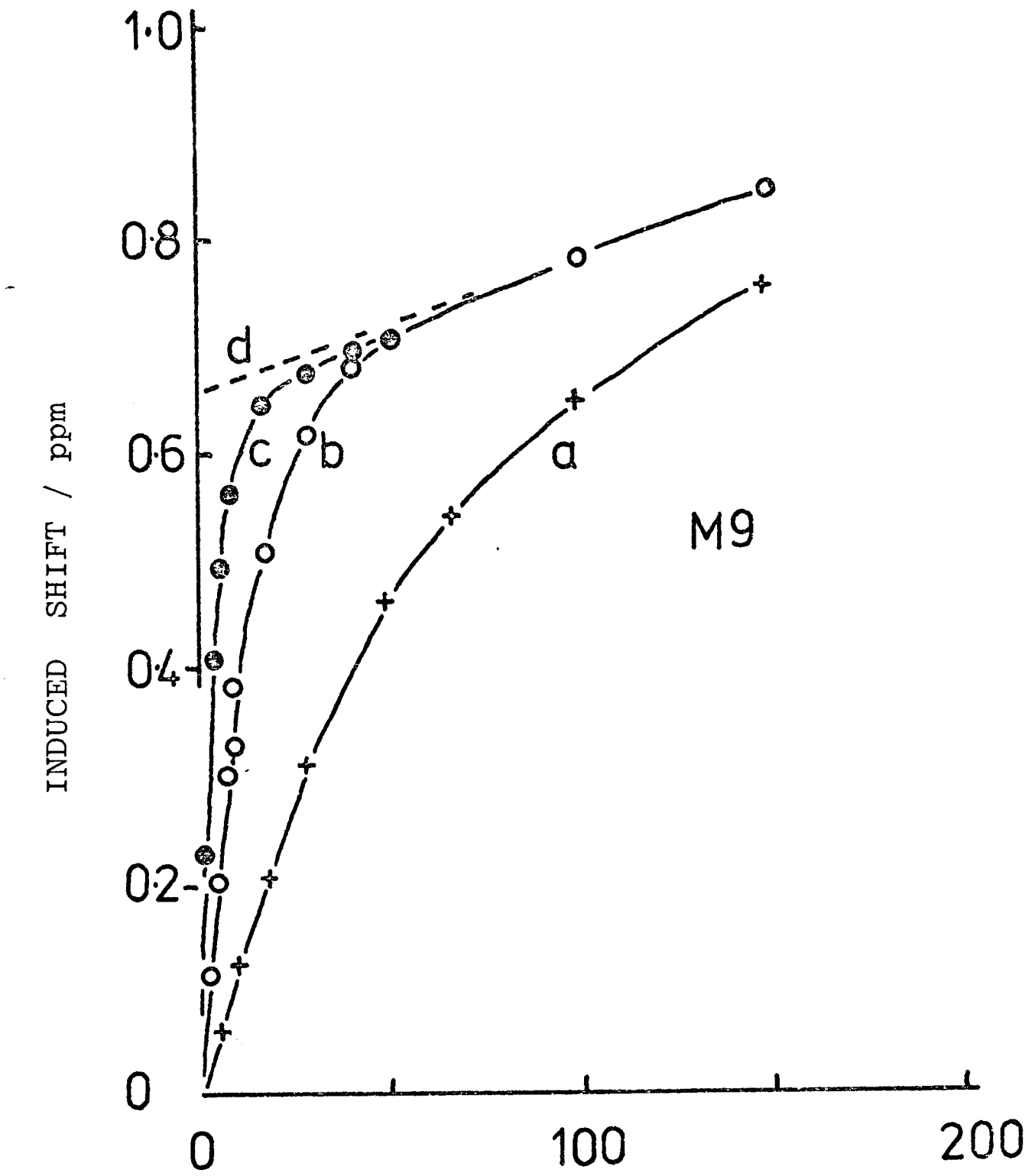

Shifts induced in the chemical shift values of M9 as a function of the concentration of Yb^{3+}. (a) pH 4.3; (b) pH 5.3; (c) pH 5.8; (d) extrapolation of linear contribution. 5mM lysozyme, 54°C.

FIGURE VI.3

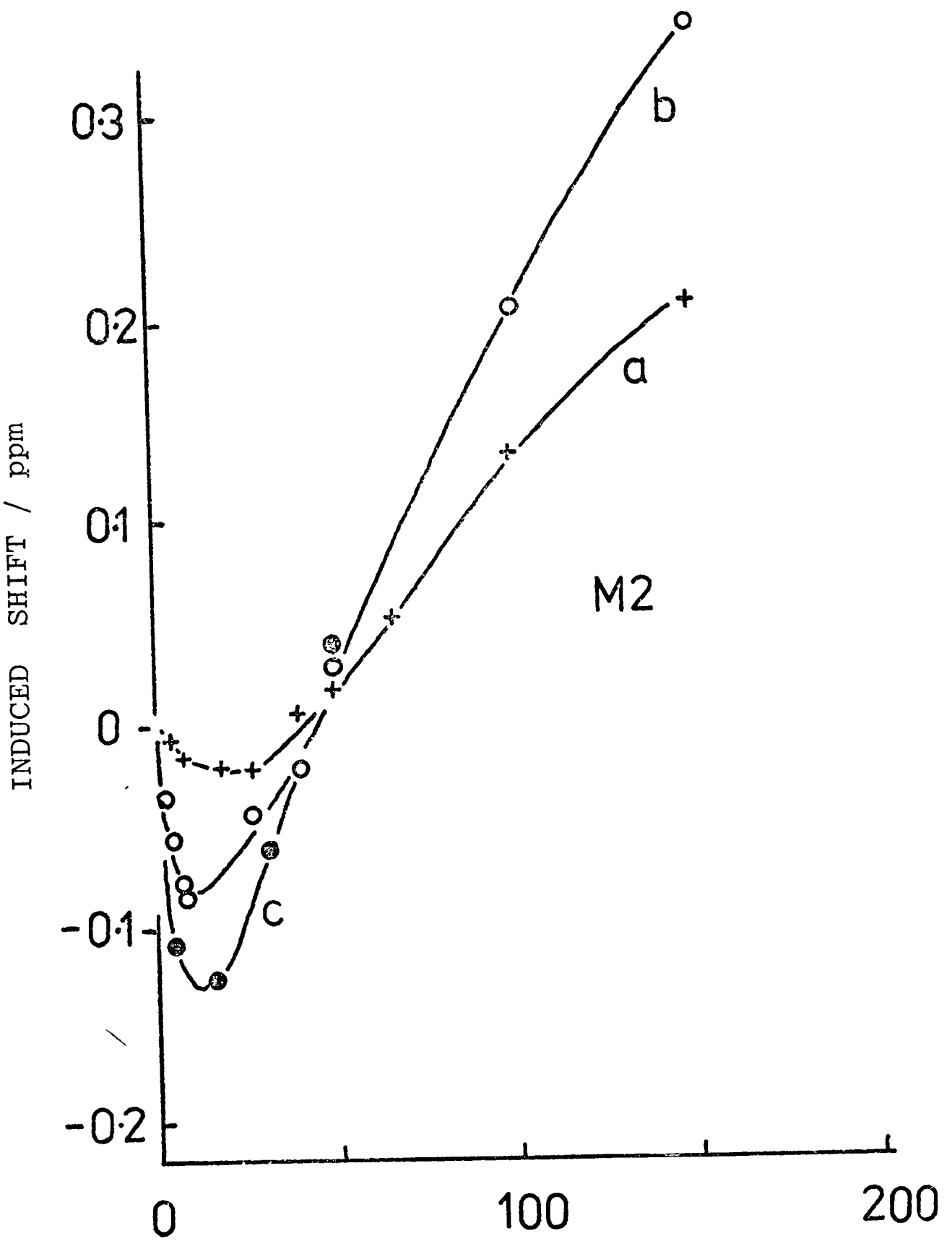

Shifts induced in the chemical shift values of M2 as a function of the concentration of Yb^{3+}.
(a) pH 4.3; (b) pH 5.3; (c) pH 5.8. 5mM lysozyme, 54°C.

FIGURE VI.4

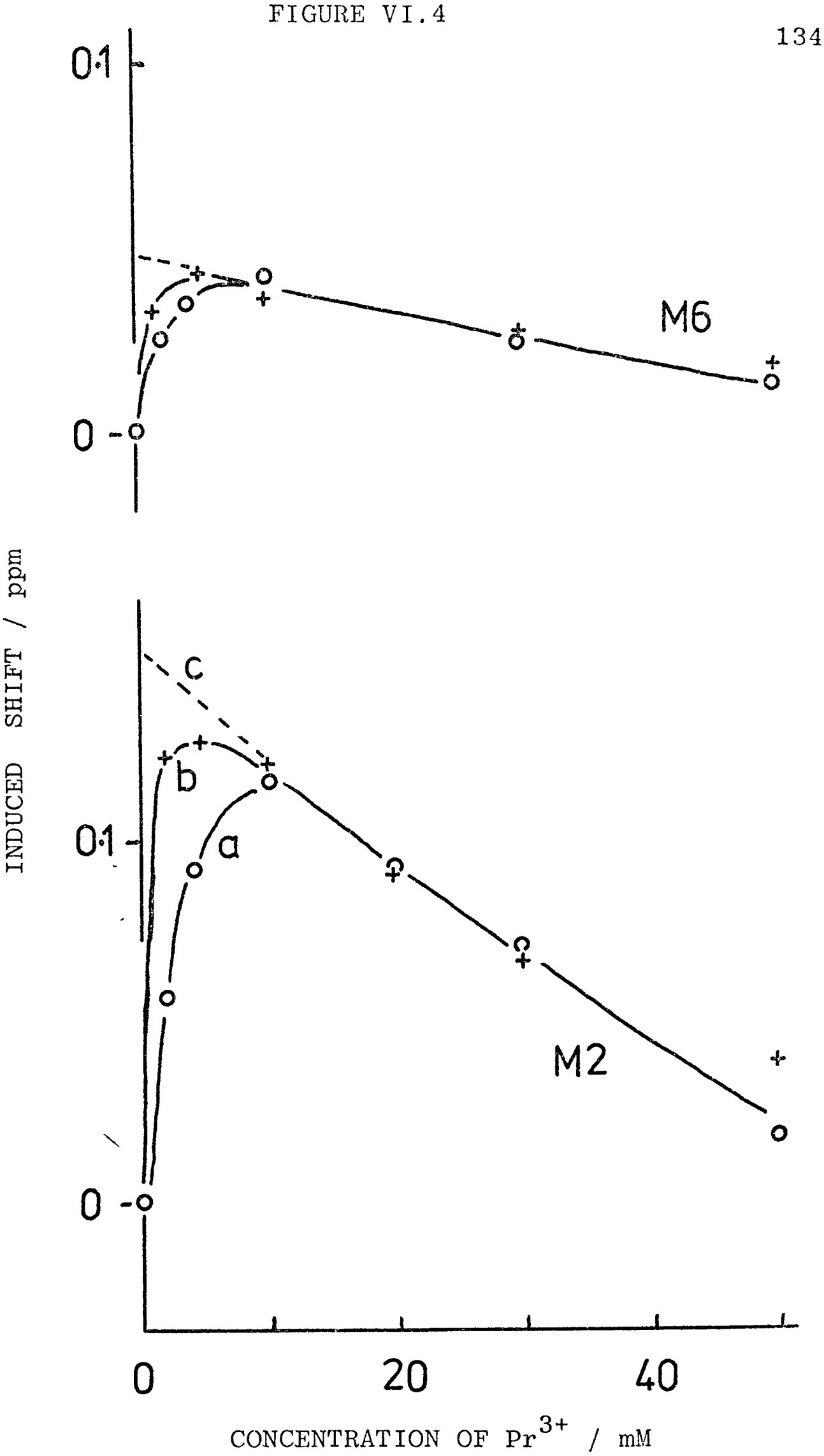

Shifts induced in the chemical shift values of M2 and M6 as a function of the concentration of Pr^{3+}. (a) pH 5.3; (b) pH 6.0; (c) extrapolation of shifts not from major site. 5mM lysozyme, 54°C.

TABLE VI.1

Ln^{3+} Titration Behaviour of Resonances[a] of Specific Residues

Behaviour Type[b]	Residue (Resonance Number)
(a)	leu 17 (M1,M3), met 12 (M22), trp 63 (A1)
(b)	thr 51 (M9), tyr 53 (A6,A12), leu 56 (M8) trp 63 (A20), met 105 (M6)[c], ala 107 (M14) trp 108 (A11,N5)
(c)	leu 8 (M5), his 15 (A23), trp 63 (A22)[d] ile 88 (M7), val 92 (M10,M13), ile 98[d] (M2,M4)

[a] for assigned resonances for which complete titration curves were observed, see Appendix D.

[b] see text; (a) has no shift from specific binding site; (b) has shift only from major site; (c) has shift from minor site, but may be from major site also.

[c] this resonance has an anomalous titration curve for Yb^{3+}.

[d] large shift from major site also.

further although comparison of titration curves at different protein concentrations is useful (Fig. VI.4.) Thus, a different type of experiment was carried out.

VI.2.3 pH Titration Curves

It was noted above that the observed binding constants are pH dependent, and that this dependence is different for binding at different sites. Therefore the effects on the observed shifts of changing pH were studied in more detail. pH titrations were carried out for solutions containing 5mM lysozyme, and various concentrations of lanthanide up to 50mM. The ionic strength of all solutions was maintained at 0.4, by using relevant concentrations of KCl. Titrations were carried out as before using Pr^{3+}, Eu^{3+} and Yb^{3+} and also diamagnetic La^{3+} and Lu^{3+}. Spectra were run at $54^{o}C$, and pH values were measured at this temperature.

VI.2.3.1 Titrations with Diamagnetic Ions

In Chapter IX, detailed consideration of the effects of pH on the lysozyme spectrum is given. Large shifts of the his 15 resonances with pH are observed as expected (see Roberts and Jardetsky, 1970) on ionisation of this group. However, the resonances of trp 108 (C(2)H and N(1)H) suffer substantial shifts with pH although the tryptophan itself is not ionisable. A pK value of 6.0 ± 0.1 (at $\mu = 0.4$, $54^{o}C$) for the ionisation effecting these resonances is obtained. This ionisation is that of glu 35 (see Appendix A), and the shifts arise from the interaction of the carboxylic acid group, in its uncharged form, with the ring of trp 108 (Chapter IX). In the presence of 50mM La^{3+}, the titration of the trp 108 resonances reflects a pK value of 4.2 ± 0.1 as

Fig. VI.5 shows. In the presence of 50mM La^{3+}, the pK value is 4.0 ± 0.1. This apparent decrease in the pK value of glu 35 indicates that the lanthanide ions compete with H^+ for the carboxylate group. Note from Fig. VI.5 that the chemical shift value of the C(2)H of trp 108 is very similar for the anionic form of glu 35 (high pH) to that for the La^{3+} or Lu^{3+} bound species.

These data provide positive evidence that the lanthanide binding is dependent on the ionisation of glu 35. This strongly implicates glu 35 as a binding group.

VI.2.3.2 Titrations with Paramagnetic Ions

From the pH titrations in the presence of paramagnetic ions, graphs of observed chemical shift against pH were plotted (see Fig. VI.5.) These were then compared to graphs obtained in the presence of diamagnetic ions, to obtain the induced paramagnetic shift. Strictly, the latter calculation of the induced shift is only valid for identical binding constants of the diamagnetic and paramagnetic ions, and also relies on the diamagnetic effects of all the lanthanides being identical. In practice these conditions are essentially satisfied. From the graphs of induced paramagnetic shifts against pH thus obtained, the conclusions concerning the binding sites are identical to those obtained in Section VI.2.2, and are summarised as follows.

(a) Certain resonances suffer a shift which is essentially independent of pH. This is attributed to the shifts of the internal standards.

(b) Many resonances show titration curves corresponding to strong binding to a group of pK value ca. 6.0, and are those observed

FIGURE VI.5

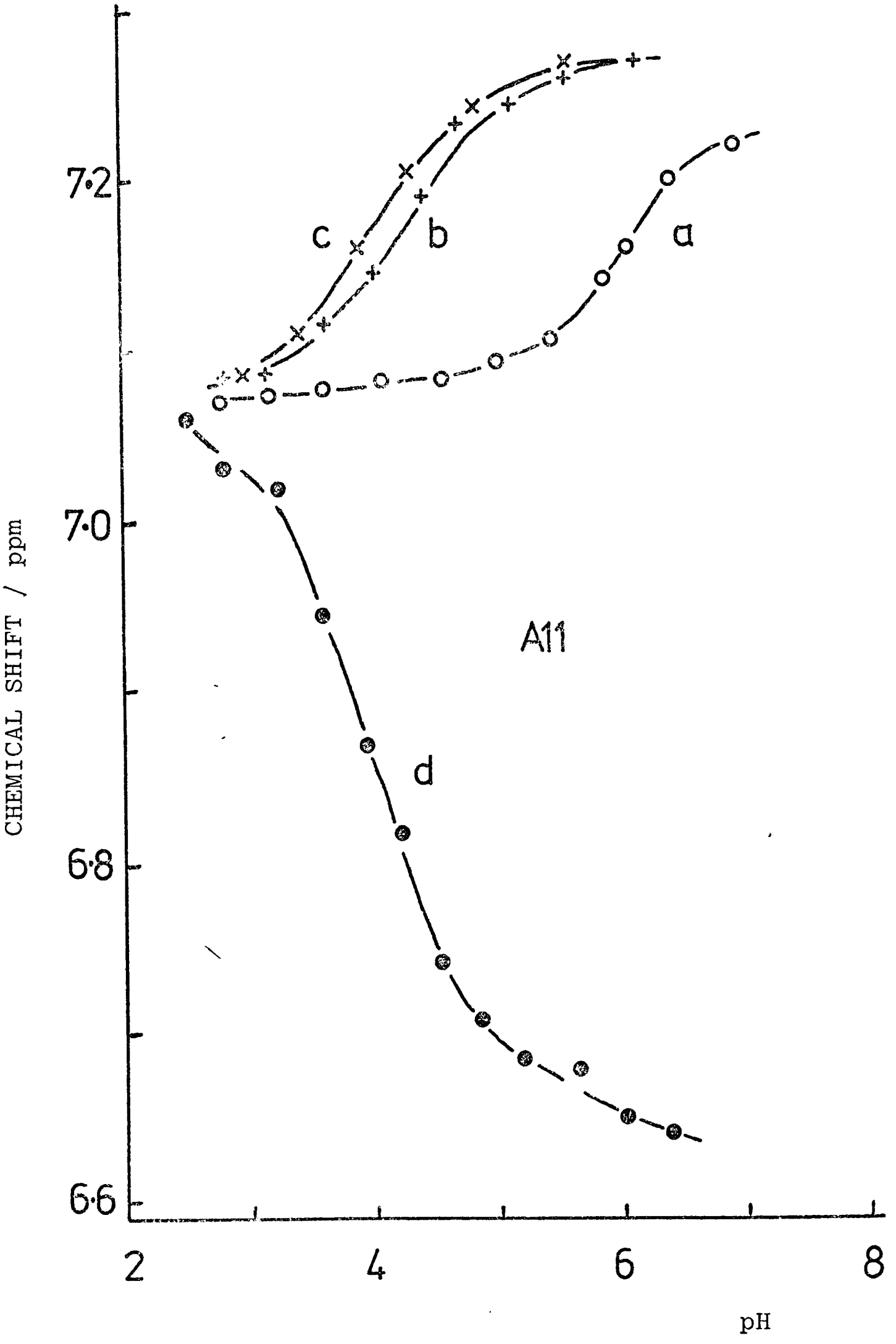

pH dependence of the chemical shift value of resonance All in the presence of (a) 0.4M KCl; (b) 0.05M La^{3+}; (c) 0.05M Lu^{3+}; (d) 0.05M Pr^{3+}. 5mM lysozyme, 54°C.

FIGURE VI.6

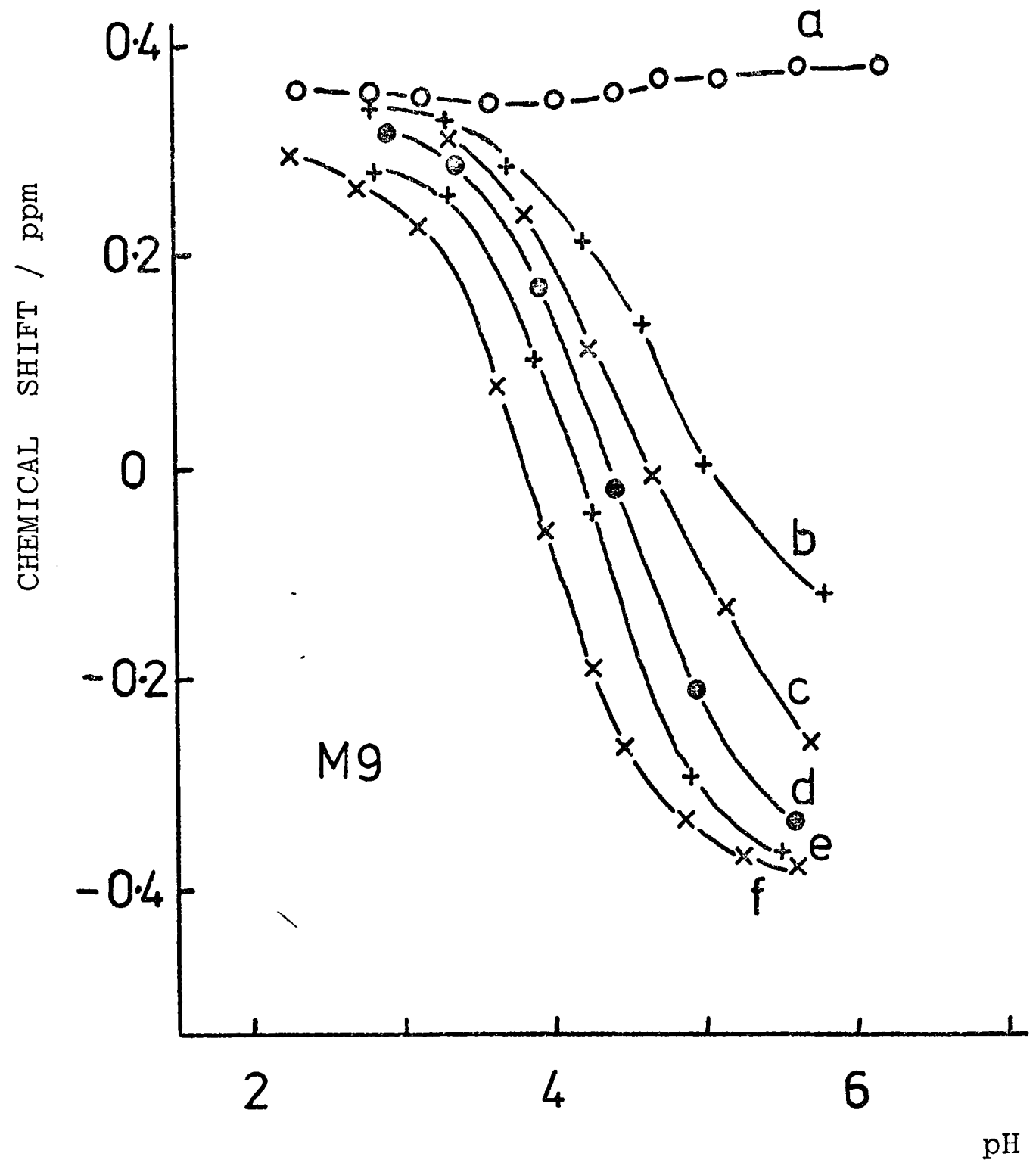

pH dependence of the chemical shift value of resonance M9 in the presence of (a) 0.05M La^{3+}; (b) 0.005M Yb^{3+}; (c) 0.009M Yb^{3+}; (d) 0.015M Yb^{3+}; (e) 0.03M Yb^{3+}; (f) 0.05M Yb^{3+}. For each solution the ionic strength was 0.4. 5mM lysozyme, 54°C.

FIGURE VI.7

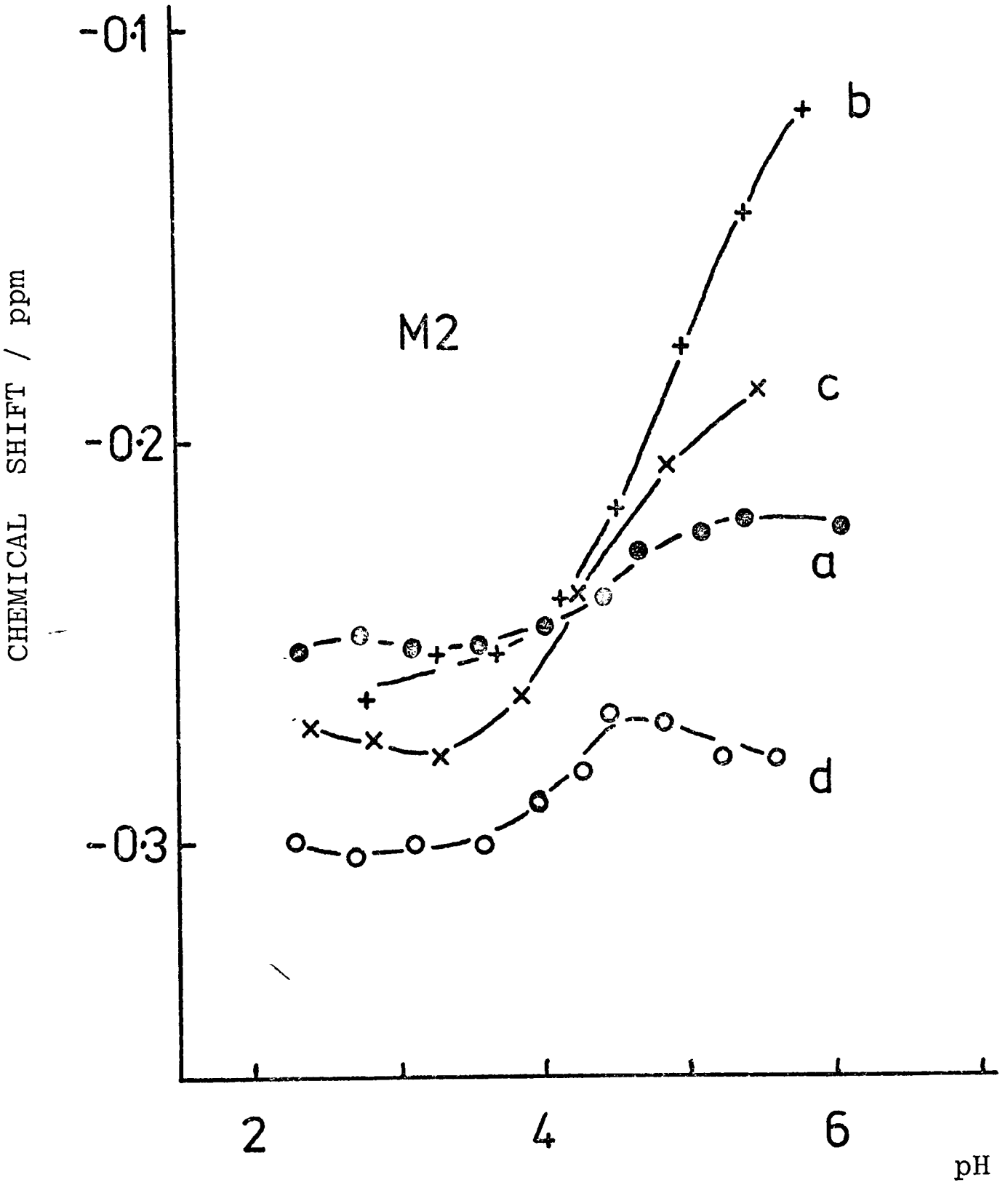

pH dependence of the chemical shift value of resonance M2 in the presence of (a) 0.05M La^{3+}; (b) 0.005M Yb^{3+}; (c) 0.03M Yb^{3+}; (d) 0.05M Yb^{3+}. For each solution the ionic strength was 0.4. 5mM lysozyme, 54°C.

to be affected by the strong binding site in Section VI.2.2.2. A series of titration curves is shown in Fig. VI.6. As the pH is decreased, the fraction of lysozyme bound to the lanthanide (f) decreases as H^+ is competitive for the carboxylate groups.

(c) All the resonances observed in Section VI.2.2.2 to have titration curves which are not simply a result of binding to the group of pK 6.0, have complicated pH dependencies of the induced shifts. Some of these curves are shown in Fig. VI.7 for the resonance M2 (Ile 98, γ-CH_3) which shows the effect of binding to a group of pK value near to 4 as well as the effect of binding to a group of pK value near to 6 (cf. Fig. VI.3).

VI.3 Characterisation of the Binding Sites

The results of the binding experiments can now be put together to define the characteristics of the binding sites. These characteristics include the values of binding constants, the number of ionisable groups involved in binding, the pK values of these groups and their position in the sequence. The resonances in category (b) in the previous sections will be considered to be perturbed by binding at the major site only, and those in category (c) by binding at weaker sites.

VI.3.1 The Major Site

The data from the binding curves recorded at fixed pH values provide values for apparent binding constants at each pH value. From Section VI.3, for binding to a single site

$$1/\delta_i = 1/\Delta_i + 1/K\Delta_i[M^{3+}]$$

Thus a plot of $1/\delta_i$ vs $1/[M^{3+}]$ allows Δ_i and K to be calculated. Provided that $[M^{3+}] \approx [M^{3+}] + [ML^{2+}]$, which is the case for a large excess of M^{3+} over L^-, $1/\delta_i$ can be plotted against

$1/[\text{total } M^{3+}]$. Data for lysozyme are plotted in Fig. VI.8. These show that the induced fully bound shift Δ_i is independent of pH for the resonance (M9) plotted. This appears to be true for essentially all the other resonances. However, the variation of binding constants with pH results in these being of little value for characterising the site. However, the data from the pH titrations effectively gives directly the variation of the binding constants with pH, and the manner of this variation provides valuable information. In order to interpret the results, it is necessary to consider specific types of behaviour.

Consider the binding of a lanthanide ion (M^{3+}) to a single ionised group on the protein (L^-) and assume that no binding to the protonated form (LH) occurs. Let the association constant for M^{3+} be K_2, and the pK value of the protein group be pK_1. The relevant processes are therefore

$$L^- + H^+ \rightleftharpoons LH$$

$$\text{and} \quad L^- + M^{3+} \rightleftharpoons LM^{2+}$$

Now, $1/K_1 = [LH]/[L^-][H^+]$, and a plot of pH ($-\log[H^+]$) against $\log([L^-]/[LH])$ is linear and can be used to determine the pK_1 value. Also, when $[L^-] = [LH]$, $K_1 = [H^+]$ and at this point (the half way point in a titration), $pK_1 = pH$.

By definition, $K_2 = [LM^{2+}]/[L^-][M^{3+}]$. Thus, $K_2 = ([LM^{2+}]/[LH][M^{3+}]).[H^+]/K_1$. Provided that $[M^{3+}] \approx [M^{3+}] + [LM^{2+}]$ over the pH range in question, as will be the case with an excess of M^{3+} in solution, a plot of pH against $\log([LM^{2+}]/[LH])$ will be linear. Also, by analogy with the previous paragraph, when $[LH] = [LM^{2+}]$, $K_2 = [H^+]/[M^{3+}].K_1$. Now, for a pH value at least one unit below the pK_1 value of LH, $[LH] \approx [LH] + [L^-]$ and the condition that $[LH] = [LM^{2+}]$ is merely that for 50% of the protein being bound to M^{3+}, and this is again a half-way point in a

FIGURE VI.8

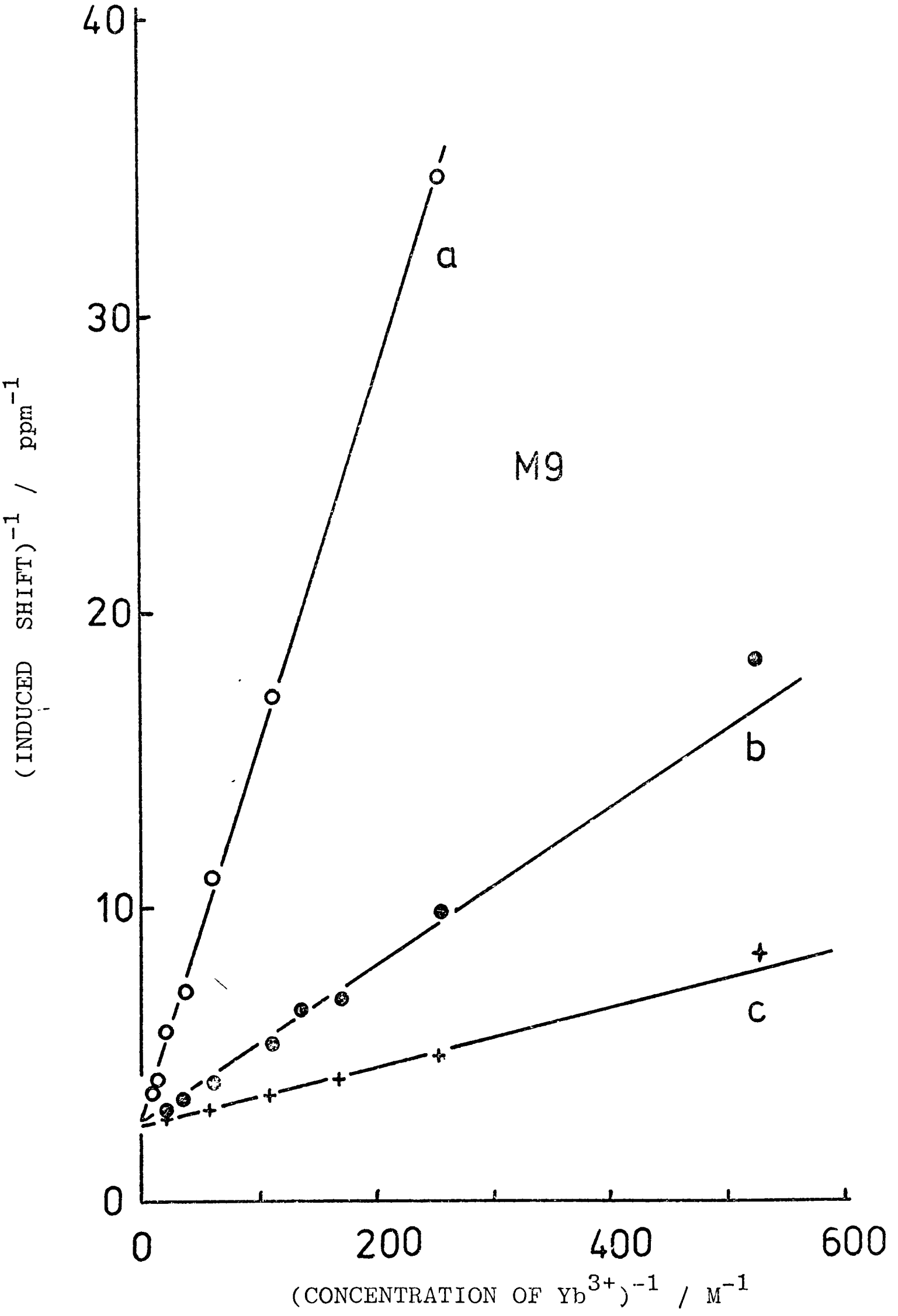

Plot of the reciprocal of the induced shift of resonance M9 against the reciprocal of the concentration of Yb^{3+}. (a) pH 4.3; (b) pH 5.3; (c) pH 5.8. 5mM lysozyme, 54°C.

titration. For a given $[M^{3+}]$, this point will be at a pH value denoted pH (50% bound) and

$$pK_1 - pH\ (50\%\ bound) = \log [M^{3+}] + \log K_2 \qquad (1)$$

This treatment can now be used to characterise the strong binding site of lysozyme, if it is a valid model for lysozyme. This may be tested because the slopes of the two linear plots described above (pH vs log $([L^-]/[LH])$ in the absence of metal ions and pH vs log $([LM^{2+}]/[LH])$ in their presence) will be equal to unity provided that the assumptions made above are correct. A slope other than unity would indicate that the assumptions are incorrect.

(i) The Metal-Free System. In Fig. VI.5 titration curves for the trp 108 C(2)H resonance are given. From this, chemical shift values for the resonance were at high pH (δ_H) and low pH (δ_L) were measured. At an intermediate pH value, an intermediate value (δ_{obs}) is obtained. On the model described above,

$$[L^-]/[LH] = (\delta_{obs} - \delta_L)/(\delta_H - \delta_{obs})$$

A plot of pH vs log $(\delta_{obs} - \delta_L)/(\delta_H - \delta_{obs})$ is shown in Fig. VI.9. This plot has a slope close to 1, and so indicates that the observed shifts arise essentially from a single ionisation $L^- + H^+ \rightleftharpoons LH$. The pK value is 6.0 ($\mu$ = 0.4, 54°C) as expected for glu 35. Except for some deviation at low pH values (arising from the effect of asp 52), no indication of other ionisations which affect trp 108 is found.

(ii) The Diamagnetic System. In the presence of 50mM La^{3+}, an exactly similar analysis may be made, except that the equation is now,

$$[LM^{2+}]/[LH] = (\delta_{obs} - \delta_L)/(\delta_H - \delta_{obs}).$$

FIGURE VI.9

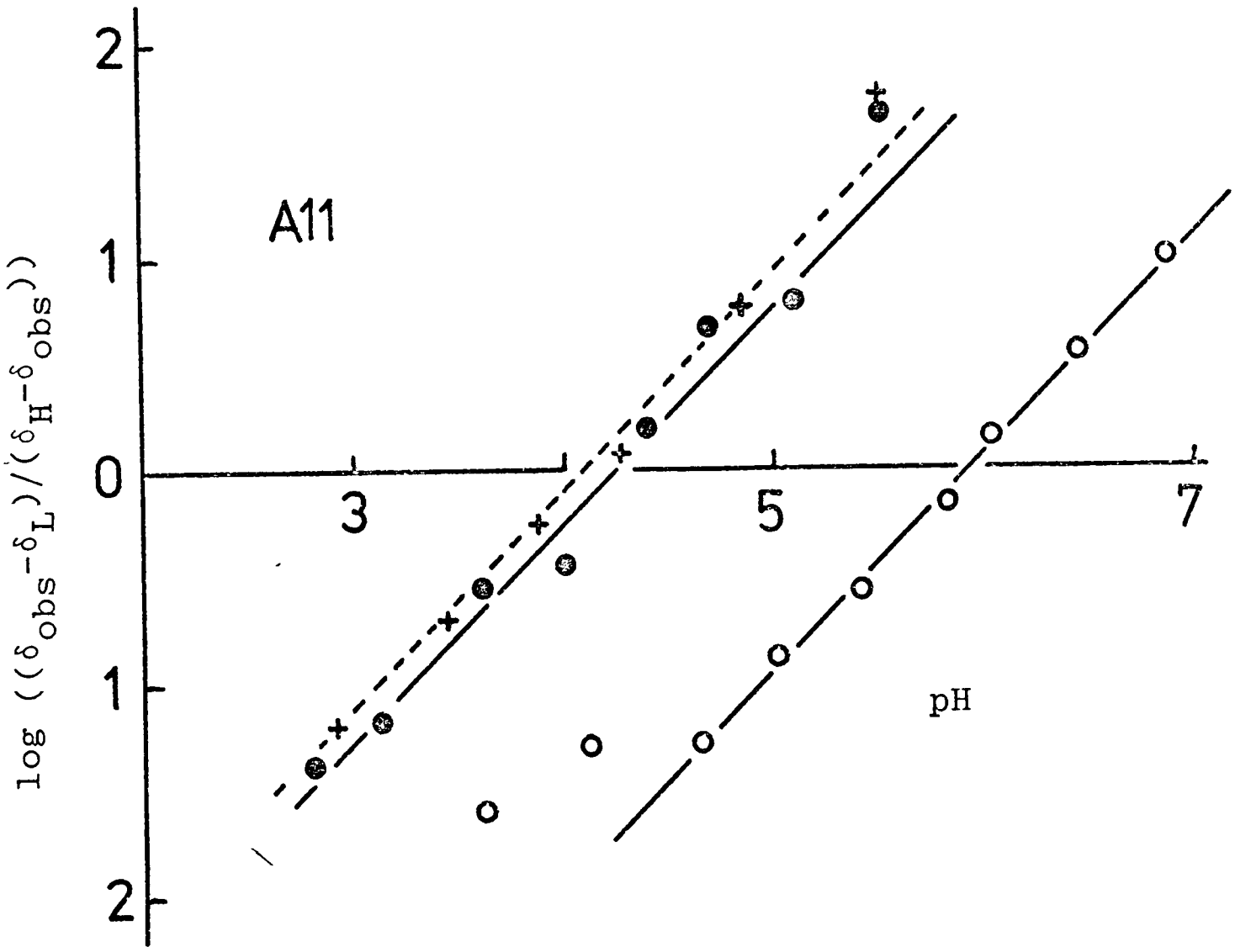

Plots of log $((\delta_{obs}-\delta_L)/(\delta_H-\delta_{obs}))$ against pH for resonance A11. Open circules, 0.4M KCl, values used $\delta_L = 7.077$, $\delta_H = 7.234$; closed circles, 0.05M La^{3+}, $\delta_L = 7.077$, $\delta_H = 7.261$; crosses, 0.05M Lu^{3+}, $\delta_L = 7.077$, $\delta_H = 7.269$. The lines are drawn with slopes of 1.00. 5mM lysozyme, $54^{o}C$.

A plot of this function (Fig. VI.9) is also nearly linear, has a slope of close to unity, and the value of the pH at 50% bound is 4.2 $\pm$ 0.1. Using equation (1) above, and knowing pK_1 (6.0) and $[M^{3+}]$ ([total M^{3+}] minus $[LM^{2+}]$ i.e. 47.5mM), K_2 is obtained to be 1.3×10^3 M^{-1}. For Lu^{3+}, analagous results are obtained, and as pH (50%) is 4.1 $\pm$ 0.1, K_2 is 1.7×10^3 M^{-1}.

(iii) The Paramagnetic System. A similar approach was taken for the paramagnetic shift data. The more extensive data on a number of resonances was utilised here. One difference from the cases above was in the calculation of δ_H, δ_L and δ_{obs}. These were not chemical shift values but were induced shift values. They were calculated from the chemical shift values in the presence of a paramagnetic ion minus the chemical shift values for La^{3+} or Lu^{3+} minus the value of the pH independent paramagnetic shift. This is indicated in Fig. VI.10.

Plots of these data again resulted, for resonances in category (b), in linear plots with slopes very close to unity (Fig. VI.11). The linearity extends from at least pH 3.5 to the highest pH value which could be used (ca. 6.0). This indicates quite conclusively that no group with pK value above 3.5 other than glu 35 can be involved in lanthanide binding. The measured binding constants are given in Table VI.2. The variation of binding constant from one lanthanide to another is similar to that found in simple carboxylate systems (see Phillips and Williams, 1966).

Summarising the results of this analysis allows the following conclusions to be drawn. The linearity and slopes of the binding graphs show that only one ionisable group with pK value above 3.5 affects the binding of lanthanides. This group has a pK value of 6.0 and is glu 35. If another group is involved in binding,

FIGURE VI.10

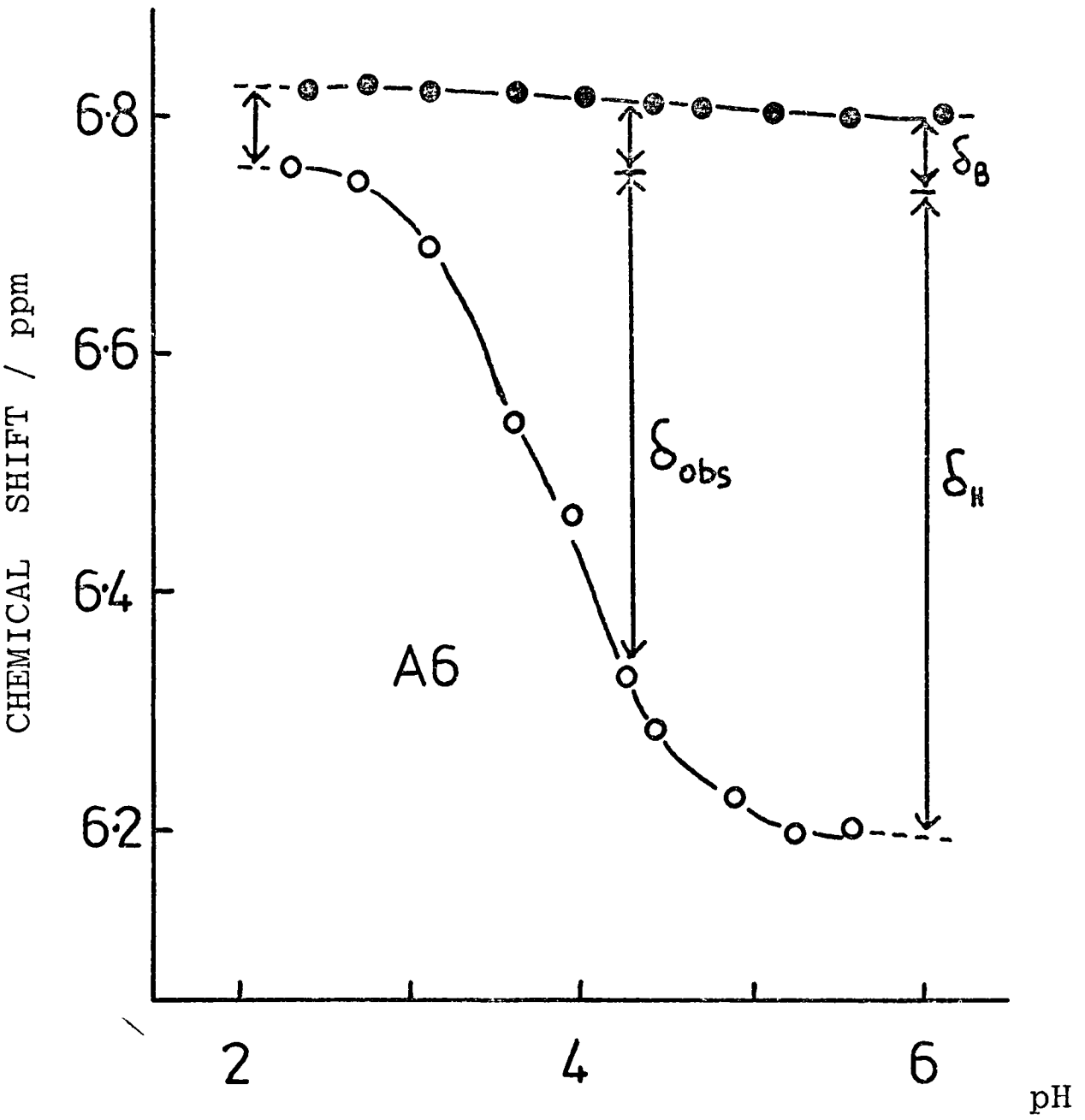

pH dependence of the chemical shift value of resonance A6. Open circles, 0.05M Yb^{3+}; closed circles, 0.05M La^{3+}. In order to calculate δ_{obs} and δ_H for paramagnetic lanthanides, correction for the pH independent shift, δ_B, must be made. 5mM lysozyme, 54°C.

FIGURE VI.11

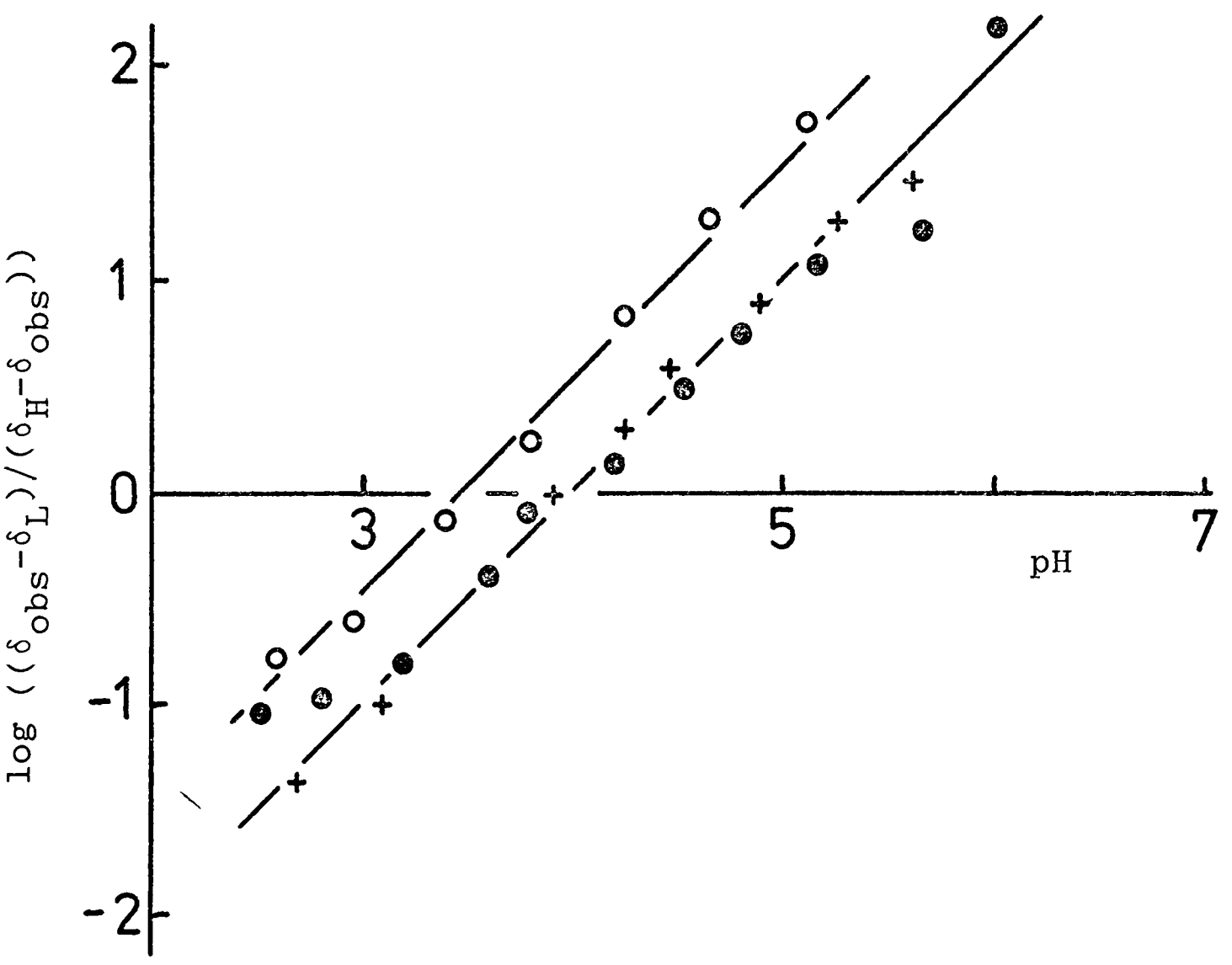

Plots of log (($\delta_{obs}-\delta_L$)/($\delta_H-\delta_{obs}$)) against pH for paramagnetic lanthanides. Open circles, resonance A6 with 0.05M Eu^{3+}, δ_H = 0.206; closed circles, resonance A11 with 0.05M Pr^{3+}, δ_H = 0.615; crosses, resonance M9 with 0.05M Yb^{3+}, δ_H = 0.702. For each case, δ_L = 0. The slopes are drawn to be 1.00. 5mM lysozyme, 54°C.

TABLE VI.2

Association Constants[a] for Different Lanthanides[b]

Lanthanide	pH (50% bound)[c] at 0.05M	K^{d} (M^{-1})
La	4.2	1.3×10^3
Pr	4.0	2.1×10^3
Eu	3.5	6.7×10^3
Yb	4.0	2.1×10^3
Lu	4.1	1.7×10^3

[a] at $54^{o}C$, $\mu = 0.40$.

[b] the binding constant for Ca^{2+} has also been calculated. At 0.5M $CaCl_2$, pH (50% bound) = 5.0, giving K = 20 M^{-1}.

[c] values ± 0.1.

[d] for binding to group of pK = 6.0.

its pK value must be less than 3.5. Asp 52 has a pK value of 3.5 $\pm$ 0.5 from other measurements (Appendix A; Rupley *et al.*, 1974). Shift data at pH values below 3.5 are not sufficiently accurate to determine whether or not asp 52 is involved in binding. However, if it is, the binding constant to asp 52 when glu 35 is not ionised is very weak. The binding constants of lanthanides to lysozyme in the ionised form of glu 35 are *ca.* 10^3 M^{-1}.

VI.3.2 The Minor Sites

From the resonances which were put into class (c) above, information about the weaker binding sites could be obtained. From a knowledge of the assigned resonances affected (Table VI.1), the regions of the protein in which these sites are placed were deduced, by making use of the X-ray structure. The sites are listed in Table VI.3 and are as follows.

(a) Asp 101. Binding at this group is proposed because of the relatively large paramagnetic shifts observed on the resonances of ile 98 (M2 and M4, see Fig. VI.3) and of trp 63 (resonances A1 and A22). The pK value of asp 101 was estimated from the pH titrations in the presence of paramagnetic ions as being *ca.* 4.5. This agrees with recent data by Rupley *et al.* (1974) and as summarised in Appendix A. The binding constant to this site is *ca.* 10 M^{-1}.

(b) asp 87 and/or glu 7. The resonances of his 15 (A14, A23) are affected by weak binding to a group of pK value *ca.* 4.0. Also affected by binding in this region of the protein are resonances of ile 88 (M7), val 92 (M10, M13) and leu 8 (M5) although these shifts are rather small. The binding constant to asp 87 and/or glu 7, which are both in this region, is less than

TABLE VI.3

Lanthanide Binding Sites

Site	Binding Groups and pK values at μ = 0.4	Approximate K (M^{-1})	Residues Affected
A	glu 35 (6.0) asp 52 (<3.5)	10^3	All in group (b) of Table VI.1
B	asp 101 (ca. 4.5)	10	ile 98, trp 63
C	glu 7 (ca. 2.0) asp 87 (ca. 4.0)	<10	leu 8, his 15, ile 88

$10\ M^{-1}$.

(c) It is likely that binding to other exposed carboxylic acid groups occurs. This has not been specifically detected, and is probably still weaker.

VI.4 Measurement of Perturbations Resulting from Binding at the Major Site

The characterisation of the major binding site permits measurement of the data required for the conformational studies. Rather than absolute shift and relaxation measurements, the relative values of induced shift and relaxation effects on different resonances are required.

VI.4.1 Shift Ratios

Shift ratios have been calculated from the titrations already described, both those at fixed pH values and those involving change of pH.

VI.4.1.1 From Titrations at Fixed pH values

Consider the binding of lanthanide ions at a specific site. Given conditions of fast exchange as described above for a resonance i, $\delta_i = f\ \Delta_i$ and for a resonance j, $\delta_j = f\ \Delta_j$. Δ is the induced shift in the fully formed complex, and δ is the observed shift at a fraction f of ligand bound to lanthanide. The required shift ratio is Δ_i / Δ_j which is the same as δ_i / δ_j. Now, consider the case where shifts arise from binding at a secondary weak site, such that $\delta_i = f\ \Delta_i + f^1 \Delta^1_i$ and $\delta_j = f\ \Delta_j + f^1 \Delta^1_j$. Then

$$\delta_i / \delta_j = (f\ \Delta_i + f^1 \Delta_i{}^1)/(f\ \Delta_j + f^1 \Delta_j{}^1).$$

However, provided that the binding sites are independent, at low

concentrations of lanthanide ion $f >> f^1$, whilst at an infinite concentration $f = f^1 = 1.0$. Thus, provided that the shift data are collected over a wide concentration range, that the binding constants are sufficiently different, and that Δ_i^1 and Δ_j^1 are not large compared to Δ_i and Δ_j, calculation of δ_i/δ_j at a fixed ligand concentration and various lanthanide concentrations followed by extrapolation of the values to zero concentration of lanthanide ion gives a close approximation to Δ_i/Δ_j. This will also remove the effects of a linear contribution (Section VI.2.1.2) to the observed titration curves. This extrapolation, which is often effectively linear (see Barry et al., 1971), also allows the shift ratios to be defined under standard conditions. The procedure can be repeated under different conditions of pH or ligand concentration. The extrapolated shift ratios should be identical if they are true ratios of Δ_i/Δ_j.

This procedure was performed for the resonances of lysozyme using the data of Section VI.2.2.2, having corrected for the diamagnetic shifts only. Some of the data are plotted in Figs VI.12 and VI.13.

VI.4.1.2 From pH titrations

Shift ratios were also calculated from the pH titrations of Section VI.2.3.2 as follows. At a constant lanthanide concentration, induced paramagnetic shifts (observed chemical shift minus chemical shift in presence of La^{3+} or Lu^{3+}) were calculated for resonances i and j at different pH values. Then, δ_i was plotted against δ_j as shown in Fig. VI.14. Only if the induced shifts have the same pH dependence, that is that they arise as a result of binding at the same site, will these

FIGURE VI.12

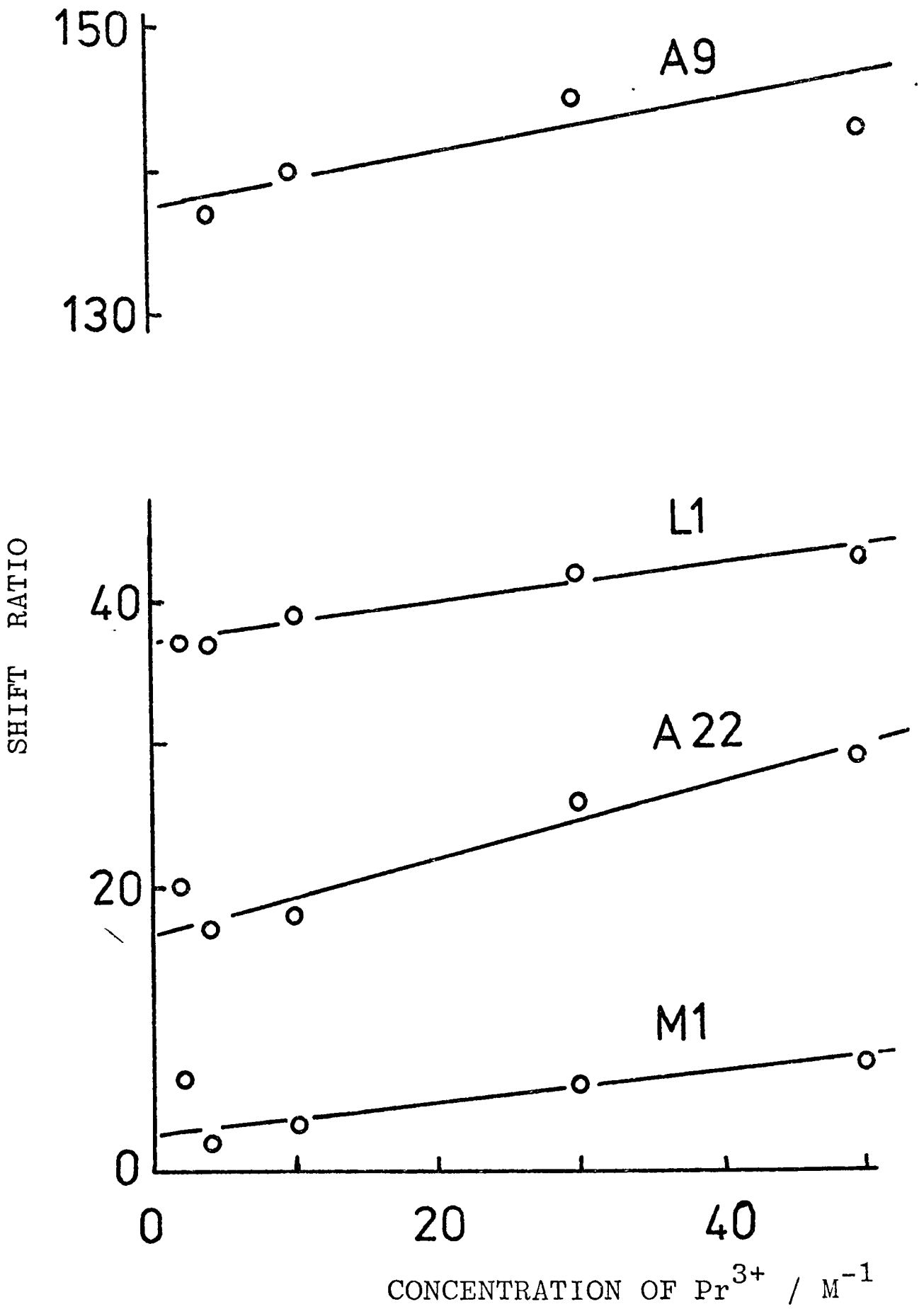

Ratios of shifts, relative to A11 = 100, with Pr^{3+} as a function of the concentration of Pr^{3+}. pH = 6.0, ionic strength = 0.4, 5mM lysozyme, 54°C.

FIGURE VI.13

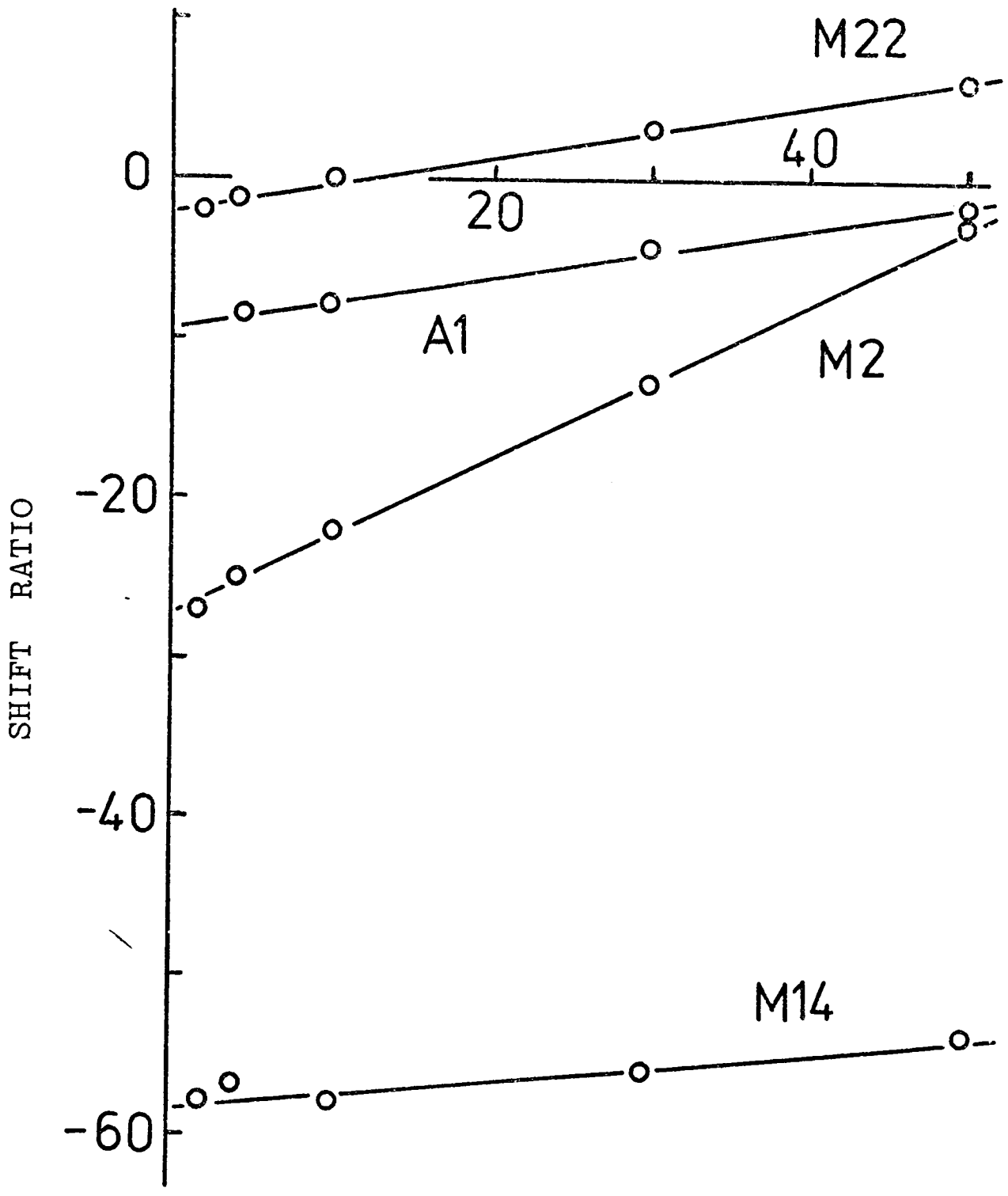

As Fig. VI.12, but the ratios shown here are negative.

FIGURE VI.14

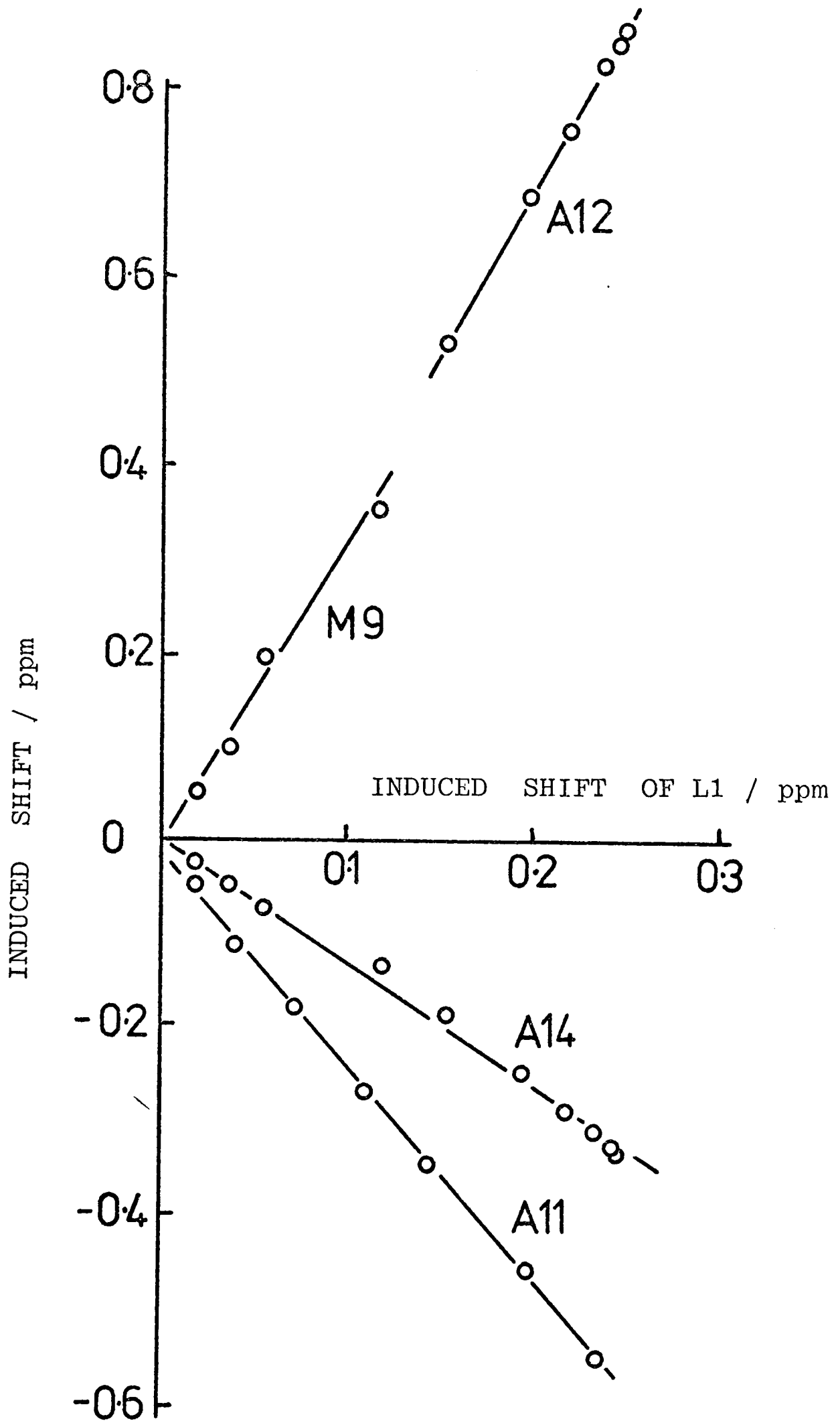

Shifts induced in various resonances by 0.05M Pr^{3+} plotted against induced shift of resonance L1. Each point represents a measurement at a different pH value. The relative slopes are values of shift ratios. 5mM lysozyme, 54°C.

TABLE VI.4

Shift Ratios[a] Determined by Different Methods

Resonance Number	Assignment	Type of Behaviour[b]	Ln^{3+}	Shift Ratio[c] A	B	C
M2	ile 98	(c)	Pr	-35		-15
			Eu	-28		-22
			Yb	-33		-15
M22	met 12	(a)	Pr	- 2		3
			Eu	9		8
			Yb	- 8		-2
A6	tyr 53 m-	(b)	Pr	159	160	164
			Eu	135	146	156
			Yb	120	140	123
A22	tyr 63 5/6	(c)	Pr	20		24
			Eu	25		41
			Yb	10		24

[a] relative to tyr 53 o-. 54°C.

[b] (a) major shift is pH independent. (b) major shift is from binding to glu 35, pK 6. (c) substantial shift from minor binding site.

[c] Method A is extrapolation to zero lanthanide concentration, method B is the pH titration method at 50 mM Ln^{3+} and method C is the use of a constant total lanthanide concentration of 24mM. Method B can only be applied to behaviour type (b).

plots be linear. The slope of the linear plot gives the shift ratio Δ_i/Δ_j. In particular it is noted that the pH independent shift is eliminated from the shift ratio.

In Table VI.4, some shift ratios obtained by the two methods are compared. For the resonances in category (b), close agreement is found. Additionally, the linearity of the plots in Fig. VI.14 shows that the shift ratios are independent of pH.

The pH independence of the shift ratios is important in considering the question of the exact nature of the major binding site. It has been shown that the variation of the binding constants with pH depends simply on the pK value of glu 35. Taken together, these two pieces of information suggest that a single mode of lanthanide binding to lysozyme is found over the whole pH range from 3.5 to 6.0. This binding is to the protein with glu 35 ionised. There is no evidence for any behaviour which would indicate the multiple modes of binding seen in the X-ray diffraction studies.

VI.4.1.3 From Titrations at Constant Total Concentration of Lanthanide

The addition of a lanthanide solution to a lysozyme solution at the same pH value results in a solution of lower pH, because of the displacement of the glu 35 proton which takes place on binding a lanthanide. Thus, all the titrations described earlier are tedious and difficult because the pH value of the solution has to be adjusted for every sample, ideally at the temperature at which the spectra are run. In addition, the titration curves for some resonances are difficult to follow. In order to overcome these difficulties, standard conditions were chosen for some titrations whereby the total lanthanide concentration was maintained constant. This concentration was 23.8mM

(50µl of 0.5M lanthanide solution added to 1ml of lysozyme solution). Solutions of lysozyme containing paramagnetic lanthanide ions at pH 5.3 were mixed with a solution containing La^{3+}, thus generating solutions of varying relative concentrations of the two ions but the same total lanthanide concentration. As the binding constants of the different lanthanides are not very different, the resulting graphs of chemical shift value against concentration of paramagnetic lanthanide ions are nearly linear. No further diamagnetic correction is needed. However, the shift ratios obtained are those for 23.8mM lanthanide, and not those extrapolated to zero ionic strength. Comparison of some values under these different conditions is shown in Table VI.4. Experiments of this type, each involving about 20 different relative concentrations of La^{3+} and paramagnetic lanthanide, were run for all lanthanides except for Pm^{3+}. These experiments allowed shift ratios to be calculated from the observed induced shifts, and the data are summarised in Table VI.5. By this means comparison between the shift ratios for different lanthanides could easily be made. This comparison is essential in order to define the symmetry of the bound lanthanide cations.

However, in order to use the shift ratios for detailed conformational studies, it is essential to obtain the shift ratios which arise solely from binding at the single strong site. The best values for these ratios are tabulated in Fig. VI.6 for Pr^{3+}, indicating the method of determination of each.

VI.4.1.4 Variation of Experimental Conditions

Other conclusions have been drawn from preliminary experiments under different conditions. First, spectra at 24mM $Eu(NO_3)_3$ appear to be identical to the spectra discussed above with the $EuCl_3$. The identity of the spectra indicates

TABLE VI.5

Shift Ratios with Different Lanthanides [a]

Resonance Number	Ce	Pr	Nd	Eu	Tb	Dy	Ho	Er	Tm	Yb
M1	0	5	12	0	6	3	5	0	0	2
M2	-8	-15	-11	-22	0	-18	-12	0	22	-15
M3	0	4	9	6	4	3	3	0	-6	2
M5					-4		-2	-6	-31	
M6	-3	-8	-5	-2	12	2	9	16	48	18
M7	0	7	12	6	0	3	0	-6	-27	-3
M8	0	-2	12	0	-4	-4	-2	-29	-92	-18
M9	105	140	100	64	61	150	110	79	57	120
M10	13	9	11	11	3	10	7	0	-23	0
M13	9	7	9	8	0	5	6	0	-7	6
M14	-45	-64	-69	-83	-48	-54	-62	-32	15	-52
M16	-55	73	-110	-190			-170	-370		-200
M17	-180	-109	-380	-410			-330	-500		-290
M18				-80						
M19	23	22	22							
M20	80	59	64							
M21	25	25	28	29	21	25	20	18	2	18
M22	0	3	7	8	0	1	2	-9	-25	-2
L1	50	45	56	56	56	42	40	53	67	45
L2	450	500	560	780	500		600	630	870	640

Continued on next page

TABLE VI.5 Continued

Resonance Number	Ce	Pr	Nd	Eu	Tb	Dy	Ho	Er	Tm	Yb
A1	0	0	0	0	5	-2	0	0	-9	0
A2	-10	-15	-14	-23	-2	-14	-6	0	25	0
A3	-7	-7	-14	-9	0	-4	-2	3	20	6
A6	100	100	100	100	100	100	100	100	100	100
A9										32
A11	-100	-56	-100							
A12	164		156	117				189		123
A16	0	0	0	0	5	2	5	5		6
A19	0	0	0	9	11	5	10	18	40	19
A20	60	41	56		100	50	55			
A21	-7	-4	-2	10	16	4	10	28	70	24
A22	33	24	33	41	39	19	24	32	70	24

[a] at 23.8mM total lanthanide, 5mM lysozyme, 54°C, pH 5.3. The shifts with Sm^{3+} were very small and the ratios are not listed.

TABLE VI.6

Pr^{3+} Shift Ratios from Major Site Alone[a]

Resonance Number	Assignment	Shift Ratios	Resonance Number	Assignment	Shift Ratio
M1	leu 17	4	A1	trp 63 5/6	-11
M2	ile 98 γ	-32	A2		-26
M3	leu 17	-4	A3		-14
M4	ile 98 δ	A	A4		
M5	leu 8	-3	A5		
M6	met 105	-14	A6	tyr 53 o-	100
M7	ile 88 δ	A	A7		
M8	leu 56	-9	A8		
M9	thr 51	151[b]	A9		
M10	val 92	-1	A10		
M11	leu 56	A	A11	trp 108 C(2)	-117
M12	leu 8	A	A12	tyr 53 m-	160
M13	val 92	A	A13		
M14	ala 107/31	-68	A14	his C(4)	A
M15			A15		
M16	val 109	-109[c]	A16		A
M17	val 109	73[c]	A17		
M18			A18		
M19		12	A19		0
M20	ala 110	59[c]	A20	trp 63 C(2)	53[b]
M21		25[c]	A21		-8
M22	met 12	-2	A22	trp 63 4/7	
			A23	his 15 C(2)	A
L2		500[c]			
L1		43	N5		-90[b]

[a] ratios calculated by extrapolation, unless otherwise indicated, relative to trp 108 C(2), and normalised to tyr 53 o-. Temp. = 54°C. A indicates that the ratio is less than - 10, but not directly determined.

[b] ratios from pH titration

[c] ratios from Table VI.5

that the shift ratios are the same in the two cases, in other words that the shift ratios are not dependent on the anion in the solutions. Secondly, the effects of temperature on the spectra have briefly been investigated for solutions containing Pr^{3+}, Nd^{3+}, Eu^{3+} and Yb^{3+}, from 25°C to 68°C. These spectra indicate that most of the shift ratios are not significantly dependent on temperature. This aspect however requires further analysis.

VI.4.2 Gd^{3+} Broadening Ratios

Quantitative measurements of the relative broadening of different resonances by Gd^{3+} were carried out using the paramagnetic difference method described in Section III.1.2. Aliquots (ca. 5µl) of relatively concentrated solutions of Gd^{3+} (10^{-5} to 10^{-3}M) were successively added to solutions (ca. 0.4ml in volume) containing 5mM lysozyme and 23.8 mM La^{3+} at pH 5.3. Spectra were run, at 54°C, of each solution at the different total concentrations of Gd^{3+}. These spectra were subtracted in turn from the spectrum of the solution recorded before addition of Gd^{3+}. The use of the high background concentration of La^{3+} was to reduce inaccuracies arising from the removal of low concentrations of metal ions from the solution which could occur for example by adsorption on the glassware. The La^{3+} and Gd^{3+} compete (under the conditions of fast exchange) for the lysozyme binding site. Also, under these conditions, the lysozyme is essentially fully bound, and the fraction bound does not alter during the Gd^{3+} titration. A change in the fraction bound could, for example, result in a pH change. Difference spectra were also recorded under different conditions but not analysed quantitatively. Qualitatively, the peaks observed in the difference spectra were the same at 90 MHz as at

270 MHz, at pH 6.0 as at pH 5.3, and in the absence as well as presence of La^{3+}. Difference spectra were also obtained by adding Gd^{3+} to solutions which contained a shift probe, Eu^{3+}, Na^{3+}, Pr^{3+} and Yb^{3+} in order to follow the shifts of certain resonances.

Very satisfactory difference spectra were obtained using the conditions described initially, and some of these are shown in Fig.VI.15. From each spectrum, the height of a given peak in the difference spectrum (I_o) was measured. Under the conditions used, the fraction of lysozyme bound to Gd^{3+} is directly proportional to the concentration of Gd^{3+}. Therefore, from Section III.1.2, a plot of $1/[Gd^{3+}]$ against $1/I_o$ should be linear with a slope proportional to $T_{2M}/T_2{}^{*2}$. Fig. VI.16 shows that these plots for different resonances are indeed linear. Now, the intercept at $1/[Gd^{3+}] = 0$ is proportional to the reciprocal of the intensity of the peak in the normal spectrum. The measured slope must be multiplied by this value to obtain values of $T_{2M}/T_2{}^{*2}$ for different resonances which are on the same scale. This correction to the slope merely allows for differences in observed heights of different peaks in the original spectrum which result, for example, from differences in multiplet structure. Relative values of the slopes for different resonances therefore give relative values of $T_{2M}/T_2{}^{*2}$. In fact, this analysis applies only to singlet resonances (Section III.1.2) or to resonances with the same multiplet structure. It is likely that little error arises from this point.

Preliminary experiments with the CPMG pulse sequence (Section III.2.3.1) to measure $T_2{}^*$ values are reported in Chapter VIII. The results indicate that $T_2{}^*$ values are similar for most resonances. Thus, it is assumed that the ratios of

FIGURE VI.15

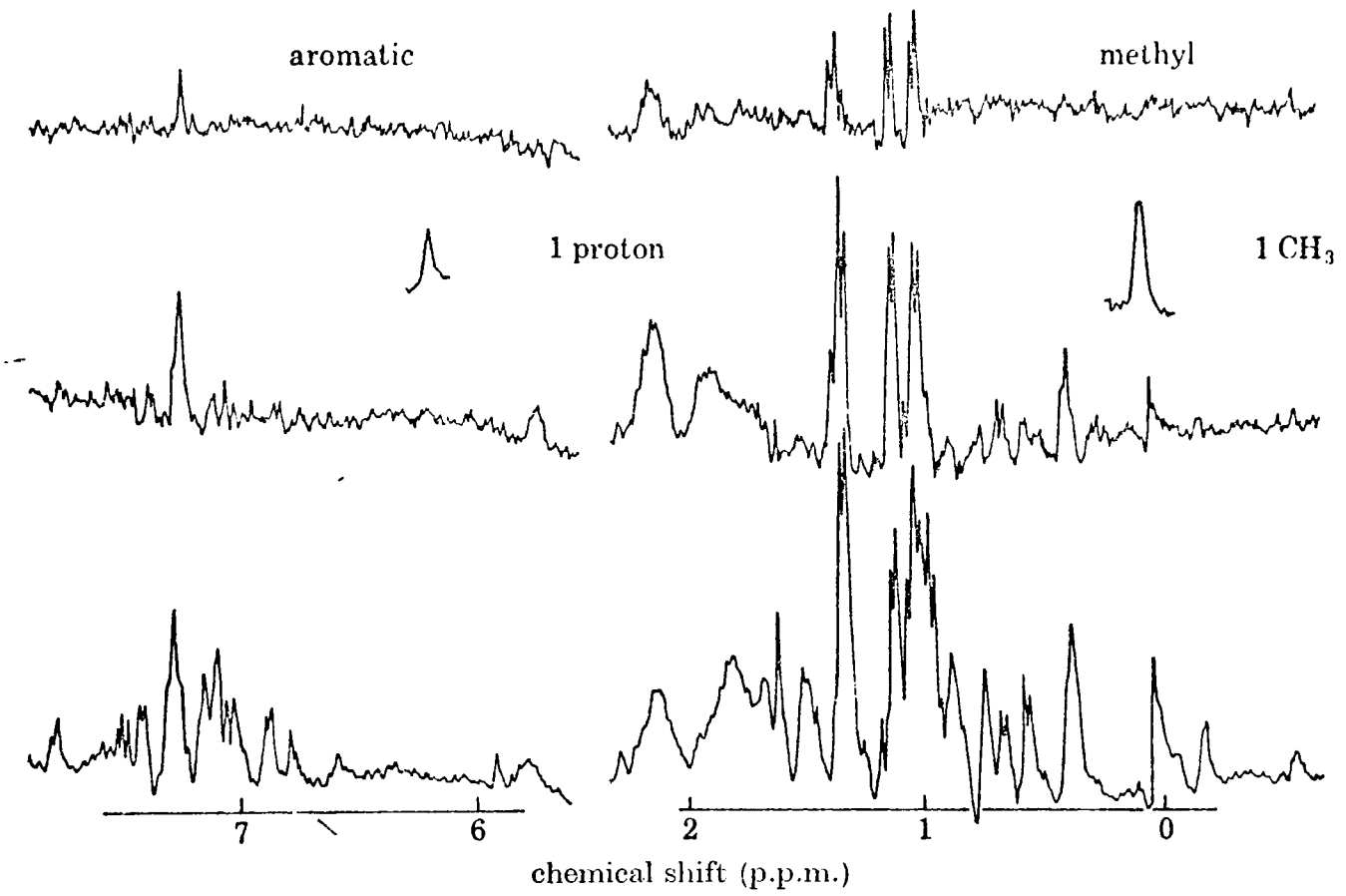

Gd^{3+} difference spectra for 5mM lysozyme with 23.8mM La^{3+}, pH 5.3, 54°C. The concentrations of Gd^{3+} were (a) 1.12×10^{-5}M, (b) 7.31×10^{-5}M and (c) 69.8×10^{-5}M. The resonances which are broadened most are A11, M20, M17 and M16 and are seen in the top spectrum.

FIGURE VI.16

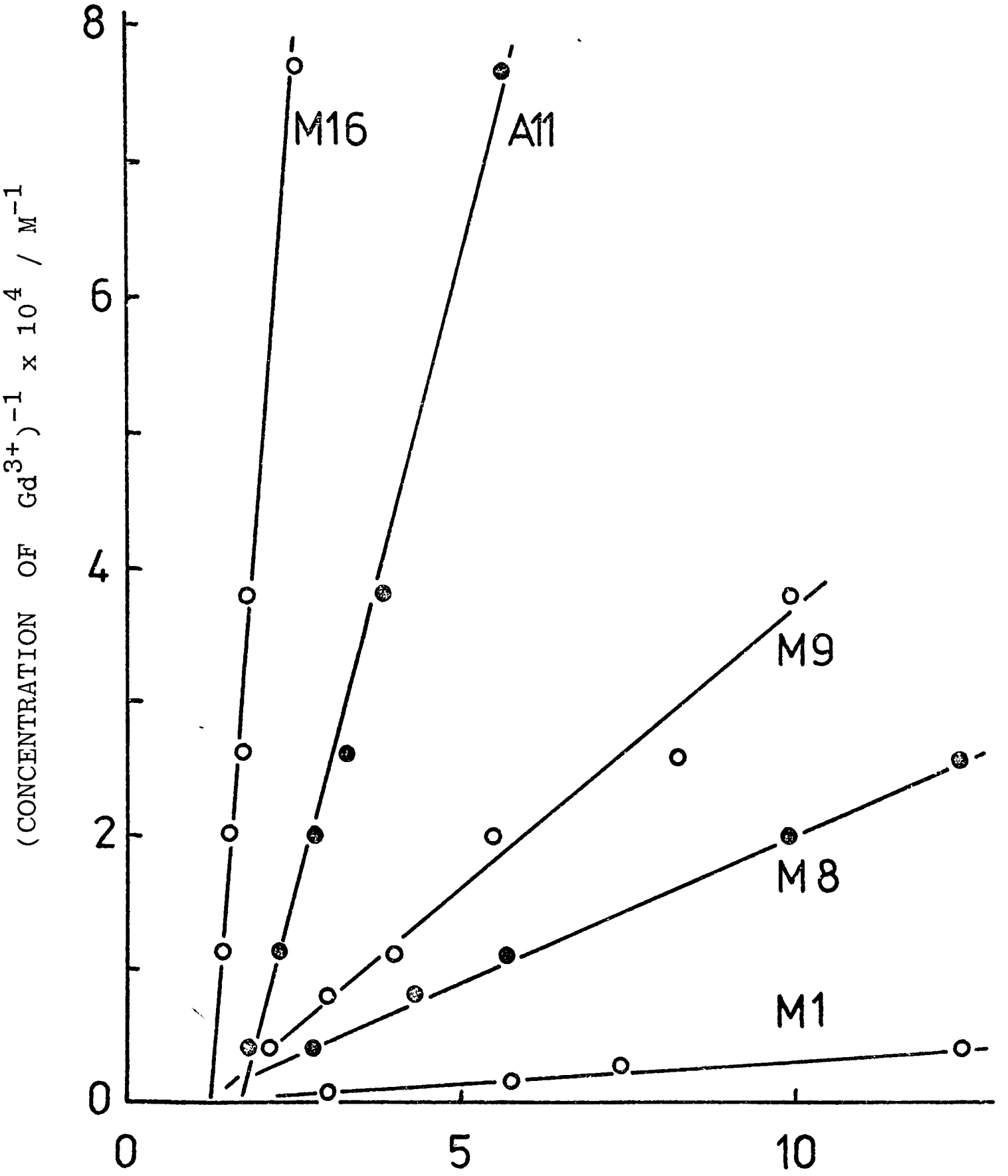

Plots of the reciprocals of the heights of peaks in difference spectra against the reciprocal of the concentration of Gd^{3+}. Solutions contained 23.8 mM La^{3+} at pH 5.3. 5mM lysozyme, 54°C.

TABLE VI.7

Relative Broadening of Different Resonances[a] by Gd^{3+}

Resonance Number	Assignment	Relative slope[b]	Relative Intercept[c]	Ratio[d] of T_{2M}^{-1}
M1	leu 17	0.26	0.84	0.22[e]
M2	ile 98 γ	0.76	0.98	0.74
M6	met 105	1.30	0.26	0.34
M8	leu 56	1.48	0.42	0.62
M9	thr 51	2.64	0.53	1.40
M11	leu 56	1.56	0.61	0.95
M14	ala 107/31	2.06	0.79	1.63
M16	val 109	36.9	0.61	22.5
M17	val 109	36.9	0.61	22.5
M20	ala 110	20.6	0.84	17.3
A6	tyr 53 o-	1.00	1.00	1.00
A11	trp 108 C(2)	12.9	0.95	12.3
L1		0.32	1.32	0.42
L2		2.16	2.25	4.85

[a] resonances discussed are either well resolved or seen without overlapping resonances in difference spectra.

[b] of plot of $1/[Gd^{3+}]$ against $1/I_o$. Relative slope is relative value of $I_o/[Gd^{3+}]$.

[c] intercept is value of $1/I_o$ for $1/[Gd^{3+}] = 0$.

[d] product of relative slope and relative intercept.

[e] no resonances can be observed to broaden less rapidly than M1.

$T_{2M}/T_2{}^{*2}$ are ratios of T_{2M} for different resonances. Data are summarised in Table VI.7. These data are not corrected for the effects of minor binding sites or of non-specific binding. This must be remembered in the subsequent conformational analyses described below.

VI.5 Summary

The analysis of various titrations with shift probes has shown that lysozyme has a single strong binding site for lanthanide cations. This site involves glu 35, and possibly asp 52. It is therefore similar to the major binding site observed in X-ray diffraction studies, although some uncertainties remain in the crystal data. A number, at least two, weaker binding sites exist.

From these titrations, ratios of induced shifts of different resonances resulting from binding at the strong site have been calculated for different lanthanides. In addition, ratios of the broadening induced in different resonances by the binding of Gd^{3+} have been measured, although these, unlike the shift data, have not been corrected for binding at the weaker sites.

References for Chapter VI

Barry, C.D., Glasel, J.A., North, A.C.T., Williams, R.J.P. and Xavier, A.V. (1971), Nature 232, 236.

Barry, C.D., Glasel, J.A., Williams, R.J.P. and Xavier, A.V. (1974), J.Molec.Biol. 84, 471.

Blake, C.C.F. and Rabstein, M.A. (1970), personal communication.

Dobson, C.M. and Levine, B.A. (1975), In New Techniques in Biophysics and Cell Biology (Pain, R.H. and Smith, B. eds). In the press.

Dwek, R.A., Richards, R.E., Morallee, K.G., Nieboer, E., Williams, R.J.P. and Xavier, A.V. (1971), Eur.J. Biochem. 21, 204.

Jensen, L.H. (1974), personal communication.

Jones, R., Dwek, R.A. and Forsén, S. (1974), Eur.J. Biochem. 47, 271.

Perkins, S.J. (1975), personal communication.

Phillips, C.S.G. and Williams, R.J.P. (1966), Inorganic Chemistry Vol. II, Clarendon Press (Oxford).

Roberts, G.C.K. and Jardetzky, O. (1970), Adv.Protein Chem. 24, 448.

Rossotti, F.J.C. and Rossotti, H. (1961), Determination of Stability Constants, McGraw-Hill (N.Y.).

Rupley, J.A., Banerjee, S.K., Kregar, I., Lapanje, S., Shrake, A.F. and Turk, V. (1974), in Lysozyme (Osserman, E.F., Canfield, R.E. and Beychok, S. eds) Academic Press (N.Y.) 251.

Secenski, I.I. and Lienard, G.E. (1974), J.Biol.Chem. 249, 2932.

CHAPTER VII

CONFORMATIONAL ANALYSIS - THE TIME-AVERAGED STRUCTURE

VII.1 Theory

Now that shift and broadening ratios have been obtained, it is required that they be used to provide conformational information. In order to do this, the origin and meaning of the ratios must be understood.

VII.1.1 Shift Ratios

The shift induced by the binding of a paramagnetic lanthanide ion can arise from three main sources (Barry et al., 1971, 1974a; Dobson and Levine, 1975). First, a shift may arise from an induced conformational change or pK change on binding. This 'diamagnetic effect' may be estimated by observing shifts induced by La^{3+} or Lu^{3+}, as described above. There are then two paramagnetic contributions to the shift, arising from through-bond (contact or scalar) or from through-space (pseudocontact or dipolar) mechanisms. However, the contact shift becomes negligible for nuclei more than two or three bonds away from the co-ordinated ion, and is unlikely to contribute to any of the observed shifts in lysozyme. The pseudocontact shift is given (Bleaney, 1972) by

$$\Delta_p^i = \frac{D\,(3\cos^2\theta_i - 1)}{r_i^3} - \frac{D^1\,(\sin^2\theta_i \cos 2\phi_i)}{r_i^3}$$

where r_i, θ_i and ϕ_i are the spherical co-ordinates of the nucleus (i) with the lanthanide ion as origin. The axes are determined by the magnetic symmetry properties of the system (Fig. VII.1) the z axis being taken as the direction of the principal magnetic axis of symmetry. D and D^1 are parameters of the ligand field

FIGURE VII.1

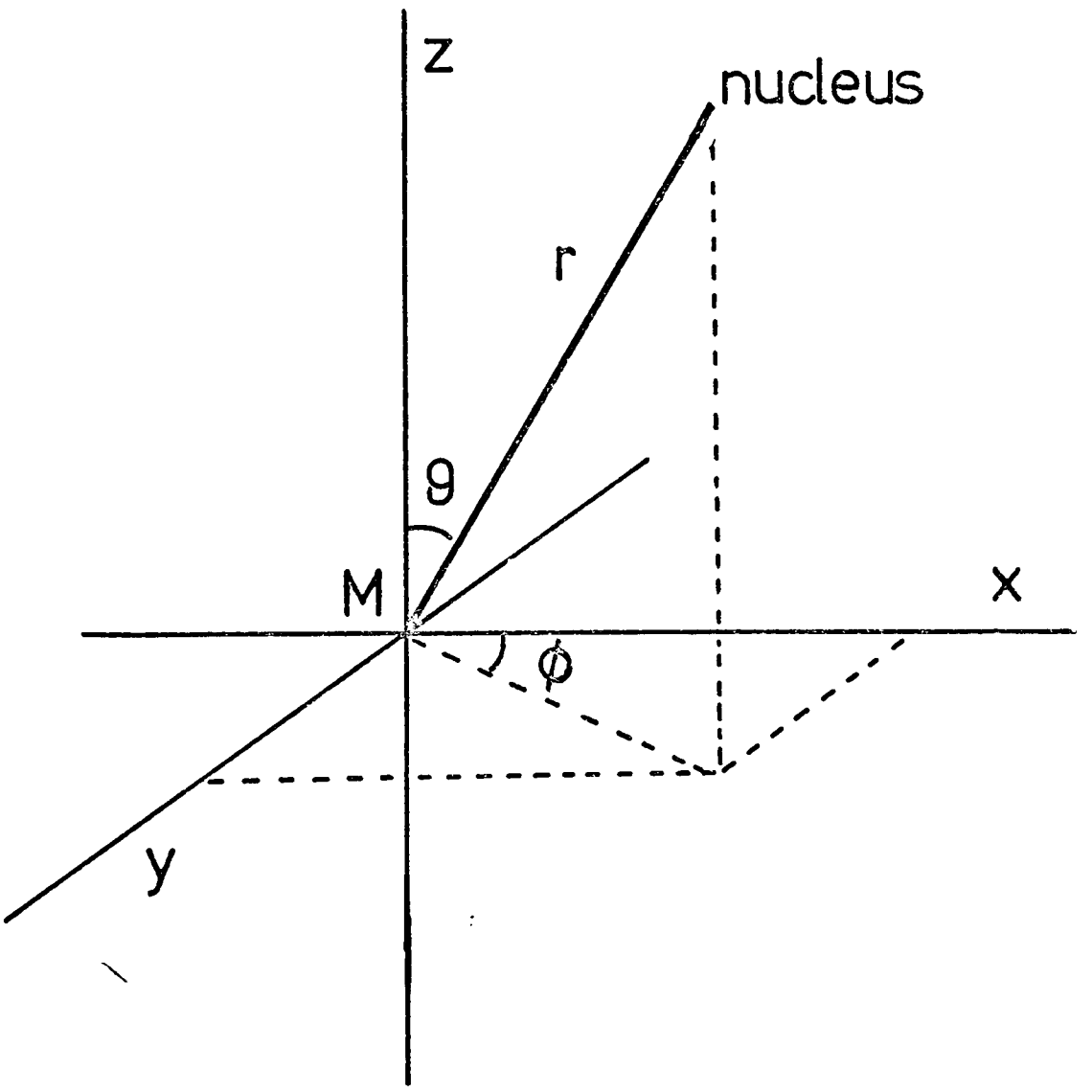

Definition of the parameters r, θ and φ in the pseudocontact shift equation. The principal axis of symmetry is in the Z direction, defined by the lanthanide cation (M). Later, the direction of the principal symmetry axis is defined with respect to the lysozyme X-ray co-ordinate axes by two angles α and β defined in an analogous manner to θ and φ.

which determines the symmetry of the bound ion.

In nearly every case studied, it appears that this equation is simplified because $D^1 = 0$. This is the situation of axial symmetry, and is thought to arise from exchange processes which average rhombic symmetries to an effective axial symmetry (see Dobson and Levine, 1975). For the axial symmetry case, the ratio (R_{ij}) of the induced shift of the resonance of nucleus i to that of the resonance of nucleus j is

$$R_{ij} = \Delta_p^i / \Delta_p^j = \frac{3\cos^2\theta_i - 1}{r_i^3} \Bigg/ \frac{3\cos^2\theta_j - 1}{r_j^3}$$

This ratio therefore contains only geometric parameters; the constants have been eliminated. A simple relationship such as this does not arise for non-axial symmetry where $D^1 \neq 0$.

Consider now the values of R_{ij} for different lanthanides. If these values are the same for different lanthanides, four conclusions may be drawn. First, the complexes must be homologous, in other words the value of r, θ and ϕ must be the same for each lanthanide. Secondly, the shifts must be solely pseudocontact in origin. Thirdly, the symmetry must be axial, so that $D^1 = 0$. Finally, fast exchange conditions are generally assumed, where the observed shift $\delta_i = f\ \Delta_i$. Values of R_{ij} are generally determined from δ_i/δ_j and this will only be the same as Δ_i/Δ_j if true fast, and not intermediate, exchange conditions are met. If the ratios are not the same for different lanthanides, then one or more of these assumptions is incorrect.

VII.1.2 Relaxation Ratios

The slow electron relaxation time of Gd^{3+} means that this ion can cause large perturbations to the relaxation times of nearby nuclei (see Dwek, 1973). If T_1^o and T_2^o are the

relaxation times of a nucleus in the absence of Gd^{3+}, and $T_{1\ obs}$ and $T_{2\ obs}$ in its presence (the ligand being fully bound to the Gd^{3+}), then the paramagnetic contributions to the relaxation times are T_{1M} and T_{2M} where

$$1/T_{iM} = 1/T_{iobs} - 1/T_i^{o} \quad (i = 1,2).$$

The diamagnetic effects on the relaxation times due to binding should also be included in T_i^{o}, and are measured using La^{3+} or Lu^{3+}.

From the equations of Solomon (1955) and Bloembergen (1957), for dipolar relaxation

$$1/T_{1M} = f(\tau_c).\ 1/r^6$$

$$\text{and} \quad 1/T_{2M} = f^1(\tau_c).\ 1/r^6$$

where τ_c is the correlation time for the dipolar mechanism.

$$\text{Thus,} \quad \frac{1/T_{iM}^{p}}{1/T_{iM}^{q}} = \left[\frac{r_q}{r_p}\right]^6 \qquad (i = 1,2)$$

for nuclei p and q. This ratio therefore gives relative distance information. In fast exchange, the observed paramagnetic relaxation is T_{ip} where $1/T_{ip} = f/T_{iM}$. In order to ensure that a dipolar mechanism operates and that fast exchange applies, both T_1 and T_2 measurements should be made, preferably at two frequencies. In systems with binding similar to that of lysozyme and investigated previously (see Dobson and Levine, 1975) these conditions have been met.

In this thesis, <u>ratios</u> of distances only are discussed. The development of the pulse sequences described in Chapter III will allow absolute values of T_{1M} and T_{2M} to be determined for certain resonances. This then allows τ_c to be calculated, and thus absolute values of distances to be measured.

VII.1.3 Requirements for Conformational Analysis

Any approach to conformational analysis must attempt to match the nmr shift and relaxation data to (a) a molecular conformation, (b) a metal ion position and (c) a symmetry axis direction. For a given set of (a), (b) and (c), values of $(3\cos^2\theta-1)/r^3$ and of $1/r^6$ can easily be calculated for different nuclei and ratios taken of each. By varying (a), (b) and (c) in turn, values of these ratios can be compared to the experimental shift and broadening ratios for each set of (a)-(c). Computer programmes have been written (Barry et al., 1971, 1973) for this purpose. In order to use the shift data in this way it is necessary to establish that the shifts are pseudocontact and also that the symmetry is axial. Otherwise, the shift ratios do not give ratios of $(3\cos^2\theta-1)/r^3$.

For lysozyme, the most straightforward approach is to compare observed shift and relaxation ratios with values of $(3\cos^2\theta-1)/r^3$ and of $1/r^6$ calculated from the X-ray structure and X-ray determined metal binding site. The only variable is then the direction of the symmetry axis which is required for the shift ratio comparison. This approach was therefore adopted as the initial stage of the conformational analysis.

VII.2. Preliminary Considerations of the Conformational Analysis

The approach outlined above is complicated by three factors. These will be briefly considered in turn.

VII.2.1 The Co-ordinates of the Bound Metal Ion

As indicated above, there are problems associated with the position in the crystal of the bound lanthanide ion. These may arise from the conditions under which the crystallography is carried out, or there may be alternative binding sites

in the region of glu 35 and asp 52, although this seems unlikely from the nmr data. In this work the co-ordinates of the bound metal ion were taken from the low-resolution work of Blake and Rabstein (1970) where a single binding position was measured. These co-ordinates are x = 15/120, y = 36/120 and z = 25.5/60 for the lysozyme unit cell a = b = 79.1 Å and c = 37.9 Å. On the scheme used for the RS5D co-ordinates, and used in Imoto et al., 1972, the co-ordinates are x = 9.89, y = 22.73 and z = 21.79. These are given in Ångstrom units in a right-handed orthogonal co-ordinate system. This position is 3.0 Å from the carboxylate carbon of asp 52 and 6.3 Å from that of glu 35, these groups being defined for the native structure.

VII.2.2 Experimental Conditions

The experimental conditions were not identical for the X-ray and nmr studies. These differences are summarised in Table VII.1. Differences in pH and in temperature are not likely to be important, as it has already been shown that the shift ratios are little affected by either. However, the major difference is that the nmr data are for the protein bound to a lanthanide cation, whilst the X-ray high-resolution studies are for the metal-free protein. It has already been noted, and will be further discussed in Chapter IX, that the binding of lanthanide cations induces a small localised conformational change.

VII.2.3 Mobility of Side-Chains

The X-ray structure is a particular time-averaged structure. It has been noted earlier that nmr experiments indicate quite unambiguously that certain of the side-chains of lysozyme have motion independent of that of the molecule as a whole. This motion will affect the shift and broadening

TABLE VII.1

Conditions for Nmr and X-ray Studies

	Nmr	X-ray
Phase	solution	solid
State	Ln^{3+} bound	Ln^{3+} free
Ionic Strength	0-0.4	ca. 0.9
Anion	Cl^-	Cl^-
pH	3.5-6.0	4.5
Temperature	54°C [a]	20°C

[a] there is no evidence for a temperature induced conformational change.

ratios for each of the different side-chain conformations involved in the averaging. Note that ratios for an average conformation are not observed (see Dobson and Levine, 1975). However, motion of this type in the crystal could result in an averaged conformation in the X-ray structure because of the fitting procedure.

At this stage, only those motions which can readily be interpreted can safely be allowed for in the conformational analysis. Thus, rotation of all methyl groups was simulated by calculating values of $(3\cos^2\theta-1)/r^3$ and of $1/r^6$ for 12 equally populated conformers generated by rotation about the $C-CH_3$ bond. A mean value of the two functions was then taken. Similarly, rapid flipping between the two equivalent orientations of a tyrosine (or phenylalanine) ring was simulated by calculating the values of the two functions in each orientation, and then taking mean values. These motions are further discussed in Chapter IX.

VII.3 Quantitative Conformational Analysis

In order to discuss the shift data, the meaning and direction of the metal symmetry axis must be defined. This is not required for the broadening data, and therefore these will be discussed first.

VII.3.1 The Gd^{3+} Broadening Data

From the Gd^{3+} broadening ratios given in Table VI.6, the relative values of effective distances were calculated, using the relationship $T_{2M}^i/T_{2M}^j = r_i^6/r_j^6$ for two nuclei i and j. The word effective allows for the possible effects of motion on the values. Also, the values of distances were calculated from the X-ray data. Allowing for the motion of methyl and

aromatic groups only, values of the effective distances were calculated for these groups, and the ratios taken of all the calculated distances or effective distances. For convenience, all the ratios, both experimental and calculated, were taken relative to the ortho protons of tyr 53. These data are given in Table VII.2, and plotted in Fig. VII.2.

The agreement between the two sets of data is reasonably good, though not excellent. From this agreement, the following conclusions may be drawn. First, the structure of the protein in solution and in the crystal must be closely similar. Secondly, the effects of internal side-chain motion are not so great that the nmr and X-ray data cannot be compared. Thirdly, the nmr effective distances become shorter than the X-ray distances at distances more than about 12 $\mathring{A}$ from the Gd^{3+}. This is undoubtedly due to the increasing importance of secondary binding sites for more distant groups. Fourthly, changes in the metal ion co-ordinates of say $\pm$ 2 $\mathring{A}$ are not likely to alter these conclusions significantly. Overall, there are no discrepancies between the experimental and calculated effective distances which are so large that they are outside the experimental and computational errors in the comparison. Given this satisfactory conclusion, the shift data are considered.

VII.3.2 The Paramagnetic Shift Data

VII.3.2.1 Comparison of Different Lanthanides

An examination of Table VI.5 shows that with the exception of the values for Tm^{3+} and Er^{3+}, the sets of shift ratios with different lanthanides are rather similar for most resonances. In small molecule systems so far examined, the shift ratios in aqueous solution induced by Tm^{3+} and Er^{3+} also differ from those induced by the other lanthanides (Barry *et al.*,

TABLE VII.2

Observed and Calculated Relative Effective Distances[a]

Residue (Proton)	Resonance Number	Relative Distances[b] Calculated	Observed
val 109	M16	0.53	0.60[c]
val 109	M17	0.73	0.60[c]
trp 108 C(2)	A11	0.73	0.65
ala 110	M20	0.81	0.62
thr 51	M9	0.84	0.93
tyr 53 o-	A6	1.00	1.00
ala 107	M14	1.08	0.94
leu 56	M11	1.18	1.01
ile 98	M2	1.19	1.05
leu 56	M8	1.36	1.08
met 105	M6	1.38	1.20
leu 17	M1	2.00	1.30

[a] relative to tyr 53 (o-) = 1.00. In fact calculated effective distance to tyr 53 (o-) is 10.0 Å.

[b] see comments in text concerning distances which are long. The experimental data have not been corrected for the effects of weak binding sites.

[c] the residue val 109 is not clearly defined in the X-ray structure.

FIGURE VII.2

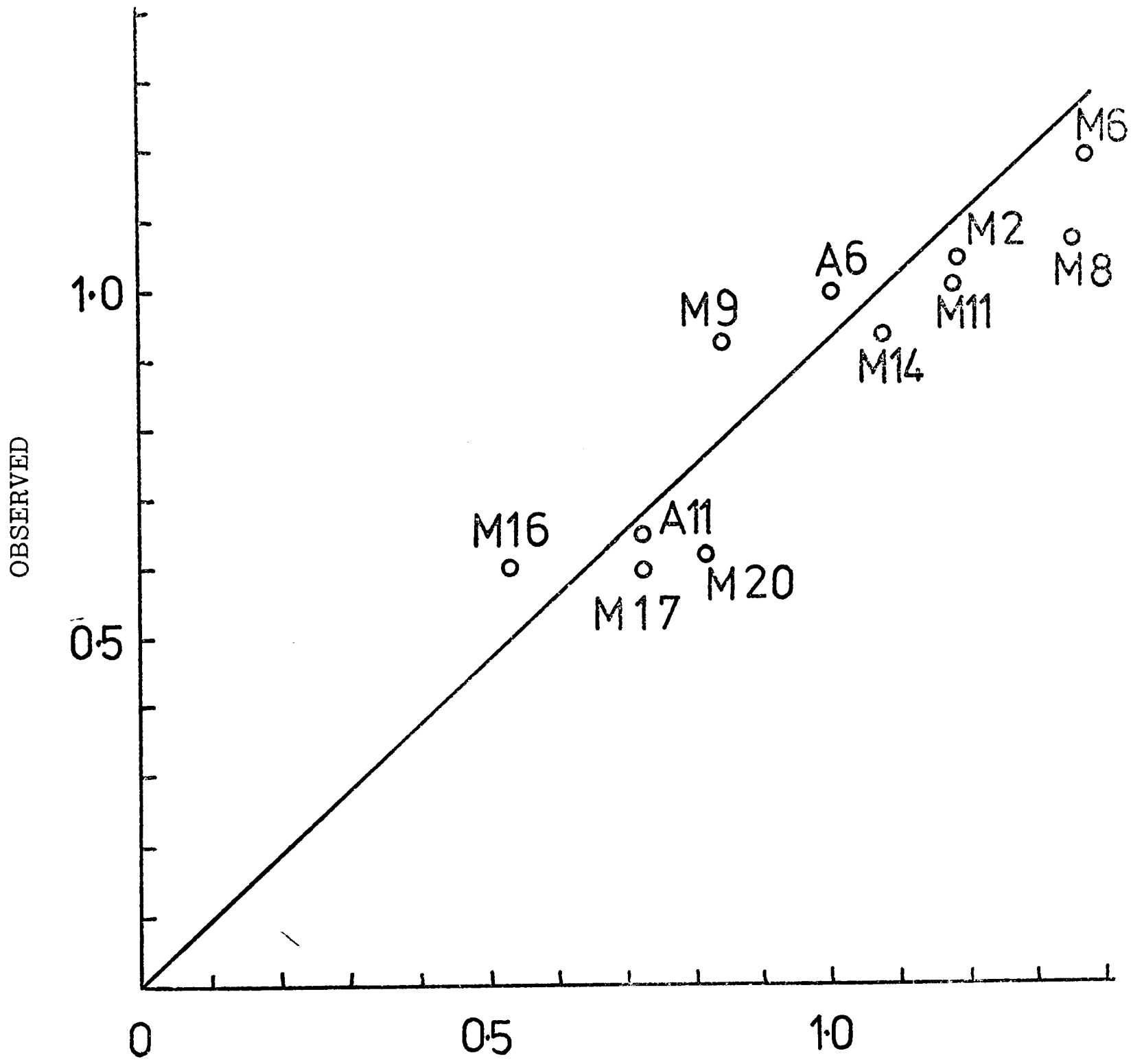

CALCULATED

Plot of observed against calculated effective distances of different groups (defined by assigned resonance numbers). from the bound Gd^{3+} cation (see text).

1974b; Levine et al., 1975; Dobson and Levine, 1974). This is thought to be involved with the size of these ions in relation to the steric requirements of an eight co-ordinate hydrated lanthanide ion complex. The ratios with Tm^{3+} and Er^{3+} will therefore not be considered further here. The similarity of the shift ratios for the other lanthanides suggests, following the argument of Section VII.1.1, that for these lanthanides the assumptions of a pseudocontact shift mechanism, fast exchange, homologous complexes and axial symmetry are valid. However, out of these ca. 100 shift ratios for Ce^{3+} to Ho^{3+} given in Table VI.5, 9 are considered to differ from the values with most lanthanides by well outside the experimental values. There is no evident pattern behind these anomalous values, except that they occur only for the residues shown from the Gd^{3+} broadening ratios to be close to the lanthanide binding site (within 10 Å). This is true whether or not the shift ratios themselves are very large. Neither the presence of a contact contribution, or lack of fast exchange conditions is a feasible explanation of these anomalous values. The explanation therefore must lie either with lack of axial symmetry or with the lack of truly homologous complexes. No general change in symmetry or homology can however occur for the different lanthanides, because the vast majority of resonances do not detect it. It is known from the slightly different effects of binding La^{3+} and Lu^{3+} that these ions do bind in a slightly different manner. The present and not entirely satisfactory explanation of the anomalous ratios is therefore that they are the result of very small changes in the binding mode of different lanthanides. Clearly further experimental evidence is required on this point. Overall, however, the shift ratios for Ce^{3+} to Ho^{3+} are very similar with each lanthanide.

A further piece of evidence concerning the origin of the lanthanide shifts has been obtained from the magnitude of the shifts induced by the different lanthanides. Values, relative to the shift observed for resonance of the ortho protons of tyr 53 in each case, are given in Table VII.3. Also given are values for the methyl group resonance of propionate (Levine, 1974), and theoretical values derived by Bleaney (1972). These theoretical values are for pseudocontact shifts in an axially symmetric system. The close agreement of the different sets of data suggest that the origin of the shifts in lysozyme is the same as that in the small molecule propionate, and is well described by the theory of Bleaney.

VII.3.2.2 Interpretation of the Shift Ratios

The shift ratios of Table VI.5 were adequate for comparison of the behaviour of different lanthanides. For the quantitative analysis described below, the more accurate values of Table VI.6 were used. These values were obtained for Pr^{3+}, but as shown above, the values for the different lanthanides (Ce^{3+} to Ho^{3+}) are closely similar.

Using the X-ray structure and bound lanthanide co-ordinates values for $(3\cos^2\theta-1)/r^3$ were calculated for the different nuclei listed in Table VII.4, allowing for the motion of methyl and aromatic groups, for different directions of the symmetry axis. These directions were defined by two angles α and β which refer to rotation angles about the crystallographic x and z axes respectively, the initial direction ($\alpha = 0$, $\beta = 0$) being the z direction (see Fig. VII.1). There is no distinction for the shift equation between directions of the symmetry axis at 180^o intervals because $\cos^2\theta = \cos^2(\theta + 180^o)$. Therefore consideration of α and β, each from 0^o to 180^o only is required.

TABLE VII.3

Induced Shift Magnitudes Relative to Dy^{3+} = -100

Lanthanide	Lysozyme[a]	Propionate[b]	Theory[c]
Ce	-5	-4	-6
Pr	-10	-14	-11
Nd	-6	-5	-4
Sm	-1	-1	-1
Eu	7	6	4
Tb	-63	-55	-86
Dy	-100	-100	-100
Ho	-41	-42	-39
Er	17	8	33
Tm	32	18	53
Yb	13	14	22

[a] tyr 53 ortho protons

[b] methyl group

[c] Bleaney (1972).

Therefore, the symmetry axis was changed by varying β from 0^{o} to 180^{o} in 10^{o} steps for all values of α from 0^{o} to 180^{o} in 10^{o} steps. Only for a small range of values of α and β were the calculated effective ratios of $(3\cos^2\theta-1)/r^3$ at all similar to the experimental shift ratios. These values were approximately $\alpha = 80^{o}$-120^{o} and $\beta = 60^{o}$-100^{o}. For these values, shifts which were upfield with the lanthanides Eu^{3+} and Yb^{3+} and downfield with the other lanthanides (see Table VII.3) corresponded to values of $(3\cos^2\theta-1)$ which were positive. This is in agreement with all other studies of small molecules in aqueous solution (see Barry et al., 1971; Dobson and Levine, 1975).

Table VII.4 lists calculated shift ratios for two values of α and β. Further values are given in Appendix D. The variation of these calculated values with changes in α and β can be seen from this Table. Some residues are very sensitive to these changes (e.g. val 109, ala 110, trp 63, ile 98 δ) and these have values of $3\cos^2\theta-1$ which are close to zero for these values of α and β. Others are relatively insensitive to the changes (e.g. tyr 53m-, trp 108 C(2)H, ile 98 (γ)).

Overall, for all the residues the observed shift ratios are well in accord with these calculated ratios. The largest discrepancy is of val 109. This is not surprising, for this exposed residue cannot be properly observed in the X-ray electron density map (see Appendix A) and appears to be a mobile group in solution. Additionally, the residue is close to the bound metal ion, and also appears to have a value of $3\cos^2\theta-1$ close to zero. Both these factors make the shift ratio very sensitive to small errors or changes in conformation. Note that for this residue the experimental shift ratios are rather variable with

TABLE VII.4

Observed and Calculated Shift Ratios

Proton	Resonance Number	Observed Shift Ratio[a]	Calculated Shift Ratio $\alpha = 100^{o}$, $\beta = 70^{o}$	Calculated Shift Ratio $\alpha = 110^{o}$ $\beta = 100^{o}$
tyr 20 o-	A3/A8	-14/A	-3	-6
tyr 23 o-	A3/A8	-14/A	-10	-3
tyr 53 o-	A6	100	100	100
tyr 53 m-	A12	160	144	93
trp 62 C(2)			-25	-30
trp 63 C(2)	A20	53	42	-20
trp 108 C(2)	A11	-117	-137	-124
trp 108 N(1)	N5	-90	-21	-84
met 12	M22	-2	-6	-12
ala 31			-35	-14
thr 51	M9	151	111	166
leu 56[b]	M8	-9	-19	-35
leu 56[b]	M11	A	-1	-23
ile 98 γ	M2	-32	-23	-35
ile 98 δ	M4	A	14	-29
met 105	M6	-14	-25	-11
ala 107	M14	-68	-49	-41
val 109[b]	M16	-109	65	631
val 109[b]	M17	73	175	271
ala 110	M20	59	-80	73

[a] A is O ± 10 but not directly measurable. Assignments of A20 and M14 are strengthened by these results. Alternative assignments to trp 62 and ala 31 appear unlikely.

[b] distinction between assignment of the two CH_3 groups of each residue cannot be made.

FIGURE VII.3

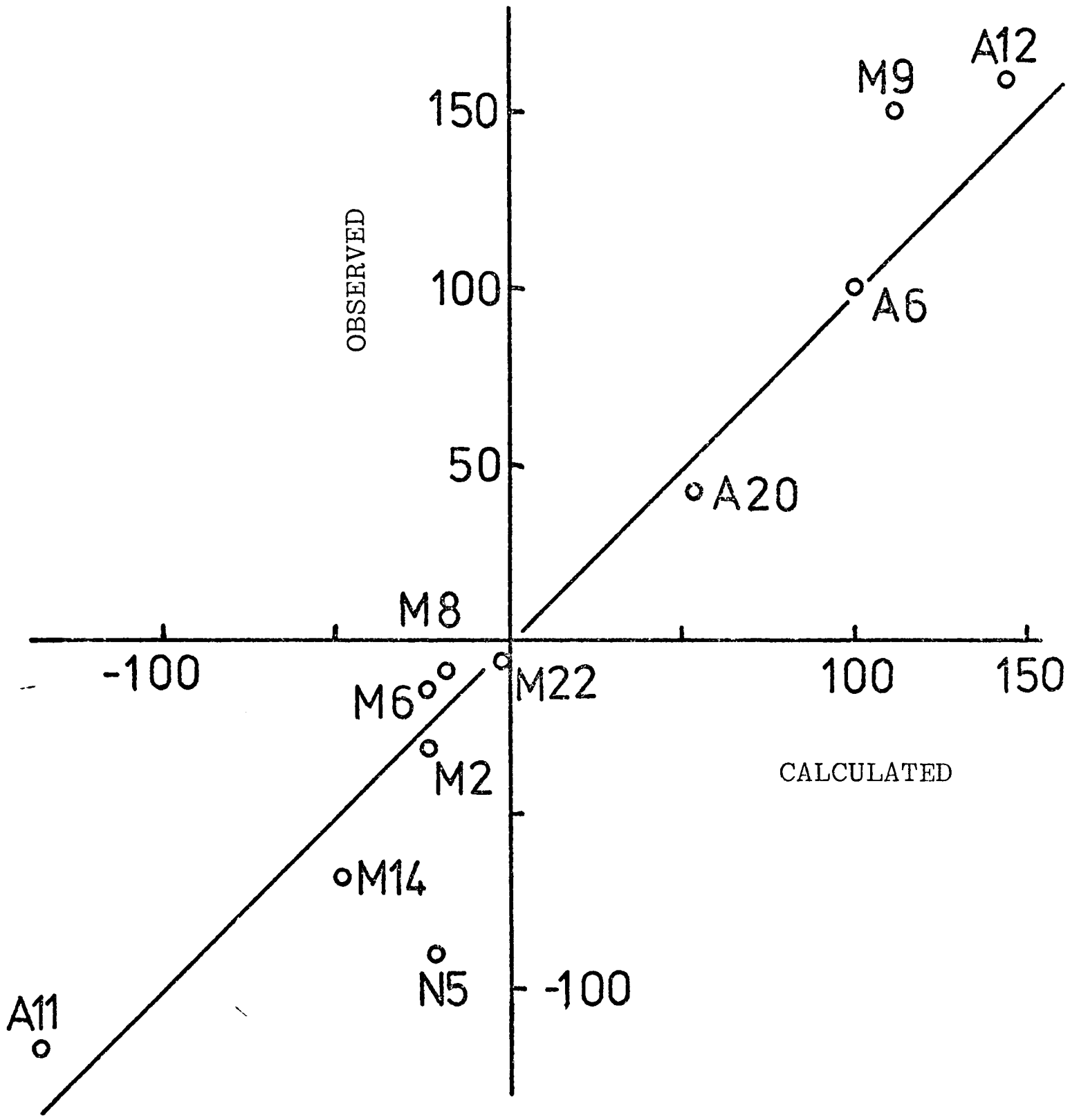

Plot of observed against calculated shift ratios for different groups with Pr^{3+} (see Table VII.4). For the calculated shift ratios, $\alpha = 100^{o}$, $\beta = 70^{o}$.

different lanthanides. A graphical illustration of the agreement between calculated and observed shift ratios is given in Fig. VII.3.

Overall, the satisfactory level of agreement shown in this analysis allows two conclusions to be drawn. First, the X-ray structure and lanthanide co-ordination position are reasonable descriptions of the solution time-averaged structure. Secondly, the assumption of axial symmetry on the basis of the experimental shift ratios and magnitudes appears to be valid. However, the observed differences are such that two aspects of the solution structure must be investigated before further progress can be made. These are the mobility of side-chains and the nature of induced conformational changes. These are considered in the next two chapters.

VII.4 Summary

Both shift and broadening data indicate that the X-ray structure is an adequate description of the time-averaged solution structure of lysozyme. The shift data overall are well described by axial symmetry of the bound lanthanide cation, although some anomalies in the observed data remain. Before further progress can be made, the dynamic behaviour of the protein, and the nature of induced conformational changes on lanthanide binding, must be considered.

References for Chapter VII

Barry, C.D., Glasel, J.A., North, A.C.T., Williams, R.J.P. and Xavier, A.V. (1971), Nature 232, 236.

Barry, C.D., Glasel, J.A., Williams, R.J.P. and Xavier, A.V. (1974a), J.Molec.Biol. 84, 471.

Barry, C.D., Dobson, C.M., Williams, R.J.P. and Xavier, A.V. (1974b), J.C.S. Dalton, 16, 1765.

Barry, C.D., Dobson, C.M., Ford, L.O., Sweigart, D.A. and Williams, R.J.P. (1973), In Nuclear Magnetic Resonance Shift Reagents (Sievers, R.E. ed.), Academic Press (N.Y.), 173.

Blake, C.C.F. and Rabstein, M.A. (1970), personal communication.

Bleaney, B. (1972), J.Mag.Resonance 8, 91.

Bloembergen, N. (1957), J.Chem.Phys. 27, 595.

Dobson, C.M. and Levine, B.A. (1975), In New Techniques in Biophysics and Cell Biology, (Pain, R.H. and Smith, B. eds), in the press.

Dwek, R.A. (1973), Nuclear Magnetic Resonance in Biochemistry, Clarendon Press (Oxford).

Imoto, T., Johnson, L.N., North, A.C.T., Phillips, D.C. and Rupley, J.A. (1972), In The Enzymes Vol. VII, 3rd ed. (Boyer, P.D. ed.), Academic Press (N.Y.), 665.

Levine, B.A. (1974), personal communication.

Levine, B.A., Thornton, J.M. and Williams, R.J.P. (1974), J.C.S. Chem. Comm., 669.

Solomon, I. (1955), Phys.Rev. 99, 559.

CHAPTER VIII

CONFORMATIONAL ANALYSIS - DYNAMIC ASPECTS

VIII.1 Introduction

In earlier parts of this thesis, comments concerning time-dependent or dynamic aspects of the protein conformation have frequently been made. One aspect of the dynamic behaviour of the protein is concerned with the rate of the changes in conformation which accompany the binding of species to the protein. Studies of this type, which resemble studies of the rate of interconversion of isomers of small molecules, are discussed in Chapter IX. Another aspect of the dynamic behaviour of the protein is concerned with the motions of groups in a given conformational state. These motions are internal rotations and vibrations of segments of the molecule, and are discussed in this Chapter. These motions can be classified by their effects on the nmr spectrum. This approximates to a division on the basis of the relative rates of the processes.

VIII.2 Detection of Rate Processes by Nmr

Nmr may be used to follow rate processes in three essentially different ways. These are summarised in Table VIII.1. For very slow processes, spectra may be obtained at different time intervals, and the spectral changes measured as a function of time. For faster processes, individual spectral features must be examined. The two methods by which rate information may be obtained in this way are (a) from analysis of relaxation times and other relaxation phenomena. These are generally informative about very fast processes. (b) From the observation of exchange effects in the spectra. These exchange effects may

be manifested in (i) line broadening (intermediate exchange), (ii) in the observation of more than one resonance from a given nucleus which can exist in more than one environment (slow exchange) and (iii) in the observation of a single resonance from more than one nucleus, or from one nucleus known to exist in more than one environment (fast exchange). Analysis of these situations for simple cases are described in standard textbooks (Pople et al., 1959; Jackman and Sternhell, 1969; Farrar and Becker, 1971). The approximate timescales of the effects are given in Table VIII.1, along with specific methods by which experimental investigation may be carried out.

VIII.3 Fast Motions - Relaxation Phenomena

In lysozyme, relaxation processes of individual resonances have been studied by measurements of T_1 and T_2, and by measurements of nuclear Overhauser effects. In order to attempt a detailed interpretation of the data, experiments have been carried out at two different frequencies, 90 MHz and 270 MHz, and at two different temperatures, generally 23°C and 68°C. The experiments were carried out at pH 4.0 using 5mM solutions of lysozyme in D_2O. Some experiments were additionally carried out with 10mM solutions.

VIII.3.1 Procedures

In Appendix B are summarised equations which describe the dependence of T_1, T_2 and the nuclear Overhauser enhancement parameter (η) on a correlation time, τ_c. These equations require that τ_c defines some isotropic motion or motions. In particular, the correlation function describing motion is assumed to be an exponential with a time constant τ_c. An example of motion which will be well described by this model is the rotation of a spherical

TABLE VIII.1

Nmr Methods for Following Rate Processes

Type of Method	Experimental Measurements	Approximate Timescale[a]
Relaxation phenomena	(a) NOE	10^{-10} to 10^{-8} sec
	(b) T_1 frequency dependence	10^{-10} to 10^{-8} sec
	(c) Relative values of T_1 and T_2	longer than 10^{-10} s
	(d) Absolute values of T_1 and T_2	wide range
Exchange effects	(a) T_1, T_2, lineshapes	10^{-5} to 10^{-2} sec
	(b) cross saturation	10^{-3} to 10^{0} sec
Consecutive spectra	Record changes in series of spectra	longer than 10^{1} sec

[a] this is an indication of the values of correlation times or lifetimes that can be directly measured at 270 MHz, assuming that a single process is involved.

object. The rotation of many small molecules in solution has been shown to be of this type.

Consider the behaviour of a proton in lysozyme. From the experimental relaxation data, values of τ_c may be calculated in several ways. Details are given in Appendix B and these are now summarised.

(i) The nuclear Overhauser effect. Measurement of η permits calculation of τ_c provided that the relaxation of the observed spin I is fully determined by the irradiated spin S. Alternatively, the fraction of the relaxation of I caused by S must be known. The dependence of η on τ_c is plotted for a frequency of 270 MHz in Fig. VIII.1. Measurement of η has been described in Section III.2.2.1.

(ii) The value of T_1 or T_2. It is possible to calculate τ_c directly from the value of T_1 or T_2, provided that the relaxation is purely from a dipolar mechanism. The distances to all the nuclei S_i relaxing a given nucleus I must be known. However, because the relaxation follows an r^{-6} law, it is generally necessary only to consider the closest nuclei. The nature of the T_1 function results in two values of τ_c being found to be consistent with the value of T_1 in each case, but only one of these should be consistent with the value of T_2. The behaviour of T_1 and T_2 are shown in Fig. VIII.2. Measurement of T_1 and T_2 has been described in Section III.2.3.1.

(iii) The frequency dependence of T_1, T_2 or η. As Fig. VIII.1 and Fig. VIII.2 indicate, the values of T_1, T_2 and η can be frequency dependent provided that $\omega_I\tau_c$ is not much less than 1. In this work, only T_1 could be measured at two frequencies. The dependence on τ_c of the ratio of T_1 at 270 MHz to T_1 at 90 MHz is shown inFig. VIII.3 (cf. Appendix B). This ratio gives τ_c

FIGURE VIII.1

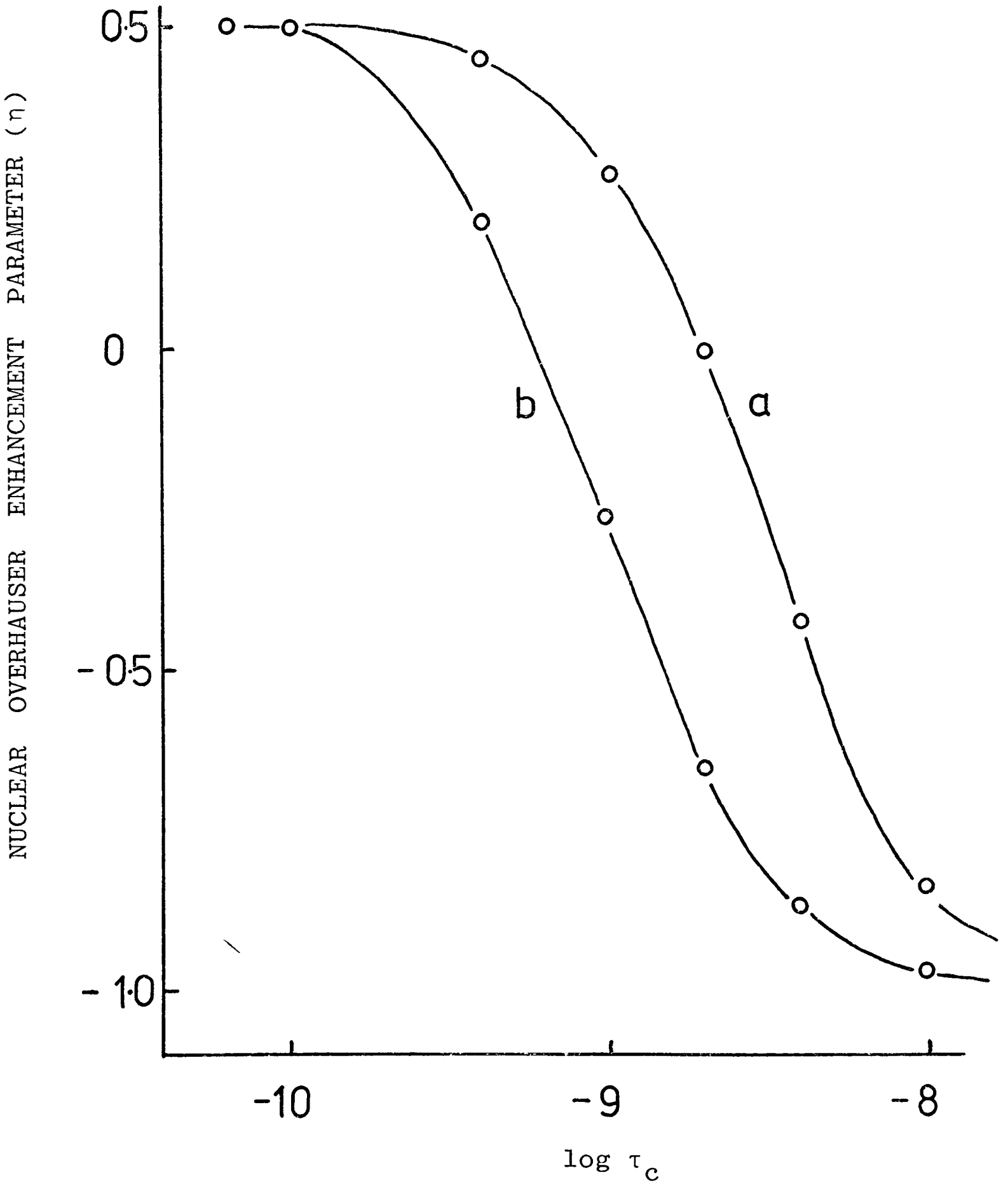

The theoretical dependence of the nuclear Overhauser enhancement parameter (η) on τ_c, according to the equation of Balaram et al., 1972 (see Appendix B). (a) 90 MHz; (b) 270 MHz.

FIGURE VIII.2

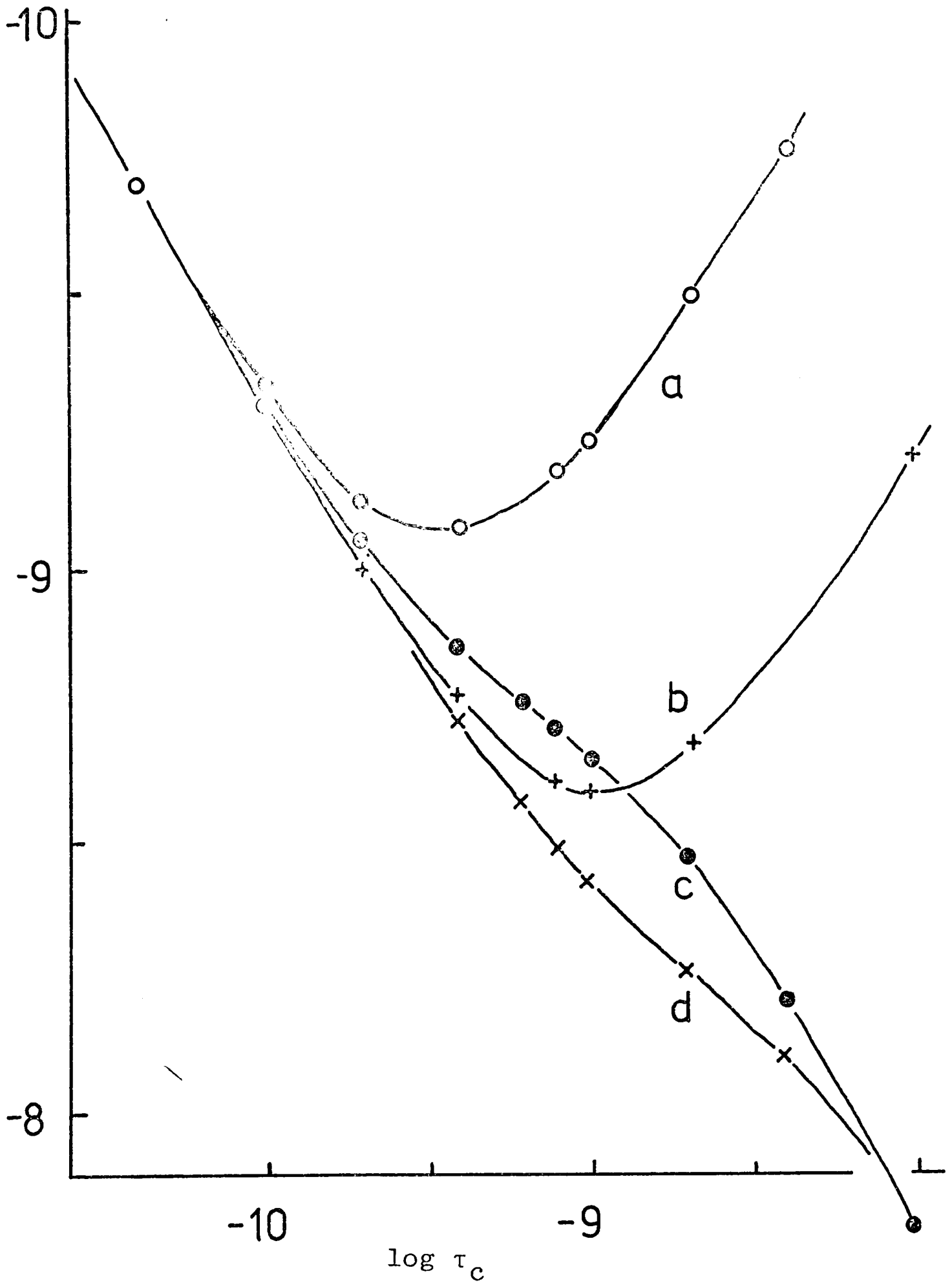

Theoretical dependence of T_1 and T_2 on τ_c. (a) T_1, 270 MHz; (b) T_1, 90 MHz; (c) T_2, 270 MHz; (d) T_2, 90 MHz. $1/T_1 = (3\hbar\gamma_o^4/10r^6)\, f_1(\tau_c)$ where $f_1(\tau_c) = \tau_c/(1+\omega_o^2\tau_c^2) + 4\tau_c/(1+4\omega_o^2\tau_c^2)$. $1/T_2 = (3\hbar\gamma_o^4/20r^6)\, f_2(\tau_c)$ where $f_2(\tau_c) = 3\tau_c + 5\tau_c/(1+\omega_o^2\tau_c^2) + 2\tau_c/(1+4\omega_o^2\tau_c^2)$. See Appendix B.

FIGURE VIII.3

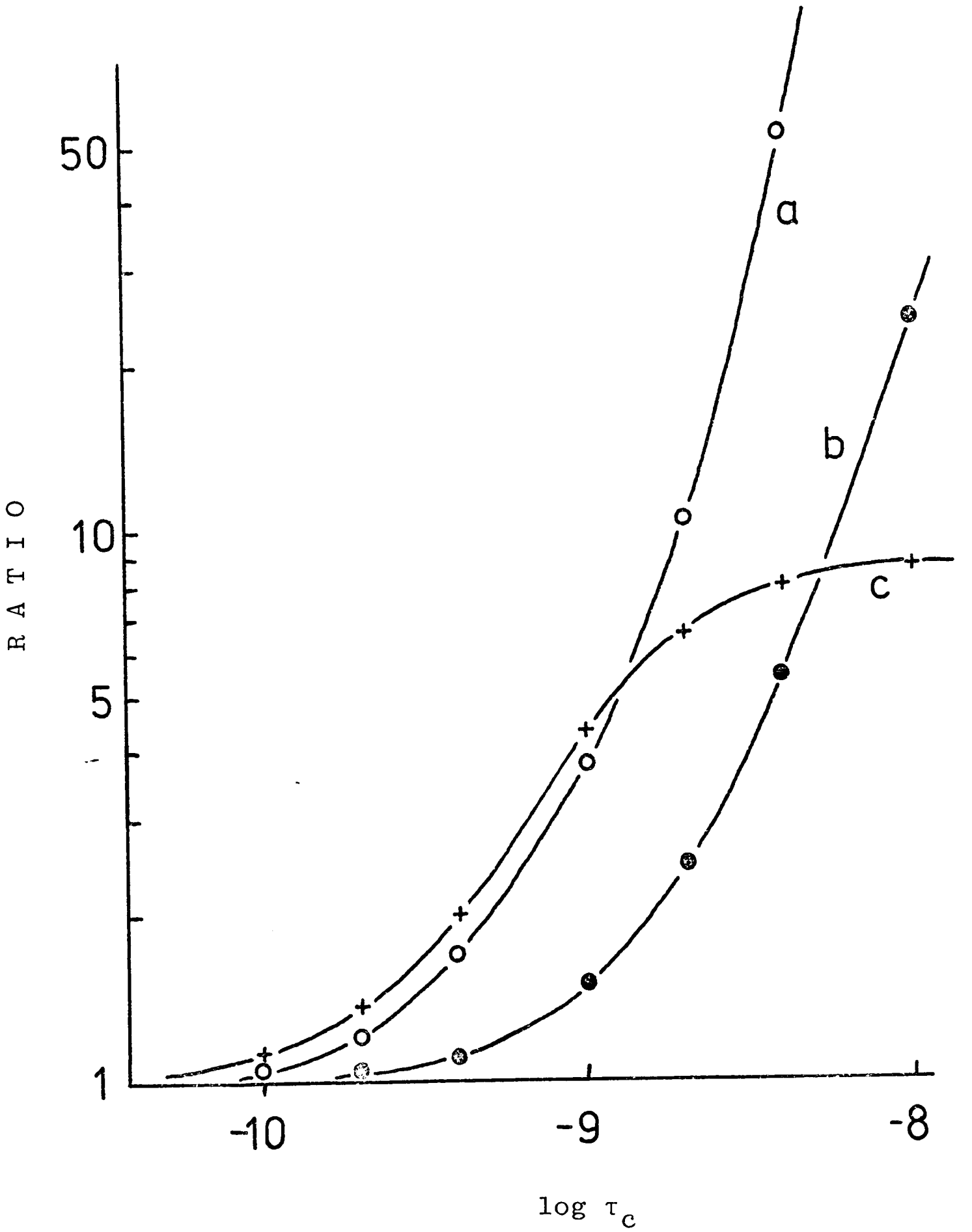

Theoretical dependence of (a) T_1/T_2 at 270 MHz, (b) T_1/T_2 at 90 MHz and (c) T_1 (270 MHz)/T_1 (90 MHz). See Appendix B.

directly, without requiring the knowledge of the distances of the nuclei causing relaxation.

(iv) The ratio of T_1 to T_2. As Fig. VIII.2 shows, the values of T_1 and T_2 are different provided $\omega_I \tau_c$ is not much less than 1. The ratio of T_1 to T_2 at 270 MHz is shown in Fig. VIII.3, and depends directly on τ_c.

Thus, by measuring the frequency dependence of T_1, and measuring the relative values of T_1 and T_2, values of τ_c may be directly obtained as described above. Additional information is available from nuclear Overhauser effect measurements, and from the absolute values of T_1 and T_2. These are dependent on the distances between protons in the molecule, which can therefore be investigated. It is essential first, however, to discover whether the relaxation effects in a protein can be described on the simple model above.

VIII.3.2 Measurement of Relaxation Times

T_1 and T_2 values were measured as described in Chapter III. These measurements were carried out for all the separately resolved resonances of lysozyme, making use of convolution difference procedures in conjunction with the pulse sequences. In addition, because it became clear that both T_1 and T_2 values for aromatic protons are rather similar for most of the protons, measurements of the average or bulk value of both T_1 and T_2 were obtained by treating the envelope of resonances as a system with a single relaxation time. This was necessary for spectra at 90 MHz where resolution of individual resonances was not possible. A similar procedure was possible for the envelope of methyl group resonances. The values of all the relaxation times measured are listed in Table VIII.2 and Table VIII.3.

TABLE VIII.2

Relaxation Times in Seconds Measured[a] at 68°C

Resonance Number	90 MHz T_1 (5mM)	270 MHz T_1 (5mM)	T_1 (10mM)	T_2 (5mM)	T_2 (10mM)
M1		0.54	0.74	0.081	0.055
M2		0.71	1.01	0.053	0.043
M3		0.58	0.84	0.072	0.065
M6		0.75	0.88	0.081	0.061
MB[b]	0.20	0.68	0.69	0.088	0.055
MB'[b]		0.65	0.88	0.113	0.082
LA[c]		0.48	0.53		
L1		0.81	1.01	0.095	0.081
L2		0.74	(1.34)	0.074	0.056
A1		0.75	1.10	0.097	0.078
A2		0.66	1.01	0.082	0.074
A3		1.04	1.15	0.138	0.090
AB[b]	0.26	0.87	1.08	0.138	0.104
A20		0.89	1.07	0.072	0.066
A21/22		0.95	1.21	0.117	0.081
A23		2.4	1.15	0.34	0.16

[a] 5mM and 10mM lysozyme concentrations at pH 4.0.

[b] Envelope of resonances at the following chemical shift values: MB (1.0 ppm); MB' (1.35 ppm); AB (7.25 ppm).

[c] Resonance at 3.0 ppm corresponding to ca. 20 equivalent protons

TABLE VIII.3

Relaxation Times in Seconds Measured[a] at 23°C

Resonance Number	90 MHz T_1	270 MHz T_1	270 MHz T_2
M1		0.95	0.033
M2		0.77	0.027
M3			
M6		0.94	0.056
MB	0.20	0.72	0.030
MB'		0.69	0.045
LA		0.55	0.049
L1		0.92	0.045
L2			
A1		0.78	0.029
A2		0.87	0.029
A3		1.04	0.046
AB	0.30	0.97	0.038
A20		1.01	0.050
A21/22		1.21	0.040
A23	0.71	1.49	0.177

[a] 5mM lysozyme solutions, pH 4.0. See Table VIII.2.

TABLE VIII.4

Ratios of Relaxation Times at 68°C

Resonance Number	T_1/T_2 10mM	T_1/T_2 5mM	T_1 (270 MHz)/T_1 (90 MHz) 5mM
M1	13.4	6.7	
M2	24.0	13.4	
M3	13.0	8.1	
M6	14.4	9.3	
MB	12.5	7.7	3.4
MB'	10.7	5.7	
LA			
L1	12.5	9.5	
L2	(24.0)	10.0	
A1	14.1	7.8	
A2	13.7	8.1	
A3	12.8	7.6	
AB	10.4	6.3	3.3
A20	16.2	12.3	
A21/22	14.9	8.1	
A23	7.2	7.1	

TABLE VIII.5

Ratios of Relaxation Times[a] at 23°C

Resonance Number	T_1/T_2	T_1 (270 MHz)/T_1 (90 MHz)
M1	29	
M2	28	
M3		
M6	17	
MB	24	3.6
MB'	15	
LA	11	
L1	20	
L2		
A1	27	
A2	30	
A3	23	
AB	26	3.2
A20	20	
A21/22	30	
A23	8.4	2.1

[a] for 5mM solutions only.

TABLE VIII.6

Correlation Times in Seconds from Measurements at 68°C and 23°C

Method	10mM solution 68°C	5mM solution 68°C	5mM solution 23°C
T_1/T_2 [a]	$2.0\text{-}2.3\times10^{-9}$	$1.4\text{-}1.9\times10^{-9}$	$2.4\text{-}3.2\times10^{-9}$
T_1(270MHz)/T_1(90MHz) [b]		0.7×10^{-9}	0.7×10^{-9}
η(trp 63, A1)	1.6×10^{-9}(min) [c]		
T_1 (A1) [d]	$1.0\text{-}2.2\times10^{-9}$		
T_1 (methyls) [a]			
(a) fixed geometry	$5.0\text{-}7.9\times10^{-9}$	$3.7\text{-}5.6\times10^{-9}$	$5.0\text{-}7.1\times10^{-9}$
(b) rapid rotation [e]	$1.0\text{-}1.6\times10^{-9}$	$0.6\text{-}1.1\times10^{-9}$	$1.0\text{-}1.4\times10^{-9}$

[a] range of values for difference resonances used, see text.

[b] envelope of resonances observed.

[c] minimum value as assumes all relaxation from neighbouring two protons, see text.

[d] range of values for relaxation of 50% to 100% from neighbouring two protons.

[e] factor of 4 applied to T_1 values, see text.

VIII.3.3 Relaxation Effects at 68°C

VIII.3.3.1 Ratios of Relaxation Times

From the data in Table VIII.2 and Table VIII.3, values of T_1/T_2 were calculated for each resonance, and values of T_1 (270 MHz)/T_1 (90 MHz) were calculated for the bulk measurements. These are listed in Table VIII.4 and Table VIII.5. These data show that the values of these ratios, under a given set of conditions, are rather similar for the different groups of the protein. There are consistent differences between the T_1/T_2 ratios for 5mM solutions and the more viscous 10mM solutions.

The values of T_1/T_2 for the 5mM solutions are between 5.7 and 9.5 for all the groups with the exception of those of resonances A20 and M2 which are slightly greater. These two resonances are however known to have an exchange contribution to $1/T_2$ under some conditions (see below), and therefore are not considered further here. From Fig. VIII.2 values of between 1.4×10^{-9} and 1.9×10^{-9} sec are obtained for τ_c for the different groups on the simple model outlined above. The ratio of T_1 (270 MHz)/T_1 (90 MHz) of 3.4 gives a value for τ_c of 0.7×10^{-9} sec as Fig. VIII.3 shows. These values of τ_c from the two methods are sufficiently similar to imply that this simple analysis may be reasonably good, and that the motion of all the groups may be described by a single correlation time of ca. 1.3×10^{-9} sec. Assuming that the viscosity is 0.5 centipoise at 68°C, if this value of τ_c corresponds to that for overall molecular rotation the hydrodynamic radius of lysozyme may be calculated from Stokes' Law as ca. 14 Å, a value which is not unreasonable.

For the 10mM solution, values of T_1/T_2 are larger, between 10.4 and 14.9, giving values of τ_c between 2.0×10^{-9} and

2.3×10^{-9} sec. This is consistent with slower molecular tumbling in a more viscous solution.

VIII.3.3.2 Absolute Values of Relaxation Parameters

In Section III.2.2.1, it was shown that for a 10mM solution of lysozyme at 68°C, a nuclear Overhauser enhancement of $\eta = -0.5$ is observed for resonance A1 as a consequence of simultaneous irradiation of resonances A4 and A5. As the maximum value of η is -1.0, at least 50% of the relaxation of the proton corresponding to A1 must arise from the protons corresponding to resonances A4 and A5. These protons are of the benzenoid ring of a tryptophan residue, assigned as trp 63.

A value of η of -0.5 corresponds to a value of τ_c of 1.6×10^{-9} sec. This is a minimum value, and a shorter value would be required if relaxation of the proton corresponding to A1 is not entirely due to the two adjacent protons of the tryptophan ring. Now, consider the T_1 value (1.10) for A1 at 270 MHz for the 10mM solution. If the relaxation of A1 does arise solely from these two adjacent protons (which are at ca. 2.45 Å from the proton corresponding to A1) this T_1 value corresponds to a value of τ_c of 1.0×10^{-9} or 1.4×10^{-10} sec, using the data of Fig. VIII.2. If only 50% of the relaxation arises from the adjacent protons, a value of τ_c of 2.2×10^{-9} or 0.6×10^{-10} sec is obtained. The previous arguments indicate that the shorter value is implausible, therefore the T_1 value at 270 MHz gives τ_c a value of between 1.0×10^{-9} and 2.2×10^{-9} sec for the 10mM solution at 68°C.

Other nuclear Overhauser experiments have not been carried out in detail, so this analysis cannot be extended rigorously to other groups. However, it is reasonable to suppose that the relaxation of a methyl group proton is totally determined by the

two other protons attached to the same carbon atom. These are at ca. 1.8 Å distances, and taking the observed T_1 values of the methyl groups (Table VIII.2), τ_c can be calculated. However, a direct calculation neglects the possibility of rapid rotation about the C-CH_3 bond. Coates et al (1973) showed that the anisotropic rotation about this bond affects T_1 by a maximum factor of 4. This maximum factor occurs when the rate is greater than 10^{11} sec^{-1}. This factor of 4, when included in the calculation of τ_c, gives τ_c values close to those found by the other methods (Table VIII.6).

Overall, the complete data suggest that the relaxation of all the groups in the protein is dominated by a single process, presumably the overall molecular tumbling. This single process has a correlation time of 1.0 - 2.3 x 10^{-9} sec for the 10mM solution, and 0.7 - 1.9 x 10^{-9} sec for the 5mM solution. Except for methyl group rotation which must be rapid with a correlation time $>10^{-11}$ sec, no other independent group motion need be considered. In order to test this theory further, two other sets of data are considered. These are the relaxation behaviour of lysozyme at 23°C, and also the relaxation behaviour of other molecules.

VIII.3.4 Relaxation Effects at 23°C

The data in Table VIII.2 and VIII.3 show that the decrease in temperature from 68°C to 23°C affects T_2 markedly, but does not greatly affect T_1 at either 90 MHz or 270 MHz. Examination of Fig. VIII.2 shows that this observation cannot be incorporated into the simple model used at 68°C.

At 23°C, values of T_1/T_2 are between 15 and 30 for most groups (Table VIII.5). The exceptions are the groups giving rise to resonances A23 and LA, which are associated with smaller

values of T_1/T_2. A23 is the C(2)H resonance of his 15. LA appears to be from a number (ca. 20) of nearly equivalent protons. These may be assigned to the ε-CH_2 protons of lysine and/or the δ-CH_2 protons of arginine from their chemical shift value (ca. 3.0 ppm, see McDonald and Phillips, 1969).

The values of T_1/T_2 of between 15 and 30 provide values of τ_c of between 2.4×10^{-9} and 3.2×10^{-9} sec for the different groups. These are rather longer than the values at 68°C as expected. However, the value of T_1 (270 MHz)/T_1 (90 MHz) of 3.4 is the same as that at 68°C giving a τ_c value of 0.7×10^{-9}. Also, as the values of T_1 themselves are not very different at the two temperatures, the values of τ_c calculated from them are not very different (Table VIII.6).

The discrepancies in the behaviour of T_1 and T_2 indicate that the relaxation behaviour cannot be interpreted at 23°C on a model whereby only overall isotropic rotation of the molecule is considered. Anisotropy or more than one type of motion is required, and this is likely to arise from the internal motion of protein side chains. However, this may be more important at a lower temperature where the overall molecule rotation is slower, for example the internal motion could have a smaller temperature dependence. This motion is not trivial to analyse. For example, the T_1 values may be dominated by the rapid internal group motions, whilst the T_2 values may be dominated by the overall molecular rotation. This arises because of the different effect of motion on T_1 and T_2 when τ_c becomes much larger than $1/\omega_I$. However, given the presence of internal motion, certain characteristics of the motion may be defined. First, certain of the resonances have small values of T_1/T_2, in particular A23 and LA. This implies that the groups giving these resonances have greater motion than the other protein groups. As his 15

(A23) and many arginine and lysine groups (LA) are on the surface of lysozyme, exposed to the solvent (see Appendix A), it is reasonable to suppose that surface groups have greater mobility than internal groups. Secondly, the T_1/T_2 ratio for most other (internal) groups is closely similar. This suggests that whatever the nature of the internal motion, it is similar for most of the groups in the protein. This suggests that there is a characteristic distribution of vibrational frequencies of the protein.

VIII.3.5 Relaxation Data for Other Molecules

As the protein molecular weight increases, the overall molecular rotation becomes slower. As Fig. VIII.2 and Fig. VIII.3 indicate, this should result in increasing values of T_1, decreasing values of T_2, and large values of T_1 (270 MHz)/ T_1 (90 MHz). Table VIII.7 summarises data at ca. 23°C for troponin (mol. wt. = 18,000, data supplied by Levine et al., 1975) and triose phosphate isomerase (mol. wt. = 50,500, data from Coates et al., 1973). T_1 has not increased from the lysozyme values, and the ratio of T_1 at the two frequencies has not increased. T_2 however has decreased as indicated by the broad spectral lines in these proteins compared to lysozyme. These data are clear indications that the T_1 values at least are not controlled by overall molecular tumbling but by internal mobility of groups (see Coates et al., 1973). This internal mobility seems to be similar in the three proteins considered, as the T_1 data are similar. In order to affect T_1, the mobility must involve frequencies with correlation times in the region of 10^{-9} sec. It is not however yet possible to state the degree of mobility concerned. T_2 however, has decreased in the larger proteins, showing its dependence on overall tumbling rates. In the next

TABLE VIII.7

Relaxation Date for Various Molecules[a,b]

Molecule	Mol. Wt.	T_1 (270 MHz) Arom.	T_1 (270 MHz) CH_3	T_1 (90MHz) Arom.	T_1 (90MHz) CH_3	T_1(270MHz)/T_1(90MHz)
Valine[c]	117		0.96		1.02	0.95
Polymyxin[c]	1200	0.71	0.32	0.29	0.20	1.6-2.5
Lysozyme	14400	0.97	0.72	0.30	0.20	3.4-3.6
Troponin[d]	18000	0.42	0.29	0.26	0.19	1.5-1.6
TIM[c,e]	50500	0.76	0.75	0.32	0.39	1.9-2.4

[a] at 18°C except for lysozyme (23°C).

[b] T_1/T_2 values are 17-30 for most groups of lysozyme.
T_1/T_2 values are estimated for the other molecules as:
Valine (1.0), Polymyxin (5.0), Troponin (>50), TIM (>50).

[c] from Coates et al. 1973.

[d] Levine et al., 1975.

[e] triose phosphate isomerase, from rabbit muscle.

sections, slower motions will be considered, and for these the nature of the motions can be more closely defined.

VIII.4 Observation of Exchange Effects

VIII.4.1 Fast Exchange

In order to detect fast exchange conditions directly, it is easiest to study a symmetrical group exchanging between geometrically equivalent positions which are magnetically inequivalent. This situation can arise in proteins for CH_3 groups and for the aromatic groups of tyrosine and phenylalanine. However, it is also possible to obtain evidence less directly as will be discussed below.

VIII.4.1.1 Methyl Groups

Each of the methyl groups in lysozyme is observed in all circumstances as a single three proton intensity resonance. This indicates that the three protons are equivalent, as it is most unlikely that the environment of all the methyl groups in the protein is such as to give this equivalence, it can be deduced that these groups are spinning rapidly about the $C-CH_3$ bond. This rate cannot be determined from the observed equivalence but is likely (see above) to be very fast ($>>10^{10}$ s^{-1}).

VIII.4.1.2 Tyrosine and Phenylalanine Residues

There are three tyrosine residues in lysozyme. It was shown in Chapter V that for each residue, only two resonances are observed, and that each of these has an area of two protons. Spin-decoupling experiments show for each tyrosine residue that the resonances of the two ortho protons are equivalent, as are those of the two meta protons. If the tyrosine ring is rigidly held in a protein structure, one would expect the environment of

all four ring protons to be different (in the absence of coincidences), thus resulting in non-equal chemical shifts for all four proton resonances. This is never observed in lysozyme.

Addition of paramagnetic Ln^{3+} ions to lysozyme results in large shifts of the aromatic resonances of one tyrosine, tyr 53. The induced shifts of the pairs of ortho and meta protons are different, but the two ortho proton resonances always remain equivalent, as do the two meta proton resonances. Again one would not expect this equivalence for a rigidly held tyrosine ring, and the orientation of the tyr 53 ring in the X-ray structure does not predict it. Even if the orientation of tyr 53 is different in solution from that in the crystal, the probability of it having an orientation to result in equivalence of the type observed is small.

The tyrosine ring however has an axis of symmetry along the C1-C4 direction. Rapid rotation about this axis can produce the effective equivalence of the resonances required provided that the rotation rate is much faster than the chemical shift difference between H2 and H6 (ortho protons) and between H3 and H5 (meta protons). Such a rotation would therefore explain all the results. It may be considered unlikely that completely free rotation occurs for all three tyrosine residues. It is however only necessary to flip a tyrosine ring through 180^{o} with sufficient frequency to gain the required equivalence. There is, of course, no distinction between the conformation before and after a 180^{o} flip. It may however be necessary to involve some sort of breathing motion in the protein to allow this proposed flipping process to take place. Although tyr 20 and tyr 23 are close to the surface of the molecule, tyr 53 is in a β- pleated sheet region of the X-ray structure, and the -OH group is hydrogen-bonded to asp 66.

In order to set a limit on the rate at which this flipping process must occur, the difference between the true chemical shift values of each of the two ortho protons or the two meta proton resonances ($\Delta\nu_{A-B}$, in Hz) must be estimated. Also, a limit on the exchange broadening ($\Delta\nu_{ex}$) must be placed. If the lifetime in a given orientation is τ,

$$\frac{1}{\tau} = \pi . \frac{\Delta\nu^2_{A-B}}{\Delta\nu_{ex}}$$

and for a first order process such as the flip, $k = 1/\tau$.

In the presence of bound Pr^{3+}, the meta proton resonance of tyr 53 is shifted by about 250 Hz, at 270 MHz. The peak can be clearly observed to low field of the envelope of the aromatic protons, and is still well resolved. $\Delta\nu_{ex}$ appears to be less than 3 Hz. The shift of the meta proton resonance is ca. 1.5 times that of the ortho proton resonance. If the difference between the two meta protons is about the same as the difference between meta and ortho proton resonances, as is likely, then $\Delta\nu_{A-B}$ = 100 Hz (the observed shift of 250 Hz being the mean of 300 Hz and 200 Hz). This results in $k \simeq 10^4$ sec^{-1}. A more accurate value cannot yet be given, however for tyr 53 it seems reasonable that the rate of flip is greater than 10^4 sec^{-1}.

An examination of published spectra of other proteins was carried out to discover whether the magnetic equivalence of tyrosine ortho and of tyrosine meta protons is a general phenomenon. The spectrum of human lysozyme (see Chapter X) shows that at least four and possibly all six tyrosine residues give rise to such equivalent resonances. The published spectra of bovine pancreatic trypsin inhibitor protein (Karplus et al., 1973), show that at least three of the four tyrosine residues are equivalent. In these diamagnetic proteins, any chemical shift

inequivalence must be produced by local perturbations such as those from ring current shifts, and may well be small. Larger perturbations are produced by paramagnetic centres. In addition to the experiments with lanthanides in lysozyme described above, shifts of tyrosine ^{13}C resonances in the paramagnetic protein ferrodoxin (Packer et al., 1972) also indicate equivalence.

Equivalence of the resonances of all tyrosine residues of the bovine trypsin inhibitor protein was noted independently of the observations on lysozyme (Wüthrich and Wagner, 1975) although it now appears likely that at low temperatures this is true only for three of the four residues (Wüthrich, 1975; Snyder et al., 1975). The change from slow exchange (inequivalence) to fast exchange (equivalence) in the nmr spectrum as the temperature is raised has been followed for the fourth residue (Wüthrich, 1975). These results have been rationalised on the basis of the X-ray structure by calculation of the potentials of the rotational barriers (Gelin and Karplus, 1975). In order to permit rapid conformational flipping, the protein had to be permitted to relax or alter its conformation as the ring orientation was changed. Rigid rotation barriers were calculated to be extremely high. However, even allowing for this relaxation, one tyrosine was calculated to be more hindered in its rotational motion, in keeping with the observations by nmr (Snyder et al., 1975).

If flipping can occur for tyrosine residues, it would be reasonable to suppose that it can occur for phenylalanine residues. Resonances from these residues have not been assigned in lysozyme, but equivalence of resonances (flipping) has been observed in cytochrome c (Dobson et al., 1975). Similarly, observations for the trypsin inhibitor protein have been made, except that one residue gives inequivalent resonances at low

temperature, and equivalent resonances at high temperature (Wüthrich and Wagner, 1975).

The nmr observations show that the protein conformation is not rigid and that even bulky aromatic groups have considerable conformational mobility. Note that it is the symmetry of tyrosine and phenylalanine which make this motion easy to detect. If other residues were undergoing motion of a similar type, its detection is less easy (see below). Finally, as described in the previous chapter, in comparing the X-ray structure and the nmr data, allowance for this aromatic ring flipping was made by taking averages over the two equivalent orientations.

VIII.4.1.3 Other Residues

Evidence that fast rotational motion of side-chain groups takes place has been given above for surface residues. Evidence for slower motions, similar to that described for tyrosine residues, has been collected for certain groups. This is more difficult to acquire, because simple two-fold symmetry does not exist for residues other than tyrosine and phenylalanine.

(a) The degree of broadening of the resonances of the two methyl groups of val 109 by Gd^{3+} (Fig. VI.15) is very similar. The X-ray structure predicts that a difference of about 5 should be observed. This could indicate that fairly fast rotational motion about the side-chain occurs for this residue, and by inference for other similar residues. Val 109 projects towards the surface of the molecule, and so the barrier to rotation would be small. Completely free rotation would result in equivalence of the chemical shift values of the two resonances. This does not occur, but nor does it occur even for the free valine molecule. Thus some hindered rotation is likely.

Finally, in the next chapter, fast exchange behaviour for induced conformational changes will be discussed.

(b) The temperature dependence of chemical shift values indicates that some rotation of the side chains of leu 17 and other groups is taking place. This is discussed in Chapter IX.

VIII.4.2 Intermediate Exchange

VIII.4.2.1 Active Site Resonances

Intermediate exchange phenomena are characterised by line broadening. Above a pH value of about 6, several resonances of groups in lysozyme are very broad at low temperatures. The pH effect depends on the pK value of glu 35 and this will be discussed in Chapter IX. Here, spectra recorded at a fixed pH value (7.0) only will be considered.

Resonances which are most easily observed to broaden substantially are assigned to the C(2)H proton of trp 63 (resonance A20), to the γ-CH_3 group of ile 98 (M2) and to the CH_3 group of met 105 (M6). As Fig. VIII.4 shows the changes in line-width with temperature are very large. Although linewidth (T_2) changes are observed, similar changes in the T_1 values of these resonances do not occur. For example, at 45°C and pH 7.0, the T_1 value of M2 (ile 98) is 0.67, whilst the T_2 value is 0.019. This value of T_1 is very close to the T_1 value of other resonances, whilst the T_2 value is different by a factor of about 2. The observation of changes in T_2 but not T_1 suggests strongly that an exchange broadening effect is being manifested. This affects T_2 considerably more than T_1 (see Pople *et al.*, 1959). Thus the broadening at low temperature is attributed to the effects of the existence of two or more conformers of the protein, each giving rise to different chemical shift values for the

FIGURE VIII.4

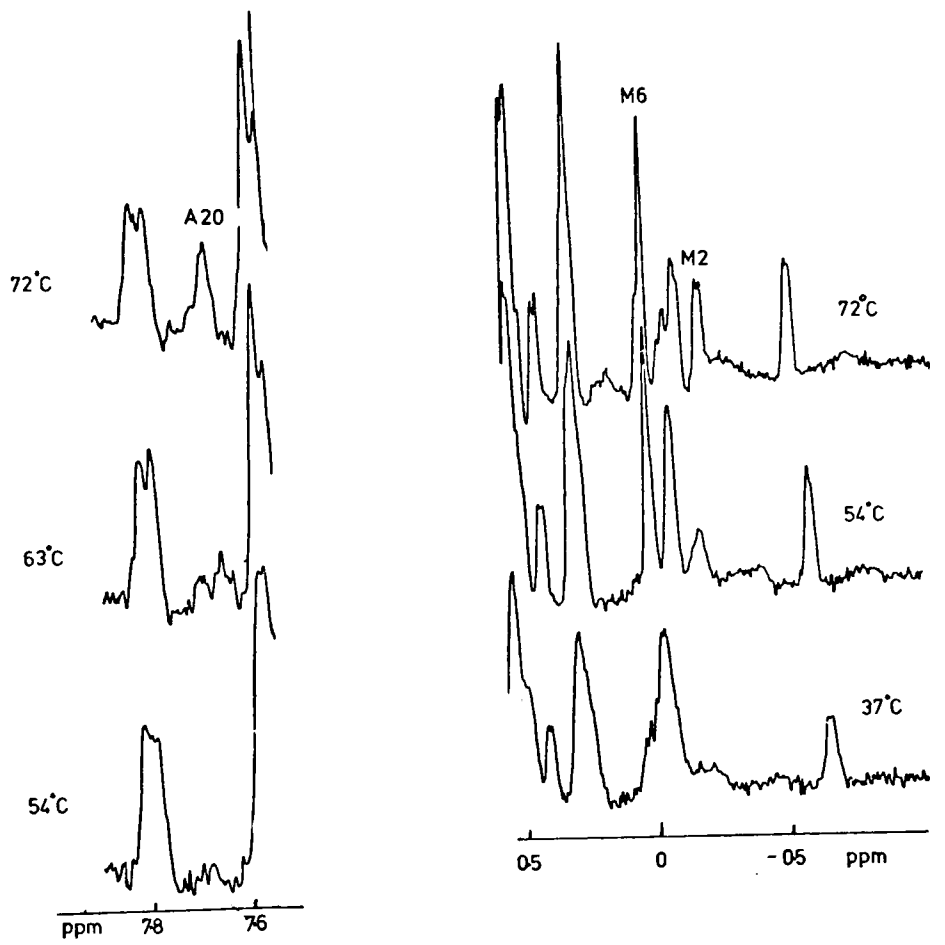

The exchange broadening of resonances at high pH values. At 72°C, all resonances are well resolved. At lower temperatures resonances A20, M2 and M6 are clearly observed to broaden more than the other resonances. 5mM lysozyme, pH 7.0.

resonances in question. At low temperatures the rate of interconversion between conformers is such that exchange broadening results. At higher temperatures the exchange is fast, resulting in sharp resonances.

Support for this hypothesis comes from a number of sources. First, it is found that each of the broadened resonances has suffered a considerable ring current shift. These shifts arise, at least in part, from the tryptophan residues (62, 63 and 108) in the active site of the protein. Thus, conformational mobility in the active site of the protein would explain the broadening of each of these resonances. Secondly, as the next chapter describes, binding of inhibitors in the active site of the protein abolishes this linebroadening presumably by reducing the conformational mobility. Thirdly, in the X-ray electron density map groups in the active site region of the protein, particularly trp 62, are not clearly observed. This indicates the existence of a variety of conformers. This situation does not occur in the presence of bound inhibitors where the groups are now well defined. Note however that the comparison of the X-ray structure is not a very good one because the pH value of the X-ray structure is 4.5, whilst the large effects in the nmr spectrum are only observed at pH values above 6.0. However, some indication that exchange effects in the nmr spectrum persist at lower pH values is available from the T_1 and T_2 values given in Table VIII.4 for resonances M2 and A20.

VIII.4.2.2 Histidine Resonances

Protonation of the ring of the single histidine residue of lysozyme (his 15) gives rise to the expected shifts of the histidine resonances (A14 and A23). At low temperature ($25^{o}C$), linebroadening of the C(2)H resonance (A23) is observed,

being a maximum at the pK value where 50% of the molecules have histidine groups which are protonated and 50% of the molecules have not. This broadening (ca. 10 Hz) gives a value for the off rate of the protonation step of 1.4×10^4 s^{-1}. All other effects in the spectrum arising from pH changes, other than those accompanying denaturation, are in fast exchange under all conditions. This includes the effects of the ionisation of glu 35 on the resonances of trp 108 (see Chapter IX).

VIII.4.3 Slow Exchange

The only slow exchange phenomena observed with lysozyme accompany induced conformational changes and are discussed in Chapter IX.

VIII.5 Observation of Separate Spectra

In Section III.1.4 the use of difference spectroscopy to observe exchangeable resonances in the nmr spectrum of lysozyme was described. The exchange of hydrogen atoms with solvent as a function of time has been studied by a variety of techniques (see Imoto et al., 1972 and references therein). The advantages of nmr studies are that solvent exchange rates may be measured by following individual observed resonances, which may be assigned to specific hydrogens in the molecule. One method of following this exchange is merely to observe the area of resolved resonances by running spectra at different time intervals, as Glickson et al. (1971) have shown for tryptophan N(1)H resonances of lysozyme. For non-resolved resonances, as shown in Fig. VIII.5, difference spectroscopy may be used. No assigned resonances have yet been studied in this way, but the method for observing these slow processes by difference spectroscopy is clearly valuable.

FIGURE VIII.5

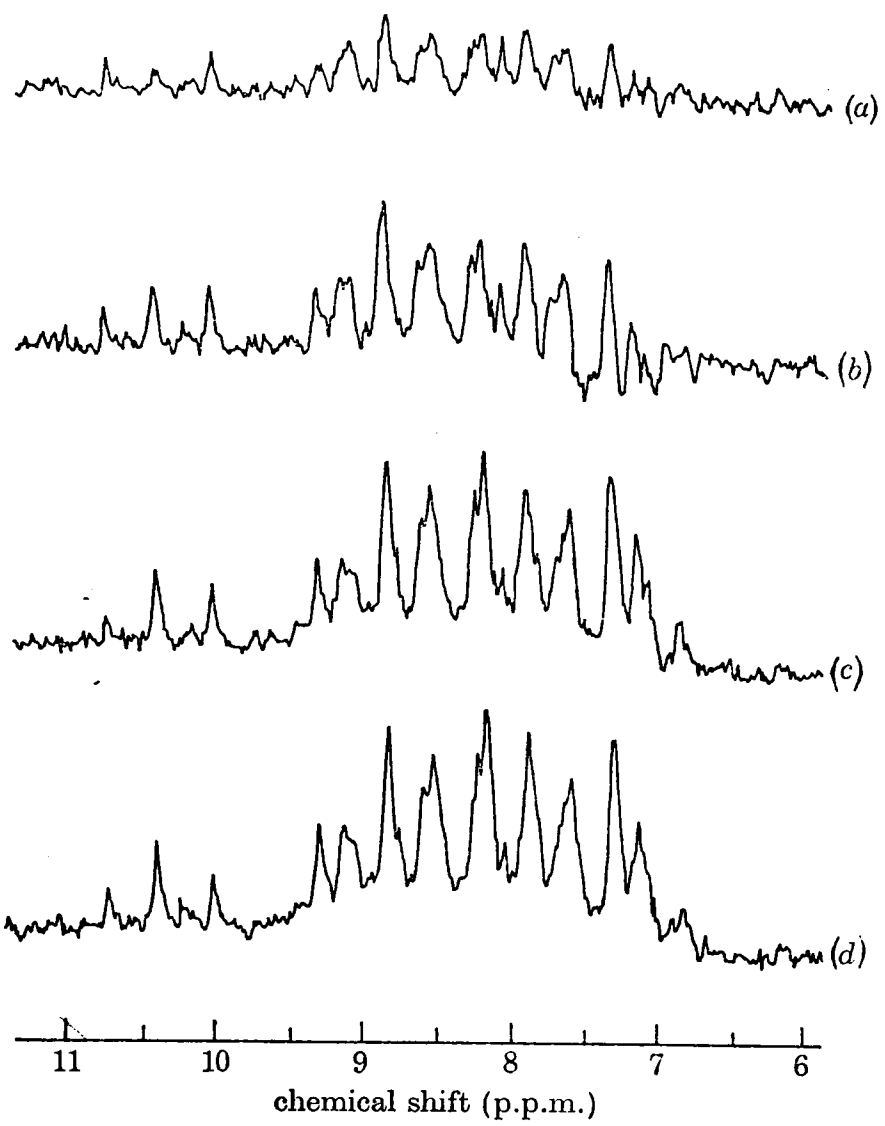

Observation of exchange of NH protons. A spectrum of freshly dissolved lysozyme was recorded and spectra recorded after (a) 25 min, (b) 79 min, (c) 128 min and (d) 237 min were subtracted from this. The resonances observed in the difference spectra are of hydrogens which have exchanged with the deuterium of the solvent after the times given.

VIII.6 Summary

The results in this Chapter have demonstrated in a preliminary manner that processes with rate constants between more than 10^{11} sec^{-1} and less than 10^{-2} sec^{-1} have been detected and followed by nmr studies of a protein. These observations indicate quite clearly that the full description of a protein structure in solution requires a knowledge of the independent motion of groups in the protein. The motions detected so far are of several types. First, there is rapid mobility (τ_c *ca.* 10^{-9} sec) of an undefined nature for all groups in the protein. This mobility is most pronounced for groups on the surface. In addition, rotation of CH_3 groups is very fast (τ_c greater than 10^{-11} sec). Secondly, even relatively bulky groups, such as tyrosine, in the centre of the molecule are performing complete rotations about single bonds. Thirdly, residues in the active site in certain circumstances possess some particular freedom of movement. This is removed in the presence of a bound inhibitor molecule. In the next Chapter, the dynamic aspects of induced conformational changes will be discussed.

References for Chapter VIII

Coates, H.B., McLaughlan, K.A., Campbell, I.D. and McColl, C.E. (1973), Biochim.Biophys.Acta 310, 1.

Dobson, C.M., Moore, G.R. and Williams, R.J.P. (1975), FEBS Lett. 51, 60.

Farrar, T.C. and Becker, E.D. (1971), Pulse and Fourier Transform NMR, Academic Press (N.Y.).

Gelin, B.R. and Karplus, M. (1975), Proc.Natn.Acad.Sci. U.S.A. 72, 2002.

Glickson, J.D., Phillips, W.D. and Rupley, J.A. (1971), J.Amer. Chem. Soc. 93, 4031.

Imoto, T., Johnson, L.N., North, A.C.T., Phillips, D.C. and Rupley, J.A. (1972), In The Enzymes, 3rd ed. (ed. Boyer, P.D.), Vol. VII, Academic Press (N.Y.), 665.

Jackman, L.M. and Sternhell, S. (1969), Applications of NMR Spectroscopy in Organic Chemistry, Academic Press (N.Y.).

Karplus, S., Snyder, G.H. and Sykes, B.D. (1973), Biochemistry, 12, 1323.

Levine, B.A., Thornton, J.M. and Mercola, D. (1975), unpublished data.

McDonald, C.C. and Phillips, W.D. (1969), J.Amer.Chem.Soc., 91, 1513.

Packer, E.L., Sternlicht, H. and Rabinowitz, J.C. (1972), Proc.Natn.Acad.Sci. U.S.A. 69, 3278.

Pople, J.A., Schneider, W.G. and Bernstein, H.J. (1959), High Resolution Nuclear Magnetic Resonance, McGraw-Hill (N.Y.).

Snyder, G.H., Rowan, R., Karplus, S. and Sykes, B.D. (1975), Biochemistry (in the press), cited in Gelin and Karplus (1975).

Wüthrich, K. (1975), Personal communication.

Wüthrich, K. and Wagner, G. (1975), FEBS Lett. 50, 265.

CHAPTER IX

CHARACTERISATION OF INDUCED CONFORMATIONAL CHANGES

In the native protein, the chemical shift values of resonances depend not only on through bond effects, but also on large through space effects. These through space effects are secondary shifts (see Chapter IV) and although generally assumed to arise primarily from the effects of ring currents also arise from anisotropic shielding effects of C = 0 groups. These through space shifts are dependent on the exact geometry of the perturbing centre (the aromatic ring or C = 0 group) with respect to the resonance observed. Thus, any changes in geometry of either can result in observed changes in shifts. The result is that resonances suffering large secondary shifts, or of nuclei close to a perturbing centre, are very sensitive to conformational changes in the vicinity of the nuclei. Therefore, having assigned the resonances, local conformational changes can be investigated. It is not, however, possible to interpret these changes in a quantitative manner. Nor is the observation that chemical shifts of certain resonances are unaffected by a given perturbation definitive evidence that the nuclei giving rise to these resonances are not affected by a conformational change. In this Chapter, spectral changes will be used to characterise in a qualitative manner, a variety of induced conformational changes.

IX.1 The Effects of Temperature

The effect of temperature on the spectrum of lysozyme was investigated in detail at several pH values between 3.8 and 8.1 (see Appendix C). Spectra were recorded at about 10^{o} temperature intervals from $5^{o}C$ to $85^{o}C$.

IX.1.1 Chemical Shift Changes

The major conformational change induced by an increase in temperature is reversible thermal denaturation at ca. 70°-80°C, and this is very clearly observed in the nmr spectrum (McDonald and Phillips 1969, 1970). The native and denatured species were in slow nmr exchange under all circumstances, and no cross-saturation effects could be observed (Section V.1.1).

As the temperature is changed between 5°C and 70°C however, there are small changes in the chemical shift values of most resonances. Some of these are shown in Fig. IX.1, and the changes are tabulated in Table IX.1. Several conclusions may be reached from an inspection of these data. First, the changes are generally small, less than 10% of the ring current shift. Secondly, the changes are gradual and continuous, and slightly more marked at higher temperatures. Both these points show that there is no discontinuous conformational change with temperature. It has been suggested from observation of the ^{13}C spectrum (Cozzone et al., 1975) that a conformational change occurs between 20° and 30°C at pH 4.75. The present data show that this is not the case.

A possible explanation of the chemical shift changes can be given from the data in Table IX.1. The changes in the chemical shifts of aromatic resonances are all indicative of a slight decrease in ring current shifts at higher temperatures. This implies a slight increase in the distance between aromatic residues, that is a swelling of the protein at higher temperatures. The chemical shift values of most methyl group resonances also indicate that this swelling occurs. However, there are two major exceptions, resonances M3 and M4. A likely explanation for these is however apparent. M1 and M3 arise from the same residue,

FIGURE IX.1

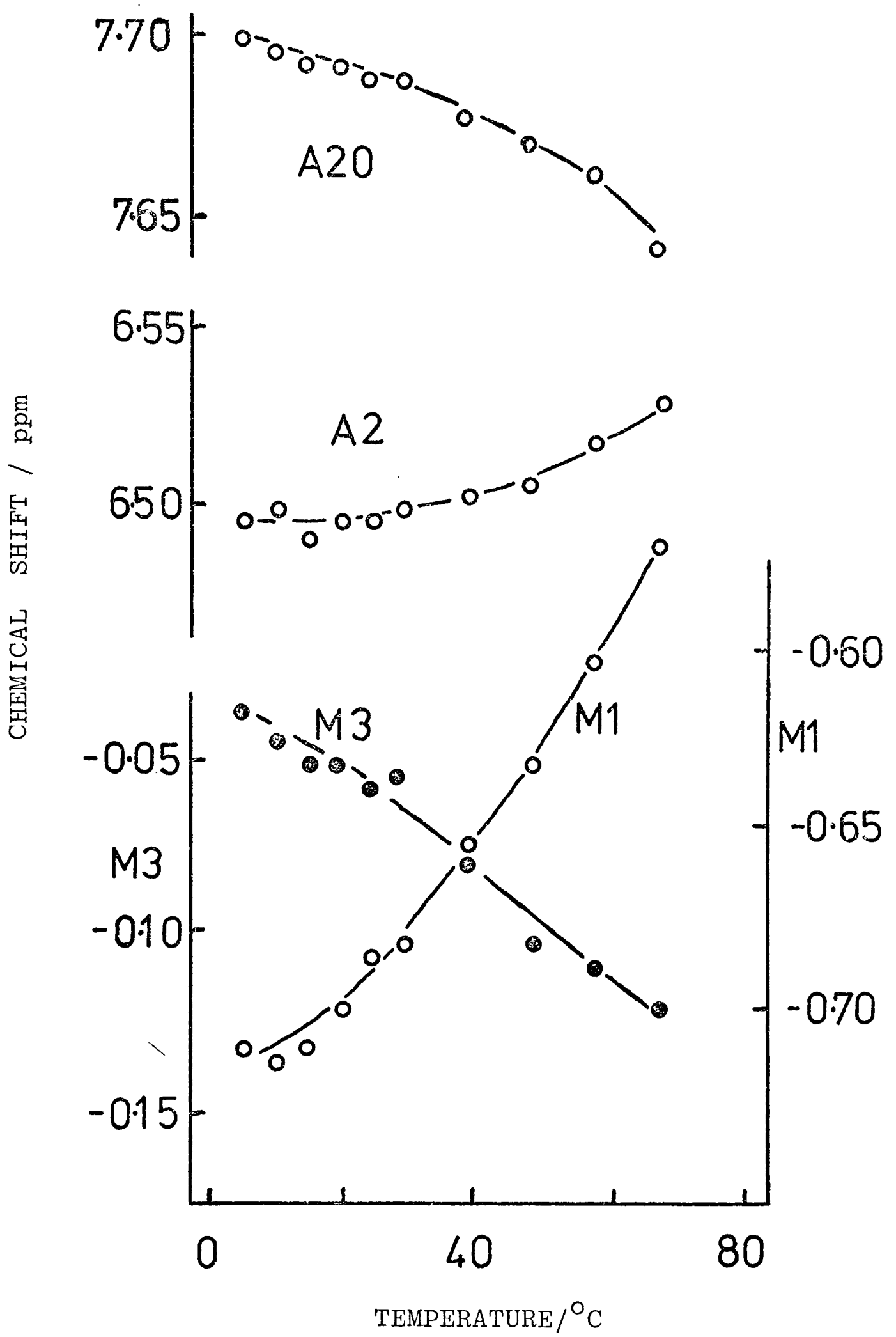

Plots of chemical shift values against temperature for several resonances. 5mM lysozyme, pH 4.75.

TABLE IX.1

Effects of Temperature on the Spectrum[a]

Resonance Number	Assignment	Shift[b]	Change in Ring Current Shift[c]
H1	ile 98 γ-CH_2	-0.162	D
M1	leu 17	-0.135	D
M2	ile 98 γ	-0.054	D
M3	leu 17	+0.072	I
M4	ile 98 δ	+0.043	I
M5	leu 8	-0.072	D
M7	ile 88 δ	-0.061	D
M13	val 92	+0.019	I
M21		+0.040	-
M22	met 12	+0.019	I
A1	trp 63 5/6	-0.033	D
A2		-0.051	D
A3		+0.033	-
A4	trp 63 4/7	-0.051	D
A6	tyr 53 o-	-0.022	
A11	trp 108 C(2)	-0.022	D
A16		-0.036	D
A20	trp 63 C(2)	+0.058	D
A21		+0.018	D
A22	trp 63 4/7	+0.018	D

[a] methyl group and aromatic proton resonances.

[b] if greater than 0.01 ppm. The shift is for 30^{o}-80^{o}C at pH 5.25. In each case the shifts are essentially linear with temperature. + indicates a shift upfield at higher temperatures.

[c] indicates whether ring current shift increases (I) or decreases (D) at higher temperatures.

leu 17. If this residue possessed completely free rotation about the C_β-C_γ bond, M1 and M3 would be equivalent. This completely free rotation does not occur in the protein, because of the observed inequivalence of M1 and M3. However, Fig. IX.1 and Table IX.1 show that at higher temperature M1 and M3 are more nearly equivalent, and that the mean ring current shift of the two resonances is reduced. This indicates that as the temperature increases, the rotation around the C_β-C_γ bond becomes less restricted. Similarly, the δ-CH_3 group of ile 98 (M4) has an increased ring current shift, but the γ-CH_3(M2) and γ-CH(H1) resonances have decreased ring current shifts. This could arise from increased rotational mobility.

Clearly it is not possible to produce a unique explanation of the temperature dependence of the spectrum. However, the chemical shift data rule out a significant conformational change at any temperature, but are consistent with increasing mobility of protein groups, possibly accompanying a slight swelling of the protein structure. The changes are fully reversible.

IX.1.2 Linewidth Changes

The effects of temperature on the relaxation times of certain resonances were discussed in detail in the previous chapter. The sharpening of resonance lines at higher temperature is due to two effects. First, the time for overall rotation of the molecule (τ_R) becomes shorter and secondly the change from intermediate to fast exchange occurs for a number of active site resonances resulting in a reduction of exchange broadening. Again, this indicates increasing mobility at higher temperatures.

IX.2 The Effects of pH

Detailed pH titrations were carried out at 54^{o}C between

pH 1 and 12. Spectra were run at intervals of no more than 0.4 pH units. Samples of the native protein dissolved in D_2O, and in 90% H_2O with 10% D_2O, were used. Less detailed titrations were carried out at other temperatures. At 54°C, the spectrum of the native protein changes to that of the random coil form below pH 2 and above pH 12. Slow exchange between the two forms is observed.

Shifts and broadening of various resonances in the spectrum between pH 2 and pH 12 arise from the effects of ionisation of specific groups. The shifts arise either from a direct through-bond mechanism associated with changes of electron density accompanying ionisation (for example shifts of the C(2)H and C(4)H proton resonances of histidine; the ortho proton resonances of tyrosine; the CH resonances next to carboxylate or amino groups) or from a through space mechanism associated with conformational changes (or in certain cases from changes for example in ring-current shifts). Some of these shifts have been mentioned in the assignment procedures of Chapter V, and pK values and resonances perturbed are listed in Table IX.2. Broadening arises from changes in mobility as described below. The main spectral changes are associated with the ionisations of his 15 and glu 35 (see Fig. IX.2). These have been rationalised in Table IX.3.

IX.2.1 Chemical Shift Changes

IX.2.1.1 The Ionisation of glu 35 and asp 52

As mentioned in Chapter V, the chemical shift values of the resonances of the C(2)H and N(1)H protons of trp 108 are perturbed by the ionisation of glu 35 and to a lesser extent by the ionisation of asp 52 (Fig. IX.3). The pK value of glu 35 may be accurately measured by the shifts of the trp 108 resonances,

TABLE IX.2

Effects of pH on the Spectrum

Resonance Number	Assignment		Shift[a]	Approximate pK value	Probable ionisable group
M1	leu 17		+0.076	several, all below 6	
M2	ile 98 γ		-0.083	6.2	glu 35
M3	leu 17		-0.076	several, all below 6	
M4	ile 98 δ	ca.	+0.054	ca. 6	glu 35
M5	leu	(a)	+0.072	<3	glu 7
		(b)	-0.036	ca. 8.5	lys 1
M6	met 105		-0.065	several	
M7	ile 88 δ	(a)	+0.022	<3	glu 7
		(b)	-0.083	5.2	his 15
M8	leu 56		0		
M9	thr 51		+0.047	3.5	asp 52
M10	val 92		+0.072	ca. 5	his 15
M11	leu 56		0		
M12	leu 8		0		
M13	val 92		+0.047	ca. 5	his 15
M14	ala 107/31		-0.058	two between 3 & 7	glu 35+1
M20	ala 110		-0.043	ca. 6.5	glu 35
M22	met 12		0		
L1			0		
L2		(a)	+0.043	ca. 3.5	asp 52
		(b)	-0.022	ca. 6.5	glu 35
L3			-0.072	<4	
L4	lys 1		+0.235	ca. 8	lys 1

Continued next page

TABLE IX.2 Continued

Resonance Number	Assignment		Shift	Approximate pK value	Probable Ionisable Group
A1	trp 63 5/6		-0.180	ca. 4.5 + others	asp 101
A2			+0.065	ca. 4	
A3			+0.252[b]	10.0	tyr 20/23
A4	trp 63 4/7	(a)	-0.036	4.5	asp 101
		(b)	+0.036	6	glu 35
A6	tyr 53 o-		0		
A11	trp 108 C(2)	(a)	+0.018	3.5	asp 52
		(b)	-0.152	6.2	glu 35
A14	his 15 C(4)		+0.650	5.2	his 15
A20	trp 63 C(2)	(a)	-0.036	ca. 4	asp 101
		(b)	+0.054	ca. 6	glu 35
A21			0		
A22	trp 63 4/7		0		
A23	his 15 C(2)		+1.103	5.2	his 15
N1			+0.029	several	
N2			+0.065	ca.4	
N3				c	
N4				c	
N5	trp 108 N(1)	(a)	+0.036	3.5	asp 52
		(b)	-0.270	6.2	glu 35

[a] at 54°C. The shifts are quoted for between pH 2 and pH 9. Upfield shifts as the pH is increased are marked +, downfield shifts are marked -. No other large shifts were observed in the spectrum.

[b] shift between pH 9 and pH 11.

[c] broadens above pH 6.

TABLE IX.3

Residues with Resonances perturbed by Ionisations

Ionisable Group	Residues Affected
lys 1	lys 1, leu 8
glu 7	leu 8, ile 88
his 15	ile 88, val 92, his 15
tyr 20/23	tyr 20/23
glu 35	ile 98, ala 107/31, ala 110, trp 63, trp 108
asp 52	thr 51, trp 108
asp 101	trp 63

FIGURE IX.2

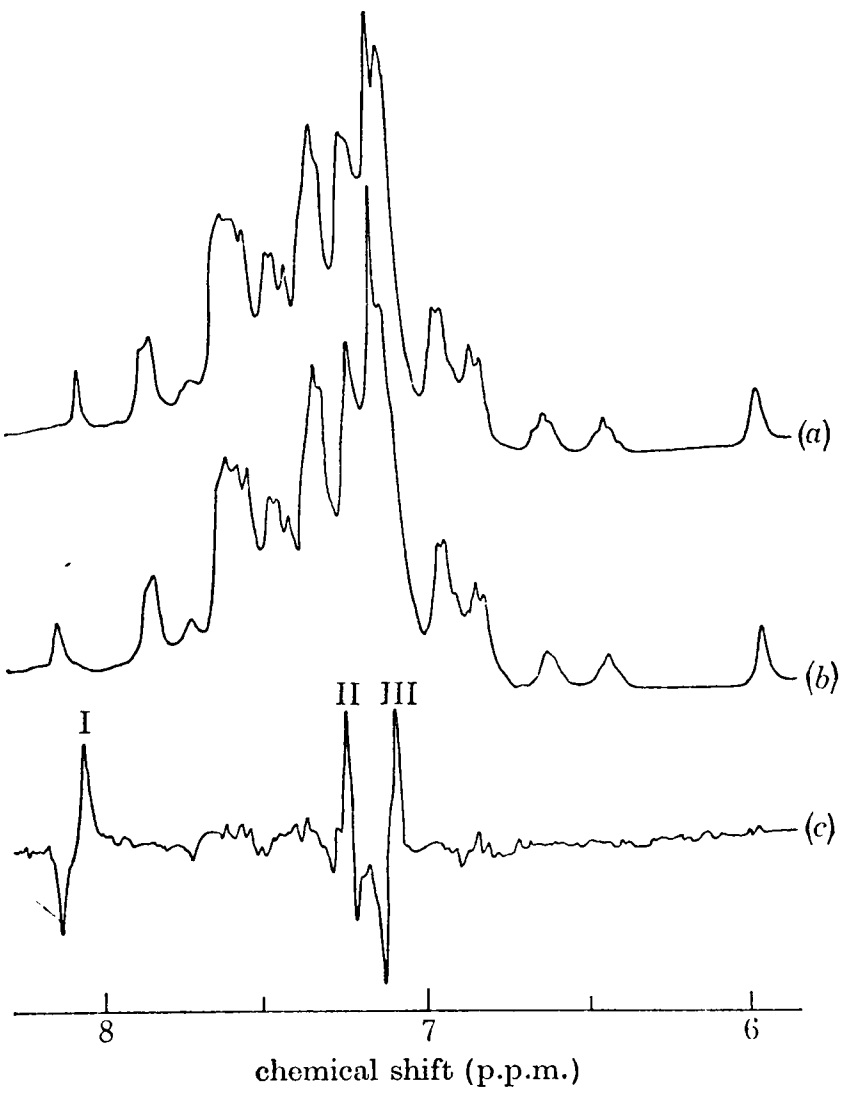

Spectra of 5mM lysozyme at 54°C. (a) pH 6.5, (b) pH 6.0, (c) difference (a)-(b) on twice the vertical scale. The resonances I (A23) and III (A14) are of his 15 and II (A11) is of trp 108.

FIGURE IX.3

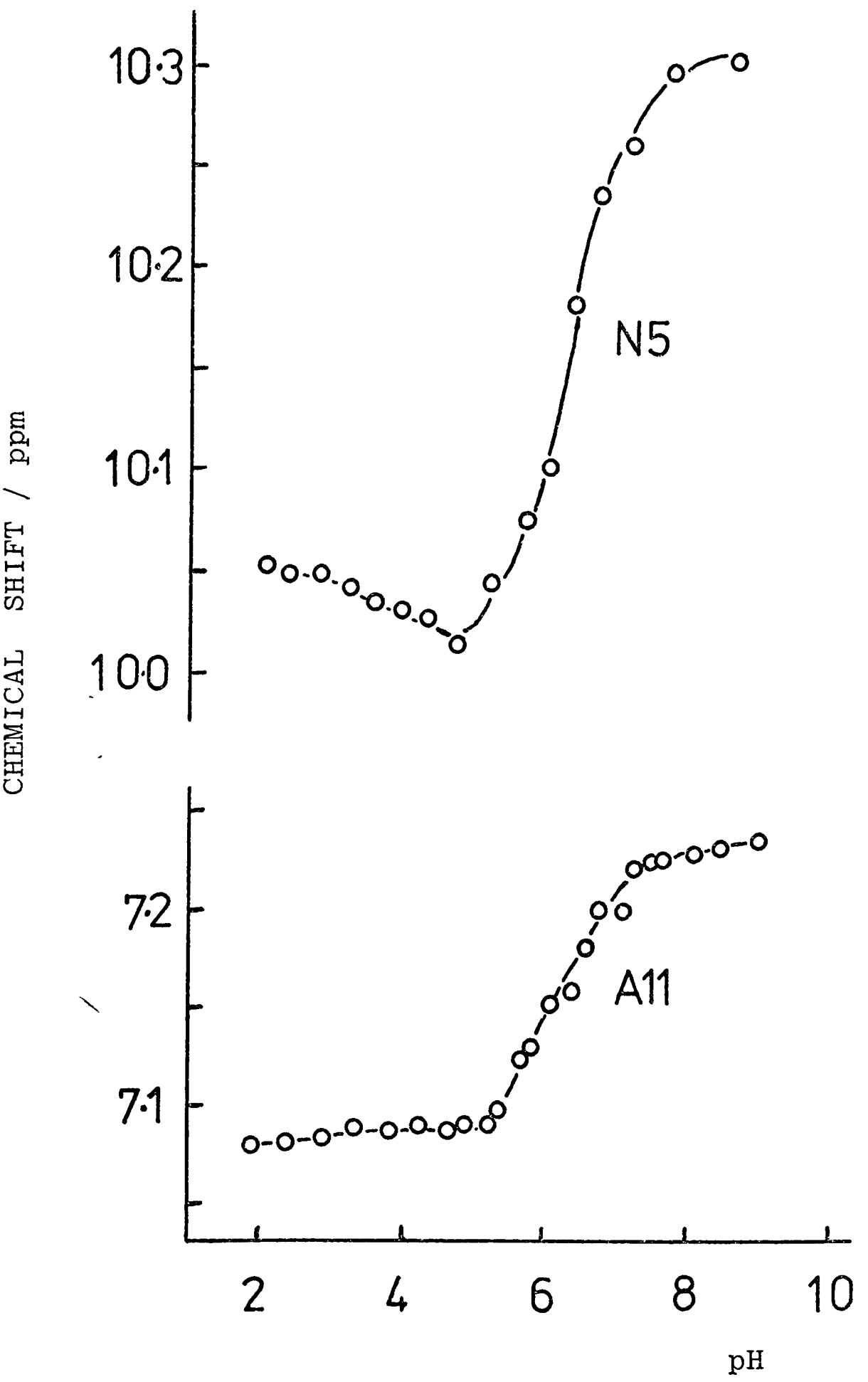

pH dependence of the chemical shift values of the resonances of trp 108. 5mM lysozyme, 54°C.

and that of asp 52 may be estimated. Both glu 35 and asp 52 are in the active site of lysozyme, and are catalytically essential.

The nmr data may be rationalised in the following way. The X-ray structure (pH 4.5) shows that the carboxylic acid group of glu 35 is very close to the five-membered ring of trp 108. This proximity could well result in a shift of the trp 108 C(2)H and N(1)H resonances, because of the anisotropic through space shielding effect of the C = 0. These shifts have been shown to occur in small molecule systems (see Dyer 1965). The observed shift observed on the trp 108 resonances on ionisation of glu 35 could therefore represent the movement of this group away from trp 108 into free solution in its charged state, resulting in a change in the shielding effect. Evidence for this hypothesis comes from several sources. (i) Similar shifts arise for human lysozyme (see Chapter X), showing that the effect is not limited to this one molecule. (ii) The chemical shifts of the trp 108 resonances in the anionic form of glu 35 ($-COO^-$) are barely affected by the binding of diamagnetic metal ions (La^{3+}, Lu^{3+} and Ca^{2+}). As these ions are thought to bind directly to glu 35, this suggests that in the ionised form the carboxylate group of glu 35 is in free solution. This observation also rules out a direct electrostatic origin for the shifts. (iii) The pK value of glu 35 is abnormally high in both hen and human lysozymes (6.0 and 7.2 respectively). This pK value indicates that the protonated state is favoured over the ionised state to an extent greater than that found in free solution. A means of obtaining this situation is to allow glu 35 to interact favourably with trp 108 in some way only in the protonated form.

It is now necessary to examine the nature of this proposed interaction between glu 35 and trp 108. This is unlikely to be from direct hydrogen bonding to the N(1)H proton (in the

X-ray structure the N(1)H of trp 108 is hydrogen bonded to the peptide carbonyl group of leu 56, see Imoto et al., 1972), because this would be expected to have a far more marked effect on the N(1)H resonance than on the C(2)H resonance (the observed pH shifts are N(1)H = 0.29 ppm, C(2)H = 0.14 ppm). However, a more likely interaction is a charge-transfer interaction, or a hydrophobic interaction between the π-electrons of the C = 0 bond and the aromatic ring.

The small shift of the trp 108 resonances as a result of the ionisation of asp 52 probably reflects a small conformational change in the active site accompanying the ionisation.

In addition to the shifts of trp 108 resonances accompanying ionisation of these groups, small shifts of other resonances occur. These shifts are tabulated in Table IX.2, and some are plotted in Fig. IX.4 (see also Fig. V.11). The residues affected (Ile 98, trp 63, ala 107/31, thr 51) are all ring current shifted and in the active site region of the protein, and any slight conformational changes, e.g. movement of trp 108 as glu 35 ionises, could produce these shifts. It is unlikely however that movement of glu 35 alone would be a sufficient explanation. It may therefore be concluded that small conformational changes occur in the active site, in addition to the movement of glu 35, as a consequence of these ionisations. These conformational changes, which cannot be closely defined yet, are local and not general changes.

IX.2.1.2 The Ionisation of asp 101

Shifts of resonances A1 and A20 of trp 63 are perturbed by a pK value of between 4 and 5. This is likely to be of asp 101, a group close to trp 63 in the X-ray structure. The shifts arise either from a small conformational change involv-

FIGURE IX.4

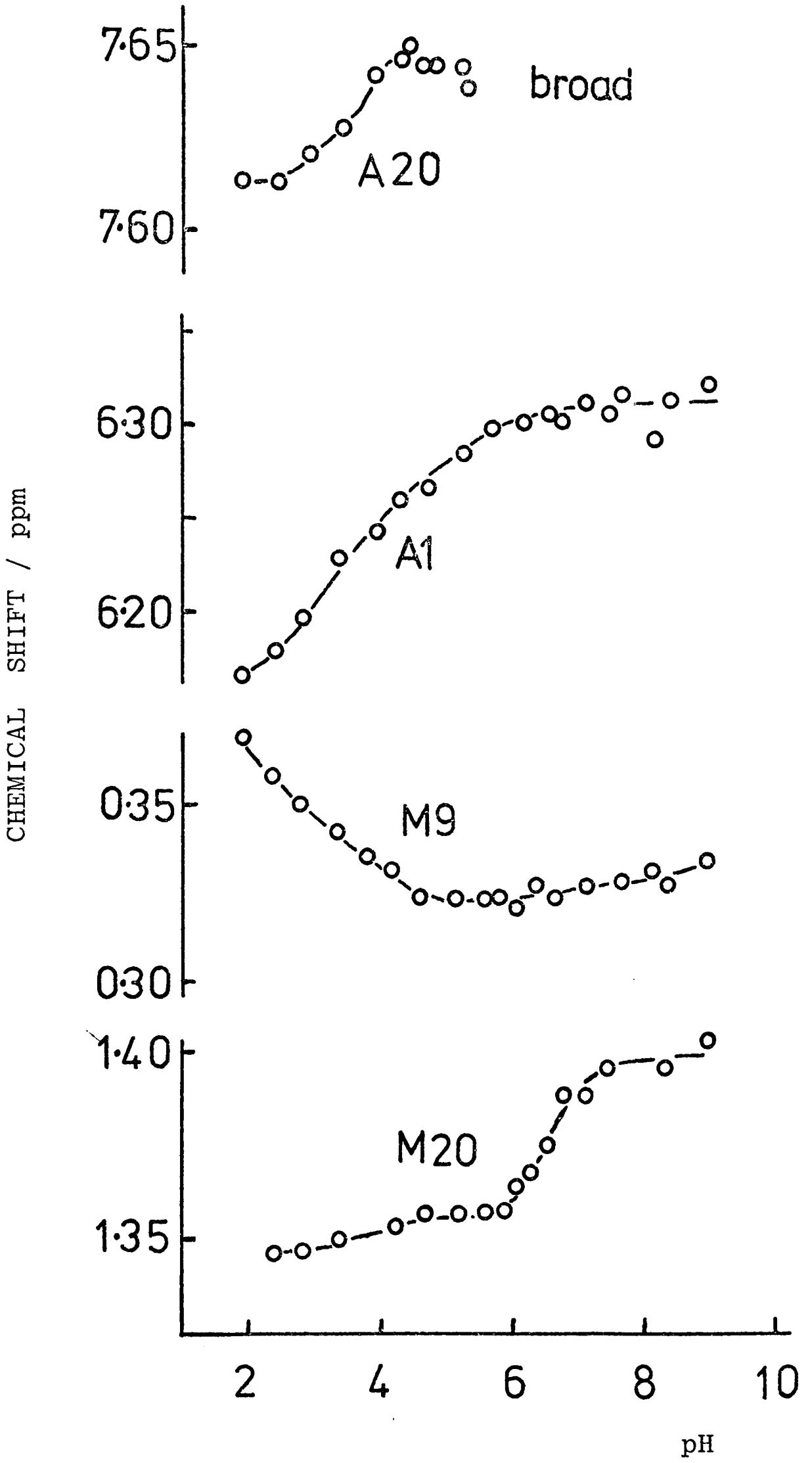

pH dependence of the chemical shift values of several resonances. 5mM lysozyme, 54°C. See also Figs V.11 and IX.13.

ing trp 63 or from a simple change in the shielding by the carboxyl group of asp 101 due to the movement of this carboxyl group on ionisation. In Fig. IX.4 these shifts are shown.

IX.2.1.3 The Ionisation of other groups

The shifts of other non-ionisable groups shown in Table IX.3 and Fig. IX.4 arise from small local conformational changes accompanying ionisation of nearby groups. These conformation changes in some cases have been indicated in the crystalline state by comparison of X-ray data at pH 2.7 and pH 4.5 (Imoto et al., 1972).

IX.2.2 Linewidth Changes

At 25°C, below pH 5, all the resolved resonances of lysozyme have similar linewidths (see Chapter VIII). As the pH value is increased above 5, the linewidths of certain resonances increase. The increase in linewidths is dependent on the pK value of glu 35 (see Fig. IX.5). At pH 8, at 25°C, the resonances of ile 98, met 105 and trp 63 are too broad to observe, and this situation continues at higher pH values. Only by increasing the temperature can these resonances be observed. This broadening is an intermediate exchange phenomenon (see Chapter VIII) and reflects an ill defined conformation of the active site region of lysozyme at pH values where glu 35 is ionised. For example suppose that when glu 35 is ionised, an aromatic residue in the active site does not have a single closely defined conformation. Instead, this residue vibrates or oscillates between different conformations. The result of this motion is that the groups which are ring-current shifted by the aromatic residue have different values of their chemical shifts as the oscillation takes place. Thus, exchange broadening of the resonances of these

FIGURE IX.5

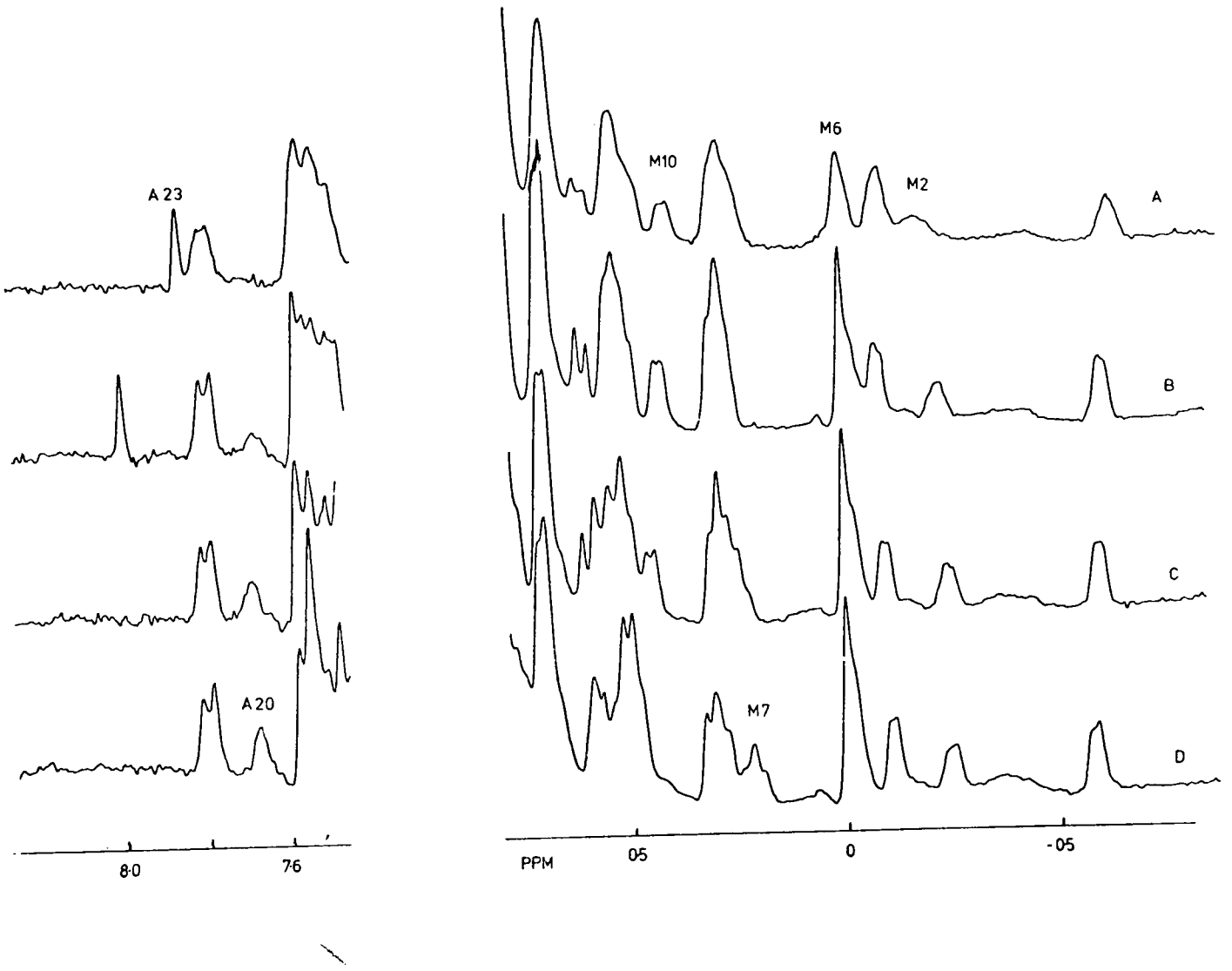

Spectra of lysozyme at different pH values showing changes in chemical shifts of resonances (e.g. M2, M7, M10, A23) and in linewidths of resonances (e.g. M2, M6) as the pH value is changed. A, pH 7.3; B, pH 6.0; C, pH 5.1; D, pH 3.8. 5mM lysozyme, $54^{o}C$.

other groups can occur as a result of the rate of the oscillation of the aromatic residue being in the region for intermediate exchange. In the active site are trp 62, trp 63 and trp 108. According to the ring-current shift calculations (Cowburn et al., 1970) and observations of the X-ray structure trp 108 is the only group which gives a ring-current shift to the three residues (met 105, ile 98 and trp 63) observed to be exchange broadened. This observation can tentatively be correlated with the movement of glu 35 on ionisation away from trp 108 and into free solution. This could result in the loss of rigidity of trp 108 in the active site by removal of a cross-linking interaction across the site. As will be shown below, the rigidity of the active site can be regained by 'cross-linking' with an inhibitor molecule.

The exchange broadening discussed above arises from oscillation of groups in a given conformational state. Because the chemical shift values of resonances of groups (particularly trp 108) are different in the two conformational states (high and low pH), exchange between these states could result in exchange broadening. This broadening is quite different from that described above and would be a maximum at the point in the pH titration where the two states were equally populated, that is at the pK value of glu 35. No such exchange broadening is observed, even on the resonances of trp 108, showing that the conformational change takes place at a rate greater than 10^3 sec^{-1} even at 25°C.

IX.3 The Effects of Inhibitor Binding

The effects on the lysozyme spectrum of the binding of the inhibitors GlcNAc, $(GlcNAc)_2$ and $(GlcNAc)_3$ were measured. Those of GlcNAc and $(GlcNAc)_3$ were studied in detail. Two types of experiment were performed. First, the effects on the spectrum

of the successive addition of inhibitor solutions at fixed temperatures and fixed pH values were studied. Secondly, at fixed concentrations of inhibitors at fixed temperatures, pH titrations were performed. These experiments will be described in turn.

IX.3.1 Titrations at Fixed pH

Detailed titrations were carried out at pH 5.3 at various temperatures between 5°C and 70°C. At this pH value, the activity of lysozyme is at a maximum (Imoto *et al.*, 1972).

Addition of GlcNAc up to concentrations of 0.25M resulted in titration curves for several resonances, Fig. IX.6, indicating a binding constant of *ca.* 43 M^{-1} at 54°C. However, GlcNAc is a mixture of α- and β- anomers, which are thought to bind in a slightly different manner (see Imoto *et al.*, 1972; Dalquist and Raftery, 1969), and so detailed analysis of the titration curves was not carried out. The largest shifts observed (Table IX.4) are of resonances assigned to the methyl groups of ile 98 (γ- and δ-) and of met 105, to a γ-CH_2 proton of ile 98, and to aromatic CH and NH protons of trp 108 and trp 63. Some of these were previously observed in the work of McDonald and Phillips (1970), and of Glickson *et al.* (1971). The following conclusions may be drawn from these data. First, the shifts observed are all of groups close to the active site cleft of lysozyme. Secondly, all the shifts can be explained by changes in ring current shifts caused by the movement of one or more of the aromatic residues trp 62, 63 and 108, which could accompany inhibitor binding. Significant shifts of resonances of groups not close to these residues have not been observed. X-ray diffraction studies (Imoto *et al.*, 1972) and pmr studies of inhibitor resonances (Dalquist and Raftery, 1969) have indicated

FIGURE IX.6

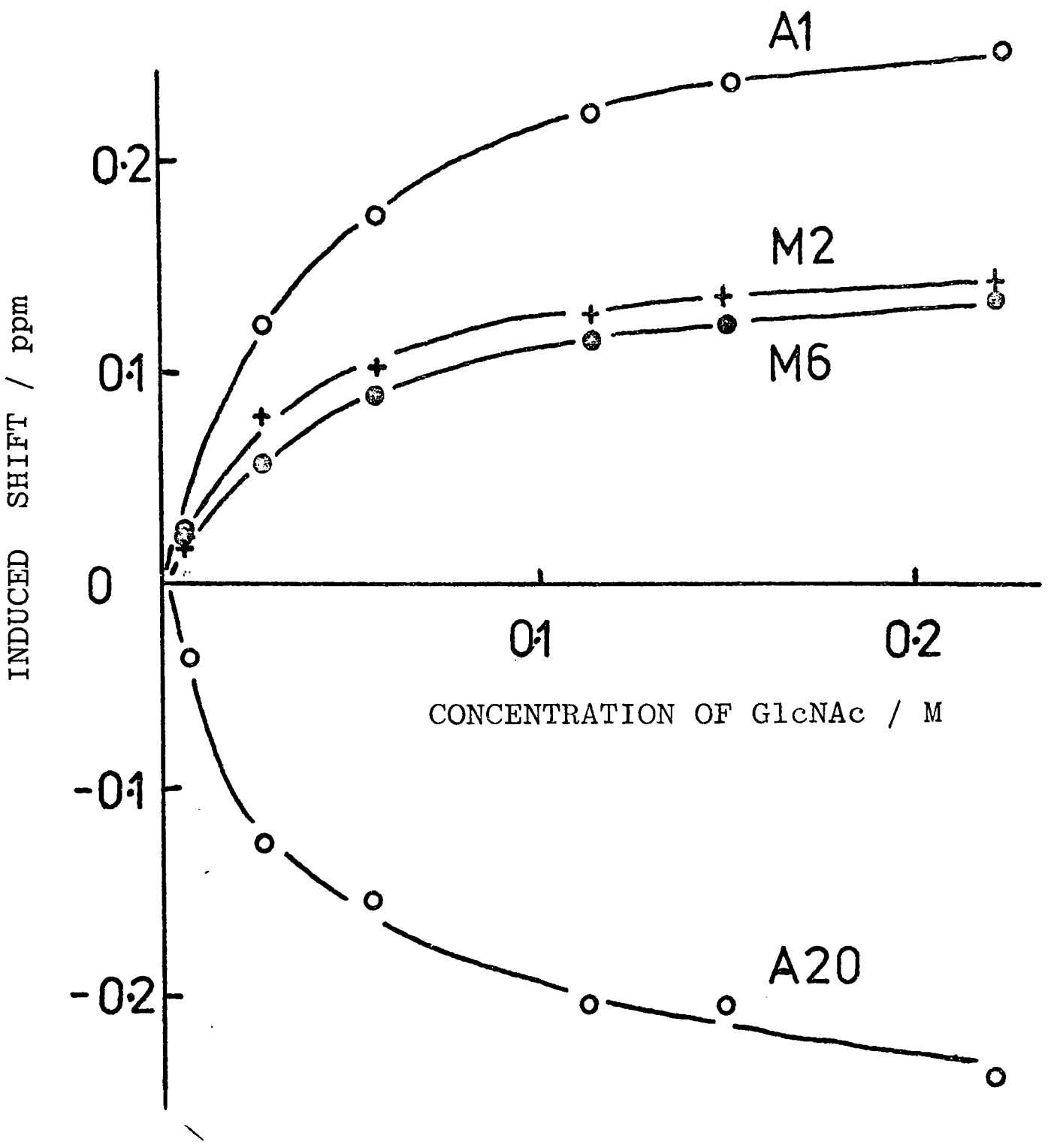

Shifts induced by the binding of GlcNAc to lysozyme as a function of the concentration of GlcNAc.
5mM lysozyme, 54°C.

TABLE IX.4

Effects of GlcNAc and $(GlcNAc)_3$ on Spectrum[a]

Resonance Number	Assignment	Shift with $(GlcNAc)_3$[b]	GlcNAc[b,c]	Change in Ring Current Shift
M2	ile 98 γ	+0.100	+0.072[d]	I
M3	leu 17	+0.058	+0.029	I
M4	ile 98 δ	+0.032	+0.054	I
M6	met 105	+0.108	+0.072	I
M8	leu 56	-0.047	-0.025	D
M11	leu 56	-0.036	-0.018	D
M13	leu 8	+0.036	0	I
M14	ala 107/31	-0.018	-0.032	D
H1	ile 98 γ-CH_2	+0.215		I
A1	trp 63 5/6	+0.198	+0.130	I
A2		+0.040	0	I
A4	trp 63 4/7	+0.126	+0.083[e]	I
A5	trp 63 5/6	+0.083	+0.054	I
A7		+0.047	+0.054	I
A16		+0.065		-
A20	trp 63 C(2)	-0.205	-0.126	I
A22	trp 63 4/7	+0.036		D
N2			-0.090	
N2			+0.086	
N4			-0.054	
N5	trp 108 N(1)		-0.234[f]	

[a] fully bound shifts at pH 5.3, 54°C which are more than 0.025 ppm. A11 (trp 108) has not been observed in the $(GlcNAc)_3$ system.

[b] shifts are very similar at temperatures from 37°C-74°C.

[c] shifts are pH independent except for those indicated.

[d] + 0.126 at pH 7.5.

[e] + 0.050 at pH 7.5.

[f] - 0.083 at pH 7.5

that both anomers of GlcNAc bind close to site C, i.e. close to trp 62, 63 and 108. The X-ray studies suggested that trp 62 moves on inhibitor binding (Imoto et al. 1972). Thirdly, note from Table IX.4 that the spectral shifts indicate an increased ring current shift for most resonances, that is the opposite effect to that of increasing temperature, Section IX.1.1. This suggests that binding of inhibitors results in a tighter structure of the protein.

The binding of GlcNAc is in fast nmr exchange under these conditions even at 5°C. Thus, because the largest shift observed on the protein resonances is ca. 60 Hz, the lifetime of the bound species must be less than 10^{-3} sec, and the first order rate constant for the observed conformational change more than 10^{3} sec^{-1}, even at this low temperature.

Similar experiments were performed with $(GlcNAc)_3$. The tighter binding of this molecule was reflected in the titration curves which indicated that no further spectral changes occurred as soon as an excess of $(GlcNAc)_3$ had been added to the lysozyme solution. The fully bound shifts induced by the binding of this molecule are very similar to those induced by the binding of GlcNAc (Table IX.4) suggesting that the induced conformational change is similar for both inhibitors. Preliminary experiments suggest that a similar situation exists for $(GlcNAc)_2$ as observed also by McDonald and Phillips (1970).

However, the exchange kinetics of $(GlcNAc)_3$ are quite different from those of GlcNAc. This is indicated in Fig. IX.7. This shows part of the spectrum of lysozyme at pH 5.3 and 37°C as the concentration of $(GlcNAc)_3$ is increased. The resonance A1, assigned to trp 63, has a different chemical shift in the spectrum of the bound and unbound protein, and slow exchange between these is observed. In Fig. IX.8 similar spectra are shown

FIGURE IX.7

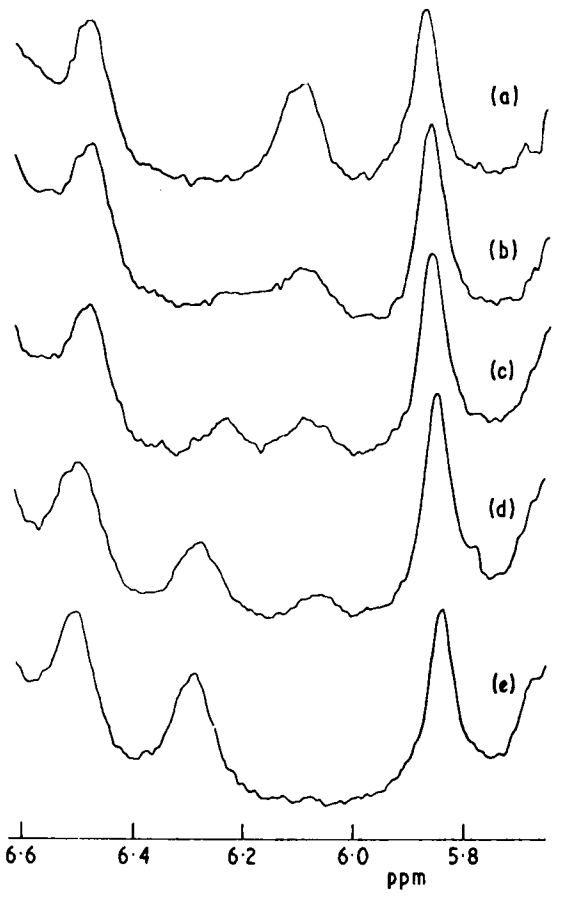

Part of the spectrum of 8mM lysozyme at 37°C, pH 5.3 in the presence of different concentrations of $(GlcNAc)_3$ which are (a) 0mM; (b) 1.9 mM; (c) 4.2mM; (d) 5.1mM; (e) 7.7mM. Resonance A1, assigned to trp 63, is observed in two environments.

FIGURE IX.8

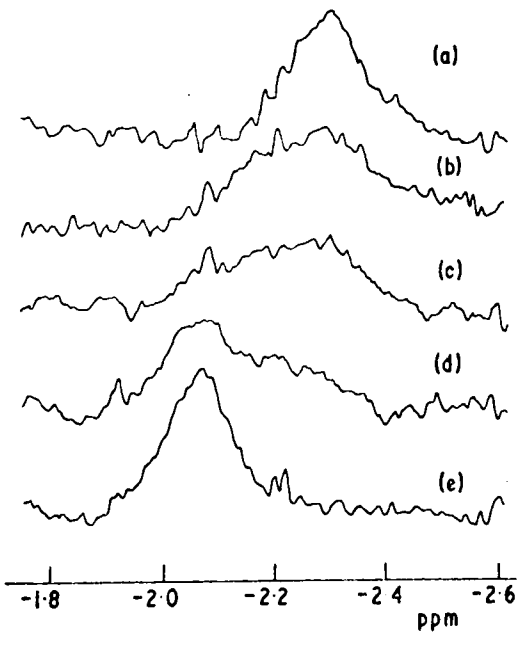

As Fig. IX.7, but for resonance H1, assigned to a γ-CH_2 proton of ile 98.

FIGURE IX.9

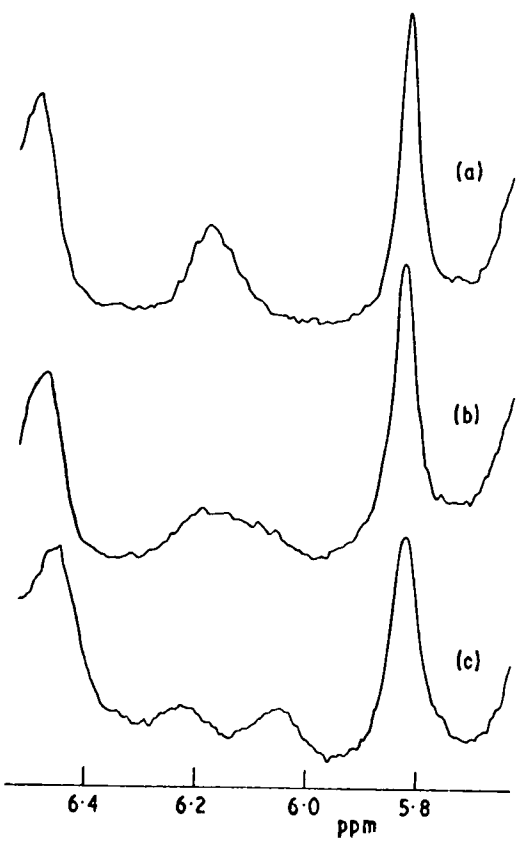

The effect of temperature on the spectrum of 8mM hen lysozyme containing 4.1mM $(GlcNAc)_3$ at pH 6.3. Temperatures are (a) $55^{o}C$; (b) $45^{o}C$; (c) $37^{o}C$. The passage from slow through intermediate to fast exchange conditions is observed.

for resonance H1 assigned to one of the γ-CH_2 protons of ile 98. In each case the difference in chemical shift values between the resonances in the bound and unbound forms is 60 Hz. The observation of these slow exchange phenomena shows that the rate of exchange between the two forms is small compared to this frequency separation. In Fig. IX.9, spectra are shown corresponding to Fig. IX.7, but of a solution in which equal concentrations of bound and unbound protein are present. As the temperature is increased, the system passes from slow through intermediate to fast exchange. At the temperature of coalescence ($45 \pm 3^{o}C$) the lifetime (τ_b) of the bound species can be estimated as 7.5×10^{-3} sec. Thus, for the first order rate process (bound conformation $\rightarrow$ unbound conformation) a rate constant (k_{obs}) of 1.3×10^{2} sec^{-1} at $45^{o}C$ is obtained. At $25^{o}C$, k_{obs} is less than 20 sec^{-1}. Exchange effects on only two resonances have been discussed here. These resonances are well resolved, and therefore easy to study. Similar effects on other resonances have been observed but not yet analysed in detail.

The results described above permit direct interpretation of the kinetics of inhibitor binding to be made. Temperature jump and stopped flow studies (Holler et al., 1969, 1970) and nmr studies of inhibitor resonances (Sykes 1969; Sykes and Parravano, 1969) have indicated that two steps are observed in the binding process of inhibitor (I) to lysozyme (E), that is

$$E + I \underset{k_{21}}{\overset{k_{12}}{\rightleftharpoons}} E I_1 \underset{k_{32}}{\overset{k_{23}}{\rightleftharpoons}} E I_2$$

The first step has been envisaged as a pre-equilibrium complex formation, the second as an isomerisation process involving a rearrangement of the protein conformation. Now, the measured value of k_{obs} for $(GlcNAc)_3$ binding was clearly that for the

conformational change which occurs on binding and results in shifts of specific resonances. This value is close to that obtained (under slightly different conditions) for k_{32} (10 sec^{-1} at pH 6.3 at 20°C) whilst k_{23} is faster (240 sec^{-1} at 20°C). k_{12} and k_{21} are of course much greater.

For β-methyl-GlcNAc, $k_{23} >> k_{32} > 10^3$ sec^{-1}, and similar values are expected for GlcNAc (both α and β anomers). In accord with these values, the conformational change was observed as described above to be rapid ($k_{obs} > 10^3$ sec^{-1} at 5°C). The present results thus provide direct evidence that the observed rate constant k_{32} corresponds to a change in protein conformation in the region of site C of lysozyme. It is unlikely that the complex EI_1 could be observed directly by nmr, first because of its very low concentration and secondly because it will be in fast exchange with E. It is interesting that for inhibitor binding the rate-controlling process is a conformational change not in the close proximity of the catalytically important groups. If this situation exists for the substrate, the enzymic rate could be limited by binding steps remote from the attacking groups.

IX.3.2 pH Titrations

The effects of pH on the spectrum of lysozyme bound to the inhibitor GlcNAc were examined. In the presence of 0.2M GlcNAc, using 5mM lysozyme, the protein is essentially fully bound at all pH values between 2 and 10. Shortage of material prevented similar experiments being performed with $(GlcNAc)_3$. The effects of pH changes on the resonances of GlcNAc bound (in fast exchange) to lysozyme were also studied and results similar to those previously published (Studebaker *et al.*, 1971) were obtained.

IX.3.2.1 The Resonances of trp 108

The effects of GlcNAc on the pH titration of the trp 108 resonances are shown in Fig. IX.10. Two effects are at once apparent. First, the pK value of glu 35 has increased slightly, and this has been observed previously (Imoto et al., 1972). Secondly, the influence of asp 52 on the N(1)H titration is much more marked. The pK value is 3.4 $\pm$ 0.2. The reason for this must be concerned with some rearrangement of the inhibitor (which is a mixture of the α- and β-anomers) in the active site cleft accompanying the ionisation of asp 52. Note however that any change in binding constant will be unimportant because a saturating concentration of GlcNAc is present.

IX.3.2.2 The Resonances of Inhibitors

In the presence of lysozyme the N-acetyl methyl group resonances of the α-and β-anomers of GlcNAc can be separately observed (Raftery et al. 1968). This arises because there are differences in ring current shifts and in binding constants for the two anomers. From pH titrations (Studebaker et al. 1971), it is clear that the ionisation of glu 35 affects both the binding constants and the observed ring current shifts experienced by the bound inhibitors. This is consistent with the conformational behaviour of lysozyme discussed above. The ring current shifts of the inhibitor are mainly from trp 108, which is perturbed by glu 35. A pK value of between 4.5 and 5.0 also affects the observed ring current shifts and the binding constants. This pK value must be of asp 101 although previously it was thought to be of asp 52 (Parsons and Raftery, 1970; Studebaker et al., 1971). That the ionisation of asp 101 affects the binding of inhibitors is not surprising as trp 63 is perturbed by the ionisation of asp 101 as described above (Section IX.2.1.2).

FIGURE IX.10

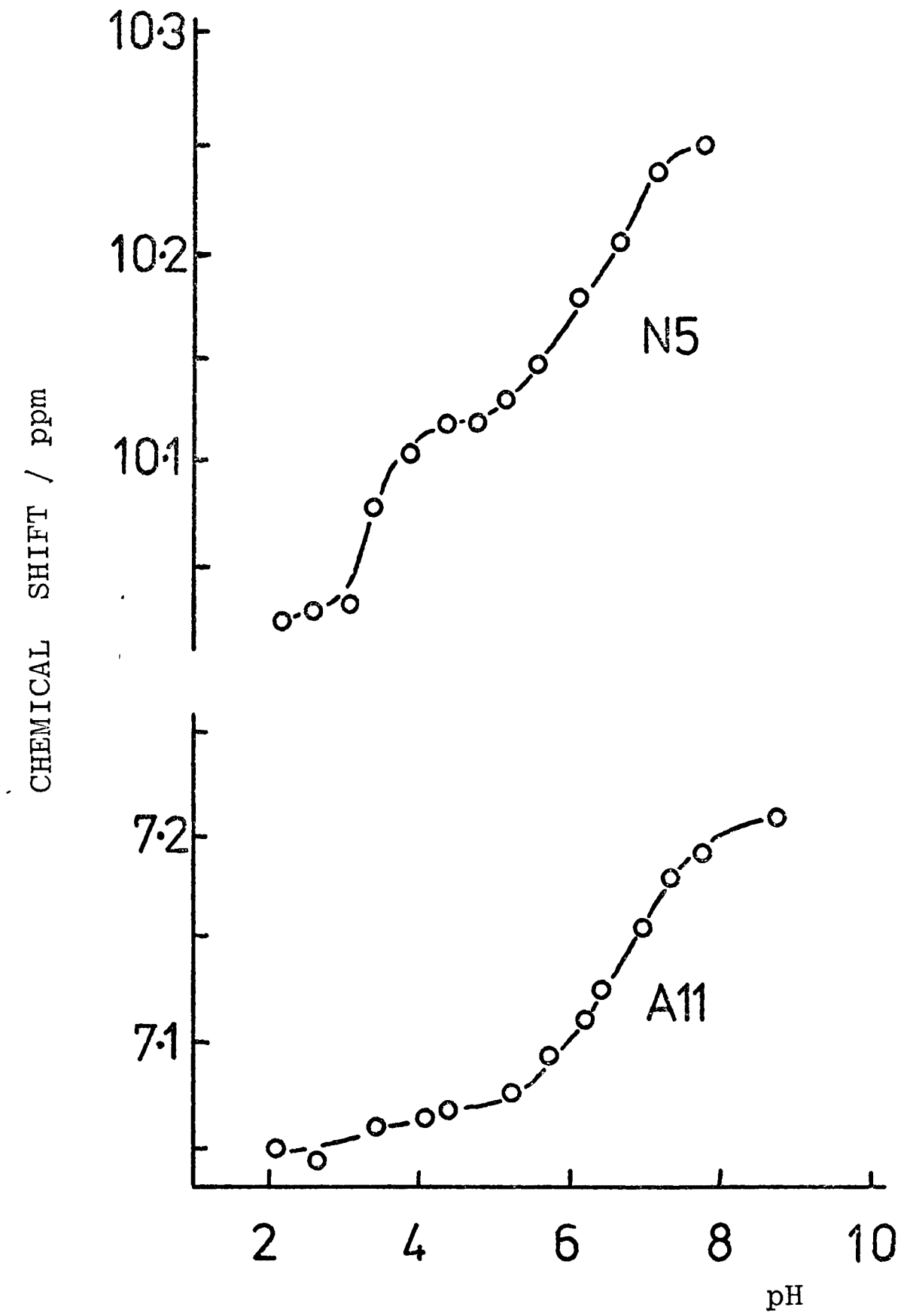

pH dependence of the chemical shift values of the resonances of trp 108, with GlcNAc bound. 5mM lysozyme, 0.22M GlcNAc, 54°C. Compare Fig. IX.3.

IX.3.2.3 Conformational and Mobility Changes

The movement of glu 35 in the active site cleft upon ionisation still occurs in the presence of GlcNAc. However, a study of the other resonances affected by the pK of glu 35 through a conformational change (see Section IX.2.1) indicates that this conformational change does not take place, or at least is much smaller, in the presence of bound GlcNAc. This conclusion follows from a comparison of titration curves in the presence and absence of GlcNAc (Fig. IX.11). Thus, it appears that the inhibitor molecule holds the active site in a fixed conformation, which is therefore unaffected by the ionisation of groups in the site. This conclusion is supported when the linewidth of resonances is observed. The broadening at pH values above the pK value of glu 35, which was observed for the native enzyme, is no longer observed in the inhibitor bound enzyme (Fig. IX.12).

Thus, the results of these experiments with the inhibitor bound protein suggest that the conformation of the active site cleft is stabilised by the presence of the inhibitor.

IX.4 The Effects of Metal Ions

The binding of the diamagnetic metal ions La^{3+} and Lu^{3+} has already been described. The shifts of different resonances are summarised in Table IX.5. Because the binding of the metal ions involves glu 35, the only way to obtain reliable information about the effects of these ions is to perform pH titrations as described in Section VI.2.3.1.

In Fig. IX.13 are shown pH titration curves in the presence and absence of metal ions (see also Fig. V.11). Ca^{2+} has similar effects to La^{3+} and Lu^{3+} and unlike the latter ions is soluble over the whole pH range of interest. The conclusions of these titrations are not very clear cut. It appears (see Fig. VI.5)

FIGURE IX.11

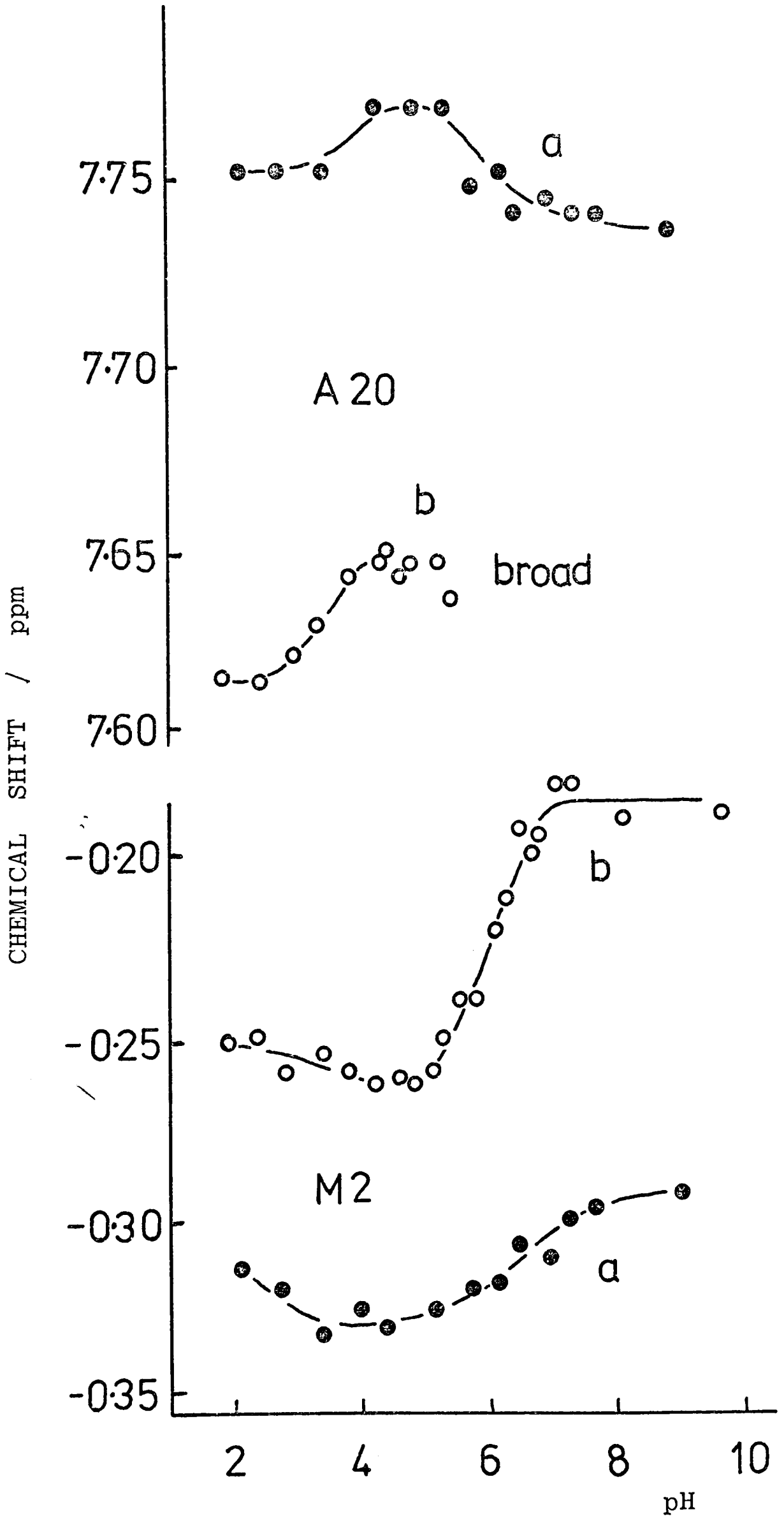

pH dependence of the chemical shift values of resonances M2 and A20 (a) with and (b) without GlcNAc bound. Both resonances are broad above pH 6 in the absence of GlcNAc. 5mM lysozyme, 0.22M GlcNAc, 54°C.

FIGURE IX.12

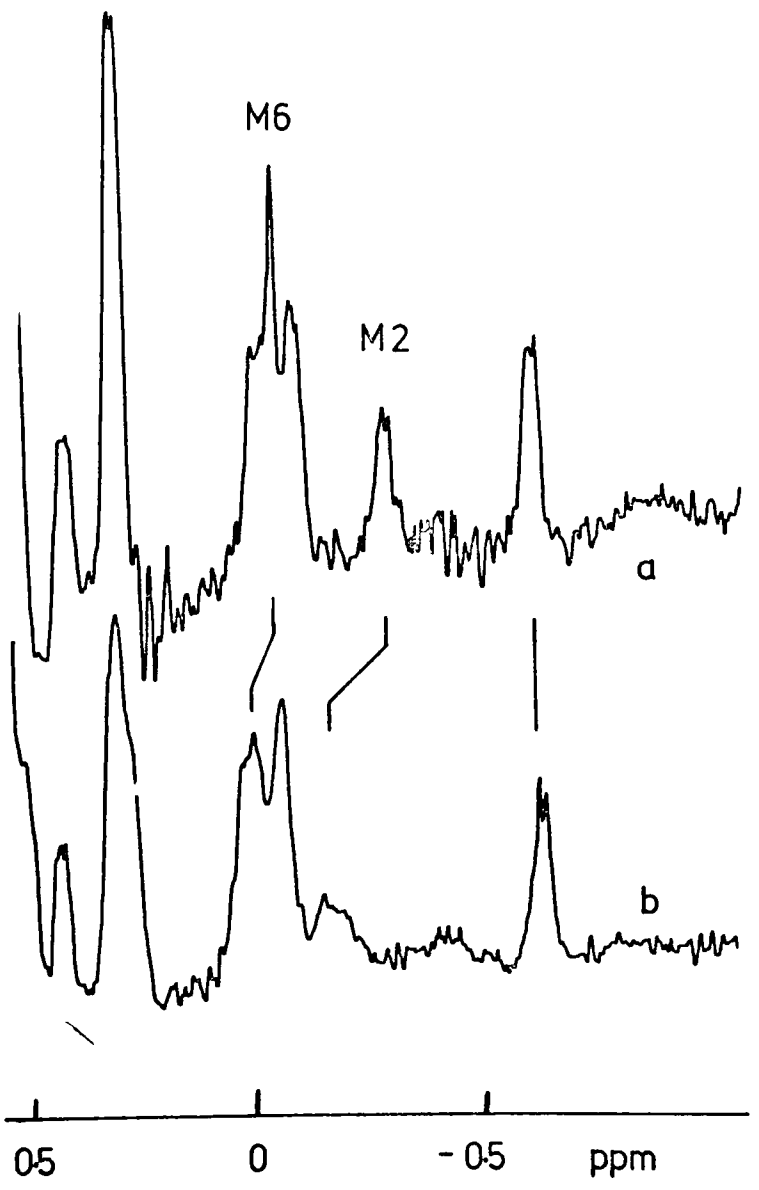

The effect of binding GlcNAc on lysozyme resonances at pH 7.0. (a) no GlcNAc; (b) 0.22M GlcNAc. Resonances M2 and M6 are broad only in the absence of GlcNAc. 5mM lysozyme, 45°C.

FIGURE IX.13

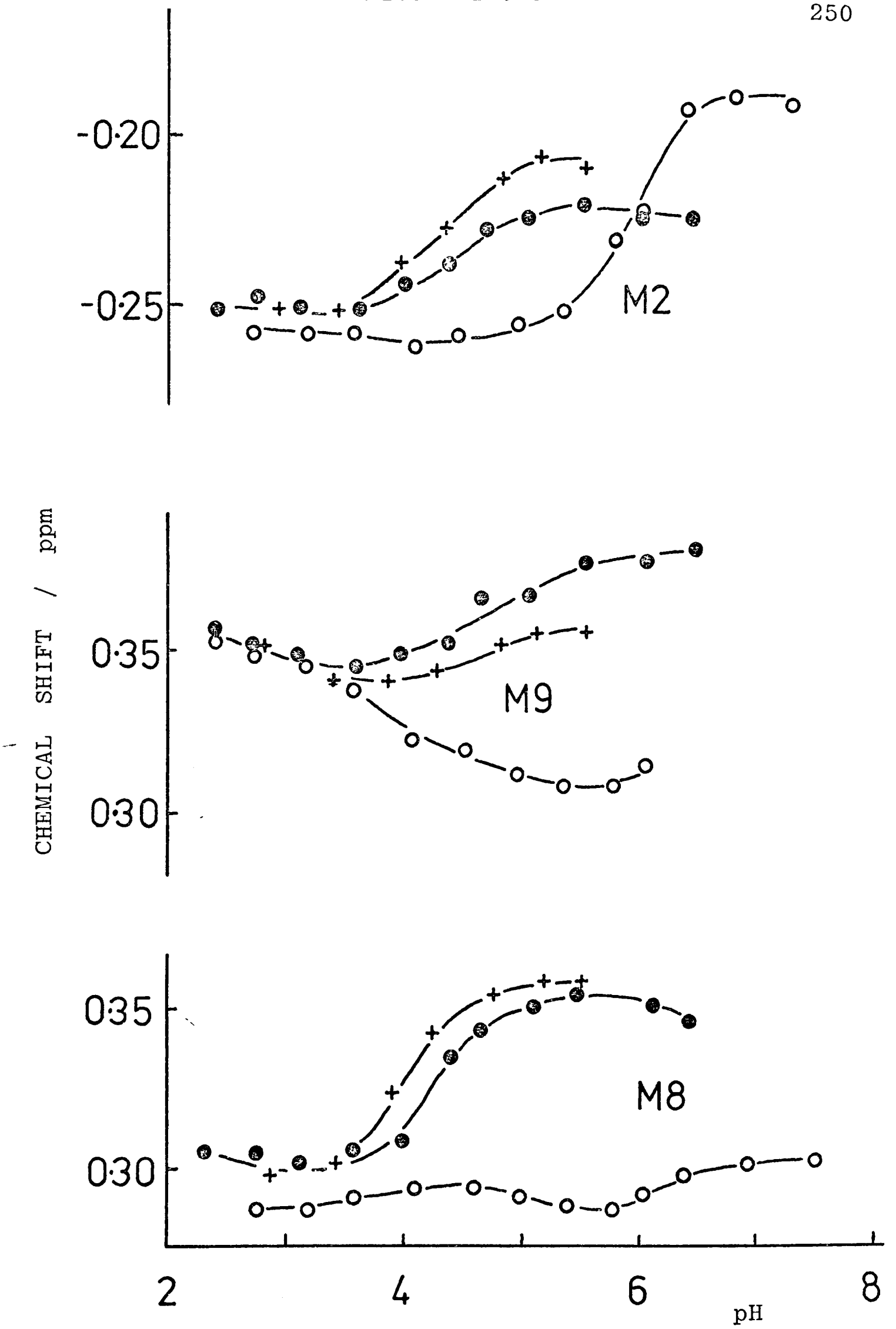

pH dependence of the chemical shift values of resonances in the presence of 0.4M KCl (open circles), 0.05M La^{3+} (closed circles) and 0.05M Lu^{3+} (crosses). 5mM lysozyme, 54°C.

TABLE IX.5

Effects of Diamagnetic Metal Ions[a]

Resonance Number	Assignment	Shift La	Shift Lu	Shift Ca	glu 35 shift[b]
M2	ile 98 γ	-0.029	-0.047	-0.022	-0.083
M8	leu 56	-0.065	-0.068	-0.018	0
M9	thr 51	-0.065	-0.047	-0.043	0
M14	ala 107/31	-0.032	-0.032	0	-0.058
M20	ala 110	-0.022			-0.043
A1	trp 63 5/6	+0.025		+0.047	(0)
A7	trp 108 C(2)	-0.133	-0.143	-0.093	-0.150
A20	trp 63 C(2)	+0.029	+0.029	+0.014	+0.054
N2		-0.082			
N5	trp 108 N(1)	-0.215			-0.290

[a] shift induced at pH 5.3 in presence of 24mM La^{3+} or Lu^{3+} or in presence of 0.5M Ca^{2+}. A negative shift is a downfield shift on binding the metal ion. Shifts larger than 0.02 ppm only are listed.

[b] shift associated with pK of glu 35 (see Table IX.2).

that as far as glu 35 and trp 108 are concerned, the conformation of the protein bound to the metal ions is similar to the conformation of the protein with glu 35 ionised (high pH). This is not surprising because the carboxylate group must move away from trp 108 to bind to the metal ion. Small shifts on the thr 51 resonances suggest that binding to asp 52 results in a slight conformational change in this region. However, overall the conformation of the bound protein differs slightly from the high pH form of the unbound protein. There are also small differences between the conformations of the La^{3+}, Lu^{3+} and Ca^{2+} bound protein (see Table IX.5 and Fig. IX.13). Finally, the linebroadening at pH values above the pK value of glu 35 is slightly less than that of the native enzyme. This presumably arises from the cross-linking effect of the metal ions in the active site, but requires further investigation.

IX.5 Summary

This Chapter has described the changes in the conformation and conformational mobility of lysozyme which accompany changes in temperature or the binding of protons, metal ions or inhibitors. Change in temperature give rise to no significant conformational changes. Binding of the different species to the protein does result in conformational changes, and the nature, extent and rates of these changes have been investigated. At pH values above the pK value of glu 35, the active site of the protein does not appear to be rigidly defined, for broadening of certain resonances indicates that exchange between different local conformers occurs. This broadening effect is abolished at lower pH, where glu 35 interacts with the nearby trp 108, and when inhibitors are bound in the active site. This implies that only under these circumstances is the active site in a fixed

conformation. This picture of the active site is summarised in Fig. IX.14.

FIGURE IX.14

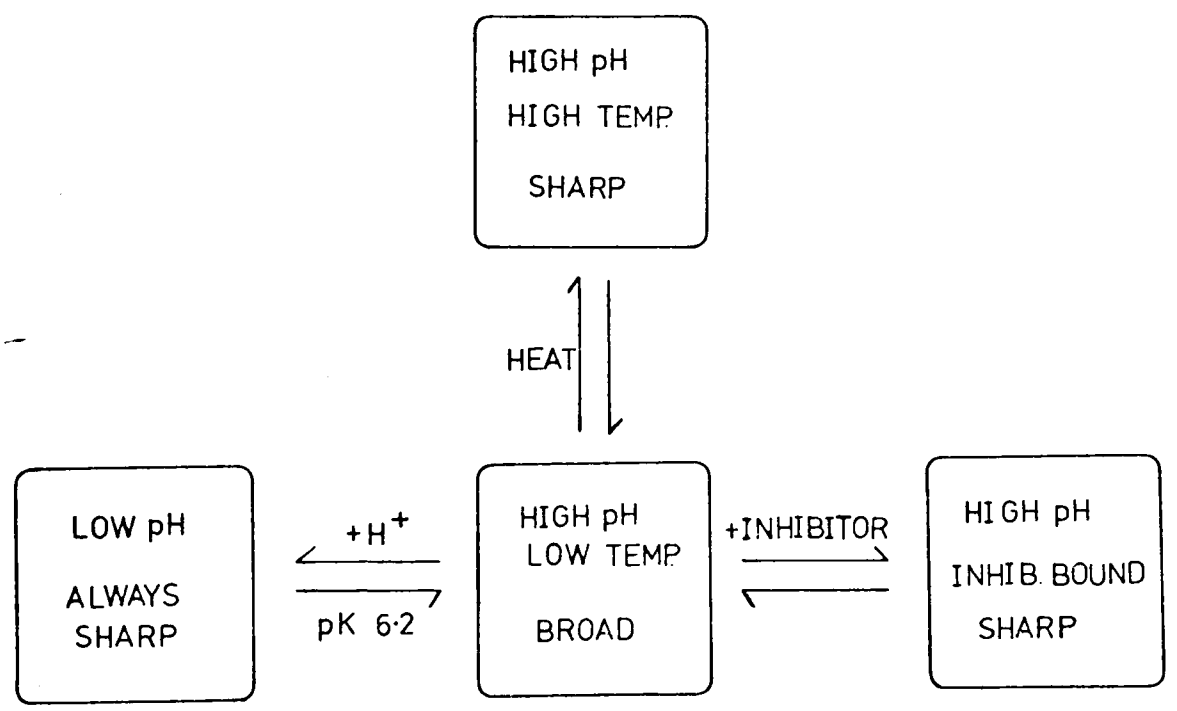

Summary of the active site conformational and mobility changes. Sharp and broad refer to resonances in the active site (see text).

References for Chapter IX

Cozzone, P.J., Opella, S.J., Jardetzky, O., Berthou, J. and Jollés, P. (1975), Proc. Natn.Acad.Sci. U.S. 72, 2095.

Dalquist, F.W. and Raftery, M.A. (1969), Biochemistry 8, 713.

Dyer, J.R. (1965), Applications of Absorption Spectroscopy of Organic Compounds, Prentice-Hall.

Glickson, J.D., Phillips, W.D. and Rupley, J.A. (1971), J.Amer.Chem.Soc. 93, 4031.

Holler, E., Rupley, J.A. and Hess, G.P. (1969), Biochem.Biophys. Res. Comm. 37, 423.

Holler, E., Rupley, J.A. and Hess, G.P. (1970), Biochem.Biophys. Res. Comm. 40, 166.

Imoto, T., Johnson, L.N., North, A.C.T., Phillips, D.C. and Rupley, J.A. (1972), In The Enzymes 3rd ed., Vol. VII (Boyer, P.D. ed.), Academic Press (N.Y.), 665.

McDonald, C.C. and Phillips, W.D. (1969), J.Amer.Chem.Soc. 91, 1513.

McDonald, C.C. and Phillips, W.D. (1970), In Fine Structure of Proteins and Nucleic Acids, Vol. IV, (Fasman, G.D. and Timasheff, S.N. eds), Marcel Dekker (N.Y.), 1048.

Parsons, S.M. and Raftery, M.A. (1970), Biochem.Biophys.Res.Comm. 41, 45.

Raftery, M.A., Dalquist, F.W., Chan, S.I. and Parsons, S.M. (1968), J.Biol.Chem. 243, 4175.

Studebaker, J.F., Sykes, B.D. and Wien, R. (1971), J.Amer.Chem. Soc. 93, 4579.

Sykes, B.D. (1969), Biochemistry 8, 1110.

Sykes, B.D. (1971), J.Amer.Chem.Soc. 93, 4579.

Sykes, B.D. and Parravano, C. (1969), J.Biol.Chem. 244, 3900.

CHAPTER X

COMPARISON OF HUMAN AND HEN LYSOZYMES

X.1 Introduction

Human lysozyme differs from hen lysozyme in about 40% of the sequence (human lysozyme has 51 replacements and 1 insertion into the 129 amino acid residues of hen lysozyme. The sequence is given in Appendix A). The X-ray structure of human lysozyme (Banyard *et al.*, 1974) is similar to that of hen lysozyme, particularly, in the active site region where much of the sequence is conserved. The purpose of the studies described in this Chapter is to compare the behaviour and structure of human with hen lysozyme in solution.

X.2 Assignment of the Spectrum

X.2.1 Description of the Spectrum

Fig. X.1 shows a spectrum of human lysozyme. The resolution of resonances is extremely good, both of the methyl group and of the aromatic proton resonances. The stability to heat and to extremes of pH is similar to that of hen lysozyme. Denaturation at high temperature ($80^{o}C$) to exchange NH protons for deuterons is fully reversible. In spectra of samples dissolved in H_2O, there are five resonances which have been assigned to tryptophan N(1)H protons (Glickson *et al.*, 1971). In this protein, which contains only five tryptophan residues, all these N(1)H resonances have therefore been observed. Additionally, all five singlet C(2)H resonances have been found using the multiplet selection method (CPA).

FIGURE X.1

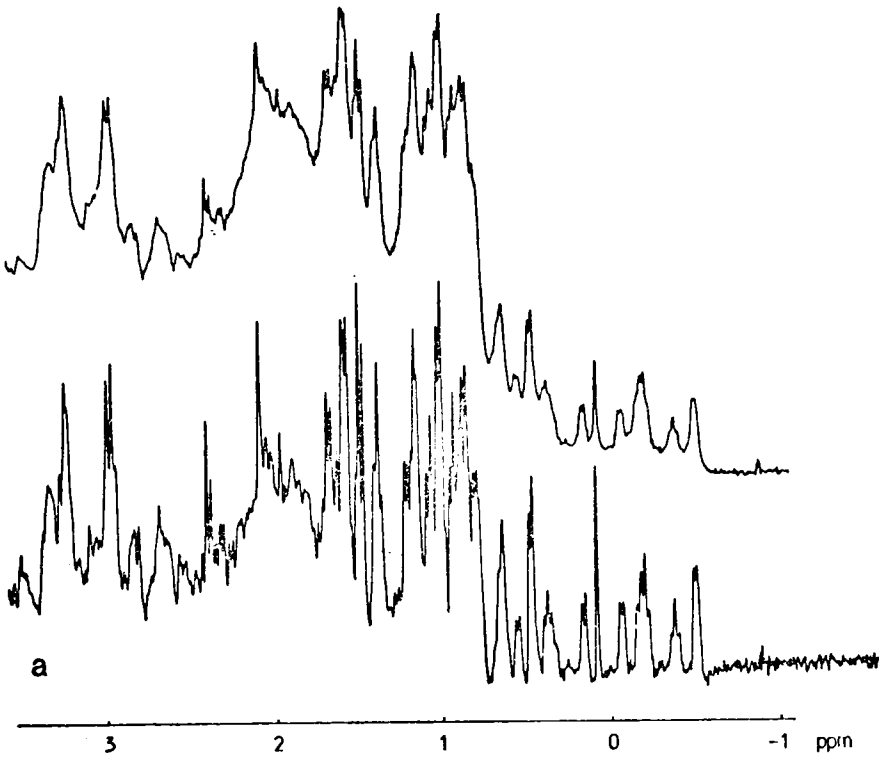

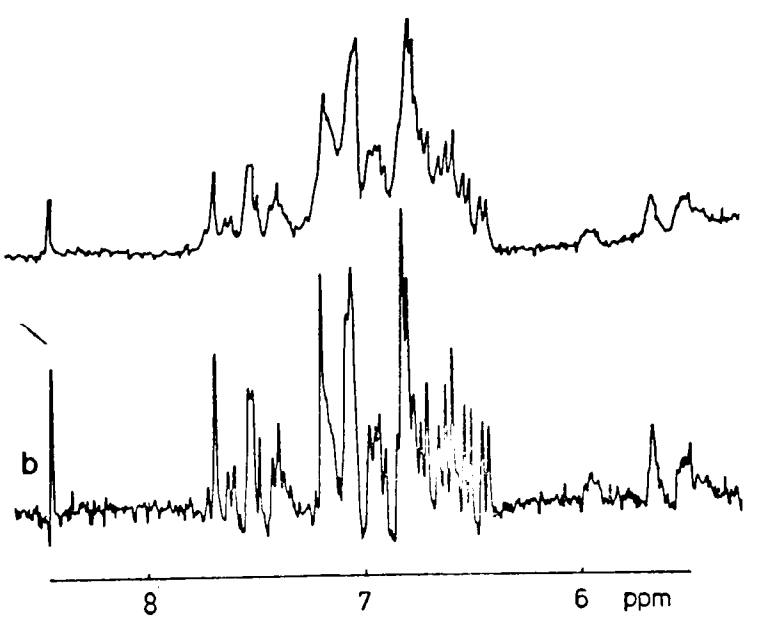

Spectra of 5mM human lysozyme with 50mM La^{3+}, pH 5.3, 54°C. Upper trace in (a) and (b) is the normal spectrum. Lower traces are CD spectra with τ_1 = 0.25 sec, τ_2 = 0.08 sec and K = 0.94.

X.2.2 Gd^{3+} Broadening

The addition of Gd^{3+} to human lysozyme results in specific broadening of certain resonances. This broadening can be observed by difference spectroscopy, and the difference spectra are extremely similar to those for hen lysozyme, as Fig. X.2 and Fig. X.3 show. In the methyl group region, resonances can be assigned to val 109, ala 110 and thr 51 (using the numbering scheme of hen lysozyme, see Appendix A) by direct comparison with hen lysozyme. These have not however been confirmed by spin-decoupling. In the aromatic proton region, the C(2)H of a tryptophan is clearly observed, and assigned to trp 108. One of the N(1)H resonances also broadens substantially (Fig. X.4) and is assigned to trp 108 also. These assignments are strongly confirmed when the effects of pH are considered. The assignments are given in Table X.1.

X.2.3 pH Titrations

The effects of pH on the spectra of human lysozyme were measured at 54°C, between pH values of 2 and 9. A pH difference spectrum is shown in Fig. X.5. This resembles very closely the analagous spectrum of hen lysozyme (Fig. IX. 2). The C(2)H and C(4)H proton resonances of the single histidine (his 77) are readily identified. The other resonance observed in the difference spectrum is of trp 108. Its titration curve is shown in Fig. X.6. The N(1)H resonance of trp 108 can be readily observed to titrate (Fig. X.7). These resonances, by analogy with human lysozyme, reflect the pK value of glu 35 (7.1 ± 0.2) and to a lesser extent asp 52 (3.5 ± 0.5). The pK values are summarised in Table X.2. The effect of added La^{3+} is to decrease the apparent pK value of glu 35 as expected. Although many resonances in the human lysozyme spectrum are observed to titrate

FIGURE X.2

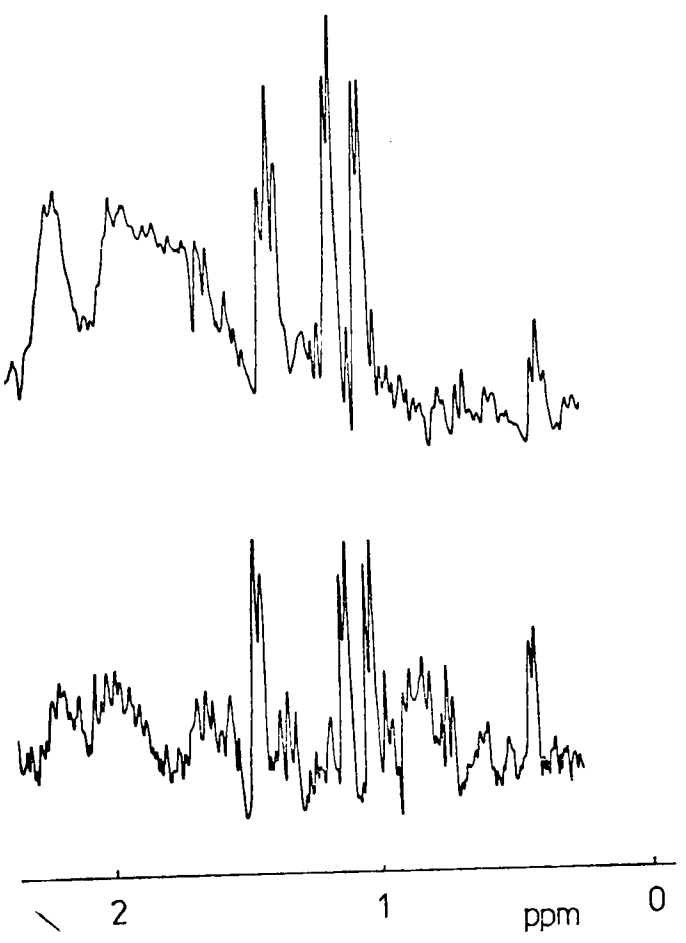

Gd^{3+} broadening difference spectra. Upper spectrum is of hen lysozyme and lower spectrum is of human lysozyme. [Lys] = 5mM, $[La^{3+}]$ = 50mM, $[Gd^{3+}]$ = 5 x 10^{-5}M, Temp. = 54^{o}C.

FIGURE X.3

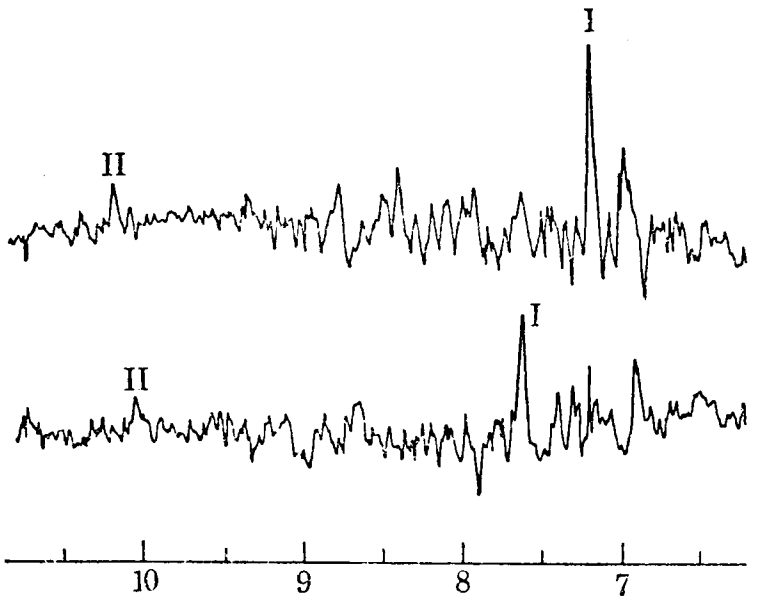

Gd^{3+} broadening difference spectra for proteins in 90% H_2O, 10% D_2O. Upper spectrum, for hen lysozyme containing 1.23×10^{-5}M Gd^{3+}. Lower spectrum, for human lysozyme containing 2.54×10^{-5}M Gd^{3+}. [Lys] = 5mM, [La^{3+}] = 23.8mM, pH 5.3, 54°C. Resonances I and II are assigned to the C(2)H and N(1)H protons of trp 108 in each case. Compare Figure V.8.

FIGURE X.4

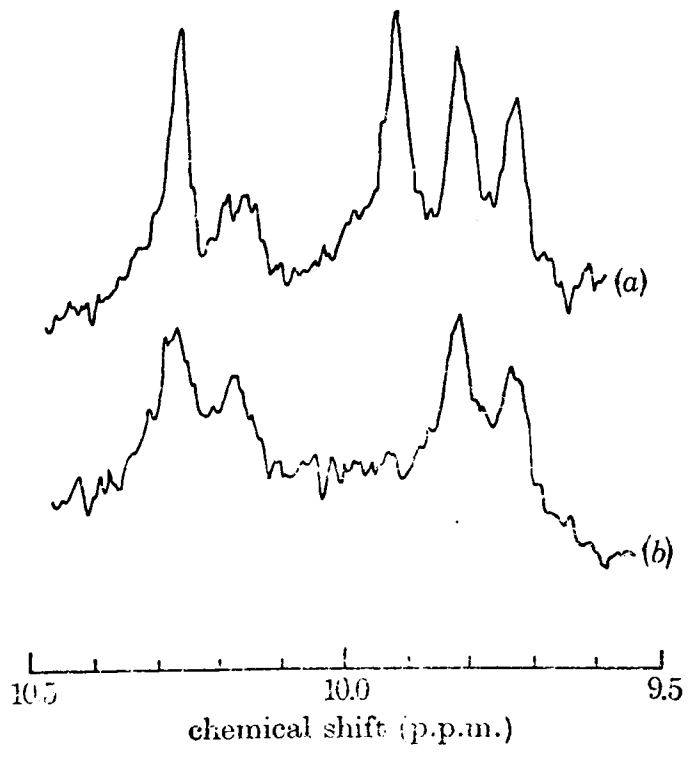

(a) Spectrum of 5mM human lysozyme in 90% H_2O, 10% D_2O at pH 5.3, 54°C. (b) Spectrum of the same solution containing 1.3×10^{-4}M Gd^{3+}. Compare Fig. V.8. The broadened resonance corresponds to resonance II above.

TABLE X.1

Assignments in the Spectrum of Human Lysozyme

Type of Proton	Multiplet Structure	Chemical Shift (ppm)[a]	Assignment	Chemical Shift in Hen (ppm)[a]	Method of Assignment[b]
CH_3	s	0.04	met 17		rc
CH_3	s	2.09	met 29		rc
CH_3	d	0.42	thr 51	0.36	Gd
CH_3	d	1.04	val 109	1.02	Gd
CH_3	d	1.15	val 109	1.13	Gd
CH_3	d	1.45	ala 110	1.37	Gd
Ar-H	s	7.28	his 77 C(4)		pH
Ar-H	s	8.57	his 77 C(2)		pH
Ar-H	s	7.33	trp 108 C(2)	7.09	Gd, pH
N-H	s	9.92	trp 108 N(1)	10.04	Gd, pH

[a] for CH_3 group resonances assigned from Gd^{3+} experiments, the chemical shift values are for 50mM La^{3+}, pH 5.3, 54°C. Otherwise the values are in the absence of La^{3+}. Values are given for hen lysozyme only if the residue is conserved.

[b] ring current calculations (rc), Gd^{3+} broadening (Gd), or pH effects (pH).

FIGURE X.5

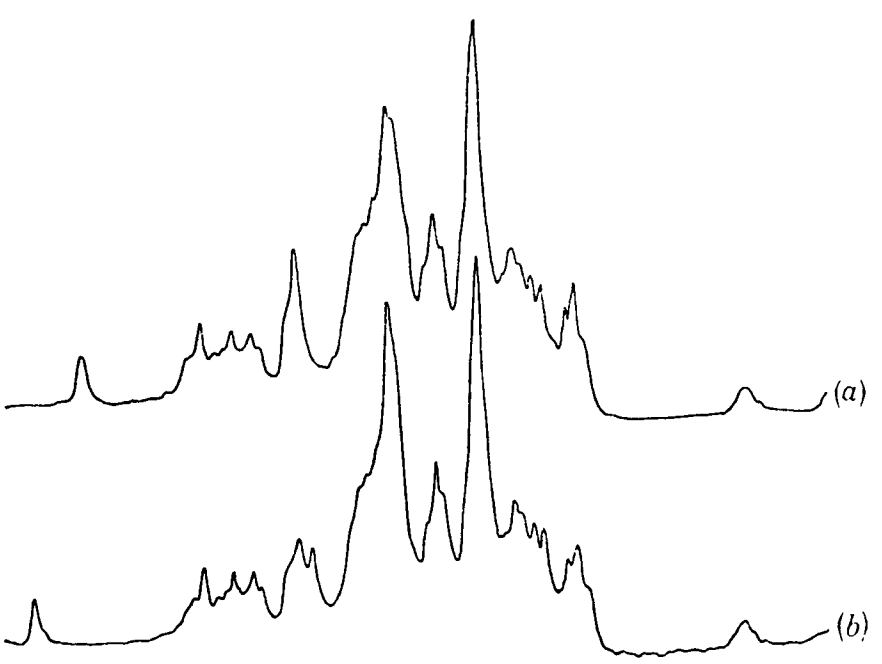

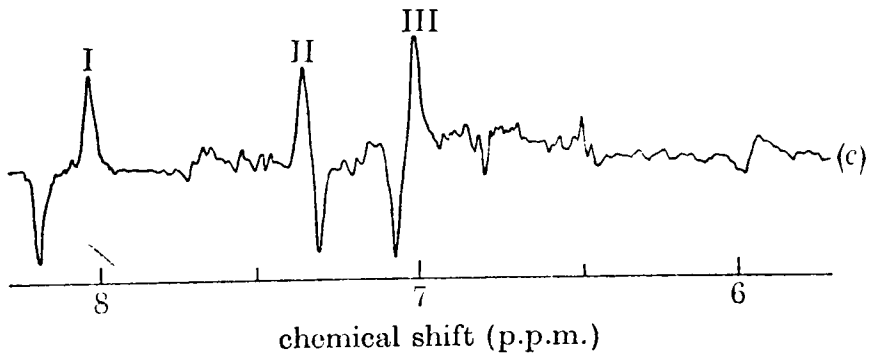

Spectra of 5mM human lysozyme, 54°C. (a) pH 7.0, (b) pH 6.5, (c) difference between (a) and (b) on twice the vertical scale. Peaks I and III are of his 77 and II is assigned to trp 108. Compare Fig. IX.2.

FIGURE X.6

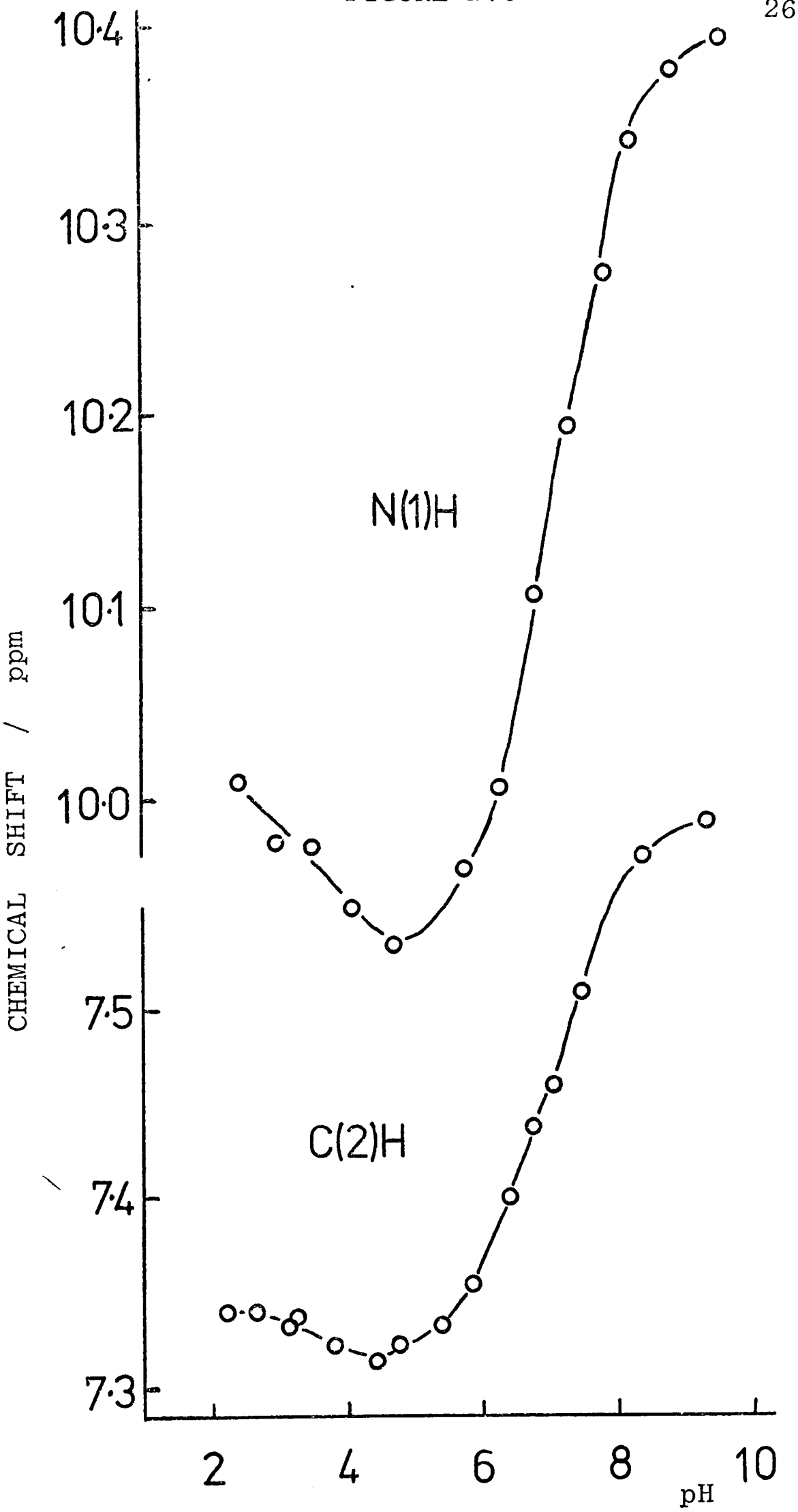

pH dependence of the chemical shift values of trp 108 resonances of human lysozyme. 5mM human lysozyme, 54°C. Compare Fig. IX.3.

FIGURE X.7

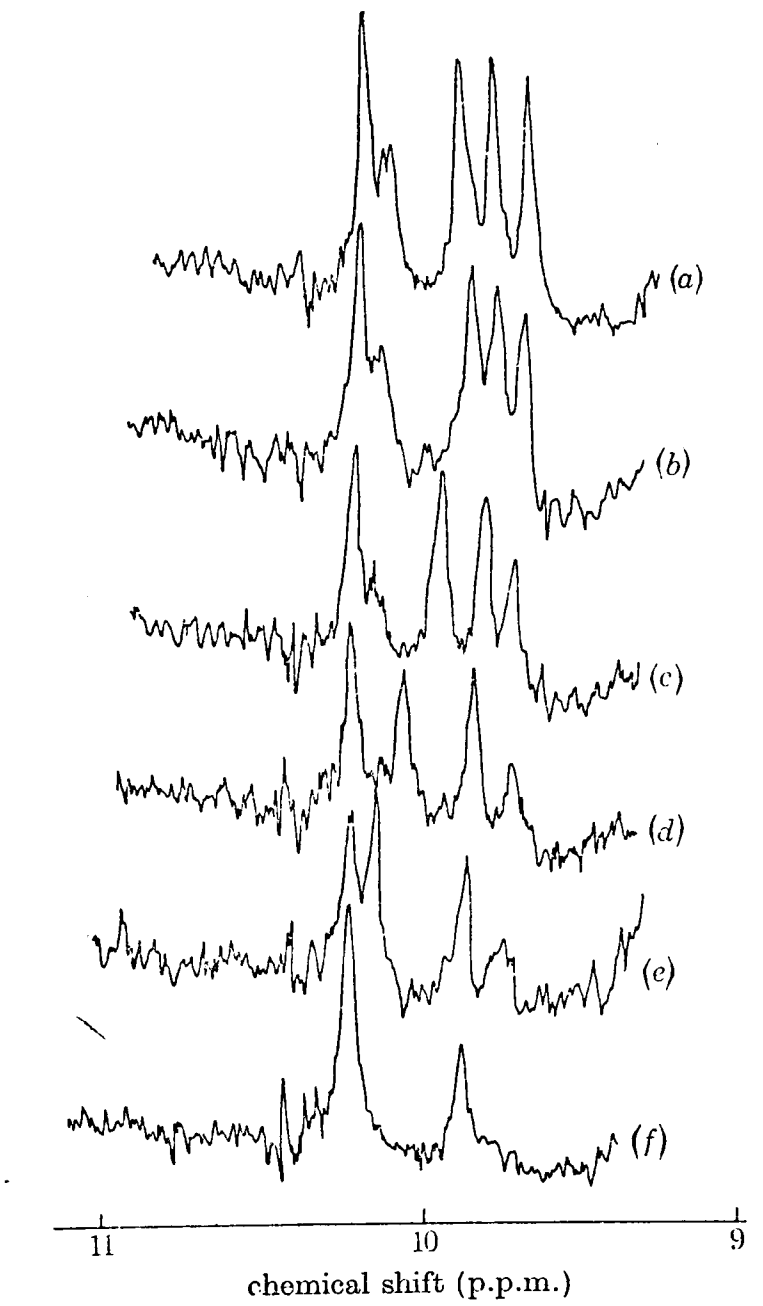

Spectra of 5mM human lysozyme in 90% H_2O, 10% D_2O at 54°C. The pH values are (a) 3.6, (b) 4.7, (c) 6.3, (d) 6.8, (e) 7.2, (f) 7.7.

TABLE X.2

pK Values for Human Lysozyme

Group	pK Value[a]	Resonance Observed
glu 35	7.1 ± 0.2	trp 108 C(2), N(1)
asp 52	3.5 ± 0.5	trp 108 C(2), N(1)
his 77	7.1 ± 0.2	his 77 C(2), C(4)

[a] at 54°C. The measured value in H_2O and D_2O are the same.

with pH, no further analysis is given here.

X.2.4 Ring Current Shifts

No calculations of ring current shifts of human lysozyme have been made. A number of large ring current shifts are observed in the spectrum, particularly of methyl groups. Two assignments can however be made at once. These are of the methionine residues, one of which experiences a very large ring current shift (Table X.1). This is clearly met 17 (cf. leu 17 in hen lysozyme) and the other methionine resonances thus arise from met 29.

X.3 Structural Conclusions

X.3.1 Outline Structure

The similarity of the paramagnetic difference spectra with Gd^{3+} of hen and human lysozyme shows that the outline structure of the two proteins is very similar. Thus, the carboxylate groups of glu 35 and asp 52 must be in very similar orientations in the two proteins. The conformation of residues 108-110 and of 51-53 must be closely similar in each protein. It is thus reasonable to suppose that the active clefts of the two proteins are essentially conserved.

X.3.2 pH Effects

A further indication of the very close similarities between the two proteins comes from the observation of a similar dependence of the C(2)H and N(1)H proton resonances of trp 108 on the pK value of glu 35 (values are 6.2 in hen, 7.2 in human lysozyme). This suggests that the unusual interaction between glu 35 and trp 108 could be important. It is an essential feature of the lysozyme mechanism that glu 35 has a high pK value in both

proteins.

The studies on human lysozyme have illustrated that the pmr methods developed here can rapidly define a small area of a protein of particular interest, and are of general applicability for comparison of proteins thought to have similar conformations.

References for Chapter X

Banyard, S.H., Blake, C.C.F. and Swan, I.D.A. (1974), in Lysozyme (Osserman, E.F., Canfield, R.E. and Beychok, S., eds), Academic Press (N.Y.), 71.

Glickson, J.D., Phillips, W.D. and Rupley, J.A. (1971), J.Amer.Chem.Soc. 93, 4031.

CHAPTER XI

CONCLUSIONS CONCERNING THE STRUCTURE OF LYSOZYME IN SOLUTION

In this Chapter, a summary is given of the information which has been collected concerning the structure of lysozyme in solution. In previous chapters it was found convenient to divide the structural features of the protein into three. First, the time-averaged structure was considered. This structure is concerned with the positions of the atoms in the molecule averaged over a period of time which is long compared to any fluctuations of these positions. Secondly, the nature of the fluctuations of atomic positions was examined. Both the extent and the rate of these conformational movements needed to be specified. Thirdly, the changes in both the time-averaged and the dynamic structure of the protein which occurred in response to external perturbations (for example ligand binding) were investigated. Again, both the extent and the rate of the changes needed to be specified. Each of the three aspects of the protein will be considered in turn.

(a) The time-averaged structure. Within the present limitations of both the X-ray methods and the nmr techniques, the time-averaged structure was found to be well described by the X-ray structure. Such a conclusion had of course been indicated previously by other physical and chemical studies of the protein (Imoto *et al.*, 1972), but this nmr study has allowed the comparison to be made quantitatively, or semi-quantitatively, in all regions of the protein. In addition, the solution structure of the active site of human lysozyme was found to be closely similar to that of hen lysozyme, in agreement with a recent crystallographic study

(Banyard et al., 1974).

(b) The dynamic structure. Information about the dynamic structure of lysozyme has come from a number of fundamentally different nmr experiments. These different nmr experiments have covered a wide range of timescales, and it was found that motions of groups in the protein were described by correlation times ranging from shorter than 10^{-11} sec to longer than 10^{-2} sec (Table XI.1). Clearly in order to understand the dynamic processes involved, a wide range of different types of motion must be defined. Now, the overall tumbling of the molecule has a correlation time of longer than 10^{-9} sec. However, relaxation time measurements show that all groups in the protein experience other motions with correlation times in the region of 10^{-9} sec which are not dependent on molecular rotation. These are internal motions of groups in the protein, and are especially pronounced for groups on the surface of the molecule, such as the histidine (his 15), some argines and some lysines. The extent of these motions cannot yet be defined, but it is interesting to note that many surface groups of lysozyme are not clearly resolved in the X-ray electron density map (see Appendix A). One process which can be defined more easily is the rotation of CH_3 groups around the C-CH_3 bond. The correlation time for this process was found from relaxation time measurements to be less than 10^{-11} sec.

Another process which can be closely defined is concerned with the behaviour of the aromatic rings of tyrosine and phenylalanine. The two-fold axis of symmetry of these rings means that there are two equivalent and isoenergetic conformation of each ring. These are indistinguishable in the time-averaged (X-ray) structure. The rate of interconversion, or flipping,

TABLE XI.1

Motion of groups in lysozyme[a]

Method of Detection		Nature of Motion	Probable τ_c (sec)
Relaxation Phenomena	(a)	CH_3 group rotation	$>10^{-11}$
	(b)	Molecular rotation	10^{-8} to 10^{-10}
	(c)	Surface side-chain motion	
	(d)	Internal side-chain motion	
Exchange Effects	(a)	Tyrosine flip or rotation	$>10^{-4}$
	(b)	Active site fluctuations	10^{-2} to 10^{-4}
	(c)	Most local induced conformational changes	$>10^{-3}$
	(d)	$(GlcNAc)_3$ induced conformational change	10^{-1}

[a] at 25°C

between the two equivalent conformations was studied by nmr, and found to be rapid, faster than 10^4 sec^{-1}, for at least one (tyr 53) and probably all of the three tyrosine residues of lysozyme. Using the X-ray structure as the time-averaged structure, this motion would require concerted fluctuations of the groups adjacent to the aromatic rings. This implies considerable mobility of groups in the protein molecule. This result is supported by calculations from the X-ray structure of the bovine pancreatic trypsin inhibitor protein where without concerted motion of nearby groups, the flipping of tyrosine residues, observed by nmr in this protein also, was shown to be impossible (Gelin and Karplus, 1975). Evidence for lysozyme has been accumulated to suggest that other groups such as valine and leucine have similar, but less easily investigated, motion to that of the tyrosines. Phenylalanine resonances have not been observed in lysozyme, but flipping has been detected in cytochrome c (Dobson et al., 1975).

Under certain conditions, the resonances of a number of groups (trp 63, ile 98, met 105) in the active site of lysozyme are very broad. Broadening of this type is not seen elsewhere in the protein spectrum. Measurement of relaxation times showed that this broadening was due to an exchange broadening mechanism, resulting from the slow conformational fluctuation of a group or groups in the active site. It appeared likely that one of the groups responsible was trp 108 (see below). Although direct comparison of this result with the X-ray structure was not possible because the effect was only observed to be large at pH values higher than that at which the crystallography was carried out, the X-ray structure did show diffuse electron density for one group (trp 62) in the active site. The conclusion was reached that in lysozyme, a group or groups in the active site experienced

mobility of a type different from that experienced in the rest of the protein. As seen below, this mobility is altered as species (including protons) are bound in the active site.

(c) Conformational changes. There are small changes in the spectrum and by inference in the conformation of lysozyme which accompany binding of protons, metal ions or inhibitors. These effects are most pronounced when binding occurs in the active site rather than elsewhere. Protonation of one of the catalytically important ionisable groups (glu 35) results in a conformational change and the association of the group with a tryptophan residue (trp 108). This suggests that a specific interaction is the cause of the pK value of glu 35 being high (6.2). This high pK value is an essential feature of the proposed mechanism of action of lysozyme (see Imoto et al., 1972). (A closely similar interaction was observed for human lysozyme, where the pK value of glu 35 was found to be even higher (7.2)). However, as well as spectral changes resulting from a conformational change, the exchange broadening of the active site resonances was abolished on the protonation of glu 35, that is when glu 35 and trp 108 are associated. Similarly, binding of inhibitors caused spectral changes indicating a conformational change, and also abolished the exchange broadening. These results show that binding of groups in the active site reduces the mobility of groups in that site. (It is noted that the X-ray electron density map shows a well defined conformation of trp 62, see above, in the presence of a bound inhibitor). A final piece of information about the dynamic behaviour of lysozyme was obtained when it was shown that the rate of the inhibitor induced conformational change was quite slow (ca. 10 sec^{-1}) in certain cases.

In summary, many groups in lysozyme possess considerable independent mobility. This is particularly clear for groups in the active site. Binding of species (even protons) in the active site can result in (i) a conformational change which may be quite slow and therefore a possible rate determining step in catalysis, and (ii) changes in the mobility of protein groups, which must be important in the energetics of the enzymic action.

References for Chapter XI

Banyard, S.H., Blake, C.C.F. and Swan, I.D.A. (1974), In Lysozyme (Osserman, E.F., Canfield, R.E. and Beychok, S., eds), Academic Press (N.Y.), 71.

Dobson, C.M., Moore, G.R. and Williams, R.J.P. (1975), FEBS Letters 51, 60.

Gelin, B.R. and Karplus, M. (1975), Proc.Natn.Acad.Sci. U.S.A. 72, 2002.

Imoto, T., Johnson, L.N., North, A.C.T., Phillips, D.C. and Rupley, J.A. (1972), in The Enzymes, 3rd. ed. (Boyer, P.D., ed.), Vol. VII, Academic Press (N.Y.), 665.

APPENDIX A

CHEMICAL AND STRUCTURAL DATA FOR LYSOZYME

All these data are taken from Imoto, T., Johnson, L.N., North, A.C.T., Phillips, D.C. and Rupley, J.A. (1972) In The Enzymes Vol. VII, (3rd ed.) (Boyer, P.D. ed.), Academic Press (N.Y.), 666.

A.1 Amino Acid Composition of Hen and Human Lysozyme

	Hen	Human
Ala	12	14
Arg	11	14
Asp	7	8
Asn	14	10
Cys	8	8
Glu	2	3
Gln	3	6
Gly	12	11
His	1	1
Ile	6	5
Leu	8	8
Lys	6	5
Met	2	2
Phe	3	2
Pro	2	2
Ser	10	6
Thr	7	5
Trp	6	5
Tyr	3	6
Val	6	9
Total	129	130

A.2 Sequences of Hen and Human Lysozymes

	1	2	3	4	5	6	7	8	9	10
Hen	Lys	Val	Phe	Gly	Arg	Cys	Glu	Leu	Ala	Ala
Human				Glu						Arg

	11	12	13	14	15	16	17	18	19	20
Hen	Ala	Met	Lys	Arg	His	Gly	Leu	Asp	Asn	Tyr
Human	Thr	Leu			Leu		Met		Gly	

	21	22	23	24	25	26	27	28	29	30
Hen	Arg	Gly	Tyr	Ser	Leu	Gly	Asn	Trp	Val	Cys
Human			Ile			Ala			Met	

	31	32	33	34	35	36	37	38	39	40
Hen	Ala	Ala	Lys	Phe	Glu	Ser	Asn	Phe	Asn	Thr
Human	Leu			Trp			Gly	Tyr		

	41	42	43	44	45	46	47	48	49	50
Hen	Gln	Ala	Thr	Asn	Arg	Asn	Thr	Asp	Gly	Ser
Human	Arg				Tyr		Ala		Arg	
							Gly			

	51	52	53	54	55	56	57	58	59	60
Hen	Thr	Asp	Tyr	Gly	Ile	Leu	Gln	Ile	Asn	Ser
Human						Phe				

	61	62	63	64	65	66	67	68	69	70
Hen	Arg	Trp	Trp	Cys	Asn	Asp	Gly	Arg	Thr	Pro
Human		Tyr						Lys		

	71	72	73	74	75	76	77	78	79	80
Hen	Gly	Ser	Arg	Asn	Leu	Cys	Asn	Ile	Pro	Cys
Human		Ala	Val		Ala		His	Leu	Ser	

	81	82	83	84	85	86	87	88	89	90
Hen	Ser	Ala	Leu	Leu	Ser	Ser	Asp	Ile	Thr	Ala
Human					Gln	Asp	Asn		Ala	Asp

	91	92	93	94	95	96	97	98	99	100
Hen	Ser	Val	Asn	Cys	Ala	Lys	Lys	Ile	Val	Ser
Human	Ala		Ala				Arg	Val		Arg

	101	102	103	104	105	106	107	108	109	110
Hen	Asp	Gly	Asn	Gly	Met	Asn	Ala	Trp	Val	Ala
Human		Pro	Gln		Ile	Arg				

	111	112	113	114	115	116	117	118	119	120
Hen	Trp	Arg	Asn	Arg	Cys	Lys	Gly	Thr	Asp	Val
Human						Gln	Asn	Arg		

	121	122	123	124	125	126	127	128	129
Hen	Gln	Ala	Trp	Ile	Arg	Gly	Cys	Arg	Leu
Human	Arg	Gln	Tyr	Val	Gln			Gly	Val

A.3 pK Values and Environments of Ionisable Groups of Hen Lysozyn

Ionisable Group	Environment	Assigned pK
Basic Groups		
Lys 1 (α-NH_2)	E	
Lys 1	E	
Arg 5	E	
Lys 13	E	
Arg 14	E	
His 15	E	5.2-5.8
Lys 33	S	
Arg 45	E	
Arg 61	E	
Arg 68	E	
Arg 73	E	
Lys 96	S	
Lys 97	E	
Arg 112	E	

Ionisable Group	Environment	Assigned pK
Basic Groups		
Arg 114	S	
Lys 116	S	
Arg 125	E	
Arg 128	E	
Acidic Groups		
Glu 7	E	2.7-4.7
Asp 18	E	
Tyr 20	S	} 9.5-10 or
Tyr 23	S	}11.3-11.8
Glu 35	S	6-6.5
Asp 48	E	
Asp 52	S	3.0-4.6
Tyr 53	S	12.4-12.9
Asp 66	I	1.5-2
Asp 87	E	2.7-4.7
Asp 101	E	4.2-4.7
Asp 119	E	
Leu 129 (α-COOH)	S	2.7-4.7

The classification of the environment is I (internal), S(surface) and E (exposed).

A.4 Groups with Diffuse Electron Density in the X-ray Map of Hen Lysozyme

Residue	Environment	Atoms[a]	Group
Lys 1	E	N(Z)	$-NH_3^+$
Met 12	I	C(E)	$-CH_3$
Asp 18	E	O(D)	-COOH
Trp 62	S	C(Z1), C(H), C(Z2), C(E2), C(D2)	-Indole
Arg 73	E	C(D), N(E), C(Z), N(HZ), N(H1)	b
Ser 86	E	O(G)	-OH
Lys 97	E	N(Z)	$-NH_3^+$
Asp 101	E	C(G), O(D2), O(D1)	-COOH
Val 109	E	C(G2)	$-CH_3$
Arg 112	E	C(G), N(H2), N(H1)	b
Glu 121	E	C(D), NO(E2), NO(E1)	$-CONH_2$
Arg 125	E	C(G), C(D), N(E), C(Z), N(H2), N(H1)	b
Arg 128	E	C(G), C(D), N(E), C(Z), N(H2), N(H1)	b

a numbering scheme of Imoto et al., 1972.

b 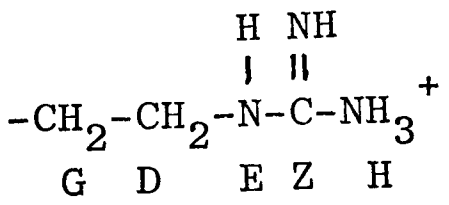

APPENDIX B

ASPECTS OF Nmr THEORY

B.1 Pulsed Nmr

Let the frequency of the applied rf pulse be ω_o. For a pulse applied for a short time, the pulse is actually a band of frequencies $\omega_o \pm \Delta\omega$. This is generally set to cause transitions in all nuclei of a given isotope (e.g. ^1H). After the application of the pulse, the net nuclear magnetisation is no longer aligned in the direction (z) of applied magnetic field, but has a component in the xy plane. This magnetisation is detected, after the application of the pulse, by a phase sensitive detector tuned to the frequency ω_o. The magnetisation in the xy plane decays at a rate which depends on T_2^*, and is followed by sampling the magnetisation at discrete time intervals. T_2^* includes the effects of magnet inhomogeneities as well as direct T_2 effects. For a nucleus with resonant frequency ω_o, the decay of magnetisation with time t is a simple exponential $f(t) = e^{-t/T_2^*}$. For a nucleus of resonance frequency ω^1, the decay of magnetisation takes the form $f(t) = e^{-t/T_2^*} \cos(\omega^1-\omega_o)t$. This results from the magnetisation processing at frequence ω^1 coming in and out of phase with the detector at frequency ω_o. The overall free induction decay (FID) is the sum of the decays for all the nuclei excited. The time domain spectrum, f(t), may be converted into the frequency domain spectrum, $F(\omega)$ because

$$F(\omega) = \int_{-\infty}^{\infty} f(t)\, e^{-i\omega t}\, dt$$

where $F(\omega)$ is defined as the Fourier transform of f(t). This transformation is carried out by an on-line computer.

The linewidth of a resonance depends on T_2^* ($\Delta\nu_{1/2}$, the linewidth at half-height in Hz, $= 1/\pi\ T_2^*$). For a nucleus of resonant frequency ω^1, the lineshape of an exponential decay in the time domain is Lorentzian in the frequency domain. The Lorentzian lineshape, $L(T_2^*)$ is $\int_0^\infty e^{-t/T_2^*} \cos(\omega-\omega^1)t\ dt$ so,

$$L(T_2^*) = T_2^*/\left[1 + T_2^{*2}\ (\omega-\omega^1)^2\right]$$

Pulsed nmr is discussed in detail by Farrar and Becker (1971).

B.2 The Nuclear Overhauser Effect

The nuclear Overhauser effect (NOE) is defined as the change in integrated intensity of a nuclear resonance signal from one nucleus caused by double resonance of the signal from a second nucleus. A detailed description of the effect is given by Noggle and Schirmer (1971). The fractional enhancement (η) of the integrated intensity of the signal of a nucleus I when saturation of a nucleus S is carried out has been considered by Balaram *et al.* (1972), as a function of τ_c. τ_c is the correlation time (see Section B.3) for the dipolar relaxation of I by S. If the spin-lattice relaxation of I arises totally from the dipolar interaction with S, then

$$\eta = \frac{5 + \omega^2\tau_c^2 - 4\ \omega^4\tau_c^4}{10 + 23\ \omega^2\tau_c^2 + 4\omega^4\tau_c^4}$$

for spin 1/2 nuclei, where ω is the resonance frequency. When $\omega\tau_c \ll 1$, which is the case for small molecules in solution, $\eta = 0.5$. When $\omega\tau_c \gg 1$, $\eta = -1.0$. When $\omega\tau_c \approx 1$, τ_c may be obtained from η provided that the relaxation mechanisms are fully characterised.

B.3 Dipolar Relaxation Times

For a spin 1/2 nucleus experiencing a magnetic field from another nucleus with spin 1/2 (see Dwek, 1973),

$$\frac{1}{T_1} = \frac{3}{10} \quad \frac{\gamma_I^4 \hbar^2}{r^6} \cdot f_1(\tau_c)$$

where $f_1(\tau_c) = \frac{\tau_c}{1+\omega^2\tau_c^2} + \frac{4\tau_c}{1+4\omega^2\tau_c^2}$

τ_c is the correlation time for the fluctuation of the magnetic field which causes relaxation, and is here assumed to be for isotropic motion. The assumption also is that τ_c is the time constant for an exponential correlation function. From this equation, it can be seen that T_1 passes through a minimum at $\omega\tau_c \simeq 0.6$. When $\omega\tau_c >> 1$, T_1 is proportional to τ_c, and is dependent on the frequency of the measurements (the ratio at different frequencies depends upon ω^2). When $\omega\tau_c << 1$, T_1 is proportional to $1/\tau_c$, and is independent of ω.

In addition,

$$\frac{1}{T_2} = \frac{3}{20} \quad \frac{\gamma_I^4 \hbar^2}{r^6} \quad f_2(\tau_c)$$

where $f_2(\tau_c) = 3\tau_c + \frac{5\tau_c}{1+\omega^2\tau_c^2} + \frac{2\tau_c}{1+4\omega^2\tau_c^2}$

when $\omega\tau_c << 1$, $T_1 = T_2$. However, otherwise

$$\frac{T_1}{T_2} = \frac{1}{2} \cdot \frac{f_2(\tau_c)}{f_1(\tau_c)} = f_3(\tau_c)$$

Thus the ratio of T_1/T_2 at a frequency ω depends only on τ_c.

T_1/T_2 will be given by the above provided that the above assumptions hold, and provided that the relaxation arises only from a dipolar mechanism. Dipolar relaxation is likely to be the only significant relaxation process for ^1H resonances of proteins, unless effects from chemical exchange occur. These affect T_2 much more than T_1.

B.4 Exchange Effects

The details of exchange effects are described by Pople et al., 1959. However, for exchange of a nucleus between two equally populated sites A and B the analysis for T_2 is straightforward (Jackman and Sternhell, 1969). If τ_A and τ_B are the lifetimes of the two sites, the lifetime of the system, defined as

$$\tau = \tau_A \tau_B/(\tau_A + \tau_B)$$

becomes $\tau = \tau_A/2 = \tau_B/2$.

Assume also that the T_2 value in each site is small compared to $1/(\nu_B-\nu_A)$ where ν_A and ν_B are the frequencies (in Hz, $2\pi\nu = \omega$ rad s^{-1}) of the nucleus in sites A and B. When $\tau<<1/(\nu_B-\nu_A)$ a single line at $(\nu_A+\nu_B)/2$ is observed (fast exchange). When $\tau>>1/(\nu_B-\nu_A)$ two lines are observed (slow exchange). As the lifetime decreases from the slow exchange situation, the two lines broaden and move together until coalescence to a broad single line occurs. The lifetime at the point of coalescence is

$$\tau = \sqrt{2}/2\pi\ (\nu_B-\nu_A)$$

The broadening in the intermediate exchange region can also be used to measure τ. The broadening of the two separate resonance before coalescence is given by

$$\frac{1}{\tau} = 2\left[\frac{1}{T_2^{ex}} - \frac{1}{T_2^{o}}\right]$$

where T_2^{ex} and T_2^{o} are the values of T_2 in the presence and absence of exchange ($1/T_2 = \pi\Delta\nu$). The broadening of the coalesced resonance is given by

$$\frac{1}{\tau} = \pi^2(\nu_B-\nu_A)^2\left[\frac{1}{T_2^{ex}} - \frac{1}{T_2^{o}}\right]^{-1}$$

The latter two equations do not hold in the region of coalescence (when $\tau \sim \sqrt{2}/2\pi\ (\nu_B - \nu_A)$) where theoretically computed spectra need to be examined to obtain τ.

B.5 References

Balaram, P., Bothner-By, A.A. and Dadok, J. (1972), J.Amer.Chem.Soc. 94, 4015.

Dwek, R.A. (1973), Nuclear Magnetic Resonances in Biochemistry, Clarendon Press (Oxford).

Farrar, T.C. and Becker, E.D. (1971), Pulse and Fourier Transform NMR, Academic Press (N.Y.).

Jackman, L.M. and Sternhell, S. (1969), Applications of Nuclear Magnetic Resonance Spectroscopy in Organic Chemistry, Academic Press (N.Y.).

Noggle, J.H. and Schirmer, R.E. (1971), The Nuclear Overhauser Effect, Academic Press (N.Y.).

Pople, J.A., Schneider, W.G. and Bernstein, H.J. (1959), High Resolution Nuclear Magnetic Resonance, McGraw-Hill (N.Y.).

APPENDIX C

SUMMARY OF EXPERIMENTS RELEVANT TO TEXT

This list does not include preliminary or incidental experiments, or experiments such as spin-decoupling or measurement of relaxation times which are fully described in the text. Unless otherwise stated, all experiments involved 5mM hen lysozyme dissolved in 99.8% D_2O, the pH values being measured at *ca* 20°C, and the spectra being recorded at 54°C.

C.1 pH Titrations

	Solution	Conditions	pH range
(i)	Protein alone	D_2O, 54°C	2-12
		H_2O[a], 54°C	2-9
		D_2O, 25°C	3-7
(ii)	+ 0.4M KCl		2.5-7
(iii)	+ 0.2M GlcNAc	D_2O	2-9
		H_2O	2.5-8
(iv)	+0.005M GlcNAc	at 54°C and 37°C	2-9
(v)	+0.5M $CaCl_2$		3.5-7.5
(vi)	+ lanthanide chlorides, see below		
(vii)	Human lysozyme	D_2O	2-9.5
		H_2O	3.5-9.5

[a] refers to 90% H_2O, 10% D_2O.

C.2 Temperature Titrations

	Solution	Conditions	Temp. Range
(i)	Protein alone	pH 3.8, 5.3, 6.1, 8.1	25°-90°C
		pH 4.8	5°-70°C
(ii)	+0.05M GlcNAc	pH 5.3	5°-70°C

	Solution	Conditions	Temp. Range
(iii)	+0.004M $(GlcNAc)_3$	pH 5.3	25^{o}-70^{o}C
(iv)	+0.008M $(GlcNAc)_3$	pH 5.3	25^{o}-70^{o}C

C.3 Inhibitor Titrations

Conditions - (a) in D_2O, pH 5.3 at 37^{o}C, 54^{o}C, 72^{o}C; (b) in H_2O, pH 5.3, 54^{o}C.

(i) GlcNAc , 0-0.25M

(ii) $(GlcNAc)_3$, 0-0.008M

C.4 Ln^{3+} titrations at constant pH, 54^{o}C

Ln^{3+}		pH	Measured at x^{o}C	[Lys] const (mM)	$[Ln^{3+}]$ max (mM)	Ionic Strength (μ)
La^{3+}	(a)	5.3	20	5	150	Variable
	(b)	5.3	54	5	50	0.4
Pr^{3+}	(a)	6.0[a]	54	5	50	0.4
	(b)	6.0[a]	54	1	50	0.4
Eu^{3+}	(a)	5.3	20	5	150	Variable
	(b)	5.3	20	5	50	0.4
Yb^{3+}	(a)	5.3[b]	20	5	150	Variable
	(b)	4.3	20	5	150	Variable
	(c)	5.6[a]	20	5	150	Variable
	(d)	5.6[a]	54	5	50	0.4
	(e)	5.6[a]	54	1	50	0.47
KCl		5.3	20	5	300	Variable

[a] The maximum pH before precipitation. La^{3+} correction calculated from La^{3+}(b) and from pH titrations (cf. App. C.2). Lu^{3+} effects v. similar (see App. C.2).

[b] Also run at 37^{o}C.

C.5 pH titrations with lanthanides[a]

Ln^{3+}		$[Ln^{3+}]$ (mM)		pH range
La^{3+}		50	(a) D_2O	2.3-6.4
			(b) H_2O	2.5-6.4
Pr^{3+}		50	(a) D_2O	2.5-6.3
			(b) H_2O	2.5-5.7
Eu^{3+}		50		2.6-5.8
Yb^{3+}	(a)	5		2.8-5.9
	(b)	9		2.8-5.7
	(c)	15		2.9-5.6
	(d)	30		2.3-5.5
	(e)	50		2.3-5.6
Lu^{3+}		50		2.9-5.6
KCl		400		2.3-7.3

[a] Lys = 5mM, μ = 0.4, pH measured at 54°C

C.6 Titrations at a Constant Total Lanthanide Concentration

With Ln^{3+}, where Ln = La, Ce, Pr, Nd, Sm, Eu, Tb, Dy, Ho, Er, Tm, Yb

total[lanthanide] = $[La^{3+}] + [Ln^{3+}]$ = 23.8mM,

and pH = 5.3.

Also, with Ln = La, Pr, Nd, Eu, Yb for $[Ln^{3+}] + [La^{3+}]$ = 50 mM and pH 5.3, 37°C.

APPENDIX D

LANTHANIDE TITRATION BEHAVIOUR OF DIFFERENT RESONANCES[a]

(a) Titrations observed clearly, but shifts small.

M1	leu 17	A1	trp 63 5/6
M3	leu 17	A2	
M8	leu 56	A3	
M22	met 12		

(b) Titrations showing large shifts from major site alone.

M9	thr 51 (Eu, Yb)	A6	try 53 o- (Eu, Yb)
M14	ala 107/31 (Pr)	A11	trp 108 C(2) (Pr, Eu)
M21		A12	tyr 53 m-
L1		A20	trp 63 C(2) (Pr)[b]
		N1	trp 108 N(1) (Pr)

(c) Titrations showing shifts from minor sites.

(i) Large effects

M2	ile 98 γ	A9	(Yb)
M4	ile 98 δ	A21	
M6	met 105 [c]	A22	trp 63 4/7

(ii) Small effects

M5	leu 8	A23	his 15 C(2)
M7	ile 88		
M10	val 92		

[a] resonances not mentioned have not been observed in a full titration, or titrations have not been analysed in detail. Titrations with Pr^{3+}, Eu^{3+} and Yb^{3+} were performed. Unless indicated, curves with all three lanthanides were observed.

[b] this resonance could not be observed at high pH values, so is a tentative inclusion in this Table.

[c] this resonance gives this behaviour with Yb^{3+} only. With Eu^{3+} and Pr^{3+} the shifts are small.

APPENDIX E

COMPUTED SHIFT RATIOS

	α =	90	90	90	90	90
	β =	60	70	80	90	100
T53Ø		100.0	100.0	100.0	100.0	100.0
T53M		185.5	154.3	134.1	117.9	102.3
T23Ø		-14.6	-11.6	-8.7	-5.7	-1.9
T2ØØ		-0.1	-3.4	-5.1	-6.0	-6.3
108C		-97.4	-142.7	-157.9	-157.1	-142.5
108N		47.4	-18.9	-54.7	-77.0	-91.5
T62C		-69.4	-60.5	-59.7	-63.7	-72.4
T63C		47.4	9.4	-15.9	-37.1	-58.3
M12		3.1	-4.5	-8.6	-11.2	-12.9
A31		-38.1	-37.2	-34.4	-30.2	-24.1
A32		-3.6	-11.8	-16.7	-20.3	-23.3
A42		37.6	31.3	24.4	16.1	5.4
T51		83.3	124.4	153.4	178.8	205.5
I55G		46.7	20.4	4.3	-7.8	-18.7
I55D		16.5	6.3	-0.5	-6.2	-12.0
L56A		11.0	-11.5	-24.0	-32.3	-38.3
L56B		25.6	4.1	-8.2	-16.7	-23.4
I58G		118.9	62.6	27.2	-0.5	-26.1
I58D		82.2	44.1	20.7	3.1	-12.6
T69		-41.0	-20.4	-9.0	-1.7	3.3
I98G		-22.2	-31.4	-35.3	-36.4	-35.4
I98D		39.6	6.5	-12.9	-26.8	-38.1
M105		-27.6	-26.6	-24.0	-19.9	-14.0
A107		-65.9	-57.5	-49.2	-39.8	-27.9
109A		-310.1	-16.9	187.2	365.1	550.1
109B		119.8	184.5	229.4	268.5	309.1
A110		-176.6	-112.8	-70.4	-34.9	0.4

	α =	100	100	100	100	100
	β =	60	70	80	90	100
T53Ø		100.0	100.0	100.0	100.0	100.0
T53M		169.1	144.0	126.6	112.0	97.7
T23Ø		-12.5	-10.3	-8.1	-5.5	-2.2
T2ØØ		0.7	-2.6	-4.3	-5.3	-5.9
108C		-103.2	-136.6	-146.6	-142.8	-126.2
108N		33.3	-21.2	-52.0	-71.3	-83.6
T62C		-17.1	-24.5	-32.1	-40.9	-52.3
T63C		89.5	41.9	10.7	-14.1	-37.5
M12		-1.3	-6.3	-9.2	-10.8	-11.7
A31		-39.2	-35.4	-31.0	-25.5	-18.0
A32		-13.7	-16.8	-18.8	-20.2	-21.1
A42		-9.7	-4.9	-6.0	-10.8	-19.4
T51		72.5	110.8	138.0	161.3	181.7
I55G		26.1	8.7	-3.0	-12.2	-20.5
I55D		1.7	-3.0	-6.8	-10.5	-14.5
L56A		-4.7	-18.7	-26.8	-32.0	-35.1
L56B		15.4	-0.5	-10.2	-16.9	-22.1
I58G		132.5	76.7	40.8	12.8	-12.6
I58D		75.2	42.2	21.1	4.7	-9.8
T69		-15.4	-0.1	9.5	16.7	23.0
I98G		-9.3	-22.7	-29.3	-32.8	-34.1
I98D		47.4	14.4	-5.6	-20.1	-32.0
M105		-26.0	-24.5	-21.6	-17.5	-11.6
A107		-50.0	-49.2	-45.7	-40.2	-32.5
109A		-187.0	64.4	250.1	417.6	594.5
109B		116.3	174.9	215.6	252.6	289.1
A110		-138.8	-80.0	-37.9	-0.6	38.7

	α =	110	110	110	110	110
	β =	60	70	80	90	100
T53Ø		100.0	100.0	100.0	100.0	100.0
T53M		156.9	135.5	119.9	106.3	92.6
T23Ø		-12.2	-10.2	-8.2	-5.9	-3.1
T2ØØ		1.0	-2.3	-4.1	-5.2	-5.9
108C		-124.7	-145.4	-149.3	-142.2	-123.9
108N		15.8	-29.6	-56.0	-73.0	-83.9
T62C		33.2	11.8	-3.2	-16.4	-30.5
T63C		128.3	71.6	34.9	6.5	-19.5
M12		-5.6	-8.6	-10.3	-11.3	-11.5
A31		-43.1	-36.2	-27.9	-22.9	-14.1
A32		-22.3	-21.4	-21.0	-20.5	-19.6
A42		-45.2	-33.3	-30.2	-32.4	-30.2
T51		57.9	95.9	122.4	144.5	165.6
T55G		9.2	-2.1	-10.2	-17.1	-23.5
T55D		-9.8	-10.6	-12.2	-14.3	-15.8
L56A		-19.4	-26.7	-31.1	-33.6	-34.5
L56B		5.9	-5.9	-13.3	-18.6	-22.7
T58G		145.7	88.9	51.8	22.9	-3.1
T58D		69.8	39.9	20.1	4.6	-9.3
T69		7.7	19.4	27.6	34.9	42.5
I98G		-0.9	-17.1	-26.0	-31.4	-34.8
I98D		53.2	19.8	-1.0	-16.3	-29.1
M105		-27.5	-24.8	-21.4	-17.0	-11.0
A107		-41.0	-45.2	-45.1	-42.9	-38.9
109A		-120.0	115.3	293.6	456.8	630.7
109B		105.4	162.2	202.6	237.0	279.7
A110		-112.4	-53.8	-10.2	29.9	73.4

	α =	120	120	120	120	120
	β =	60	70	80	90	100
T53Ø		100.0	100.0	100.0	100.0	100.0
T53M		146.2	127.1	112.8	99.9	86.4
T23Ø		-13.3	-11.2	-9.2	-7.1	-4.6
T2ØØ		0.7	-2.5	-4.4	-5.6	-6.5
108C		-165.3	-170.4	-166.5	-155.2	-135.5
108N		-8.9	-45.5	-67.5	-82.4	-92.7
T62C		42.3	55.2	31.7	13.6	-3.2
T63C		172.1	104.0	60.7	27.9	-1.3
M12		-10.9	-11.9	-12.4	-12.6	-12.2
A31		-50.4	-39.5	-30.9	-22.3	-12.0
A32		-31.4	-26.6	-23.7	-21.4	-18.8
A42		-77.3	-59.2	-52.4	-52.2	-47.4
T51		36.7	77.0	104.1	125.7	145.2
I55G		-8.0	-13.7	-18.7	-23.4	-28.2
I55D		-20.7	-18.1	-17.6	-18.1	-19.4
L56A		-46.2	-37.0	-37.6	-37.5	-36.4
L56B		-5.0	-12.9	-18.2	-22.2	-25.4
I58G		161.7	101.3	62.1	31.6	4.2
I58D		64.6	36.6	17.8	2.7	-11.2
T69		33.3	41.5	48.5	56.0	65.2
I98G		5.3	-13.7	-24.7	-32.0	-37.8
I98D		58.4	23.6	1.7	-14.8	-28.9
M105		-32.2	-27.5	-23.2	-18.3	-12.2
A107		-36.7	-44.6	-47.5	-48.2	-47.7
109A		-91.1	115.5	324.7	489.0	664.7
109B		85.3	144.3	185.2	219.0	251.0
A110		-91.0	-29.4	17.3	61.3	110.3

APPENDIX F

ILLUSTRATIONS OF THE X-RAY STRUCTURE OF LYSOZYME

FIGURE F.1

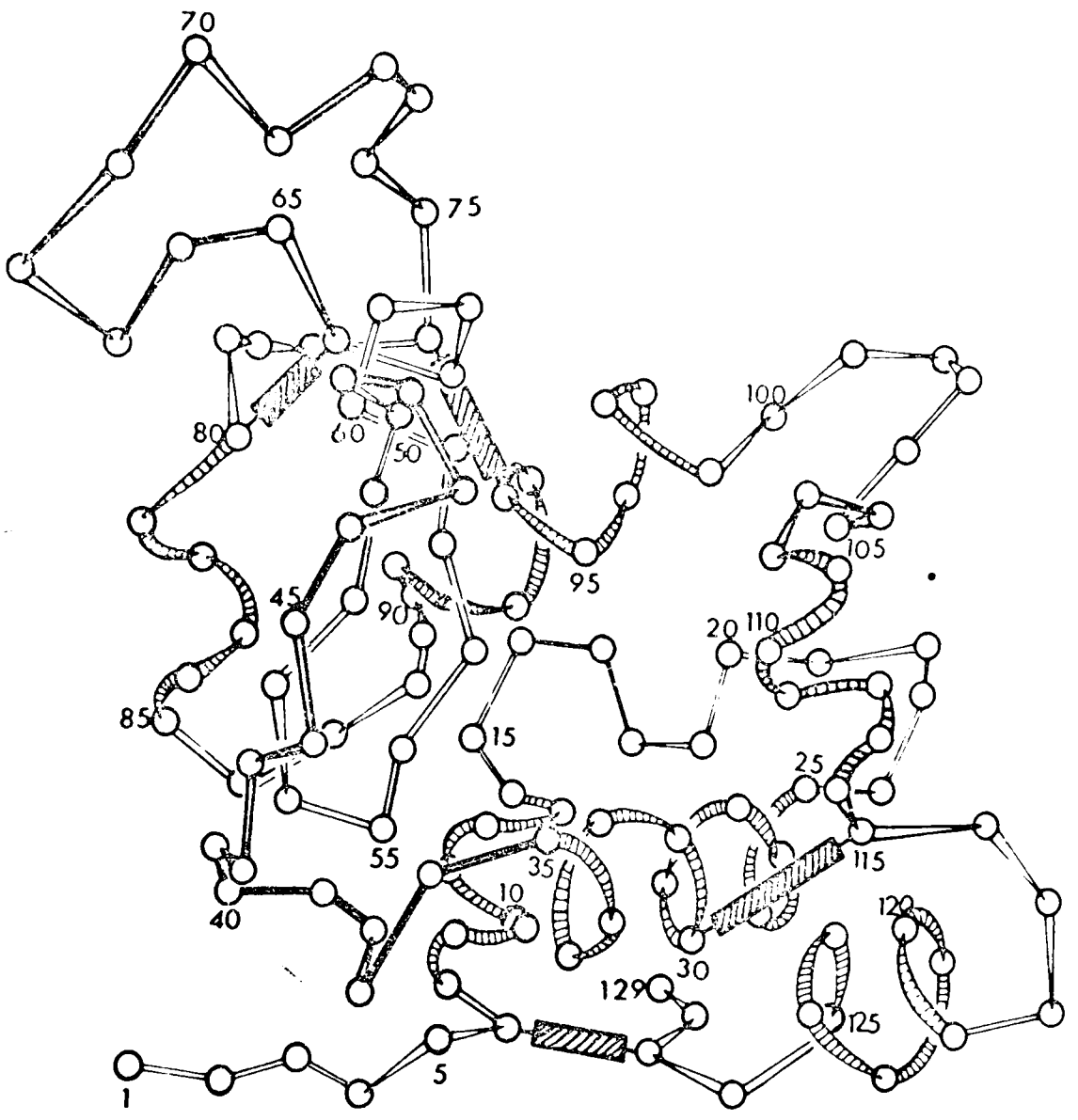

Sketch of the course of the main polypeptide chain in the lysozyme model of Blake et al. (1967). This view is from the front of the model. (From Phillips, 1974).

FIGURE F.2

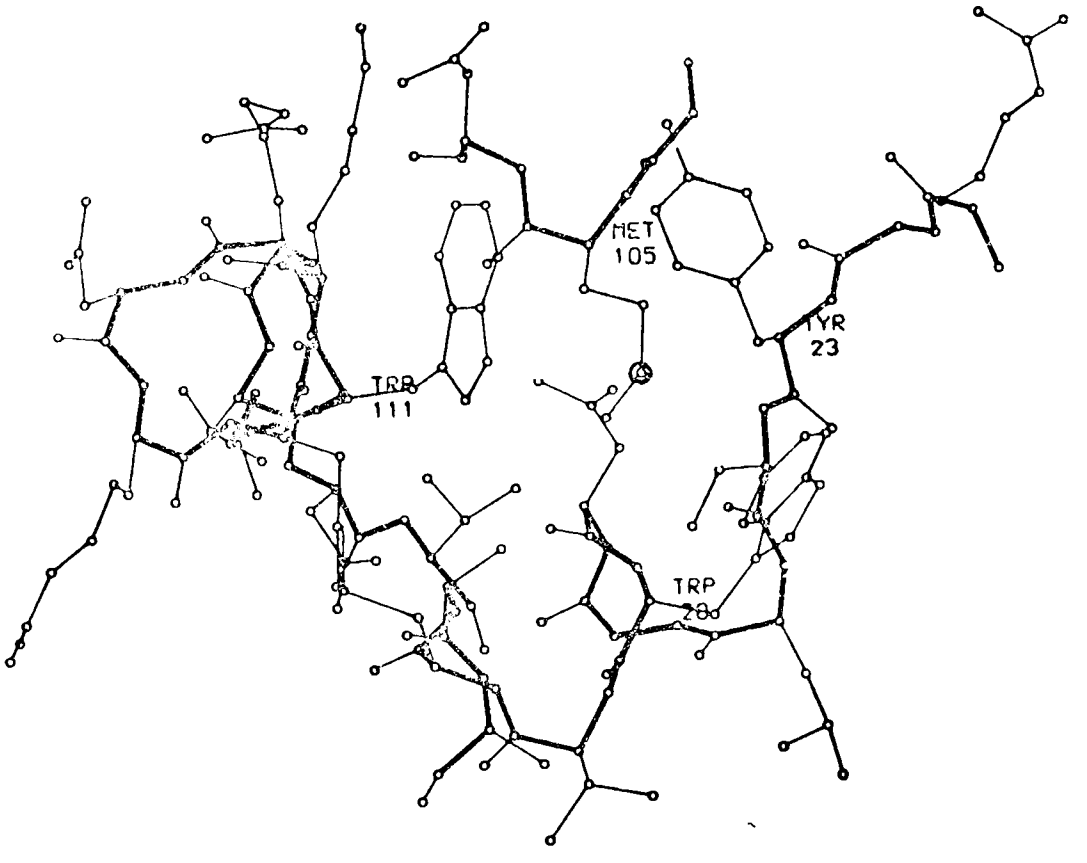

The right hand side of the lysozyme model, showing the hydrophobic box region around met 105. (From Banyard et al. 1974).

FIGURE F.3

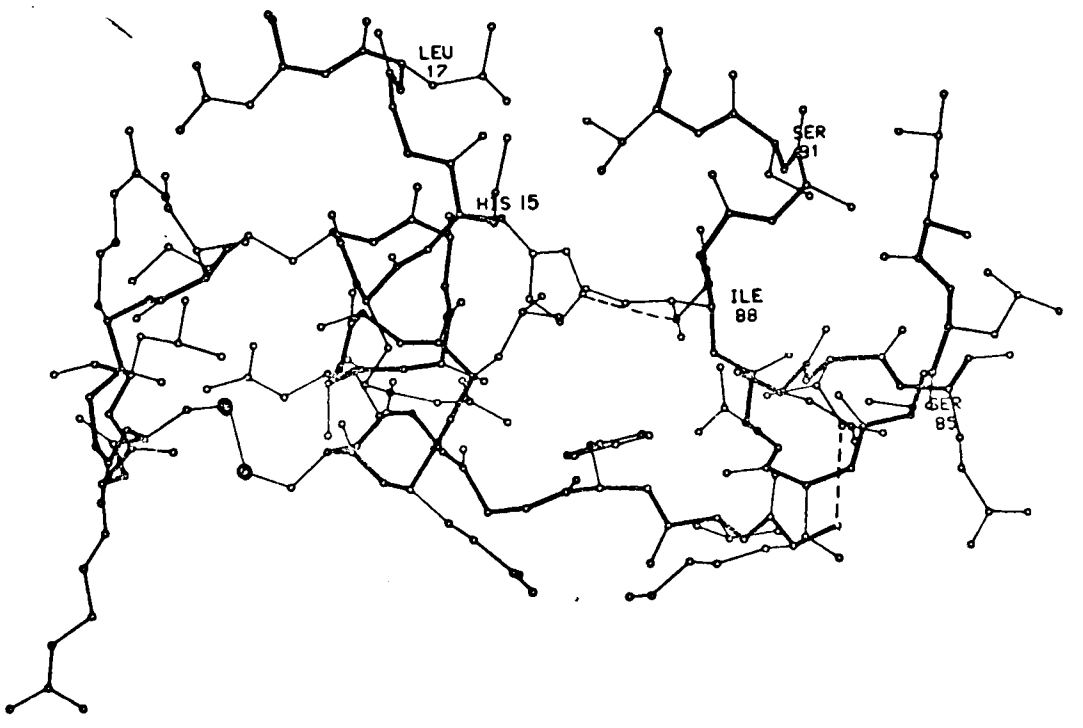

The back of the lysozyme model showing the region around his 15. (From Banyard et al. 1974).

FIGURE F.4

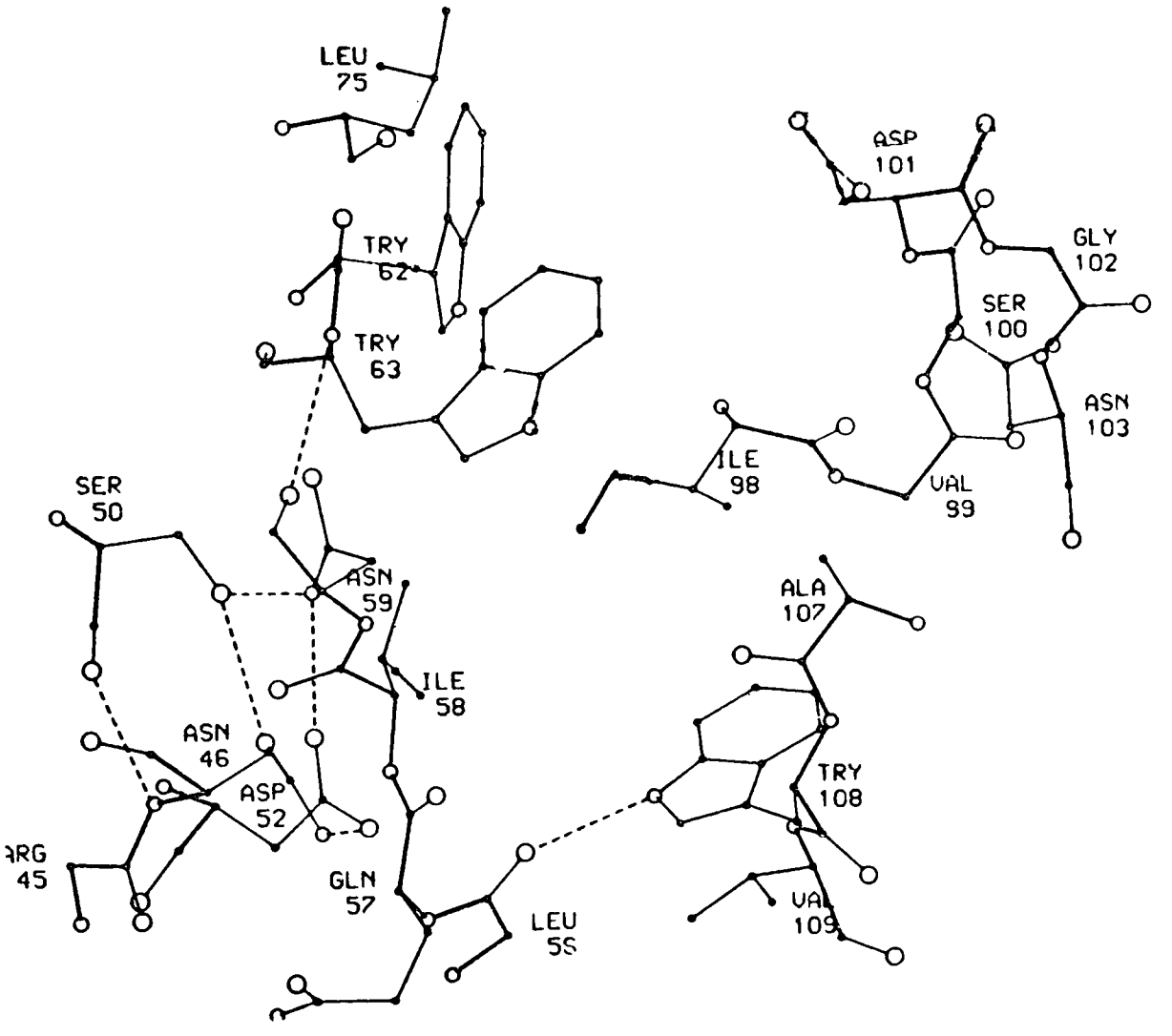

The upper part of the active cleft of lysozyme, viewed from the front of the model. (Adapted from Phillips, 1974).

FIGURE F.5

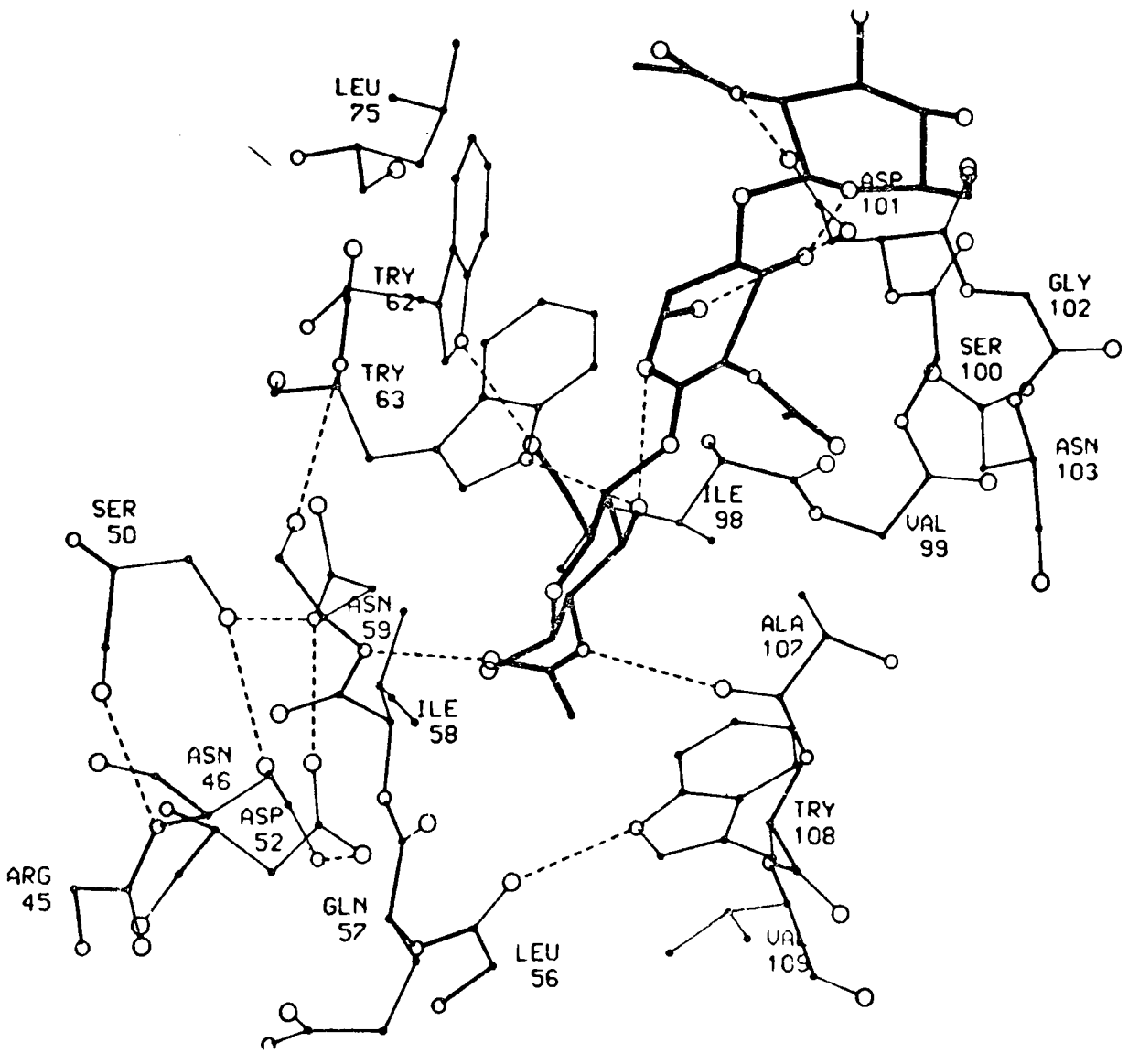

As Fig. F.4, but showing the position of $(GlcNAc)_3$ in the crystal (From Phillips, 1974).

FIGURE F.6

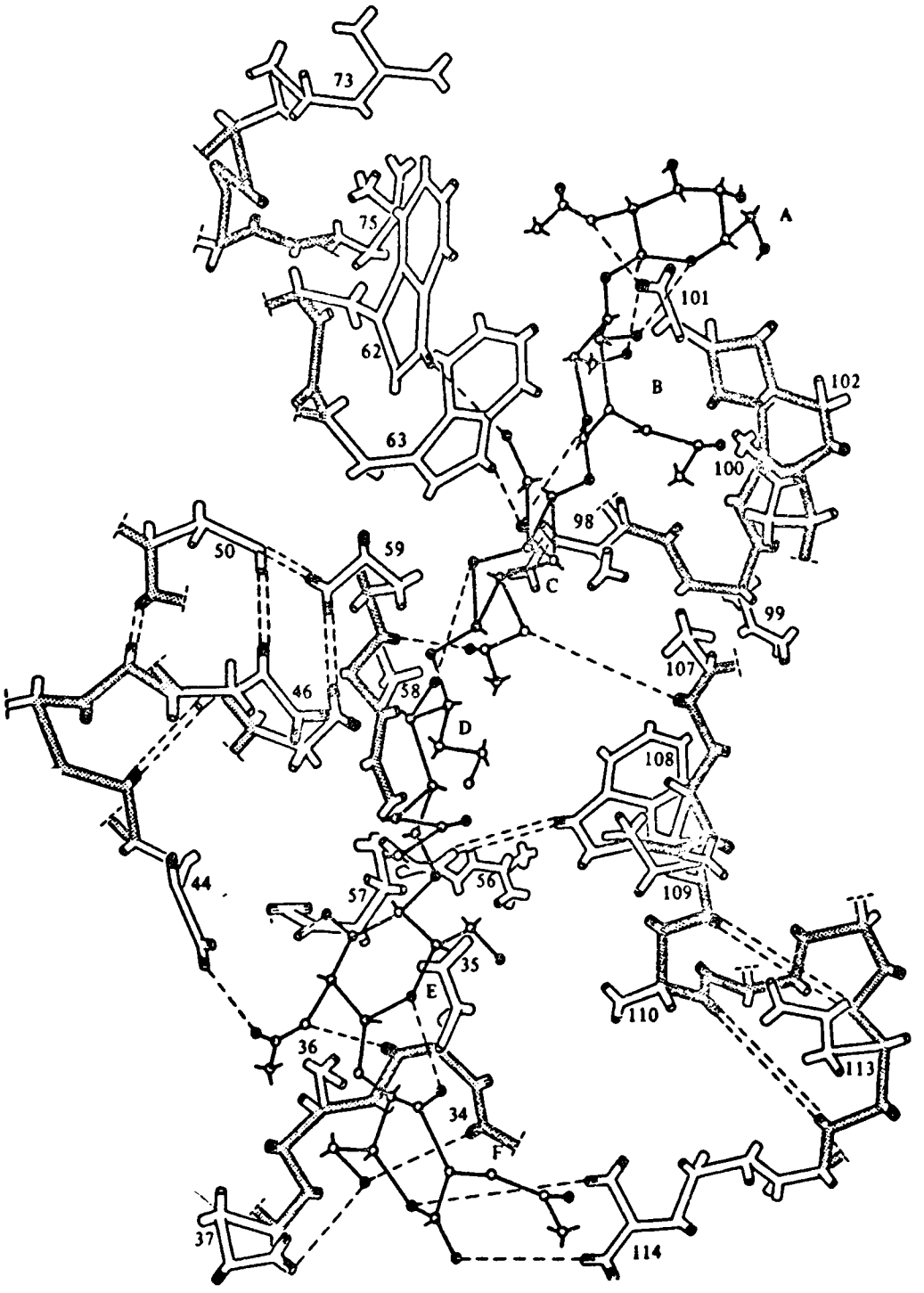

The whole of the active site cleft of the lysozyme model, showing the proposed binding of $(GlcNAc)_6$ in sites A to F. The polypeptide chain is shown speckled, with NH and O atoms indicated by line and full shading respectively. (From Phillips, 1967).

References for Appendix F

Banyard, S.H., Blake, C.C.F. and Swan, I.D.A. (1974), In Lysozyme (Osserman, E.F., Canfield, R.E. and Beychok, S. eds). Academic Press (N.Y.), 71.

Blake, C.C.F., Mair, G.A., North, A.C.T., Phillips, D.C. and Sarma, V.R. (1967), Proc.Roy.Soc. B167, 365.

Phillips, D.C. (1967), Proc.Natn.Acad.Sci. U.S.A. 57, 484.

Phillips, D.C. (1974), In Lysozyme (Osserman, E.F., Canfield, R.E. and Beychok, S. eds). Academic Press (N.Y.), 9.